universität wien

DIPLOMARBEIT / DIPLOMA THESIS

Titel der Diplomarbeit / Title of the Diploma Thesis

„Lanostane Triterpenes from Tyrolean Mushrooms:

ASE Based Extraction Protocol, Metabolite Profiling and

Isolation “

verfasst von / submitted by

Julia Zwirchmayr

angestrebter akademischer Grad / in partial fulfilment of the requirements for the degree of

Magistra der Pharmazie (Mag.pharm.)

Wien, 2017 / Vienna, 2017

Studienkennzahl lt. Studienblatt / degree programme code as it appears on the student record sheet:	A 449
Studienrichtung lt. Studienblatt / degree programme as it appears on the student record sheet:	Diplomstudium Pharmazie
Betreut von / Supervisor:	Univ.-Prof. Dr. Judith M. Rollinger
Mitbetreut von / Co-Supervisor:	Mag. Dr. Ulrike Grienke

In natural sciences the basic of truth

must be confirmed by observations.”

(Carl von Linnée)

ACKNOWLEDGEMENT

First of all I would like to thank the head of the Department **Univ.-Prof. Dr. Verena M. Dirsch** for giving me the opportunity to perform my diploma thesis at the Department of Pharmacognosy.

Especially, I would like to express my gratitude to **Univ.-Prof. Dr. Judith M. Rollinger** for the excellent supervision and her precious support during the whole process of my diploma thesis. I am more than grateful that I had the possibility to learn from you and dig deeper into the fascinating world of pharmacognosy and pharmaceutical sciences.

Likewise I also express my gratitude to my co-supervisor **Mag. Dr. Ulrike Grienke** for her never ending advice and continuous assistance during the whole work in the laboratory as well as for proofreading of my thesis.

I would also like to thank **Dr. Martin Zehl** for the HRMS, and **Prof. Ernst Urban** for the NMR measurements, respectively.

Additionally I would like to thank the whole team of the Pharmacognosy Department and all the other diploma students for creating a warm and friendly atmosphere. It had always been enjoyable and funny to listen to all the stories during coffee break. In particular I would like to thank Agata, Franzi and Thomas.

Last but not least I thank my family and friends for always supporting and helping me achieving my goals. Especially to my parents and my brother: I am very thankful not only for the financial but also for the mental support during my studies.

TABLE OF CONTENTS

LIST OF ABBREVIATION

^{13}C-NMR	Carbon-12 Nuclear Magnetic Resonance
17 β-HSD	17 β-Hydroxysteroid Dehydrogenase
^{1}H-NMR	Hydrogen-1 Nuclear Magnetic Resonance
ACE	Acetone
ACN	Acetonitrile
APT	Attached Proton Test
ASE	Accelerated Solvent Extraction
CAD	Charged Aerosol Detector
$CHCl_3$	Chloroform
Col.	Column
Config.	Configuration
COSY	Correlation Spectroscopy
DCM	Dichlormethan
DHEA	Dehydroepiandosterone
DHEAS	Dehydroepiandosterone Sulfate
DMSO	Dimethylsulfoxid
E_1	Estrone
E_1S	Estrone Sulfate
ER	Endoplasmatic Reticulum
et al.	et alii (lat.: and others)
EtOAc	Ethyl Acetate
EtOH	Ethanol
H_2O	Water
H_2SO_4	Sulfuric Acid
HA	Hemagglutinin
HMBC	Heteronuclear Multiple Bond Correlation
HPLC	High Pressure Liquid Chromatography
HSQC	Heteronuclear Single Quantum Coherence
IAV	Influenza A Virus
IC_{50}	Half Maximal Inhibitory Concentration

Inj. Vol.	Injection Volume
LC	Liquid Chromatography
MDCK	Mardin-Darby Canine Kidney
MeOH	Methanol
MeOH-d4	Deuterated Methanol
NA	Neuraminidase
n-hex	n-Hexane
PE	Petroleum Ether
SD	Standard Deviation
SFC	Supercritical Fluid Chromatography
SSo	Stock Solution
STS	Steroid Sulfatase
TCM	Traditional Chinese Medicine
Temp.	Temperature
TLC	Thin Layer Chromatography
UHPLC	Ultra High Pressure Liquid Chromatography
Vis	Visible
Wavel.	Wavelength

1 ABSTRACT

In this diploma thesis the natural compounds of interest are tetracyclic lanostane-type triterpenes derived from various mushroom species collected in Tyrol. The following work can be thematically split into two main sections: (i) the generation of an extraction protocol with Accelerated Solvent Extraction (ASE) for non-polar triterpenes of various mushroom species for a subsequent separation with Supercritical Fluid Chromatography (SFC) and (ii) the purification of selected triterpene-enriched fractions of *Gloeophyllum odoratum* (Wulffen) Imazeki.

For the generation of the extraction protocol with ASE, the fruit body of *Ganoderma lucidum* (Curtis) P. Karst was used as a model organism for the preliminary tests and thereafter 10 different mushroom species and more specifically 30 different strains thereof were extracted in small scale with the generated extraction method and, in addition, investigated for their secondary metabolite profile. The point of interest herein was to compare the secondary metabolite profile of the various strains of each species both, qualitatively and quantitatively. This was possible since all extracts were prepared in the exact same way. In a final step, a comparison of the secondary metabolite profiles of the non-polar extracts was achieved via SFC-ELSD.

The second part of this thesis was dedicated to the purification of selected triterpene-enriched fractions of *G. odoratum* strain 0054. This appeared to be very challenging since the compounds to be separated were very similar regarding their chemical structure. In total, five different fractions of *G. odoratum*, namely GO10_01, GO10_02, GO12_04, GO15_01 and GO27_07 were mycochemically investigated. For the separation of these fractions, a semi-preparative UHPLC (Ultra High Pressure Liquid Performance) was developed since other chromatographic separation techniques, e.g. SFC, were unsuccessful. NMR- and HRMS investigations of these fractions revealed to contain 6 different compounds: GO36_01 (21-hydroxylanosterol), GO36_02 (eburicodiol), GO37_01 (a new natural compound), GO37_02 [(15α)-15-hydroxy-3-oxo-lanosta-8,24-dien-21-oic acid], GO38_01 (3-ketodehydrosulfurenic acid) and GO38_02 (fomefficinic acid D). Out of these

fractions GO36_01 and GO36_02 were isolated as pure compounds and identified by NMR structure elucidation. Fraction GO27_07 turned out to be a single compound identical with a previously isolated pure compound, namely GO33_03 (Gloeophyllin A). All of these compounds have never been identified from *G. odoratum* before.

From previous test results it was known that the ethanolic crude extract (GO54E) as well as the dichlormethan (DCM) fraction of *G. odoratum* (GO54ED) shows an inhibition of the cancer related target steroidal sulfatase (STS) and the anti-viral target influenza neuraminidase (NA). Hence, the isolated pure compounds obtained in this work as well as other previously isolated constituents [11 pure compounds (GO54-A to GO54-O) and one mixture (GO54-E)] were prepared as stock solutions (SSo) in DMSO and were sent to collaboration partners for bioactivity testing. In addition GO54E and GO54ED were also tested for their STS and NA inhibition. Furthermore, IR spectra and the optical rotation of several isolated pure compounds were experimentally derived within this thesis.

STS analysis revealed that the inhibition of GO54E is higher than of the isolated compounds or GO54ED, suggesting that the active compounds of GO54E are not enriched in GO54ED. Further investigation and isolation of other fractions of GO54E are ongoing. The results of the NA analysis showed promising results for several compounds of *G. odoratum*. Five compounds showed activity against both influence A viruses IAV HK/68 and IAV Jena/8179, namely GO54-A [(3β)-Hydroxy-lanosta-8,24-dien-21-oic acid], GO54-E [mixture of: (3β)-3-hydroxy-lanosta-8,24-dien-21-oic acid and (3β)-3-hydroxy-24-methylene-lanost-8-en-21-oic acid], GO54-H (diastereomere of GO54-A) as well as GO54-M (=GO36_01; 21-hydroxylanosterol) and GO54-N (=GO36_02; eburicodiol), whereas GO54-D [(3β,15α)-acetyloxy-2,26-dihydroxy-lanosta-8,24-dien-21-oic acid] is only active against IAV Jena8179. The lowest half maximal inhibitory concentration (IC_{50}) against both virus strains IAV HK/68 (IC_{50} = 16,72 µM) and IAV Jena/8179 (IC_{50} = 8,98 µM) was recorded for the two component mixture GO54-E.

ABSTRACT (DEUTSCH)

In dieser Diplomarbeit wurden tetracyclischen Triterpene vom Lanostan-Typ untersucht, die aus verschiedenen in Tirol gesammelten Pilzarten gewonnen wurden. Die folgende Arbeit kann thematisch in zwei Abschnitte gegliedert werden: (i) die Generierung eines Extraktionsprotokolls mit Accelerated Solvent Extraction (ASE) für nichtpolare Triterpene verschiedener Pilzarten für eine anschließende Auftrennung mittels überkritischer Flüssigchromatographie (SFC) und (ii) die Aufreinigung ausgewählter Triterpen-angereicherter Fraktionen von *Gloeophyllum odoratum*.

Für die Entwicklung des Extraktionsprotokolls mit ASE wurde der Fruchtkörper von *Ganoderma lucidum* als Modellorganismus für die Vorversuche verwendet, um im Anschluss daran 30 Pilzstämme von 10 verschiedenen Pilzarten im Kleinmaßstab zu extrahieren. Mit dem optimierten Extraktionsverfahren wurde das Sekundärmetabolitenprofil der verschiedenen Stämme jeder Spezies sowohl qualitativ als auch quantitativ verglichen. Dies wurde ermöglicht, da alle Extrakte auf die gleiche Weise erzeugt wurden. In einem weiteren Schritt wurde ein Vergleich des Sekundärmetabolitenprofils der unpolaren Extrakte über SFC-ELSD vorgenommen.

Der zweite Teil dieser Arbeit umfasste die Aufreinigung ausgewählter Triterpen-angereicherter Fraktionen von *G. odoratum* Stamm 0054. Diese Aufgabe stellte sich als sehr anspruchsvoll heraus, da die zu trennenden Verbindungen hinsichtlich ihrer chemischen Struktur sehr ähnlich waren. Insgesamt wurden fünf verschiedene Fraktionen von *G. odoratum* - nämlich GO10_01, GO10_02, GO12_04, GO15_01 und GO27_07 - mykochemisch untersucht. Zur Trennung dieser Fraktionen wurde eine semi-präparative UHPLC verwendet, da andere chromatographische Trenntechniken, z.B. SFC, nicht erfolgreich waren. Eine HRMS- und NMR-Analyse dieser Fraktionen zeigte, dass 6 verschiedene Verbindungen enthalten sind: GO36_01 (21-Hydroxylanosterol), GO36_02 (Eburicodiol), GO37_01 (ein neuer Naturstoff), GO37_02 [(15α) -15-Hydroxy-3-oxo- Lanosta-8,24-dien-21-oic acid], GO38_01 (3- Ketodehydrosulfurenic acid) und GO38_02 (Fomefficinic acid D). Von diesen wurden GO36_01 und GO36_02 als Reinsubstanzen isoliert und mit NMR-Strukturaufklärung

identifiziert. Die Fraktion GO27_07 erwies sich als Reinsubstanz, die mit einem zuvor im Labor isolierten Inhaltsstoff identisch war, nämlich GO33_03 (Gloeophyllin A). Alle diese Verbindungen wurden noch nie für *G. odoratum* beschrieben.

Aus früheren Testergebnissen war bekannt, dass der ethanolische Rohextrakt (GO54E) sowie die Dichlormethan-Fraktion (GO54ED) von *G. odoratum* eine Hemmung des Krebs-relevanten Targets STS und des antiviralen Targets Influenza-NA zeigen. So wurden von den in dieser Arbeit isolierten Reinsubstanzen, sowie anderen bisher isolierte Substanzen [11 Reinsubstanzen (GO54-A bis GO54-O) und einer Mischung (GO54-E)] Lösungen (Stock solutions) in DMSO hergestellt und an Kooperationspartner für die Bioaktivitätstests verschickt. Zusätzlich zu den isolierten Verbindungen wurden auch GO54E und GO54ED auf ihre STS- und NA-Hemmung getestet. Des Weiteren wurden in dieser Arbeit IR-Spektren und die optische Drehung mehrerer isolierter Reinsubstanzen experimentell ermittelt.

Die STS-Analyse ergab, dass die Hemmung von GO54E höher ist als jene der daraus isolierten Verbindungen und von GO54ED. Dies deutet darauf hin, dass die aktiven Verbindungen in GO54E nicht in GO54ED angereichert sind. Weitere Untersuchungen und Isolierungen aus anderen Fraktionen von GO54E werden derzeit vorgenommen.

Die NA-Analyse ergab vielversprechende Ergebnisse für mehrere Verbindungen aus *G. odoratum*. Fünf Verbindungen zeigten eine deutliche Aktivität gegen beide Influenza-A Viren IAV HK/68 und IAV Jena/8179, nämlich GO54-A [(3β) -Hydroxy-lanosta-8,24-dien-21-oacid], GO54-E [Mischung aus: (3β) -3-Hydroxy-lanosta-8,24-dien-21-oacid und (3β) -3-Hydroxy-24-methylen-lanost-8-en-21-oacid], GO54-H (Diastereomer von GO54-A) sowie GO54-M (=GO36_01; 21-Hydroxylanosterol) und GO54-N (=GO36_02; Eburicodiol), während GO54-D [(3β, 15α) -Acetyloxy-2,26-dihydroxy- Lanosta-8,24-dien-21-oacid] nur gegen IAV Jena/8179 eine antivirale Aktivität zeigt. Die niedrigste halbmaximale Hemmkonzentration (IC_{50}) gegen beide Virusstämmen IAV HK/68 (IC_{50} = 16,72 µM) und IAV Jena/8179 (IC_{50} = 8,98 µM) wurde für die Zweikomponentenmischung GO54-E ermittelt.

2 AIM OF THE WORK

2.1 Generation of an Extraction Protocol with ASE for non-polar Triterpenes for Subsequent Separation with SFC

The aim of this work was to find an extraction method suitable for non-polar triterpenes contained in various mushrooms for a subsequent separation with supercritical fluid chromatography (SFC). From previous experiments it was known which area of polarity is suitable for the analysis with SFC. Therefore ASE was used as a convenient way to perform variations of several parameters e.g. solvent composition, pressure and temperature in a very short time compared to conventional extraction methods. In addition, a qualitative and quantitative comparison of the produced extracts was done. This was possible since all of the extracts were produced in the exact same way.

2.2 Purification of Selected Fractions of *Gloeophyllum odoratum*

The aim of this work was to separate selected fractions of the fruit body of *G. odoratum* by UHPLC since previous tests showed a promising bioactivity of the ethanolic extract regarding inhibition of STS and NA. The compounds to isolate in this diploma thesis were present in the fractions GO10_01, GO10_02, GO12_04, GO15_01 and GO27_07 which were originally derived from the ethanolic extract of *G. odoratum*. Of all 6 obtained pure compounds, 4 pure compounds, namely GO36_01 (21-Hydroxylanosterol), GO36_02 (Eburicodiol), GO38_01 (3-Ketodehydrosulfurenic acid) and GO38_02 (Fomefficinic acid D), as well as previously isolated pure compounds – GO54-A, GO54-D, GO54-E, GO54-H, GO54-I, GO54-J, GO54-K, GO54-L - were then tested for their bioactivity. Detailed information of all tested samples, substances and CAS Registry Number is given in Table 11. In addition, further work such as measurements of optical rotation and IR spectra of previously isolated pure compounds was done.

3 INTRODUCTION

3.1 Generation of an Extraction Protocol with ASE for non-polar Triterpenes for Subsequent Separation with SFC

3.1.1 Traditional Use of Mushrooms in Folk Medicine

Dried mushrooms have a longstanding use especially in Traditional Chinese Medicine (TCM) (Money, 2016). They have been used in Asian countries for centuries as a source for food as well as medicines to cure several diseases (Duru et al., 2015). Nonetheless the western world only recently raised awareness of these marvellous mushroom qualities and started to welcome natural products from the TCM. Hence, interest was raised for the isolation of bioactive compounds, elucidation of mechanisms responsible for biological effects and further development of new drugs for alternative or adjuvant cancer therapy (Sliva, 2006). The reasons therefore are not only the long history of mushrooms in the Asian world, but also the newly developed laboratory methods for isolation and investigation of natural products (Stamets et al., 2014). Especially terpenoids of mushroom origin “are associated with various pharmacological activities like anticancer, antimalarial, anticholinesterase, antiviral, antibacterial and anti-inflammatory activities”, as reported by Duru et al., 2015. Not only because of the longstanding ethnomedicinal use of mushrooms in the eastern world but also because of enhanced possibilities for pharmacological and chemical investigation leads us to the assumption that medicinal mushrooms have an enormous potential for the development of new drugs (Lindequis et al., 2005).

3.1.2 Botanical Description of “Mushrooms”

With the term “mushroom” we mostly mean “a macrofungus with a distinctive fruiting body, which can be either hypogeous or pigeous, large enough to be seen with the naked eye and to be picked by hand”, according to the definition of Chang et al., 1992). It is not a taxonomic category, but mostly basidiomycetes and some ascomycetes are associated as mushrooms. There exist probably 150 000 mushroom species on earth, whereas only 10 % are known and even less are well investigated (Wasser, 2011).

3.1.3 Chemical Constituents

Being the major constituents of the fungal cell wall, polysaccharides like α-glucans and β-glucans as well as their derivatives are largely present in mushroom fruit bodies and show biological effects. Anti-tumor, anti-viral and immune-regulatory activities are just a few of them and notably polysaccharides show no reported side effects. Concerning the secondary metabolite profile, terpenoids, i.e. lanostanes with various functional groups such as esters, acids, aldehydes and many more, represent the biggest part of the secondary metabolite classes in mushrooms,. Terpenoids are associated with manifold biological activities such as anti-inflammatory, antimicrobial and cytotoxic effects (Grienke et al., 2014). According to previous studies, the fruit bodies of different polypore strains of e.g. *F. fomentarius* (L.) Fr.) and *F. pinicola* (Sw.) P. Karst differed in qualitative and quantitative secondary metabolite production as well in bioactivity (Dresch et al., 2015). For the identification of various mushroom strains, rDNA ITS sequencing is widely used as a distinguishing feature for species identification (Quin et al., 2014).

3.1.4 Accelerated Solvent Extraction

ASE is a convenient technique for the extraction of e.g. dry plant material using different solvents at increased pressures and temperatures, which enables faster extractions and reduces the solvent consumption up to 90 % compared to traditional extraction techniques like sonication or Soxhlet. This leads to an elevated efficiency of the whole extraction process. The extraction process works as follows: The ASE extraction cell filled with (ground) sample is loaded into a preheated oven and is then filled with the solvent of choice, heated and pressurized. During this process, the cell is held at a constant temperature for a certain period of time for the static extraction. After this, the extract will be released into collection vessels. This whole process can be repeated for further extractions steps, thus allowing an exhaustive extraction as well. In the last step, the extraction cell will be flushed with nitrogen in order to unload the cell. All parameters as extraction cycles, temperature, pressure or the chosen solvents are programmable, which allows for an unattended extraction for up to 24 ASE cells (dionex.com; accessed on: September 2016) and enables to receive reproducible extracts.

3.2 Purification of Selected Fractions of *Gloeophyllum odoratum*

3.2.1 *Gloeophyllum odoratum*

G. odoratum is a wood-rotting mushroom which grows mainly on stumps of spruces, but has also been found to grow on stumps of pine trees. Because of its anise-like scent the mushroom fruit-bodies have been investigated intensely for their volatile but also non-volatile compounds but only a few constituents like ergosterol and lanostane derivates have been isolated so far (Rösecke, 2000). The fruit body of the young fungus shows a bulbous-bulging shape, with a mat, velvety-miserly and orange-brown surface, whereas the older ones are console shaped with an irregular mat-miserly surface of a dark brown-black color. Perennial mushrooms increase their surface area, which varies from a dark red-brown, a bright-orange to a shiny-yellow color. As already mentioned before, the name “odoratum” derives from the anise-like scent of the fresh fruit bodies but also older mushrooms smell like anise when they are not too arid. *G. odoratum* is not edible but according to literature, it has a bitter-sourish taste (Pilzforum.eu; accessed on August 2016).

3.2.1.1 Classification of *Gloeophyllum odoratum*

Kingdom:	Fungi
Phyllum:	Basidiomycota
Class:	Agarycomycetes
Order:	Gloeophyllales
Family:	Gloeophyllaceae
Genus:	Gloeophyllum
Species:	*Gloeophyllum odoratum*

Figure 1 – *G. odoratum*
[mycoweb-stv.ru; accessed on: June 2016]

3.2.1.2 Known Compounds from Literature

Volatile compounds from *G. odoratum* fruit bodies were investigated by (Rösecke et al., 2000). Reported compounds are e.g. aliphatic alcohols, ketones and aldehydes, as well as terpenes and aromatic compounds. Non-volatile compounds were reported by Cateni et al., 2015 and Rösecke et al., 2000. Table 1 gives an overview of the reported non-volatile compounds sorted by substance class, CAS number, molecular weight and structure.

Table 1 - Known non-volatile compounds of *G. odoratum* from literature (Scifinder)

Substance Class		CAS Number	Substance Name	Molecular Weight	Structure
TRITERPENE	**1**	1310359-31-9	(3α,4β,12β)-12-(acetyloxy)-3-hydroxy-Lanosta-8,24-dien-28-oic acid	514.74	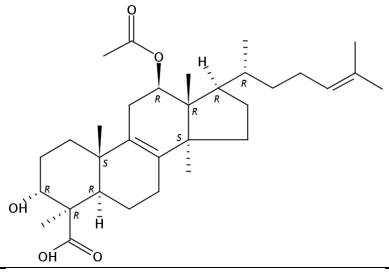
	2	1660105-49-6	Gloeophyllin B	514.74	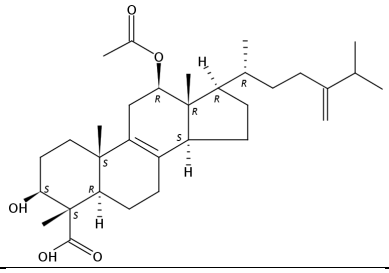
	3	1660105-50-9	(3β,4α,5α,12β)- 12-(acetyloxy)-3-hydroxy-4-methyl-Ergosta-8,24-diene-4-carboxylic acid	514.74	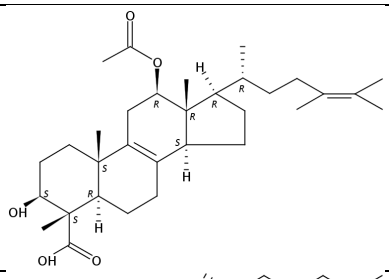
	4	79-63-0	(3β)-Lanosta-8,24-dien-3-ol	426.72	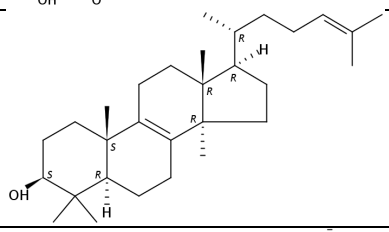
	5	2061-64-5	Ergosterol peroxide	428.65	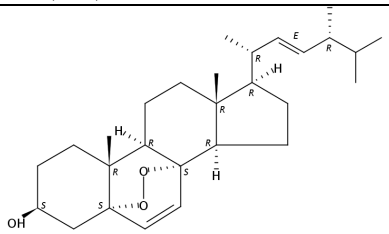

Substance Class		CAS Number	Substance Name	Molecular Weight	Structure
TRITERPENE ACID	**6**	19262-52-3	15α-Hydroxytrametenolic acid	472.70	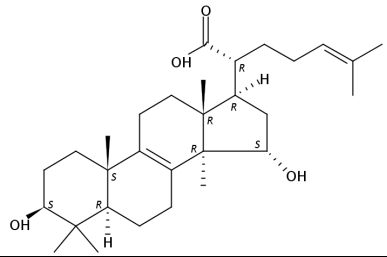
	7	6879-05-6	Dehydrotrametenolic acid	468.71	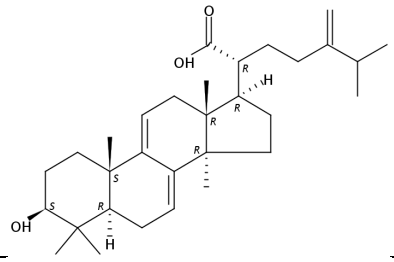
	8	24160-36-9	Trametenolic acid B	456.70	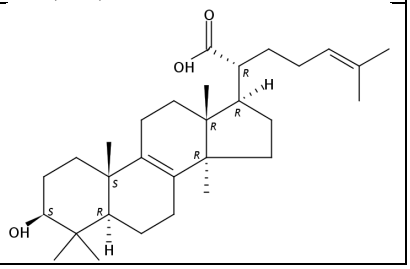

3.2.2 Bioactivity of Pure Compounds from *Gloeophyllum odoratum*

According to Ma et al., 2013, **8** and **5** isolated from the mushroom *Inonotus obliquus* (Donk) show inhibitory effects on NF-κB luciferase activity and additionally it was also investigated that **8**, **5** and **4** inhibit nitric oxide production. These activities are responsible for various signaling pathways in inflammation and cancer.

2 and **3** are also already known to inhibit thrombin, a serine protease responsible for blood coagulation and therefore play important roles in the pathogenic pathway of thrombosis (Cateni et al, 2015). Bioactivity investigations of the ethanolic extract, the dichlormethan fraction thereof as well as selected fractions of *G. odoratum* have shown inhibition of the STS and NA enzymes, reported in the dipoma theses of N. Lukovic and N. Prenner (2015).

3.2.2.1 Steroid Sulfatase and Hormone Dependant Cancers

Steroidal sulfatase (STS) is an enzyme capable of cleaving the biologically inactive sulfated steroids into the biologically active unsulfated steroids (Shah et al., 2016). These steroids promote the growth of several „gynaecological diseases such as endometriosis, adenomyosis

and uterin fibrosis, and gynaecological cancers including endometrial cancer and ovarian cancer“, according to Rižner, 2016.

In human cells 17 individual sulfatases have been found, whereof Arylsulfatase C, known under the name STS, is involved in the desulfation of estrone sulfate (E_1S) and dehydroepiandrosterone sulfate (DHEAS) to their unsulfated active forms estrone (E_1) and dehydroepiandrosterone (DHEA), respectively (see Figure 2). E_1 can then be converted by aromatase 17β-HSD to potent estrogens such as estradiol (E_2), whereas DHEA is further converted to androstenedione, testosterone and dihydrotestosterone. Consequently the STS enzyme has great impact on the regulation of steroid action in steroidogenic and non-steroidogenic tissues (Mueller et al., 2015). For instance, the highest STS levels were found in breast, ovary, adrenal gland, lung and endometrium, whereas the concentration of STS can modify from physiological to pathophysiological conditions. Thus the so called STS pathway is clearly involved in the local estrogen formation as well as increased estrogen actions. Therefore the development of STS inhibitors could have beneficial use for the treatment of gynaecological diseases (Rižner, 2016).

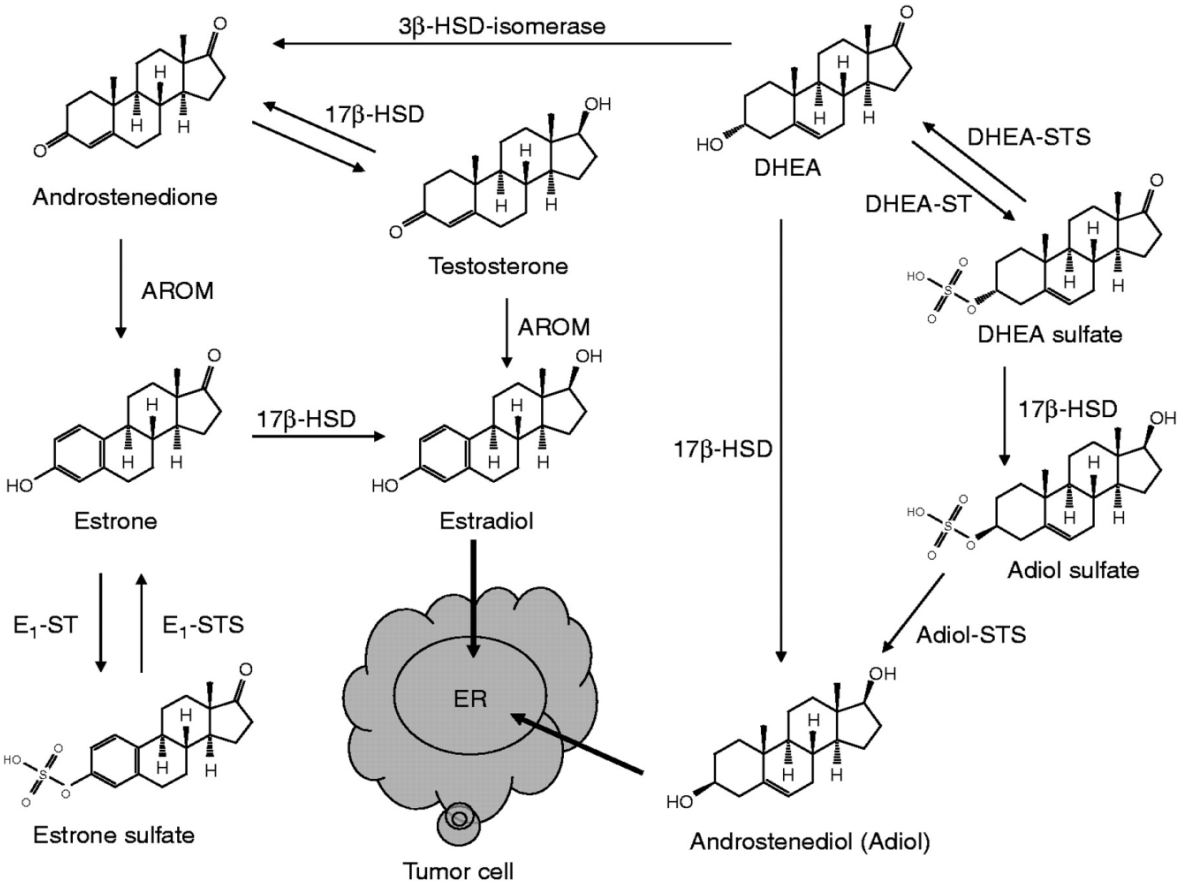

Figure 2 - The origin of estrogenic steroids
(joe.endocrinology-journals.org; accessed on: June 2016)

3.2.2.1.1 Structural Information

The crystal structure of the protein STS provides an insight into the architecture of the steroid sulfatase enzyme (see Figure 3): the protein has a mushroom-like shape, consisting of a polar globular domain and a hydrophobic, non-polar stem domain; latter consists of two anti-parallel a-helices capable for anchoring to the membrane surface in the endoplasmatic reticulum (ER). The polar globular domain contains the active catalytic site of the protein which is responsible for the hydrolysis of the sulfated inactive hormones (Nussbaumer et al., 2004).

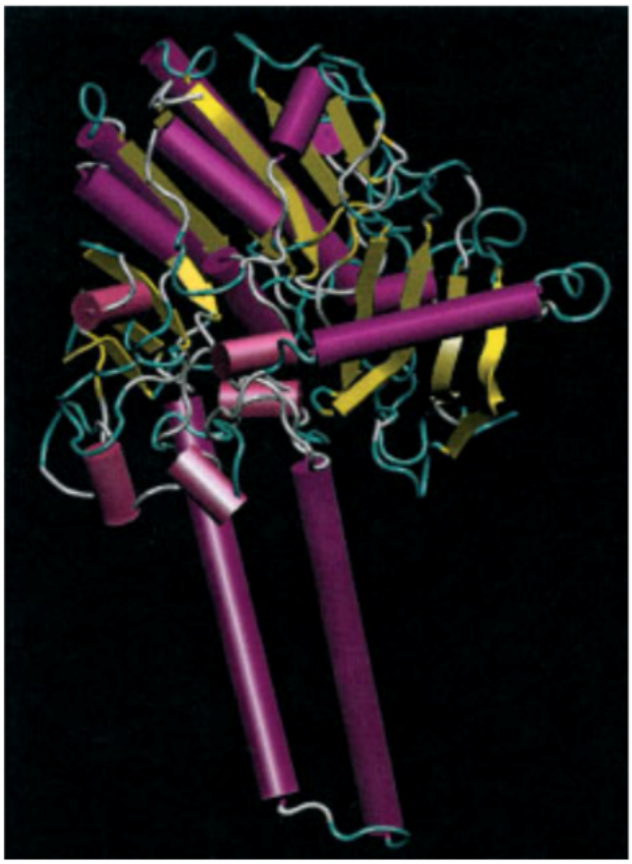

Figure 3 – Mushroom-like shape of the STS enzyme

(Nussbaumer & Billich, 2004)

3.2.2.2 Influenza

Influenza, the most common infectious disease, plays an important role in human health as it often leads to high morbidity and mortality due to its infectious nature and high transmissibility (Jagadesh et al., 2016). Influenza A and B belong to the *Orthomyxoviridae* and are responsible for flu characterized symptoms as fever, cough, sore throat but can also lead to life- threatening conditions such as pneumonia. These epidemics reoccur periodically but also pandemics are no exception. The surface of the virus possesses two surface glycoproteins: the enzyme Influenza Neuraminidase (NA) and Hemagglutinin (HA) (see Figure 4).

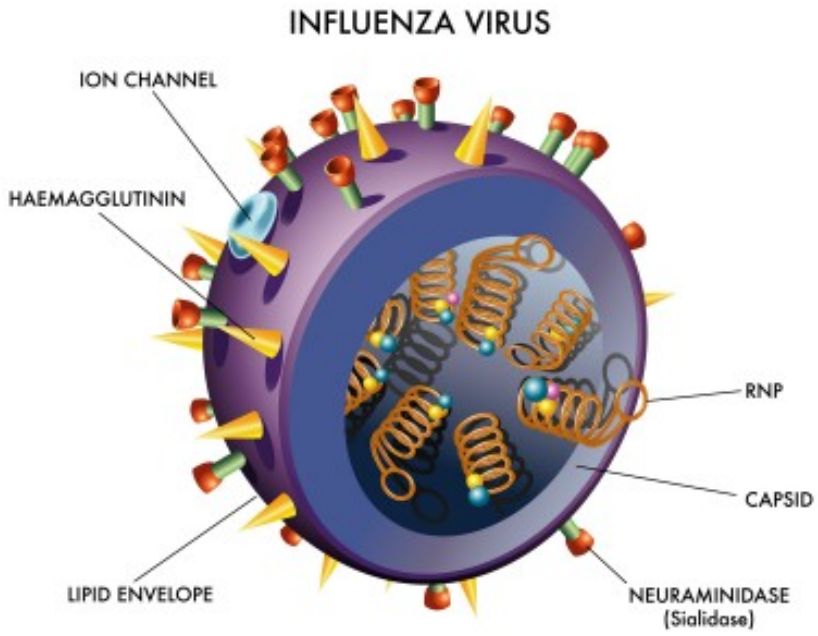

Figure 4 - Influenza virus; (images.tutorvista.com; Accessed: August 2016)

These enzymes play an important role in viral replication and pathogenesis and are therefore a main target for the treatment of influenza infections (Grienke et al., 2012). Last but not least it must be mentioned that annually reoccurring influenza epidemics results in approximately 5 million cases of severe illness and are estimated to cause 250.000 to 500.000 deaths per year worldwide. A huge problem is the virus alteration by mutation of the glycoproteins NA and HA on its surface, also known as antigenic drift if the changes are minor, antigenic shift if these antigenicity changes are major. Resulting in new virus strains these cause pandemic outbreaks periodically. Thus, there is an urgent need in updating vaccine strains frequently and finding new drugs (Jagadesh et al., 2016).

3.2.2.2.1 NA Structure

NA is present in influenza virus A and B whereas the enzyme is non-present in influenza C virus (Jagadesh et al., 2016). The structure of NA on the viral surfher iace consists of four identical subunits, which form a homo-tetramer of a mushroom-like shape with four catalytic domains on its head, whereas the stem is formed by the N-terminal sequences of the subunits. In the centre of each subunit the catalytic active site is located (Grienke et al., 2012). In addition, the surface loops which surround the active site carry the antibody-binding sites (Jagadesh et al., 2016), which is shown in Figure 5.

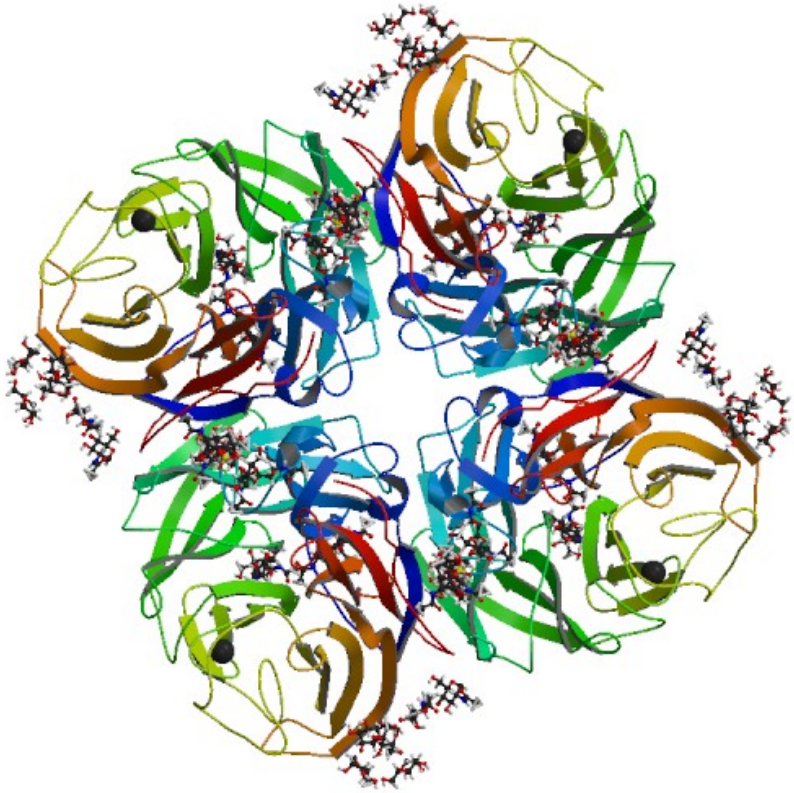

Figure 5 - Three-dimensional structure of the neuraminidase of influenza virus A/Tokyo/3/67 at 2.2 A resolution; (rcsb.org; Accessed: August 2016)

3.2.2.2.2 Neuraminidase

NA as well as HA are capable of recognizing carbohydrate structures and are able to bind to terminal sialic acid (receptor) on the surface of the host cell. After binding to the receptor, HA facilitates the viral entry in the host cell, such as NA, which additionally has an impact on virus spread in the infected tissue. NA is also capable on cleaving the glycan structure of mucus and therefor is able to increase the agility of influenza virus in the respiratory tract (Grienke et al., 2012). There is evidence that NA facilitates the HA fusion and increases the virus spread in the epithelium of the human respiratory tract. It was shown that the antigenic drift of NA appears at a slower rate than in HA, which emphasizes that NA antibodies are capable of long-term protection. Thus, NA represents an interesting target for the treatment of influenza viruses (Jagadesh et al., 2016).

4 RESULTS AND DISCUSSION

4.1 Generation of an Extraction Protocol with ASE for non-polar Triterpenes for Subsequent Separation with SFC

4.1.1 Preliminary Tests and Optimization

Both, the preliminary tests and the further optimization of the ASE were performed with the fruit bodies of the fungus *G. lucidum*, as we had a lot of source material enabling extensive experiments beforehand. The so performed extractions were subsequently examined with TLC as well as Dionex High Performance Liquid Chromatography (HPLC) connected to a Charged Aerosol Detector (CAD) to ensure that the chosen changes of parameters would lead to an enrichment of triterpenes in the focussed polarity range. The detailed process of the preliminary tests as well as the labelling of the mushroom samples is described in Chapter 6.3.4, Page 49.

After finding an appropriate extraction method with the ASE based on *G. odoratum*, 10 different mushroom species including different strains thereof (30 in sum) were extracted with the generated protocol in order to obtain the contained non-polar triterpenes. Figure 6 gives an overview of the developed extraction scheme.

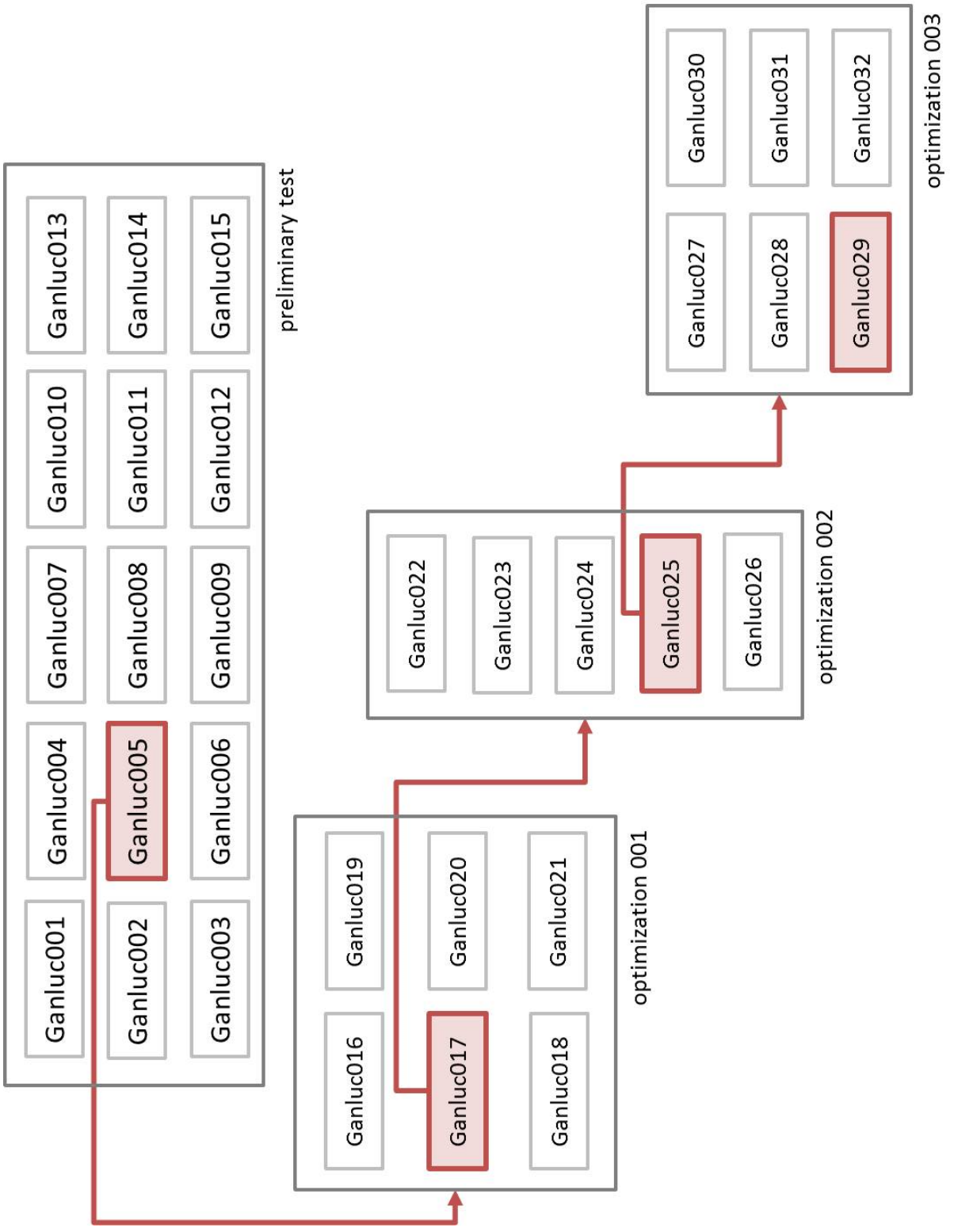

Figure 6 – Extraction scheme of *G. lucidum* with ASE

After finding an appropriate method for the extraction of non-polar triterpenes (see Table 2), the fruit bodies of the following mushroom species and their corresponding strains were investigated for their secondary metabolite profile (see Table 3).

Table 2 - Final parameters for ASE extraction

Ganluc029			
preheat (min)	5	pressure (psi)	1450
heat (min)	6	temp. (°C)	125
static (min)	5	solvent A (%)	-
flush (%)	90	solvent B (%)	-
purge (sec)	60	solvent C (%)	PE (100)
cycles	3	solvent D (%)	-

Since there were different strains of various species available, the point of interest was to compare the samples by chromatographic methods to receive insights into possible variations of the secondary metabolite profile. Therefore 3 g ground mushroom material of each strain was extracted once with 100 % PE (extract A) and afterwards the same sample was extracted with 100 % MeOH (extract B) in order to see differences in the secondary metabolite profile after the PE extraction. In addition, another 3 g fresh mushroom material was extracted with 100 % MeOH (extract C). In total, 3 different extracts (A, B and C) per strain were produced in small scale with ASE (Figure 7).

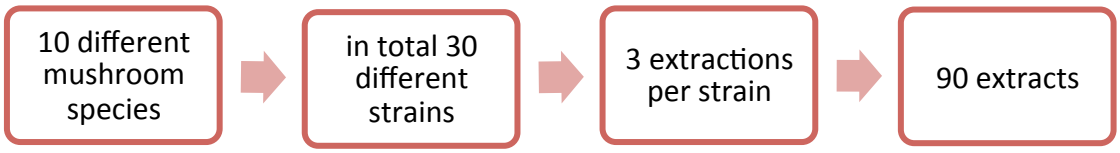

Figure 7 - Workflow mushroom extractions

4.1.2 Extraction of Mushroom Species with ASE

The 30 fruit bodies of local Tyrolean mushroom species and strains were obtained from a collaboration partner at the Institute of Microbiology of the University of Innsbruck, Austria. PE and MeOH extracts were produced in small scale with ASE. In Table 3 all mushroom species are listed with full name and labels for the raw material of the various strains. Detailed information of the various mushroom species is given in Chapter 6.1.

Table 3 - Mushroom species for ASE extraction

Genus/Species	Label
Fomes fomentarius(L.) Fr.	Fomfom0011
	Fomfom0016
	Fomfom0019
	Fomfom0022
	Fomfom0033
Fomitopsis pinicola(Sw.) P. Karst.	Fompin0010
	Fompin0013
	Fompin0015
	Fompin0018
	Fompin0021
	Fompin0024
	Fompin0026
	Fompin0030
	Fompin0037
	Fompin0040
	Fompin0053
	Fompin00374
	Fompin00442
Ganoderma applanatum(Pers.) Pat.	Ganapp0012
Ganoderma lucidum(Curtis) P. Karst.	Ganluc0027
	Ganluc0032
Gloeophyllum odoratum(Wulfen) Imazeki	Gloodo0023
	Gloodo0028
	Gloodo0054
Ischnoderma benzoinum(Wahlenb.) P. Karst.	Isben0038
Laetiporus sulphureus(Bull.) Murrill	Laesul0043

Phellinus robustus(P. Karst.) Bourdot & Galzin	Pherob0025
Genus/Species	**Label**
Phellinus robustus(P. Karst.) Bourdot & Galzin	Pherob0025
Piptoporus betulinus(Bull.) P. Karst.	Pipbet0029
	Pipbet0039
Trametes gibbosa(Pers.) Fr.	Tragib0052

After the extraction with ASE was performed, the extracts were transferred from ASE vials in round bottom flasks in order to reduce the solvent volume on the rotary evaporator. Therefore the PE extracts were transferred with DCM, whereas the MeOH extracts were transferred with MeOH: after the extract was evaporated to total dryness, each extract residue was resolved in 6.0 ml solvent and sonicated, in detail: each PE extract was resolved with 6.0 ml DCM, each MeOH extract with 6.0 ml MeOH. Of each resolved extract 100 µl were taken, using an Eppendorf-pipette, and transferred in prelabelled HPLC vials. In a next step the 100 µl of the transferred PE extract was diluted with ACN (for analysis); the 100 µl of the transferred MeOH extract was diluted with MeOH (for analysis). The residual extract in the round bottom flask was then transferred to pre-labelled and pre-weighed glass vials for solvent evaporation and for storage. As the HPLC vials of all extracts were prepared in the exact same way, a qualitative as well as quantitative investigation of the secondary metabolite profile with HPLC-CAD and SFC was possible in order to compare all mushroom strains. Another point of interest was to figure out what differences an extraction with MeOH after PE extraction in comparison with the plain MeOH extraction (extract C) makes. The chosen parameters for HPLC-CAD are given in Chapter 6.3.3, Page 49.

It was shown that there are differences between the different mushroom strains of the same species despite the fact that all of the extracts were produced with the same parameters in exactly the same way, e.g. Fompin0053 (see Figure 8): The comparison of the different extracts A, B and C shows that PE as solvent only extracts the non-polar compounds (Figure 8, A; retention time between 20.0 – 60.0 min), whereas an extraction with MeOH extracts both, the polar as well the non-polar compounds (Figure 8, C). In addition, it was shown that an extraction with MeOH after PE extraction mainly extracts the polar compounds since the non-polar compounds were already extracted with PE before (Figure 8, B; retention time

between 0.0 – 5.0 min). This gives also information about the quality and effectiveness of the ASE extraction method, as almost the whole spectrum of the non-polar compounds was extracted in the first step. In the Appendix all of the further chromatograms are shown.

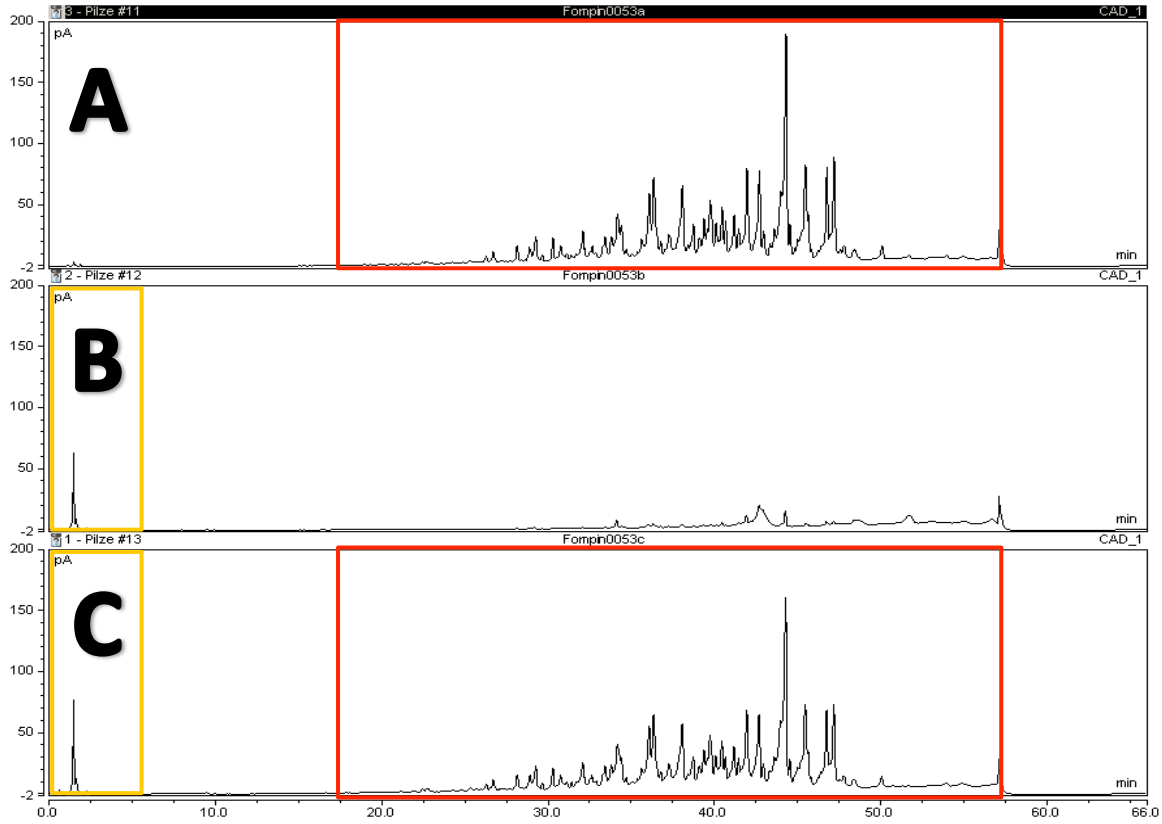

Figure 8- HPLC-CAD chromatogram Fompin0018 A-C; A: PE extract; B: MeOH extract after PE extraction; C: only MeOH extract with fresh mushroom material

4.1.3 TLC of MeOH Extracts

The MeOH extracts (extract C) of the different mushroom strains were also investigated with a collective TLC-analysis as it shows the whole spectrum of the containing secondary metabolites. 3 µl of each HPLC vial of the extracts were applied. Out of all *F. pinicola* strains only Fompin0010, Fompin0018 and Fompin0021 show a blue spot “a” (Figure 9). It is also evident that spot “b” is only present in seven *F. pinicola* strains. TLC parameters are described in Chapter 6.3.2, page 48.

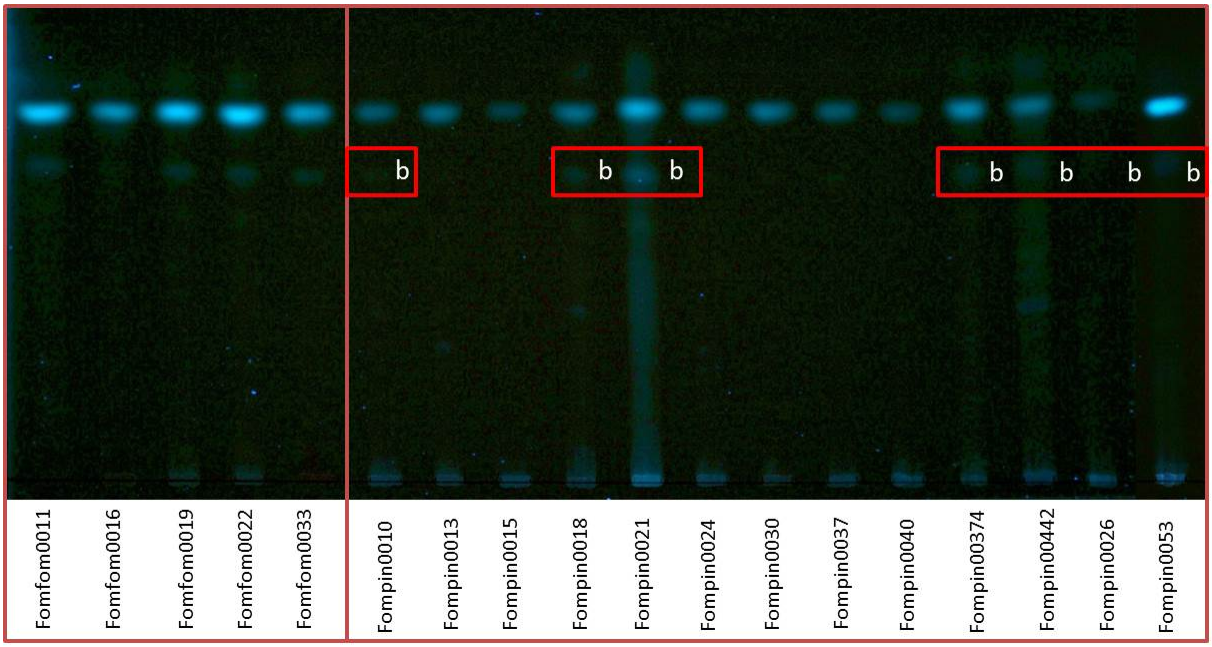

Figure 9 – Collective TLC-analysis of the MeOH extracts C from the mushroom samples Fomfom0011 – Fompin0053; detection at 366 nm

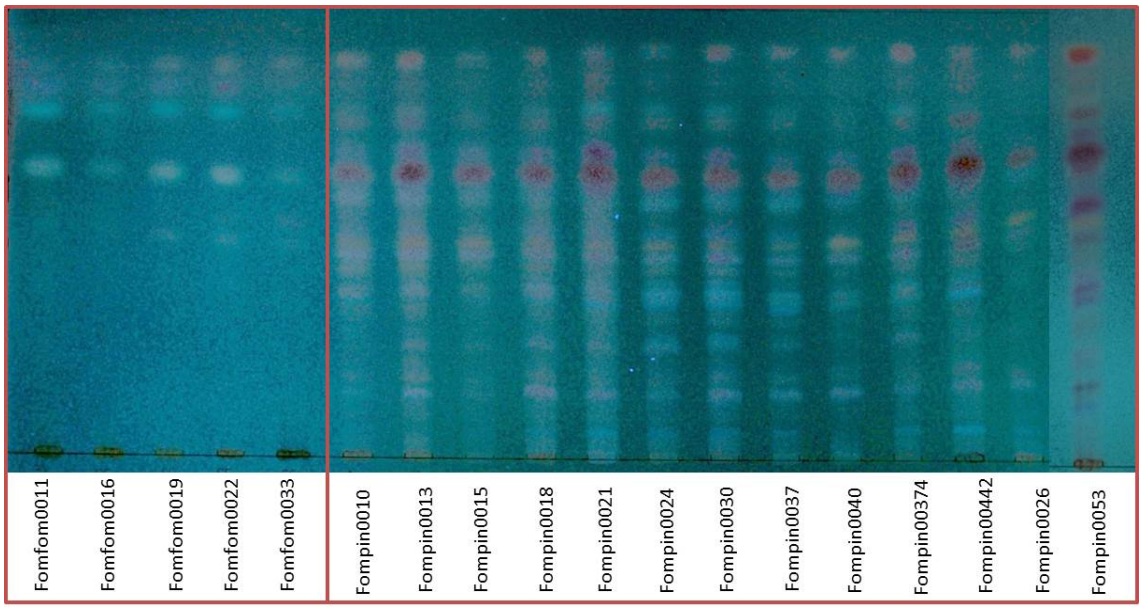

Figure 10 – Collective TLC-analysis of the MeOH extracts C from the mushroom samples Fomfom0011 – Fompin0053; detection in 366 nm after using spraying reagent Vanillin/H_2SO_4

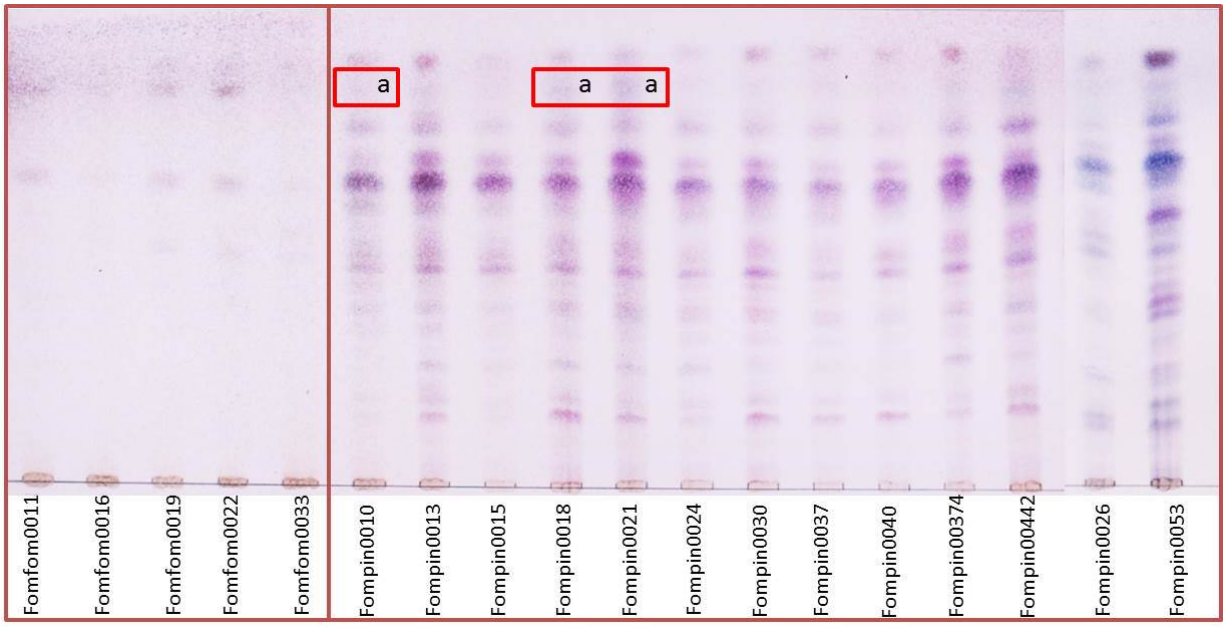

Figure 11 – Collective TLC-analysis of the MeOH extracts C from the mushroom samples Fomfom0011 – Fompin0053; detection in VIS after using spraying reagent Vanillin/H_2SO_4.

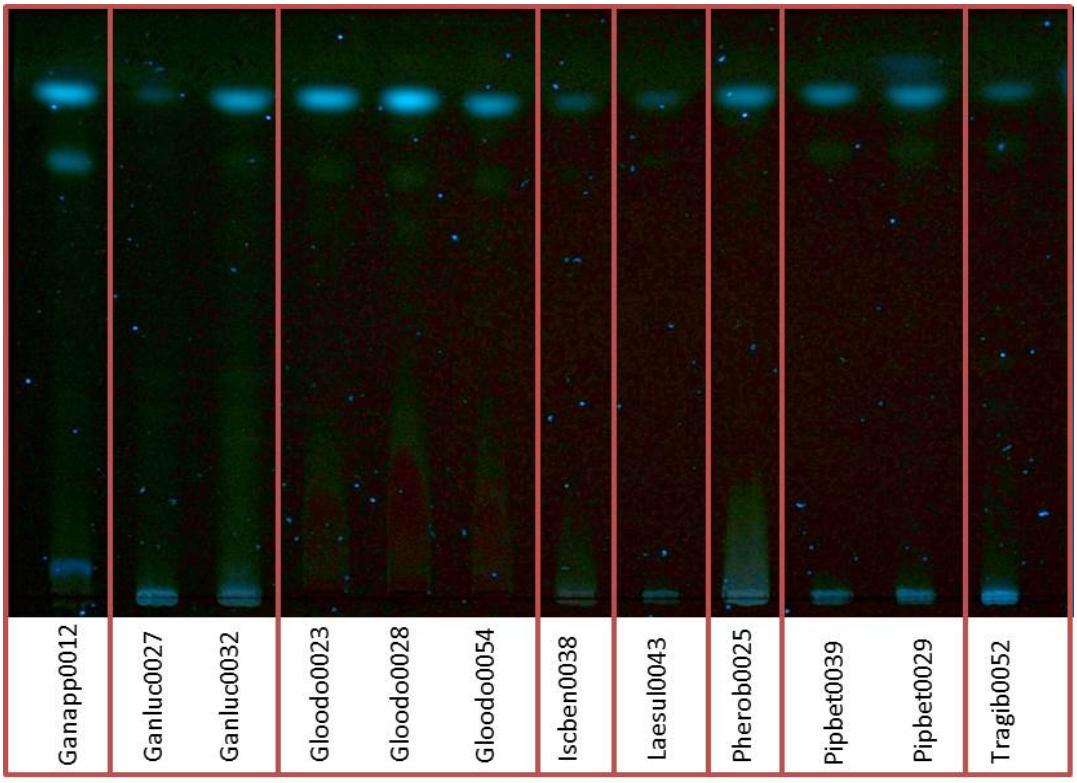

Figure 12 - Collective TLC-analysis of the MeOH extracts C from the mushroom samples Ganapp0012 – Tragib0052; detection at 366 nm

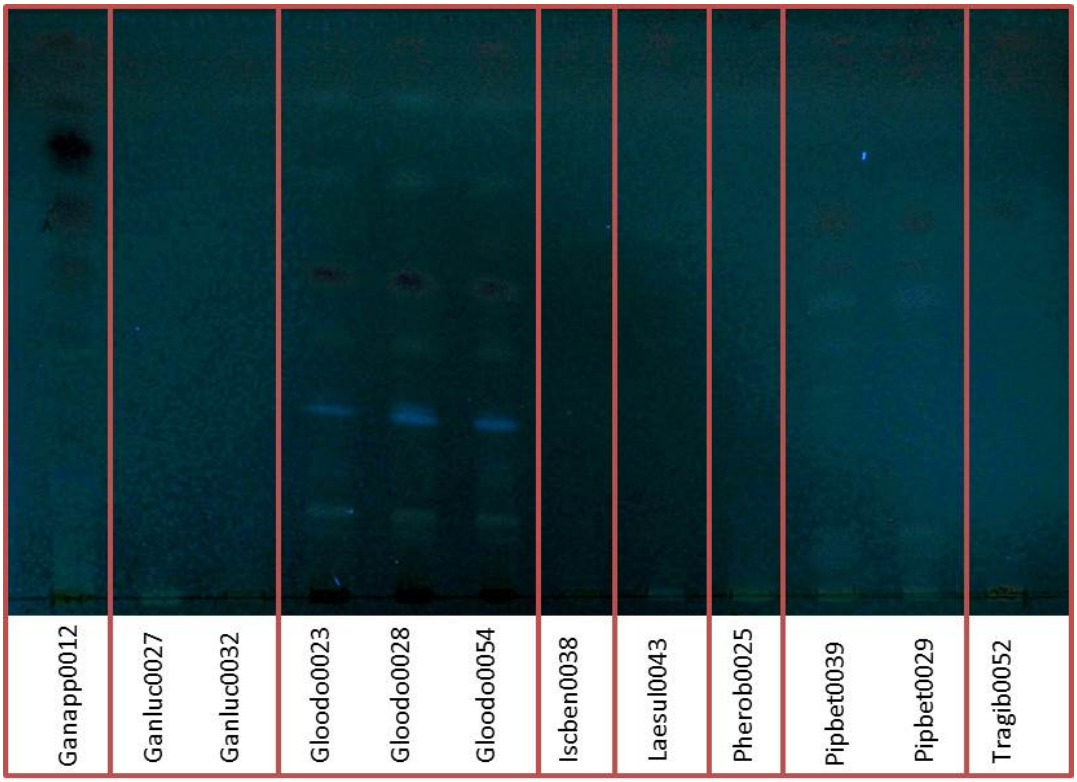

Figure 13 - Collective TLC-analysis of the MeOH extracts C from the mushroom samples Ganapp0012 – Tragib0052; detection in 366 nm after using spraying reagent Vanillin/H_2SO_4

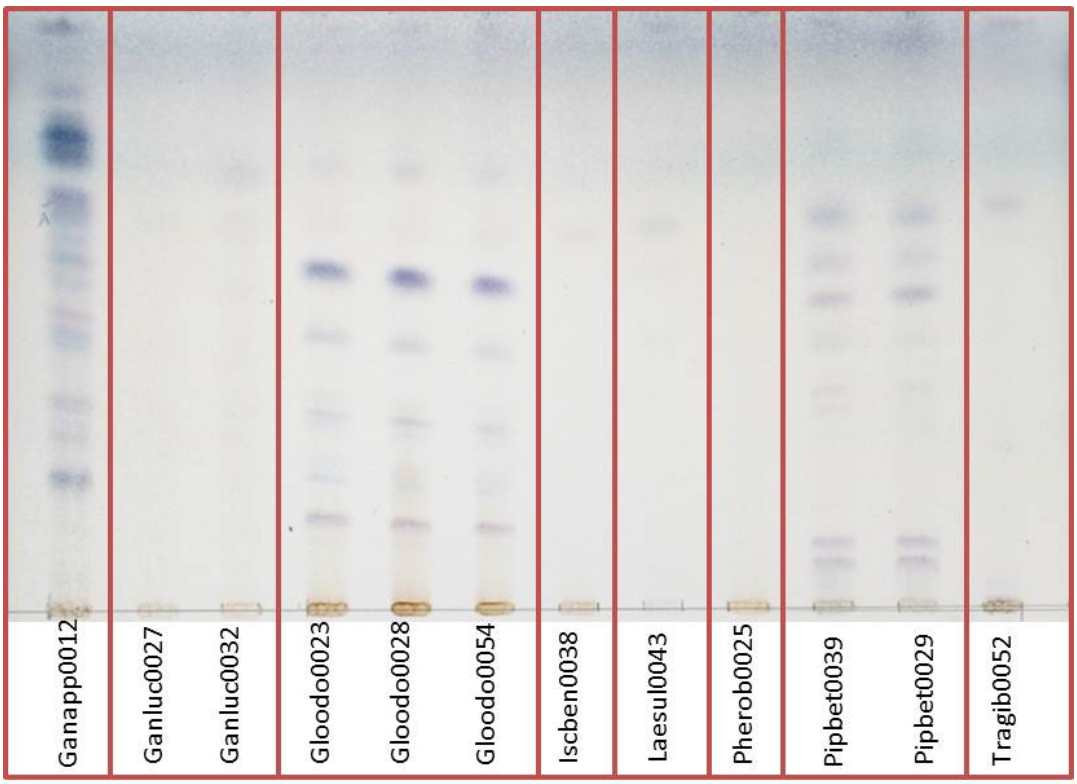

Figure 14 - Collective TLC-analysis of the MeOH extracts C from the mushroom samples Ganapp0012 – Tragib0052; detection in VIS after using spraying reagent Vanillin/H_2SO_4

4.1.4 Further Separation of the non-polar Triterpenes with SFC

All of the PE extracts (A) were then separated with preparative SFC in order to see further differences in the secondary metabolite profile and to distinguish the various mushroom strains of each species in detail. Therefore a Waters Prep 15 SFC Purification System was used. The chosen parameters for SFC are given in 6.3.7, Page 60. To exemplify, in Figure 15 it is shown that there are differences in the metabolite profile of 3 different strains of the same species of *F. pinicola* (Figure 15, A: Fompin0021a, B: Fompin0024a, C: Fompin0026a). This was obvious for all of the investigated mushroom species as well as their different strains. The mushroom samples have been injected quantitatively. All further SFC chromatograms are attached in the Appendix (see 8.1.3, Page 114).

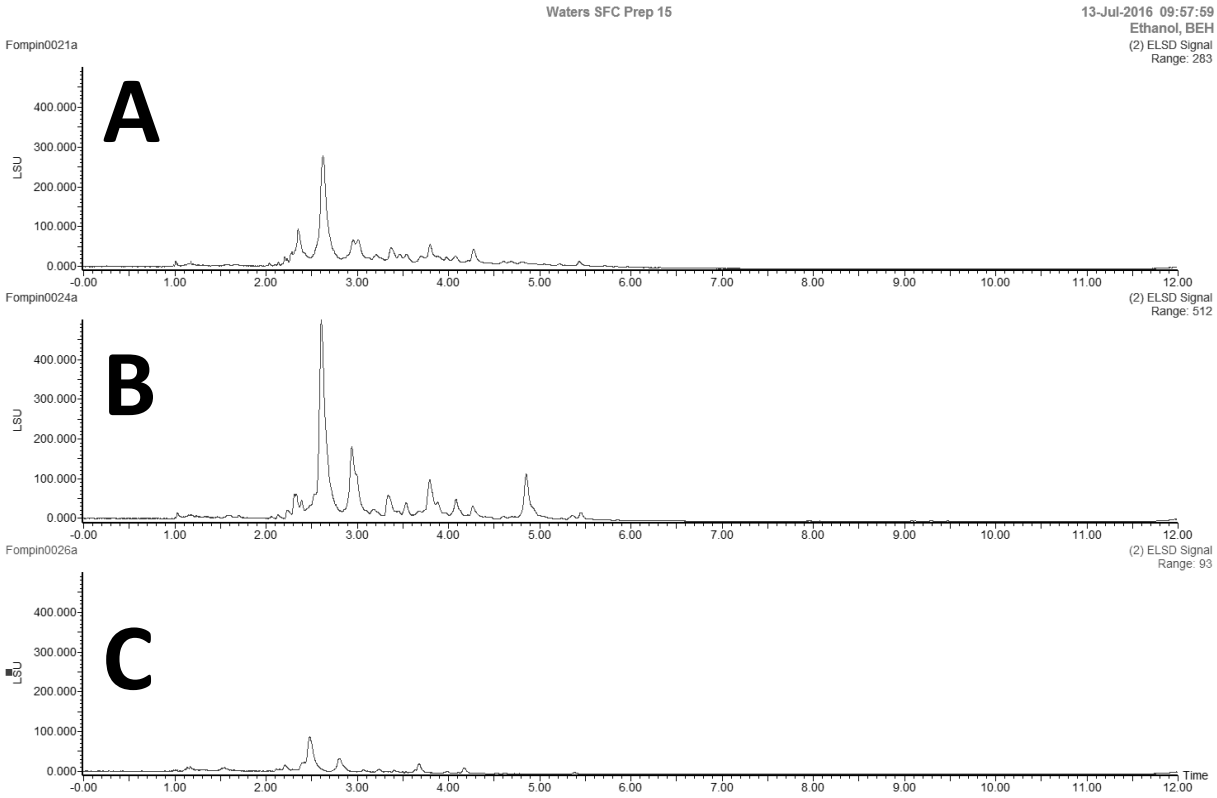

Figure 15 – SFC chromatogram of *F. pinicola* strains A: Fompin0021a, B: Fompin0024a, C: Fompin0026a; ELSD signals

4.2 Purification of Selected Fractions of *Gloeophyllum odoratum*

4.2.1 Workflow

Bioactivity tests of several mushroom strains were performed previously. Strain GO0054 of the polypore *G. odoratum* showed the best results according to STS inhibition and NA inhibition. Therefore the extraction and isolation of constituents from this strain was of high interest. Previous diploma students performed the following steps (see Figure 16): the ground fruit body of *G. odoratum* (GO0054) was extracted with EtOH, resulting in the ethanolic extract GO54E which showed both, NA and STS inhibition. Several fractionation steps with solvents of different polarity were performed, of which the DCM fraction (GO54ED) showed the highest STS inhibition. Therefore silica gel column chromatography had been performed with the DCM fraction GO54ED, resulting in 14 fractions, among them the fractions GO01_09 (9^{th} fraction) and GO01_12 (12^{th} fraction). The 9^{th} fraction had been further separated resulting in the fractions GO10_01, GO10_02, GO12_04 and GO15_01, which contained 2 compounds each. Within this thesis I aimed to isolate and identify the constituents from these fractions using different chromatographic steps. Whereas the 12^{th} fraction had been further purified resulting in the substance GO27_07, a single compound for which a purification step was still necessary.

At first, a separation with SFC was envisaged but it was not possible to separate the single compounds with this technique since the structural scaffolds were too similar. Therefore the separation with UHPLC was used and turned out to be the method of choice for the separation of the selected fractions of *G. odoratum*: due to higher system pressures in ultra-high pressure LC (15000 – 19000 psi), columns packed with smaller particles can be used for analysis resulting in superior separation of complex samples. Another big advantage of UHPLC is clearly the high throughput up to 10 fold in comparison to conventional HPLC by maintaining high resolution, rapid method development and thereby ensuing fast analysis. Consequently due to shorter analysis time significant solvent saving can be maintained (Dong, 2013) on the one side, but on the other side many runs must to be performed to separate the compounds as you can only inject little substance per run. Nevertheless the advantages outweigh the disadvantage since this was the only way for the separation and therefore isolation of the pure compounds.

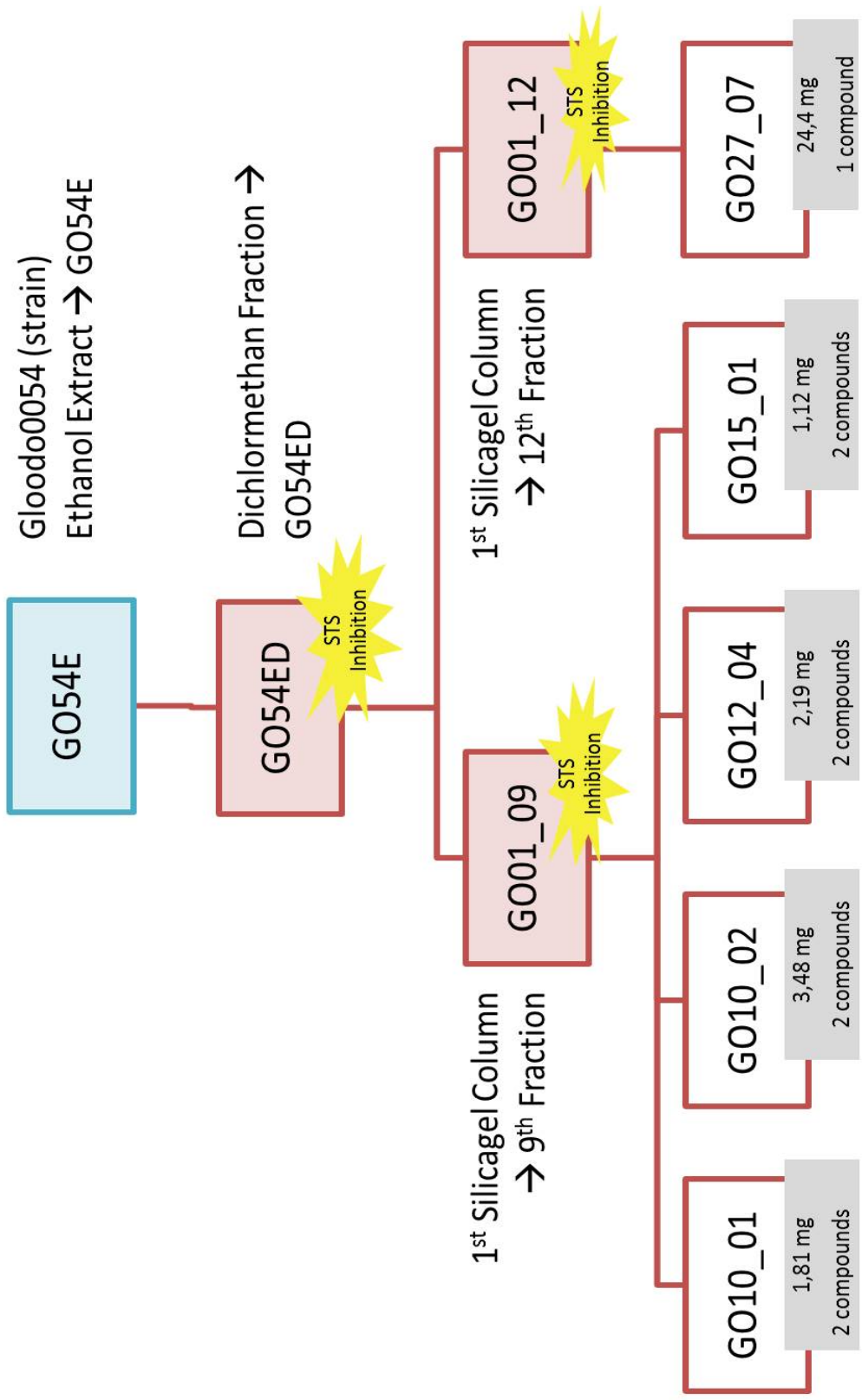

Figure 16 - Workflow *Gloeophyllum odoratum*

4.2.2 UHPLC Optimization of *Gloeophyllum odoratum* Extracts

For UHPLC optimization a small amount of each fraction, i.e. GO10_01, GO10_02, GO12_04, and GO15_01, respectively, was dissolved in MeOH. For the development of a suitable UHPLC method the following parameters were adjusted accordingly to evaluate performance of the best separation:

- Different columns:, BEH Phenyl 100 mm, BEH C18 100 mm, BEH C18 50 mm, HSS T3 100 mm, CSH C18 100 mm and CSH Fluoro-Phenyl 100 mm
- Gradients
- Injection volume
- Flow rate
- Detector: ELSD and PDA

Detailed information about all used parameters is given in Chapter 6.4.2, page 61. In this chapter all following UHPLC chromatograms show the PDA traces only, since the collection of peaks is only possible by triggering via the UV signal. Thankfully, the triterpenes present in the different fractions could be detected with both, ELSD and PDA (however not as good as ELSD).

4.2.3 Structure Elucidation and Identification of Pure Compounds

For structure elucidation, one-dimensional (^{1}H-NMR, ATP) and two-dimensional (HSQC, HMBC, HH-COSY and NOSEY) spectra have been recorded by Prof. Dr. Ernst Urban (Department of Pharmaceutical Chemistry, University of Vienna). Measurements were performed on a 500 MHz NMR instrument with cryo probe. The interpretation of the spectra was performed by my co-supervisor Dr. Ulrike Grienke. Spectral data of pure compounds is attached in the Appendix (see 8.2.1, Page 126). For the structure elucidation the chemical formula of the isolated pure compounds was ascertained by HRMS analysis, as ion trap measurements remained unsuccessful. HRMS analysis as performed by Dr. Martin Zehl (Department of Analytical Chemistry, University of Vienna) (see Table 4, page 29). HRMS parameters are attached in the appendix (see Chapter 8.2.2).

Table 4 - Molecular weight and chemical formula of isolated pure compounds

Fraction	Pure Compound	Substance Name	CAS Number	Molecular Weight	Chemical formula
GO12_04	GO36_01	21-Hydroxylanosterol	56362-97-1	442.34	$C_{30}H_{50}O_2$
	GO36_02	Eburicodiol	35241-56-6	456.40	$C_{31}H_{52}O_2$

4.2.3.1 GO12_04

Fraction GO12_04 was separated with UHPLC as described in Table 18 in Chapter 6.4.2. The resulting pure compounds were labelled GO36_01 and GO36_02, respectively (see Figure 17).

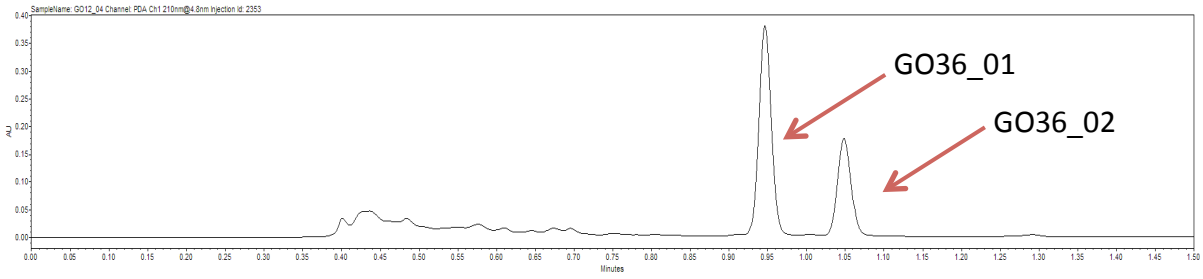

Figure 17 UHPLC chromatogram of fraction GO12_04 including compound GO36_01 and GO36_02; Channel: PDA 210 nm

Spectral data of both pure compounds is given in Chapter 6.4.3, Page 63. For NMR-analysis about 1 mg of both pure compounds was dissolved in MeOH-d4. GO36_01 could be identified as 21-Hydroxylanosterol, GO36_02 was identified as Eburicodiol (see Table 5). This is the first time these compounds were isolated from *G. odoratum*, but have already been reported as constituents in other mushrooms: 21-Hydroxylanosterol was already isolated from *Polyporus pinicola* (Sw.) Fr. [= *Fomitopsis pinicola* (Sw.) P. Karst.] (Carbide et al., 1961) and *Inonotus obliquus* (Ach. ex Pers.) Pilát (Taji et al., 2008), whereas Eburicodiol was already isolated from *Fomes officinalis* (Batsch) Bres. (Anderson et al., 1971), respectively.

Table 5 - GO36_01 and GO36_02

GO12_04				
Pure Compound	**CAS Number**	**Substance Name**	**Molecular Weight**	**Structure**
GO36_01	56362-97-1	21-Hydroxylanosterol	442.72	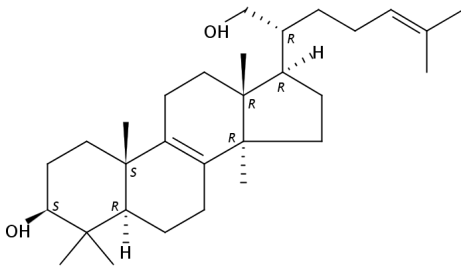
GO36_02	35241-56-6	Eburicodiol	456.74	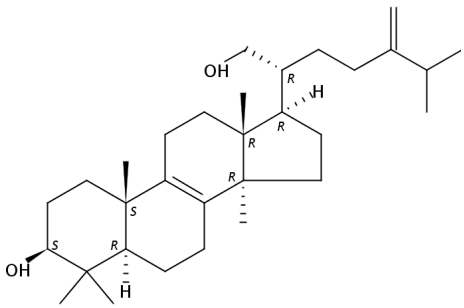

Table 6 - 1H and 13C NMR spectral data of GO54ED36_01

pos.	H	multiplicity (J [Hz])	δ H [ppm]	δ C [ppm]	δ C HMBC [ppm]	δ H COSY [ppm]	δ H NOESY [ppm]
24	1	t	5.12	126.2	-	2.07/1.96	
3	1	overlapped	3.16	79.6			1.22/1.06/ 0.99
21	1	d (J 10.7)	3.71	62.7		3.54/1.49	
	1	dd (J 4.9, 10.6)	3.54			3.71/1.49	
5	1		1.06	51.9			
17	1		1.88	45.7			
20	1		1.49	44.0			0.76
1	1		1.76	36.9			
	1		1.22				
15	1		1.66	31.9			0.76
	1		1.23				

pos.	H	multiplicity (J [Hz])	δ H [ppm]	δ C [ppm]	δ C HMBC [ppm]	δ H COSY [ppm]	δ H NOESY [ppm]
12	1		1.84	31.7		2.07	
	1		2.07			1.84	0.76
16	1		1.29	30.7			
	1		1.38				
22	1		1.38	30.7			
	1		1.48			2.07	
7	2		1.36	28.5			
28	3		0.99	28.6	79.6/51.9/39.9/16.1		
2	2		2.01	27.6	-	-	
27	3		1.67	25.9	131.8/126.2/17.7		
23	1		2.07	25.7	-	5.12/1.96/1.48	
	1		1.96		-	5.12/2.07	
30	3		0.92	24.6	135.7/51.0/45.5/31.9		
6	2		2.07	22.1	-		
19	3		1.02	19.6	136.0/51.9/38.2/36.9		
11	1		1.55	19.4	-	2.07	
	1		1.73		-	2.07	
26	3		1.62	17.7	131.8/126.2/25.9		
18	3		0.76	16.6	51.0/45.5/31.7/45.7		
29	3		0.81	16.1	79.6/51.9/39.9/28.6		
9	-	-	-	136.0	-	-	
8	-	-	-	135.7	-	-	
25	-	-	-	131.8	-	-	
14	-	-	-	51.0	-	-	
13	-	-	-	45.5	-	-	
4	-	-	-	39.9	-	-	
10	-	-	-	38.2	-	-	

Table 7 - 1H and 13C NMR spectral data of GO54ED36_02

pos.	H	multiplicity (J [Hz])	δ H [ppm]	δ C [ppm]	δ C HMBC [ppm]	δ H COSY [ppm]	δ H NOESY [ppm]
3	1	overlapped	3.16	79.6			
21	1	d (J 10.7)	3.71	62.7		3.54/1.49	0.98/1.05
	1	dd (J 4.9, 10.6)	3.54			3.71/1.49	
5	1		1.06	51.9			
17	1		1.88	45.7			
20	1		1.49	44.0			
1	1		1.76	37.0			
	1		1.25				
23	1		2.15	32.2			
	1		1.99				
15	1		1.66	31.9			
	1		1.24				
12	1		1.66	31.7		2.07	
	1		1.85			1.84	
22	1		1.48	29.5			
	1		1.62				
7	2		1.63	28.5			
16	1		1.42	28.6			
	1		1.96				
28	3		0.99	28.6	79.6/51.9/39.9/16.1		
2	2		2.08	27.6	-	-	
30	3		0.92	24.6	135.7/51.0/45.5/31.9		
6	2		2.07	22.1	-		
19	3		1.02	19.6	136.0/51.9/38.2/36.9		
11	1		1.55	19.4	-	2.07	
	1		1.73		-	2.07	
18	3		0.76	16.6	51.0/45.5/31.7/45.7		1.49/1.66/ 2.07
29	3		0.81	16.1	79.6/51.9/39.9/28.6		
9	-	-	-	136.0	-	-	
8	-	-	-	135.7	-	-	
14	-	-	-	51.0	-	-	
13	-	-	-	45.5	-	-	

pos.	H	multiplicity (J [Hz])	δ H [ppm]	δ C [ppm]	δ C HMBC [ppm]	δ H COSY [ppm]	δ H NOESY [ppm]
4	-	-	-	39.9	-	-	
10	-	-	-	38.2	-	-	
27	3		1.04	22.3	34.9/157.7/22.5		
26	3		1.04	22.5	34.9/157.7/22.3		
24[1]	1		4.73	107.0	32.1/34.9		
	1		4.70		32.1/34.9		
25	1		2.27	34.9			
24	-	-	-	157.7	-	-	

4.2.3.2 GO10_01

The used method for the separation of the fraction GO10_01 with UHPLC is shown in Table 19 in Chapter 6.4.2. The corresponding UHPLC Chromatogram is given in Figure 18. The resulting pure compounds were labelled GO37_01 and GO37_02. For NMR-analysis both pure compounds were dissolved in $CDCL_3$. Unfortunately the separated amount of both pure compounds was not enough for NMR analysis - no signals were recorded. Nevertheless, previous NMR analysis of the mixture GO10_01 allowed for the structure elucidation of the containing compounds: GO37_01 is a new compound, whereas GO37_02 could be identified as a triterpene acid, which is also new for *G. odoratum*. Detailed information is shown in Table 8.

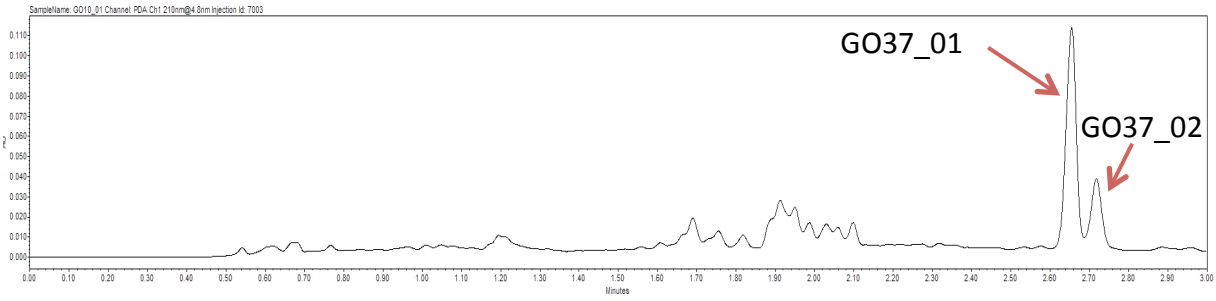

Figure 18 - UHPLC chromatogram of fraction GO10_01 including compound GO37_01 and GO37_02; Channel: PDA 210 nm

Table 8 - GO37_01 and GO37_02

GO10_01				
Pure Compound	**CAS Number**	**Substance Name**	**Molecular Weight**	**Structure**
GO37_01	NEW	NEW	426.60	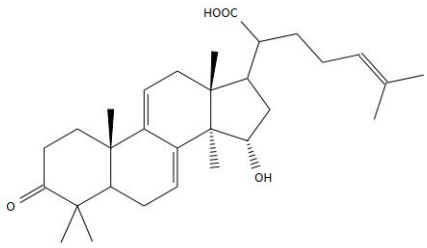
GO37_02	862109-75-9	(15α)-15-hydroxy-3-oxo-Lanosta-8, 24-dien-21-oic acid	470.68	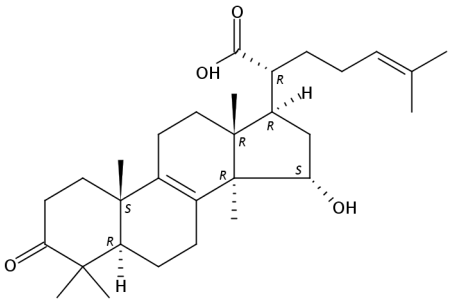

4.2.3.3 GO10_02

Fraction GO10_02 was also separated with UHPLC (see Figure 19). The used method is shown in Table 20, Chapter 6.4.2. For NMR-analysis both pure compounds were dissolved in $CDCL_3$. Again, the amount of both pure compounds was not enough for NMR analysis - no signals were recorded. A previous NMR analysis of fraction GO10_02 has shown the containing compounds: Both, GO38_01 and GO38_02 are new for *G. odoratum*. Detailed information is shown in Table 9.

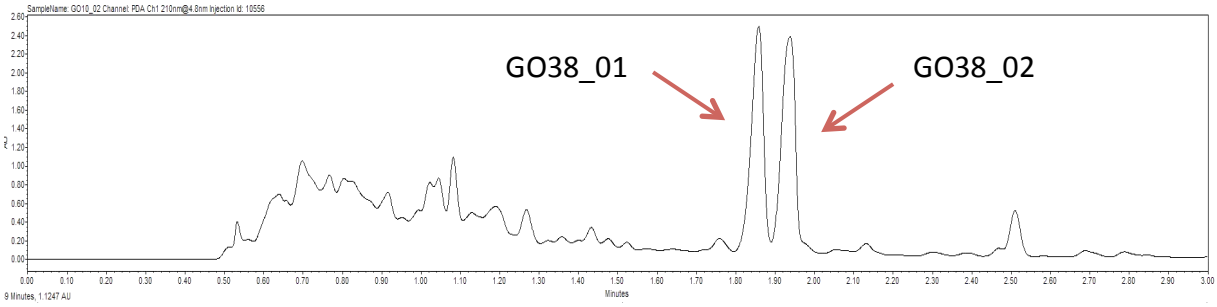

Figure 19 - UHPLC chromatogram of fraction GO10_02 including compound GO38_01 and GO38_02; Channel: PDA 210 nm

Table 9 - GO38_01 and GO38_02

GO10_02				
Pure Compound	**CAS Number**	**Substance Name**	**Molecular Weight**	**Structure**
GO38_01	38611-64-2	3-Ketodehydrosulfurenic acid	482.69	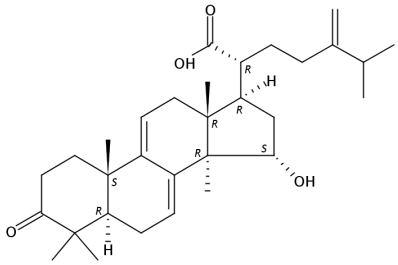
GO38_02	823202-91-1	Fomefficinic acid D	484.71	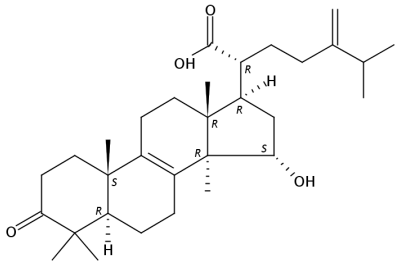

4.2.3.4 GO27_07

An NMR analysis of the fraction GO27_07 turned out to be identical with the previous isolated pure compound GO33_03, which was elucidated as Gloeophyllin A before (see Table 10). Again, the compound Gloeophyllin A has never been isolated from *G. odoratum* before.

Table 10 - GO27_07

GO27_07				
Pure Compound	**CAS Number**	**Substance Name**	**Molecular Weight**	**Structure**
GO27_07 = GO33_03	1709833-88-4	Gloeophyllin A	454.68	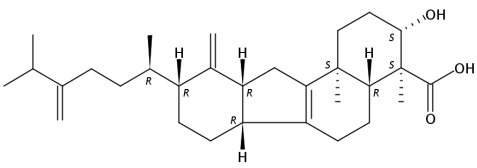

4.2.3.5 GO15_01

Unfortunately it was not possible to separate fraction GO15_01 due to scant time and the fact that there were only 1.12 mg left. No separation and structure elucidation was done. In Figure 20 an UHPLC chromatogram of Fraction GO15_01 is shown.

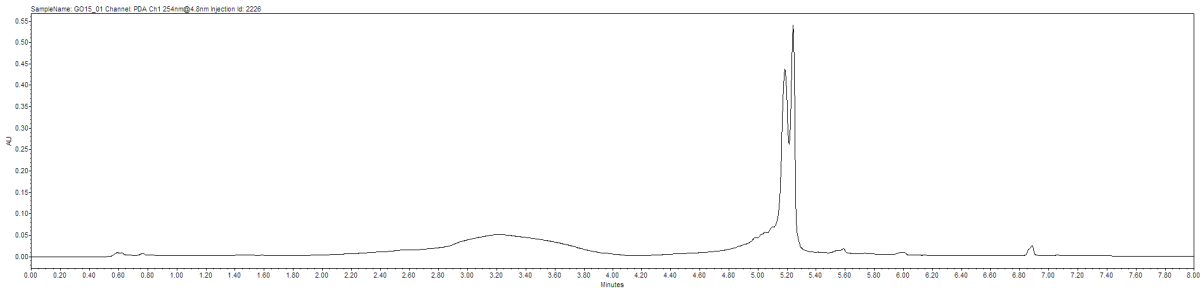

Figure 20 - UHPLC-chromatogram of fraction GO15_01 with the compounds of interest for separation: PDA 254 nm

4.2.4 Bioactivity Investigations of Pure Compounds

After the separation of the selected fractions of *G. odoratum* was finished, collaboration partners in the UK and Germany performed *in vitro* bioactivity tests. During this thesis, Fraction GO12_04 was separated in its pure compounds GO36_01 and GO36_02, whereas Fraction GO10_02 was separated in its pure compounds GO38_01 and GO38_02, respectively. As the amount of the fraction GO10_01, separated in GO37_01 and GO37_02 was not enough for NMR analysis, these two pure compounds were not tested for its bioactivity, as well as Fraction GO15_01, which could not be separated at all with UHPLC. This means that 4 pure compounds were obtained within this diploma thesis. Since other diploma students managed to isolate further compounds before, a set of 11 pure compounds, 1 mixture (GO54-E), the ethanolic extract (GO54E) as well as the DCM fraction of the ethanolic extract (GO54ED) was tested for its bioactivity. The 11 pure compounds and the mixture GO54-E were prepared and sent as Stock Solutions (SSo) in DMSO. The collaboration partner in the UK tested all of the 14 samples on STS inhibition, whereas the collaboration partner in Germany tested only 12 of the samples on NA inhibition, due to the fact that the amount of GO38_01 and GO38_02 was not enough for both bioactivity test systems. Since each partner performs different bioactivity tests, a mixed pool of information has been collected.

In order to facilitate the testing of these samples, an additional labeling for all of the samples was invented. Detailed information of the samples, CAS-Number, class, molecular weight and executed bioactivity test system is given in Table 11. Results for STS inhibition are shown in chapter 4.2.4.1 and for NA inhibition in chapter 4.2.4.2, respectively.

Table 11 - Samples for bioactivity tests

Code	Fraction	Substance	CAS Number	Class	Molecular Weight	Bioactivity Tests
GO54-A	GO54ED01_10_r	Trametenolic Acid B	24160-36-9	Triterpene Acid	456.70	STS / NA
GO54-D	GO54ED25_02	3-O-Acetyl-15α,26-dihydroxytrametenolic acid	new	Triterpene Acid	530.00	STS / NA
GO54-E	GO54ED23_01	(3β)-3-Hydroxy-lanosta-8,24-dien -21-oic acid : (3β)-3-Hydroxy-24-methylene-lanost-8-en-21-oic acid	24160-36-9 : 560-66-7 (53:47)	Triterpene Acids + Phtalat?	456.7 470.73	STS / NA
GO54-H	GO54ED19_02	Diastereomere of GO54-A		Polymer?	?	STS / NA
GO54-I	GO54ED31_02	Gloeophyllin B	1660105-49-6	Triterpene Acid	514.37	STS / NA
GO54-J	GO54ED32_02	Derivative of Gloeophyllin A	new	Triterpene Acid	440.33	STS / NA
GO54-K	GO54ED33_03	Gloeophyllin A	1709833-88-4	Triterpene Acid	454.68	STS / NA
	= **GO54ED27_07**					
GO54-L	GO54ED34_17	Ergosterol Peroxide	2061-64-5	Triterpene	428.33	STS / NA
***GO54-M**	**GO54ED36_01**	21-Hydroxylanosterol	56362-97-1	Triterpene	442.34	STS / NA
***GO54-N**	**GO54ED36_02**	Eburicodiol	35241-56-6	Triterpene	456.74	STS / NA
***GO54-O**	**GO54ED38_01**	3-Ketodehydrosulfurenic acid	38611-64-2	Triterpene	482.69	only STS
***GO54-P**	**GO54ED38_02**	Fomefficinic acid D	823202-91-1	Triterpene	487.71	only STS

*isolated in the frame of this diploma thesis

4.2.4.1 STS Inhibition

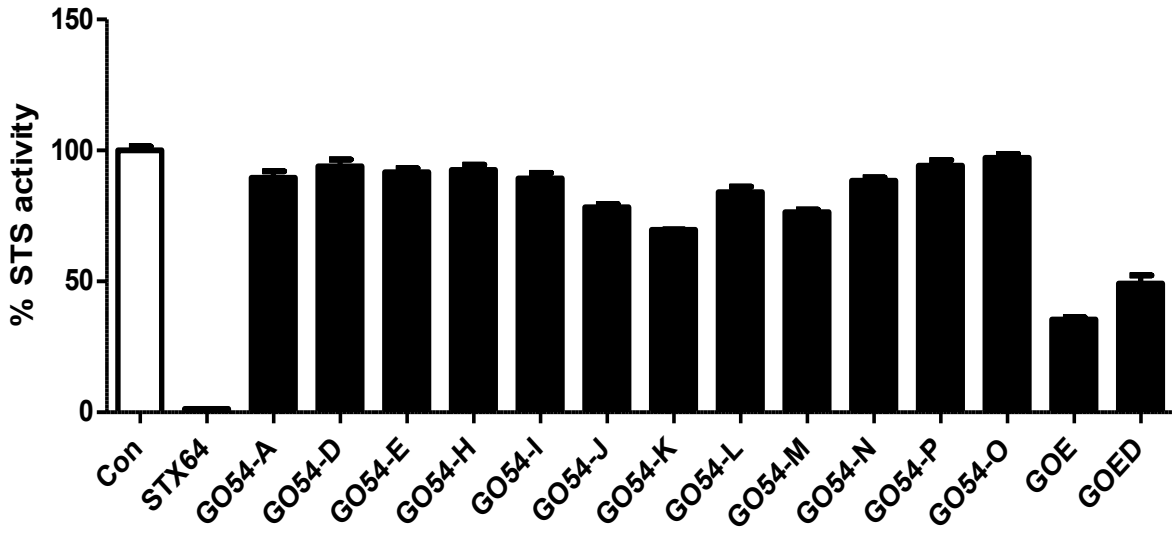

Figure 21 - STS enzyme activity after treatment with STX64 as positive control and *G. odoratum* samples GO54-A to -O, GOE and GOED

STS activity was confirmed by a STS assay, using STX64 as positive control, which is also known as Irosustat or 667 Coumate (CAS Registry Number 288628-05-7; Scifinder). This coumarin sulfamate has been reported as potent and successful STS inhibitor (Purohit, 2012). The STS bioactivity testing was performed by Dr. Paul A. Foster and his team at the University of Birmingham, UK. Results are shown in Figure 21: to evaluate the STS activity, the activity of each sample was expressed as a percent activity value (% STS activity) relative to the negative control (Con). Unfortunately none of the 12 isolated compounds GO54-A to GO54-O decreased the STS activity significantly. In addition to these 12 samples, the ethanolic extract of *G. odoratum* (GOE) and the dichlormethan fraction thereof (GOED) were also tested for their activity. Interestingly the STS inhibition of GOE was higher than the STS inhibition of GOED, suggesting that the active compounds are not enriched in the dichlormethan fraction of the ethanolic extract of *G. odoratum*. Investigations concerning the isolation and identification of the active compounds in GOE are ongoing.

4.2.4.2 NA Inhibition

compound		50% cytotoxic concentration		50% inhibitory concentration IAV HK/68		IAV Jena/8178	
		mean	SD	mean	SD	mean	SD
GO54- A	µM	>100		14,11	4,47	25,23	20,86
GO54- D	µM	>100		n.a.		46,42	8,61
GO54- E	µM	**>100**		**16,72**	11,36	**8,98**	4,20
GO54- H	µM	>100		77,82	12,19	24,63	9,14
GO54- I	µM	35,52	6,88	n.a.		n.a.	
GO54- J	µM	45,48	7,55	n.a.		n.a.	
GO54- K	µM	17,76	1,69	n.a.		n.a.	
GO54- L	µM	7,31	3,54	n.a.			
GO54- M	µM	>100		34,49	9,39	8,98	1,67
GO54- N	µM	>100		31,17	14,61	18,99	4,05
Osel	µM			0,004	0,005	0,076	0,016

Figure 22 - Neuraminidase bioactivity results after treatment with Oseltamivir (Osel) as positive control and *G. odoratum* samples GO54-A to –N

NA activity was confirmed by a NA assay, using Oseltamivir (Osel) as positive control, which is also known as Enfluvir or Tamiflu (CAS Registry Number 196618-13-0; Scifinder). This antiviral agent has been reported as potent and successful NA inhibitor, which interferes with the influenza virus release from the infectious host cell (Moscona, 2005). The NA bioactivity testing was performed by Dr. Michaela Schmidtke and her team of the Department of Virology and Antiviral Therapy (IVAT), Friedrich Schiller University Jena, Germany. Results are shown in Figure 22: Whereas GO54-I, GO54-J, GO54-K and GO54-L show cytotoxic effects against Mardin-Darby canine kidney (MDCK) II cells, GO54-A, GO54-D GO54-E, GO54-H as well as GO54-M and GO54-N show no cytotoxicity against MDCK II cells. In addition to the cytotoxic effect of GO54-I, GO54-J, GO54-K and GO54-L, these compounds show no activity against IAV (Influenza A virus) HK/68 and IAV Jena/8179. On the contrary the samples GO54-A, GO54-E, GO54-H as well as GO54-M and GO54-N show activity against both IAV HK/68 and IAV Jena/8179, whereas GO54-D is only active against IAV Jena/8178. Especially GO54-E, the only sample consisting of a mixture of two compounds, shows the most potent activity against both influenza virus strains.

4.2.5 Specific Optical Rotation of Pure Compounds

Optical rotation is the ability of chiral substances to rotate the plane of polarisation of polarised light. There are those compounds that rotate the plane of polarisation in a clockwise direction, considered to be postitive (+) dextrorotatory substances, and negative (-) laevorotatory substances that rotate the plane of polarisation counterclockwise. In addition, the specific optical rotation $[\alpha]_{\mathrm{D}}^{20}$ of substances in solution is the angle of rotation in degrees read at 20 °C at the wavelength of the D-line of sodium (λ = 589.3 nm) (Ph. Eur. 8th edition, method 2.2.7).

A Perkin-Elmer 341 polarimeter was used to measure the optical rotation of the following pure compounds. About 1 – 4 mg substance was weighted and dissolved in MeOH or chloroform, respectively. The angle of rotation α of the solution was measured at 20°C and the specific optical rotation was calculated using the following formula:

$$[\alpha]_{\mathrm{D}}^{20} = \frac{1000\alpha}{l \cdot c}$$

Figure 23 - Specific optical rotation formula
[uspbpep.com; accessed on: August 2016]

α - angle of rotation in degrees read at 20 ± 0.5 °C

l - length in decimetres of the polarimeter tube

c - concentration of the solution in g/L

The chosen parameters for the measurement of all pure compounds are given in Table 12.

Table 12 - Optical rotary power

Code	Fraction	Value	Condition
GO54-A	GO54ED01_10_r	+ 53,6 °	Conc: 0.110 g/100 mL; Solv: MeOH; Wavel.: 589.3 nm; Temp: 20 °C
GO54-D	GO54ED25_02	+ 43.6 °	Conc: 0.101 g/100 mL; Solv: MeOH; Wavel.: 589.3 nm; Temp: 20 °C
GO54-H	GO54ED19_02	+ 2.0 °	Conc: 0.101 g/100 mL; Solv: MeOH; Wavel.: 589.3 nm; Temp: 20 °C
GO54-I	GO54ED31_02	+ 37.0 °	Conc: 0.208 g/100 mL; Solv: MeOH; Wavel.: 589.3 nm; Temp: 20 °C
GO54-J	GO54ED32_02	+ 21.9 °	Conc: 0.334 g/100 mL; Solv: MeOH; Wavel.: 589.3 nm; Temp: 20 °C
GO54-K	GO54ED33_03	+ 29.9 °	Conc: 0.178 g/100 mL; Solv: MeOH; Wavel.: 589.3 nm; Temp: 20 °C
GO54-L	GO54ED34_17	- 112,7 °	Conc: 0.166 g/100 mL; Solv: $CHCl_3$; Wavel.: 589.3 nm; Temp: 20 °C

4.2.6 IR-Spectroscopy of Pure Compounds

An IR of the following Samples was recorded with an Miracle Diamond ATR. For the measurement a small christal of the pure compound was used. Data is shown in Figure 24 and Figure 25, respectively.

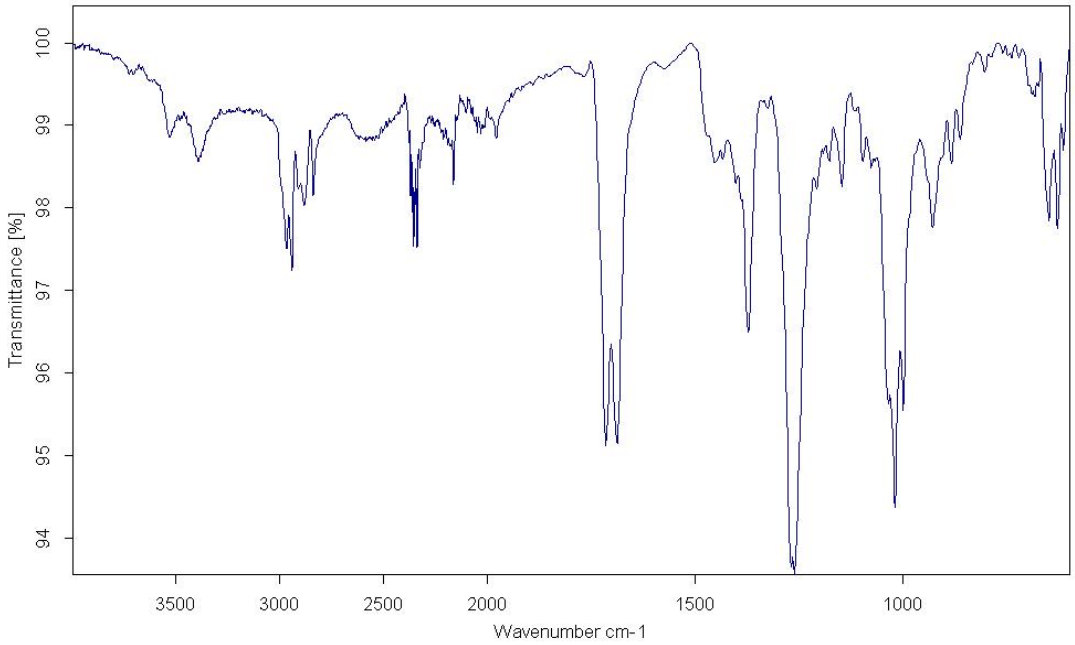

Figure 24 - IR-Spectra of GO25_02 / GO54-D

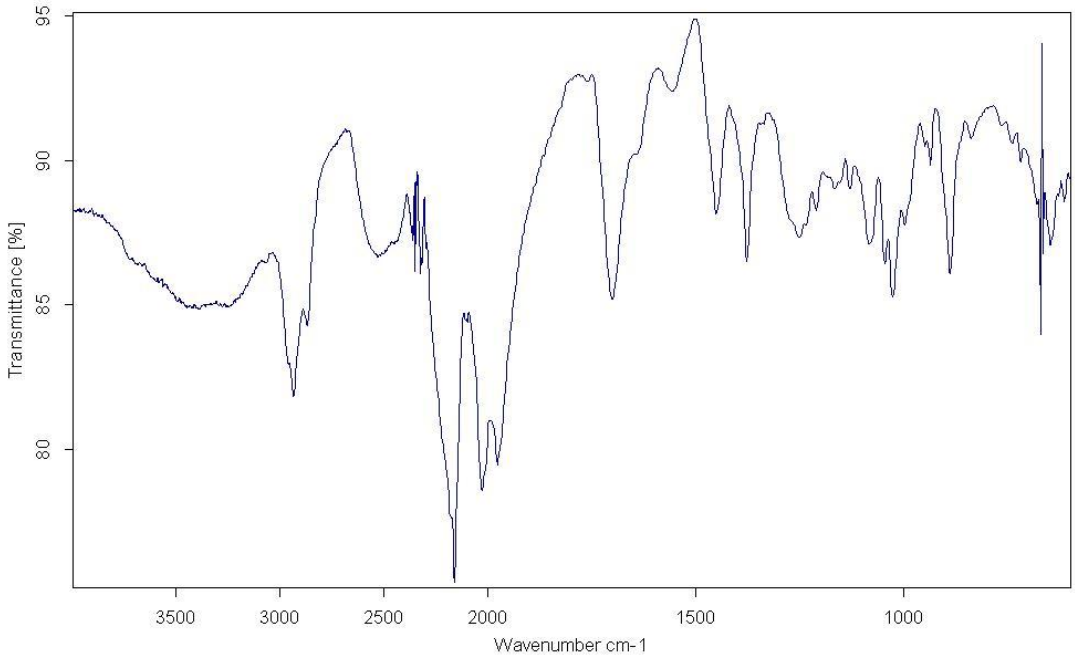

Figure 25 – IR-Spectra of GO32_02 / GO54-J

5 CONCLUSION

In the first part (i) of this diploma thesis MeOH and PE extracts of 30 fruit bodies of Tyrolean mushroom species and their corresponding strains were produced in small scale with ASE. As all extracts were produced in the exact same way, a qualitative and quantitative investigation of the secondary metabolite profile with different chromatographic methods was possible. Within the scope of this work the differences of an extraction with MeOH (extract B) after PE extraction (extract A) in comparison with the plain MeOH extraction (extract C) was examined. Therefore all prepared extracts (extract A, B and C) were investigated with HPLC-CAD which revealed there are not only differences between the different mushroom strains of the same species. Further, the analysis revealed that an extraction with MeOH after PE mainly extracts the polar compounds as the non-polar compounds were already extracted with PE. This has proven that the chosen parameters for a PE extraction with ASE were accurate for the non-polar compounds. Likewise the separation of the non-polar triterpenes (extract A) with SFC showed clearly the differences between the different mushroom strains and their secondary metabolite profile. These results were also proven by a collective TLC investigation of the plain MeOH extracts (extract C) which showed that out of all *F. pinicola* strains only 3, namely Fompin0010, Fompin0018 and Fompin0021, show a blue spot “a”. A further spot “b” was only present in seven *F. pinicola* strains. Further research concerning the *F. pinicola* strains is currently under investigation.

A further aim of this thesis (ii) was the purification of selected fractions of *G. odoratum* since previous bioactivity tests of the ethanolic extract showed promising STS and NA inhibition. The fractions GO10_01, GO10_02, GO12_04, GO15_01 and GO27_07 derived from the DCM fraction each and had to be purified. For the separation of these fractions a semi-preparative UHPLC was developed, resulting in 6 pure compounds: The isolation of constituents from GO15_01 failed due to insufficient amount; for all the other fractions, isolates could be obtained and identified.

GO12_04 was separated in GO36_01 and GO36_02, GO10_01 in GO37_01 and GO37_02 and GO10_02 in GO38_01 and GO38_02. Of all these compounds GO36_01 (21-Hydroxylanosterol) and GO36_02 (Eburicodiol) were identified with NMR structure elucidation. These two compounds are new for *G. odoratum*. Unfortunately the separated

amount of the other 4 isolated pure compounds GO37_01, GO37_02, GO38_01 and GO38_02 was not enough for NMR analysis, although a previous NMR analysis allowed structure elucidation of the mixture GO10_01 and GO10_02, respectively. GO10_01 contained the triterpene acid (15α)-15-hydroxy-3-oxo-Lanosta-8,24-dien-21-oic acid (=GO37_02) and a new compound (=GO37_01). GO10_02 consisted of 2 triterpene acids, 3-Ketodehydrosulfurenic acid (=GO38_01) and Fomefficinic acid D (=GO38_02). None of them have ever been reported for *G. odoratum*. Fraction GO27_07 turned out to be identical with a previous isolated pure compound (=GO33_03), namely Gloeophyllin A, which has also never been identified from *G. odoratum* before.

The ethanolic crude extract (GO54E) previously showed a promising inhibition of the STS enzyme. In contrast to this, the herein isolated compounds of the DCM fraction were not or only moderately active on STS. This implies that the more potent STS inhibitors are enriched in another fraction of the ethanolic extract than the DCM one (GO54ED). Investigations concerning these compounds are ongoing.

The NA bioactivity assay was performed with the IAV HK/68 and IAV Jena/8179, using Oseltamivir as positive control and showed promising outcomes: compound GO54-A [(3β)-Hydroxy-lanosta-8,24-dien-21-oic acid], GO54-E [Mixture of: (3β)-3-Hydroxy-lanosta-8,24-dien-21-oic acid and (3β)-3-Hydroxy-24-methylene-lanost-8-en-21-oic acid], GO54-H (Diastereomere of GO54-A) as well as GO54-M (=GO36_01; 21-Hydroxylanosterol) and GO54-N (=GO36_02; Eburicodiol) show activity against both IAV HK/68 and IAV Jena/8179, whereas GO54-D [(3β,15α)-Acetyloxy-2,26-dihydroxy-lanosta-8,24-dien-21-oic acid] is only active against IAV Jena/8178. Hardly surprising the lowest inhibitory concentration against both virus strains was recorded for GO54-E, the only sample containing two compounds. Additionally the remaining samples GO54-I (Gloeophyllin B), GO54-J (Derivative of Gloeophyllin A), GO54-K (Gloeophyllin A) and GO54-L (Ergosterol Peroxide) showed cytotoxic effects against MDCK II cells.

The present work anticipates additional studies to further elucidate the potential of the secondary metabolites contained in *G. odoratum* for novel anti-cancer or anti-viral drugs. Natural products deriving from mushrooms used in TCM can be an important source for the development of new lead-compounds.

6 MATERIALS AND METHODS

This chapter contains detailed information about the procedure of preparation and all used parameters described in Chapter 4.

6.1 Generation of an Extraction Protocol with ASE for non-polar Triterpenes for Subsequent Separation with SFC

This material was obtained from Plantasia (wholesale company for Asian medicinal herbs in Oberndorf, Salzburg). The mushroom materials for further investigations were obtained from a collaboration partner (Prof. Dr. Ursula Peintner) at the Institute of Microbiology of the University of Innsbruck, Austria. In total 10 different mushroom species and respectively 30 different mushroom strains were investigated. Voucher specimens are deposited in the Herbarium of the Department of Pharmacognosy, University of Vienna, Austria. Table 13, gives an overview of all species including Author and Family.

Table 13 - Mushroom Species ASE Extraction

Genus/Species	Author	Family	Label
Fomes fomentarius	(L.) Fr.	Polyporaceae	Fomfom0011
			Fomfom0016
			Fomfom0019
			Fomfom0022
			Fomfom0033
Fomitopsis pinicola	(Sw.) P. Karst.	Fomitopsidaceae	Fompin0010
			Fompin0013
			Fompin0015
			Fompin0018
			Fompin0021
			Fompin0024
			Fompin0026
			Fompin0030
			Fompin0037
			Fompin0040
			Fompin0053
			Fompin00374
			Fompin00442

Genus/Species	Author	Family	Label
Ganoderma applanatum	(Pers.) Pat.	Ganodermataceae	Ganapp0012
Ganoderma lucidum	(Curtis) P. Karst.	Ganodermataceae	Ganluc0027
			Ganluc0032
Gloeophyllum odoratum	(Wulfen) Imazeki	Gloeophyllaceae	Gloodo0023
			Gloodo0028
			Gloodo0054
Ischnoderma benzoinum	(Wahlenb.) P. Karst.	Fomitopsidaceae	Isben0038
Laetiporus sulphureus	(Bull.) Murrill	Fomitopsidaceae	Laesul0043
Phellinus robustus	(P. Karst.) Bourdot & Galzin	Hymenochaetaceae	Pherob0025
Piptoporus betulinus	(Bull.) P. Karst.	Fomitopsidaceae	Pipbet0029
			Pipbet0039
Trametes gibbosa	(Pers.) Fr.	Polyporaceae	Tragib0052

Dresch et al., 2015 provides detailed information of the used polypore strains and their voucher ID, Genbank accession number and natural substrate (host) for each isolate.

6.2 Mycochemistry

6.2.1 Chromatographic Methods

6.2.1.1 High Performance Liquid Chromatography

High Performance Liquid Chromatography (HPCL) is a sophisticated and potent analytical technique. The principle of HPLC is that a mixture to be separated is applied on top of a column filled with adsorbent (stationary phase) which will be eluted with a liquid (mobile phase). Because of different interactions of the components in the mixture with the stationary phase, a separation of the weakly adsorbent to the stronger adsorbent compounds is possible as the elution of the analytes is varying. The time taken for the analyte to pass through the column is called retention time, which is a characteristic for a particular set of conditions, as well as the UV spectra of an analyte (Lindsay, 1992).

6.2.1.2 Ultra-High Pressure Liquid Chromatography

An advance in LC referring to instrumentation and column technology is the Ultra-High Pressure Liquid Chromatography (UHPLC). Columns filled with smaller particles (1.7 – 1.8 µm) and pressures up to 15.000 psi (1030 bar) result in an incensement of resolution and shortening in analysis-time (waters.com; accessed: August 2016).

6.2.1.3 Supercritical Fluid Chromatography

Similar to reversed phase LC, SFC is a chromatographic method using carbon dioxide as main mobile phase and represents therefore a normal-phase chromatography. At high pressures CO2 is a supercritical fluid which leads to low viscosity and high diffusivity (waters.com; accessed: September 2016). These conditions lead to high mobile phase flow rates resulting in a reduction of time used for the isolation of pure compounds in preparative SFC. This improvement of productivity in purification steps leads to lower organic solvent consumption compared to LC, as the main mobile phase is CO_2 which can be mixed with various co-solvents, between 2 and 40 %. Consequently, the SFC is also known as green approach, as the consumption of organic solvents and waste are reduced. In addition, chiral as well as achiral separations can be achieved by SFC, using the same type of mobile phase and instrument (Desfontaine et al., 2015).

6.3 Generation of an Extraction Protocol with ASE for non-polar Triterpenes for Subsequent Separation with SFC

6.3.1 Labeling of Mushroom Samples

The first three letters of both genus and species name (e.g. *Ganoderma lucidum*) are taken and merged whereas the number at the end represents the consecutive number of the extraction method. Page 17 shows an overview of the executed extraction steps.

6.3.2 TLC-System for Mushroom TLC Analysis

Stationary phase:	TLC Silica gel 60 F_{254}
System:	DCM : MeOH : H_2O (10 : 1 : 0.25)
Spraying reagent:	Vanillin / H_2SO_4
Detection:	UV_{254}, UV_{366}, VIS

6.3.3 Method for HPLC-CAD Investigation of Mushroom Samples

Method: GUS_5to95w2ppm_CAD_130315						
instrument	**col.**	**temp. [°C]**	**flow rate [mL/min]**	**inj vol [µL]**	**config.**	**det. wavel. [nm]**
Dionex HPLC-CAD	Agilent Zorbax SB-C18	40	1.0	10	CAD	210

time [min]	**mobile phase A [%] H_2O**	**mobile phase C [%] ACN**
0.00	95	5
45.00	2	98
55.00	2	98
66.00	95	5

6.3.4 Preliminary Tests and Optimization Steps

In the following chapter the ASE parameters for the preliminary tests and optimization steps for the development of an extraction method of *G. lucidum* fruit bodies are shown (see Figure 26 - Figure 29, pages 51 to 52). Furthermore, all extraction yields are listed (see 6.3.6, page 57).

The dried mushroom *G. lucidum* was ground and for each extraction 3 g of the so prepared material was filled into 11 ml ASE cells. Next, the ASE was programmed to perform the different extraction methods.

All preliminary tests were performed with default settings: 1500 psi, 1 cycle, 10% flush and 60 seconds purge as constant parameters (Ganluc001-015). Figure 6, Page 17 shows an overview of the so performed workflow. Initially the effect of both solvent and temperature on the extraction of triterpenes was investigated (see Figure 26, page 51).

As the focused compounds are non-polar, the experiment was started with 100% non-polar solvents using on the one hand n-hexane at 100°C, 125°C, and 150°C (Ganluc001-003) and on the other hand petroleum ether at 100°C, 125°C, and 150°C (Ganluc004-006).

Other extractions were performed with mixtures of a non-polar solvent with a more polar solvent in order to investigate the changes of polarity on the extraction efficacy. The mixture ratio of non-polar solvent : polar solvent varied from 70:30, 80:20 and 90:10. These extractions were carried out with n-hex:ACE at 70°C (Ganluc007-009) and 100°C (Ganluc013-015) as well with n-hex:EtOAc at 70°C (Ganluc010-012).

These extracts seemed to be not suitable for our aim due to the fact that more polar compounds were extracted as well. Additionally the yield of these extracts was higher and it was also shown that a rise of temperature increases the extract yield as well (see Table 14, Chapter 6.3.5).

Nonetheless, the extraction method using petroleum ether at 125°C (Ganluc005) seemed to be most suitable as mainly the non-polar compounds were extracted according to the HPLC-CAD chromatogram. Hence Ganluc005 was chosen for the first optimization step (optimization 001, see Figure 27, page 51): the first variable in this step is the number of cycles used for each extraction, which varied from 2, 3, 4 to 5 cycles (Ganluc016-019). As a second variable the percentage of flush was raised from 10% to 50% (Ganluc020) and to 60% (Ganluc021) using one cycle each. According to TLC analyses, 3 extraction cycles (Ganluc017) seemed to be best. For that reason Ganluc017 was chosen for the second optimization step (optimization 002, see Figure 28, page 52) where the flush percentage was raised from 10% to 60%, 70%, 80%, 90% up to 100% using 3 cycles each (Ganluc022-026). The efficacy of the extraction was likewise investigated with TLC, whereby a flush percentage of 90 (Ganluc025) seemed to be best. In the third optimization step (optimization 003, see Figure 29, page 52) the effect of pressure was examined on Ganluc025. The extractions were performed with 1250 psi, 1350 psi, 1450 psi, 1650 psi, 1850 psi and 2000 psi as a maximum (Ganluc027-032). Finally, Ganluc0029 seemed to be most suitable for the extraction of non-polar triterpenes, therefore 1450 psi was chosen for the last optimization.

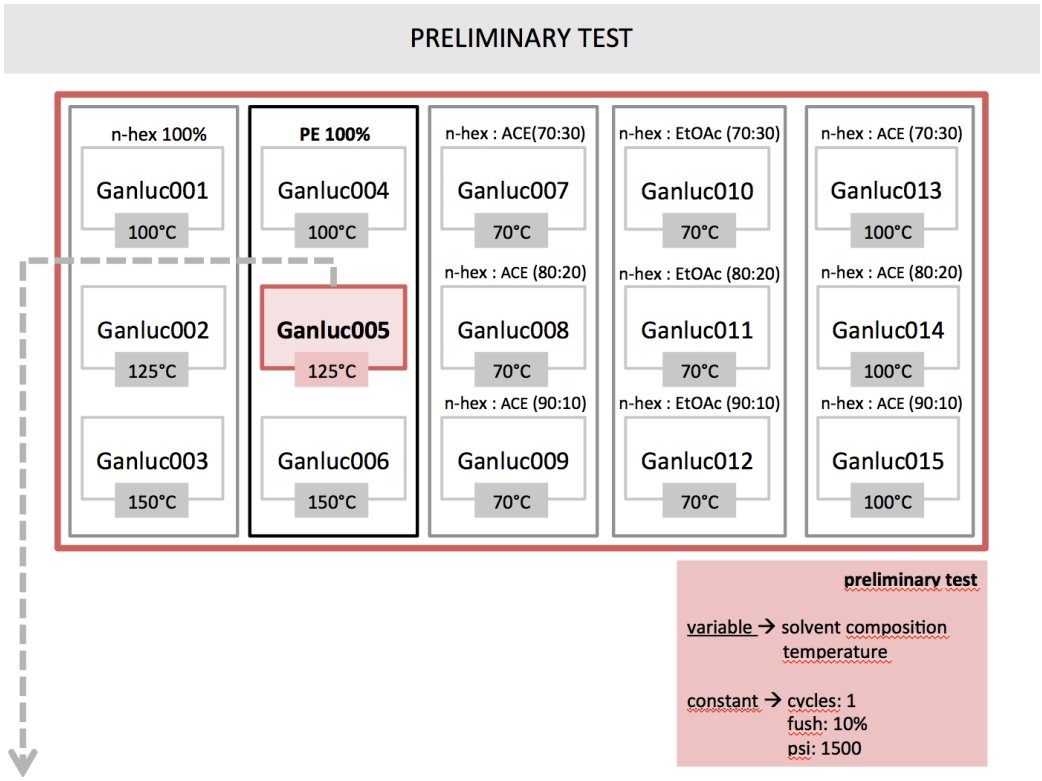

Figure 26 – Preliminary Tests

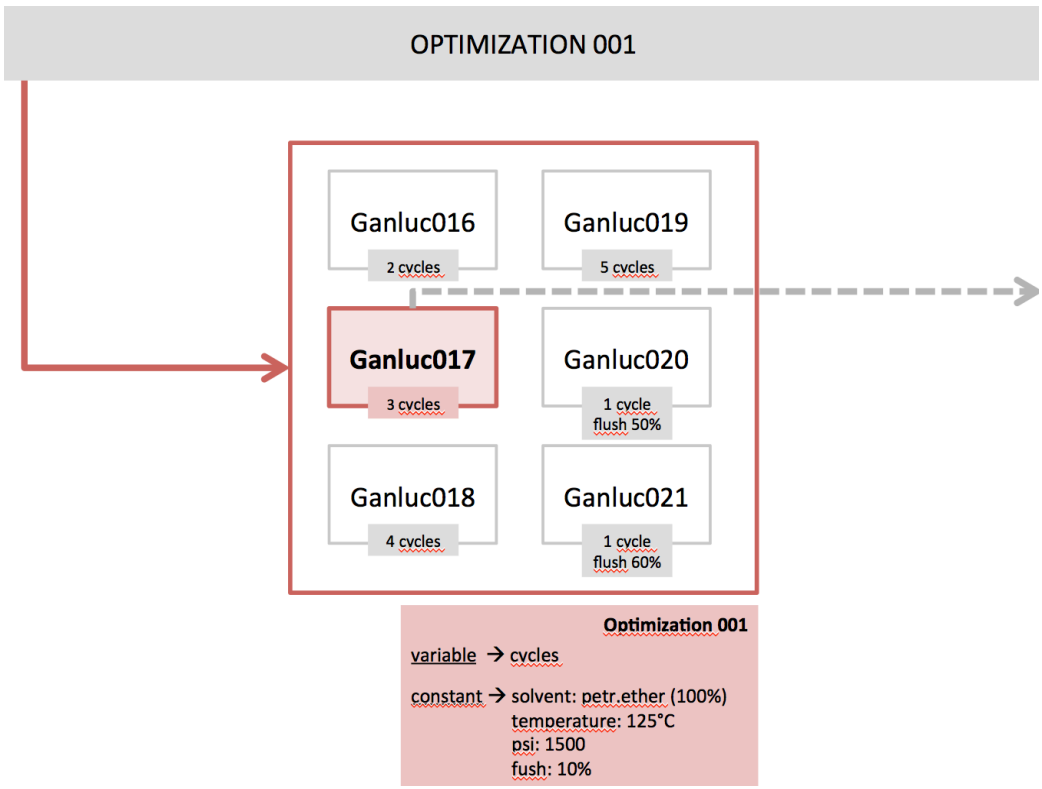

Figure 27 - Optimization001

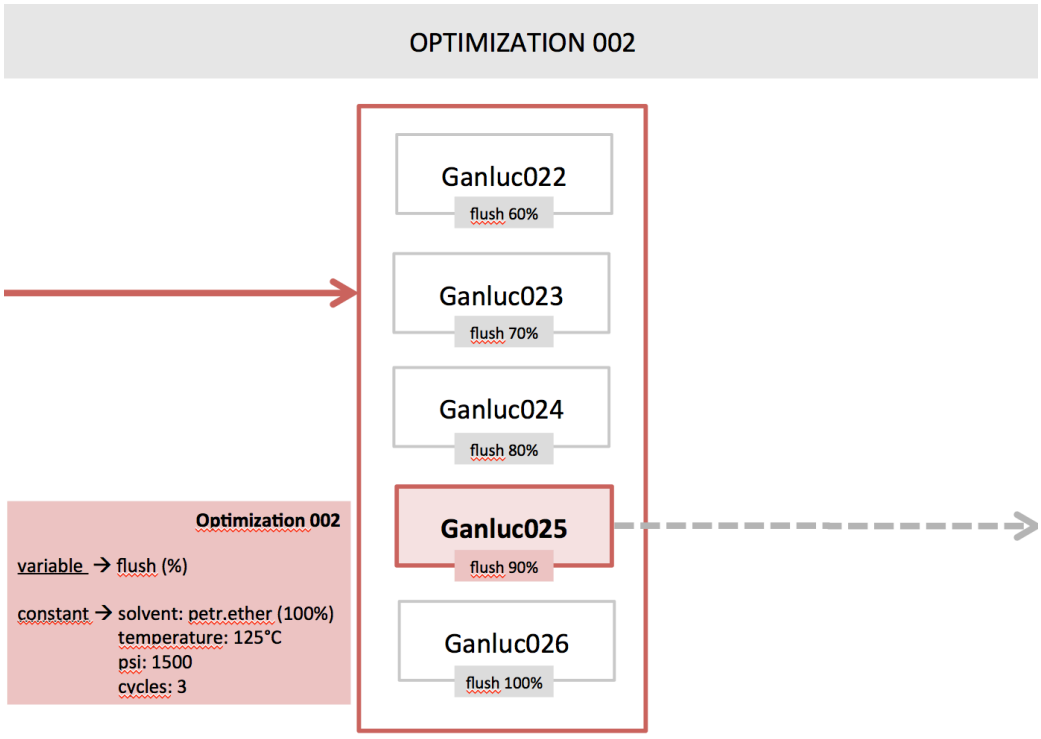

Figure 28 - Optimization002

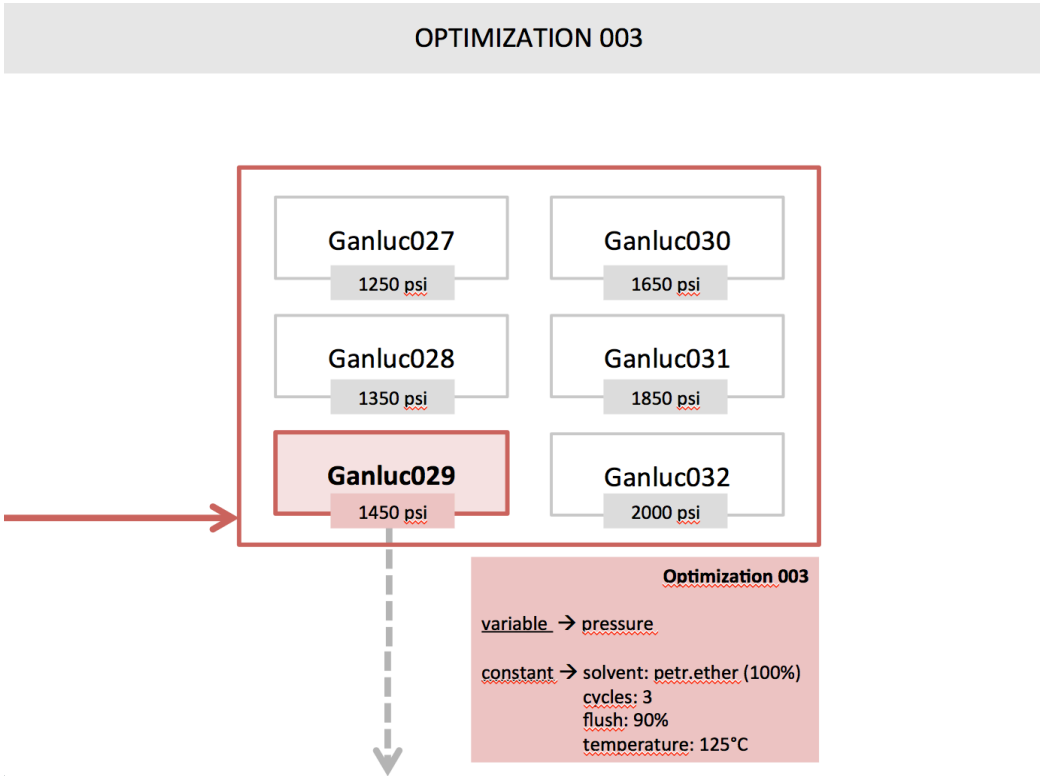

Figure 29 - Optimization003

6.3.5 Extraction Yields of *Ganoderma lucidum* for the Preliminary Tests

Table 14- Extraction yields of *G. lucidum*

label	solvent	temperature [°c]	pressure [psi]	vial weight [mg]	extract yield [mg]
Ganluc001	n-hexane	100	1500	9856.38	15.06
Ganluc002	n-hexane	125	1500	9682.05	13.23
Ganluc003	n-hexane	150	1500	9820.49	19.00
Ganluc004	PE (100)	100	1500	9845.03	12.73
Ganluc005	PE (100)	125	1500	9818.97	15.95
Ganluc006	PE (100)	150	1500	9754.66	18.20
Ganluc007	n-hex : ACN (70:30)	70	1500	9686.12	41.37
Ganluc008	n-hex : ACN (80:20)	70	1500	9797.80	38.99
Ganluc009	n-hex : ACN (90:10)	70	1500	9671.88	28.42
Ganluc010	n-hex : ACN (70:30)	100	1500	9751.66	38.52
Ganluc011	n-hex : ACN (80:20)	100	1500	9574.38	35.77
Ganluc012	n-hex : ACN (90:10)	100	1500	9758.03	11.63
Ganluc013	n-hexane : EtOAc (70:30)	70	1500	9681.23	30.95
Ganluc014	n-hexane : EtOAc (80:20)	70	1500	9660.05	22.50
Ganluc015	n-hexane : EtOAc (90:10)	70	1500	9848.27	16.62
Ganluc016	PE (100)	125	1500	9587.50	21.93
Ganluc017	PE (100)	125	1500	9658.58	20.17
Ganluc018	PE (100)	125	1500	9691.52	20.48

label	solvent	temperature [°c]	pressure [psi]	vial weight [mg]	extract yield [mg]
Ganluc019	PE (100)	125	1500	9704.64	22.13
Ganluc020	PE (100)	125	1500	9652.34	22.79
Ganluc021	PE (100)	125	1500	9754.06	19.26
Ganluc022	PE (100)	125	1500	9691.94	17.28
Ganluc023	PE (100)	125	1500	9693.53	20.93
Ganluc024	PE (100)	125	1500	9821.75	20.89
Ganluc025	PE (100)	125	1500	9556.23	18.75
Ganluc026	PE (100)	125	1500	9808.55	19.50
Ganluc027	PE (100)	125	1250	9733.53	15.94
Ganluc028	PE (100)	125	1350	9793.21	18.58
Ganluc029	PE (100)	125	1450	9894.46	21.35
Ganluc030	PE (100)	125	1650	9879.32	21.94
Ganluc031	PE (100)	125	1850	9696.29	18.03
Ganluc032	PE (100)	125	2000	9874.61	17.93

Additionally we wanted to figure out what differences in the extracted compounds an extraction with MeOH after the PE extraction makes. Therefore, with the final ASE extraction parameters, the mushroom material was extracted with PE (Ganluc0033) and afterwards, the same ASE cell was extracted with 100 % MeOH (Ganluc0034). Another ASE cell was filled with fresh mushroom material and then extracted with 100 % MeOH (Ganluc0035). The Chromatograms are given in Figure 30, Page 56.

Table 15- Used solvent for the extraction of Ganluc0033-Ganluc0035, inclusive extraction yields.

label	solvent	temperature [°c]	pressure [psi]	vial weight [mg]	extract yield [mg]
Ganluc033	PE (100)	125	1450	9748.55	24.44
Ganluc034	MeOH (100)	125	1450	9777.45	86.50
Ganluc035	MeOH (100)	125	1450	9774.06	109.76

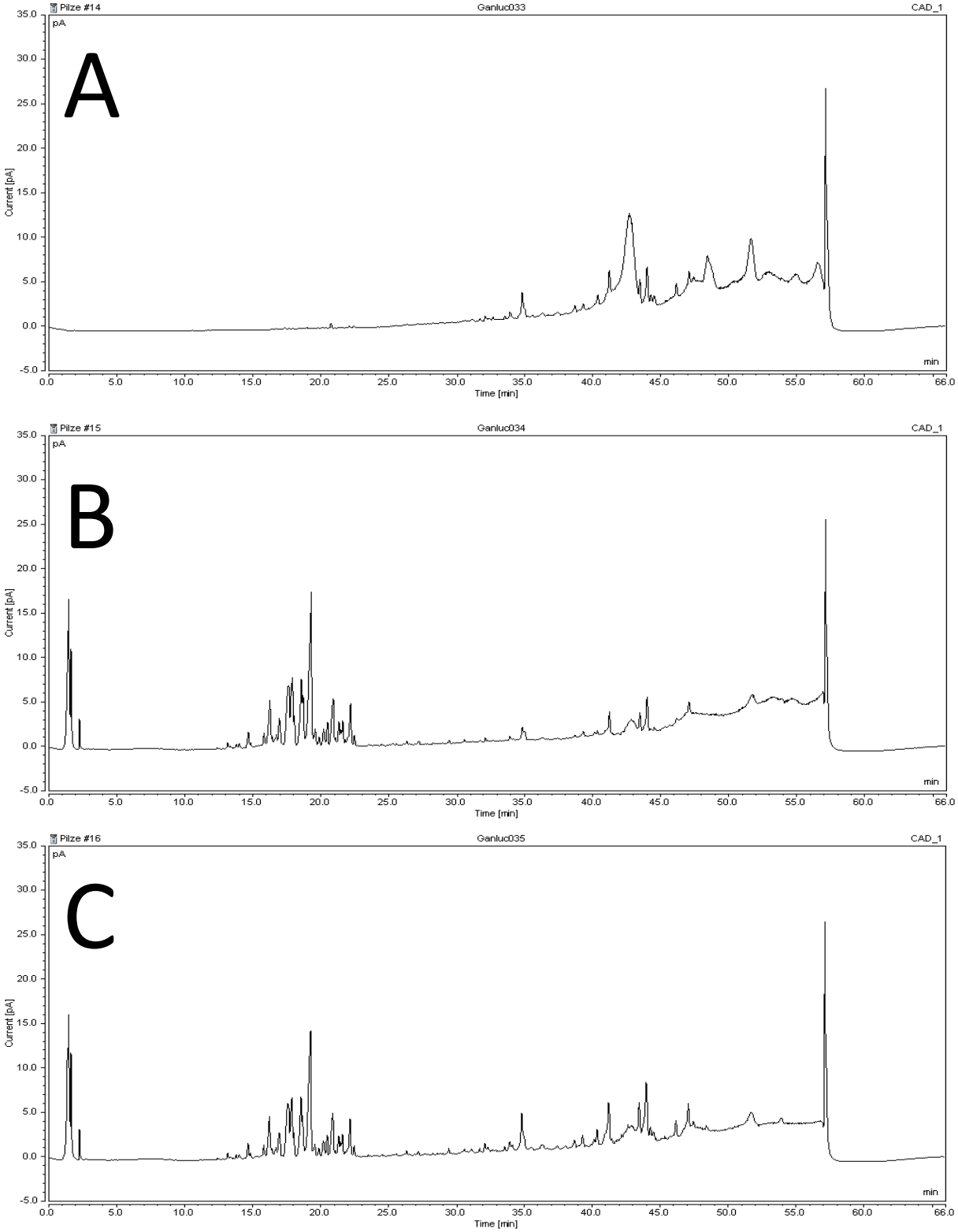

Figure 30 – A: Ganluc0033; B: Ganluc0034; C: Ganluc0035

6.3.6 Extraction Yields of Mushroom Species

In Table 16 all extracts are listed with full name, strain and sample label and used solvent for extraction. Additionally, total extract yields are given.

Table 16 - Extraction yields of mushroom species

sample	strain	label	solvent	vial weight [mg]	extract yield [mg]
Formes fomentarius	Fomfom0011	Fomfom0011a	1. PE	9549.51	67.89
		Fomfom0011b	2. MeOH	9577.62	79.15
		Fomfom0011c	only MeOH	9582.28	200.39
	Fomfom0016	Fomfom0016a	1. PE	9573.00	76.43
		Fomfom0016b	2. MeOH	9558.88	55.06
		Fomfom0016c	only MeOH	9580.84	191.41
	Fomfom0019	Fomfom0019a	1. PE	9574.47	68.56
		Fomfom0019b	2. MeOH	9551.91	58.00
		Fomfom0019c	only MeOH	9547.65	171.28
	Fomfom0022	Fomfom0022a	1. PE	9560.96	64.83
		Fomfom0022b	2. MeOH	9550.33	88.57
		Fomfom0022c	only MeOH	9566.60	188.15
	Fomfom0033	Fomfom0033a	1. PE	9584.45	79.22
		Fomfom0033b	2. MeOH	9563.28	73.54
		Fomfom0033c	only MeOH	9619.41	205.53
Fomitopsis pinicola	Fompin0010	Fompin0010a	1. PE	9592.01	307.82
		Fompin0010b	2. MeOH	9571.84	285.76
		Fompin0010c	only MeOH	9581.47	614.28
	Fompin0013	Fompin0013a	1. PE	9597.24	617.47
		Fompin0013b	2. MeOH	9581.89	126.15
		Fompin0013c	only MeOH	9573.89	718.58
	Fompin0015	Fompin0015a	1. PE	9556.41	517.89
		Fompin0015b	2. MeOH	9606.02	57.51
		Fompin0015c	only MeOH	9580.71	472.37
	Fompin0018	Fompin0018a	1. PE	9589.45	416.79
		Fompin0018b	2. MeOH	9582.12	417.18
		Fompin0018c	only MeOH	9637.50	844.54
	Fompin0021	Fompin0021a	1. PE	9570.18	800.42
		Fompin0021b	2. MeOH	9560.66	91.86
		Fompin0021c	only MeOH	9580.46	925.48
	Fompin0024	Fompin0024a	1. PE	9633.51	463.26
		Fompin0024b	2. MeOH	9595.78	82.99
		Fompin0024c	only MeOH	9551.52	536.22

sample	strain	label	solvent	vial weight [mg]	extract yield [mg]
Fomitopsis pinicola	Fompin0026	Fompin0026a	1. PE	9623.79	327.66
		Fompin0026b	2. MeOH	9642.14	210.39
		Fompin0026c	only MeOH	9523.04	294.53
	Fompin0030	Fompin0030a	1. PE	9438.72	569.82
		Fompin0030b	2. MeOH	9545.81	108.05
		Fompin0030c	only MeOH	9618.77	618.27
	Fompin0037	Fompin0037a	1. PE	9625.60	320.82
		Fompin0037b	2. MeOH	9559.68	207.53
		Fompin0037c	only MeOH	9570.62	482.61
	Fompin0053	Fompin0053a	1. PE	9640.93	753.9
		Fompin0053b	2. MeOH	9625.97	115.44
		Fompin0053c	only MeOH	9612.83	922.91
	Fompin0040	Fompin0040a	1. PE	9583.14	355.23
		Fompin0040b	2. MeOH	9598.27	84.99
		Fompin0040c	only MeOH	9570.02	451.81
	Fompin00374	Fompin00374a	1. PE	9638.57	539.20
		Fompin00374b	2. MeOH	9586.05	100.20
		Fompin00374c	only MeOH	9596.78	636.95
	Fompin00442	Fompin00442a	1. PE	9594.40	823.23
		Fompin00442b	2. MeOH	9485.80	114.05
		Fompin00442c	only MeOH	9554.27	948.02
Ganoderma applanatum	Ganapp0012	Ganapp0012a	1. PE	9443.54	478.9
		Ganapp0012b	2. MeOH	9546.18	279.49
		Ganapp0012c	only MeOH	9662.19	764.13
Ganoderma lucidum	Ganluc0027	Ganluc0027a	1. PE	9753.49	85.41
		Ganluc0027b	2. MeOH	9468.29	75.59
		Ganluc0027c	only MeOH	9470.60	167.83
	Ganluc0032	Ganluc0032a	1. PE	9611.18	227.61
		Ganluc0032b	2. MeOH	9593.53	50.28
		Ganluc0032c	only MeOH	9567.33	156.89
Gloeophyllum odoratum	Gloodo0023	Gloodo0023a	1. PE	9581.91	279.64
		Gloodo0023b	2. MeOH	9624.49	134.25
		Gloodo0023c	only MeOH	9605.28	536.84
	Gloodo0028	Gloodo0028a	1. PE	9889.66	245.66
		Gloodo0028b	2. MeOH	9798.48	170.58
		Gloodo0028c	only MeOH	9690.15	550.73
	Gloodo0054	Gloodo0054a	1. PE	9860.45	214.65
		Gloodo0054b	2. MeOH	9737.46	118.99
		Gloodo0054c	only MeOH	9619.99	444.01

sample	strain	label	solvent	vial weight [mg]	extract yield [mg]
Ischnodermal benzoinum	Iscben0038	Iscben0038a	1. PE	9813.79	50.02
		Iscben0038b	2. MeOH	9693.61	86.56
		Iscben0038c	only MeOH	9631.87	181.82
Laetiporus sulphureus	Laesul0043	Laesul0043a	1. PE	9836.99	66.52
		Laesul0043b	2. MeOH	9731.08	85.25
		Laesul0043c	only MeOH	9663.24	142.63
Phellinus robustus	Pherob0025	Pherob0025a	1. PE	9878.55	7.20
		Pherob0025b	2. MeOH	9809.81	125.93
		Pherob0025c	only MeOH	9743.98	158.27
Piptoporus betulinus	Pipbet0029	Pipbet0029a	1. PE	9658.05	85.25
		Pipbet0029b	2. MeOH	9794.67	252.89
		Pipbet0029c	only MeOH	9777.26	237.5
	Pipbet0039	Pipbet0039a	1. PE	9853.14	57.22
		Pipbet0039a	2. MeOH	9816.27	122.12
		Pipbet0039a	only MeOH	9780.49	413.40
Trametes gibbosa	Tragib0052	Tragib0052a	1. PE	9737.51	100.05
		Tragib0052b	2. MeOH	9784.45	423.20
		Tragib0052c	only MeOH	9728.26	527.63

6.3.7 Method Development for Secondary Metabolite Characterization via SFC

Within the scope of this thesis all SFC runs were performed with the parameters given in Table 17. As co-solvent EtOH was chosen. The corresponding chromatograms are shown in Chapter 8.1.3, page 114.

Table 17 - Used method for secondary profile characterization of mushroom extracts

instrument	column	temp. [°C]	make-up flow rate [mL/min]	inj vol [µL]	config.	det. wavel. [nm]
SFC Waters	BEH Viridis 4.6 x 250	40	3	5	ELSD + PDA	254

time [min]	Co-Solvent [%] EtOH
0.00	5
1.00	5
9.50	50
10.50	50
11.00	5
12.00	5

6.4 Purification of Selected Fractions of *Gloeophyllum odoratum*

6.4.1 Ultra High Performance Liquid Chromatography

6.4.2 Method Development for the Separation of GO10_01, GO10_02, GO12_04 and GO15_01

Table 18 - Used method for the separation of GO12_04

Method: GOallg8_PDA_ELSD_col1						
instrument	**col.**	**temp. [°C]**	**flow rate [mL/min]**	**inj vol [µL]**	**config.**	**det. wavel. [nm]**
UHPLC Waters	BEH Phenyl 100 mm	40	0.6	5	PDA + WFMA	210

time [min]	**mobile phase A [%] H2O**	**mobile phase C [%] ACN**
0.00	16	84
1.50	14	86
1.60	2	98
2.90	2	98
3.00	16	84

Table 19 - Used method for the separation of GO10_01

Method: GO10_01_collect01_PDA_WFMA_col1						
instrument	**col.**	**temp. [°C]**	**flow rate [mL/min]**	**inj vol [µL]**	**config.**	**det. wavel. [nm]**
UHPLC Waters	BEH Phenyl 100 mm	40	0.4	5	PDA + WFMA	210

time [min]	**mobile phase A [%] H2O**	**mobile phase C [%] ACN**
0.00	60	40
3.40	28	72
4.00	27	73
4.10	2	98
4.90	2	98
5.00	60	40

Table 20 - Used method for the separation of GO10_02

Method: GO10_02_collect03_PDA_WFMA_col1						
instrument	**col.**	**temp. [°C]**	**flow rate [mL/min]**	**inj vol [µL]**	**config.**	**det. wavel. [nm]**
UHPLC Waters	HSS T3 100 mm	40	0.4	1	PDA + WFMA	210

time [min]	**mobile phase A [%] H2O**	**mobile phase C [%] ACN**
0.00	25	75
1.80	10	90
2.20	10	90
2.30	2	98
2.90	2	98
3.00	25	75

6.4.3 Spectral Data of the Isolated Pure Compounds

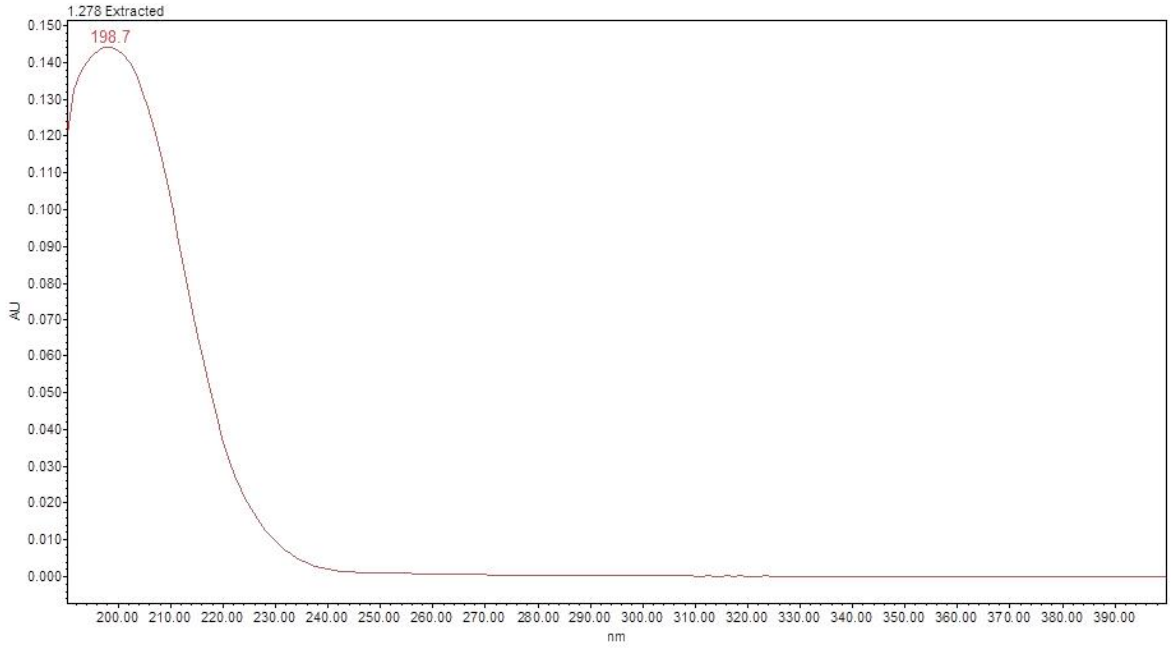

Figure 31 - UV-spectra GO36_01

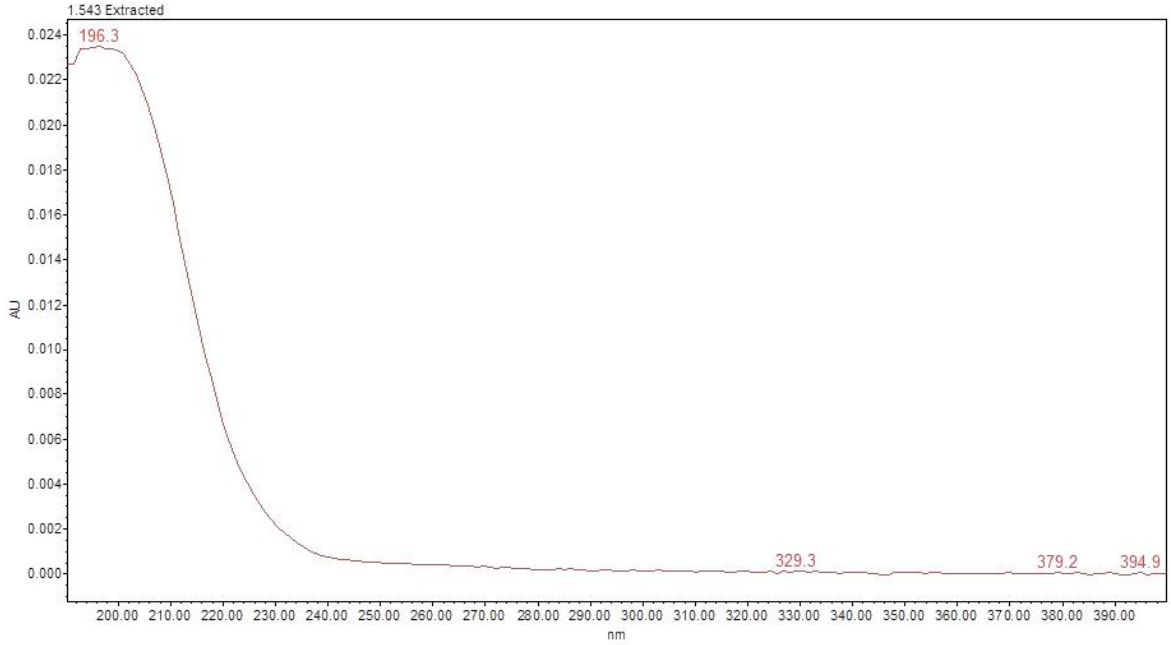

Figure 32 - UV-spectra GO36_02

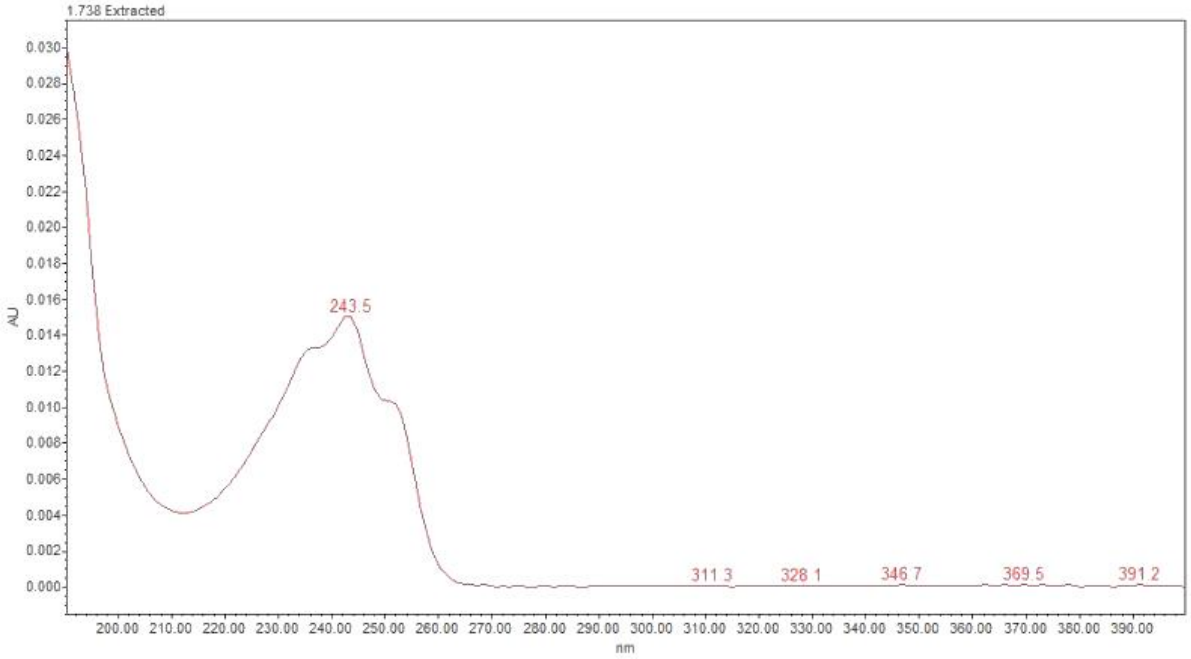

Figure 33 - UV-spectra GO38_01

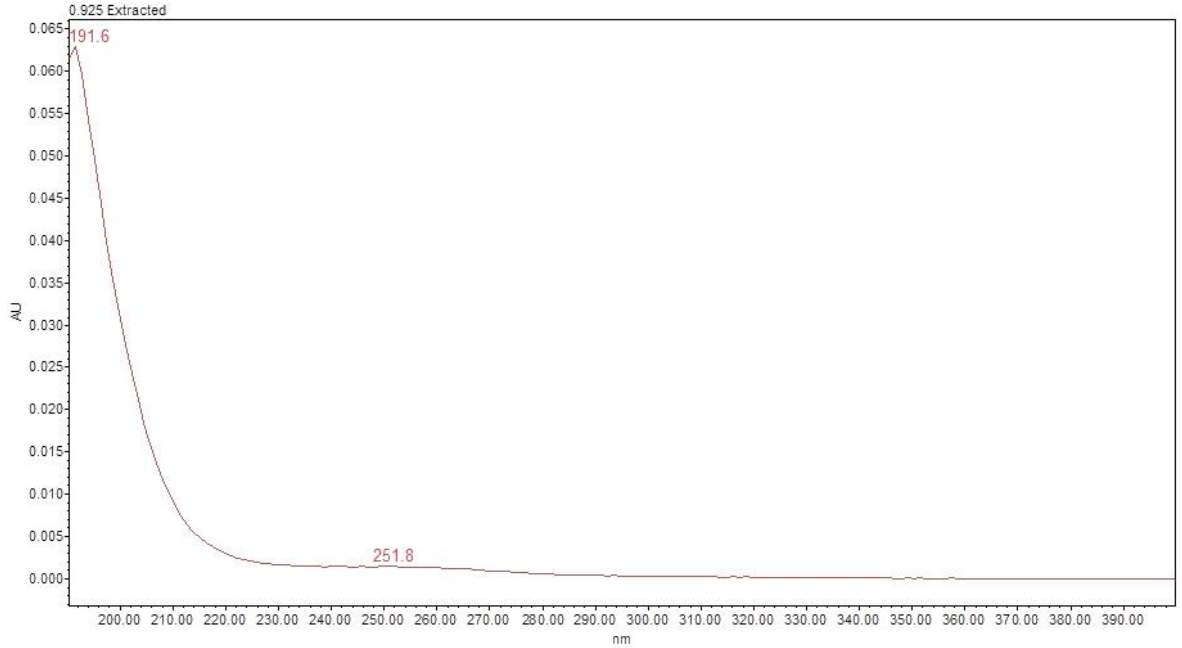

Figure 34 - UV-spectra GO38_02

6.5 Instruments, Solvents and Reagents

6.5.1 Miscellaneous Instruments

Device	Technical Features / Description
Accelerated Solvent Extraction	ASE 200 Accelerated Solvent Extraction, Dionex
Analytical Balance	BP210D, Sartorius
Chiller (SFC)	Accel 500 LC, Thermo Scientific Polar Series
Concentrator	Sample concentrator FSC400D, Techne
Grinder	Bosch Grinder MKM 6003
Hot Air Dryer	HG 2000 E, Steinel
HPLC-CAD	Dionex Ultimate 3000 Charged Aerosol
FT-IR	Bruker Tensor 27
Mass Spectrometer	Bruker Esquire Ion Trap
Nitrogen generator (SFC)	GENIUS NM32LA, Peak Scientific
NMR	Bruker NMR 500 MHz with cryo probe
Polarimeter	Perkin Elmer 341
Rotary Evaporator	Rotavapor R II, Büchi
Supercritical Fluid Chromatography	Prep 15 SFC Purification System, Waters
TLC Spray Cabinet	CAMAG TLC Spray Cabinet II
TLC Visualizer	CAMAG
Ultra-High Pressure Liquid Chromatography	ACQUITY UPLC H-Class System, Waters
Ultrasonic Bath	Transsonic T 460, Elma
UV Lamp	CAMAG
Vacuum Pump	V-710, Büchi
Vortex	Genius 3, IKA

6.5.2 Solvents and Reagents

Acetone,	Rectapur; ÖAB, distilled
Acetonitrile for HPLC,	Hypersolv Chromaorm VWR BDH 83639.320
CO_2 for SFC	Messer, S/No: 53172245, Quality 4.5, purity 99,995%
DMSO p.a.,	Emsure; Merck 1.02952.1000
DCM p.a.,	Rectapur; ÖAB, distilled VWR BDH 25631.362
Ethanol 96% p.a.,	ÖAB, distilled Brenntag CEE
Ethyl acetate p.a.,	Rectapur; ÖAB, distilled
H_2O for HPLC,	purified by ion exchanger
Methanol p.a.,	ÖAB, distilled
Methanol for HPLC,	HiPerSolv Chromaorm VWR BDH 83638.320, 16Z0432
N_2 for ASE	AlphagazTM 1 N2 , 99,999%, S/No: 102.020.121
n-Hexane p.a.,	Normapur; VWR BDH 24577.460
Petroleum ether 40 – 60°C,	Rectapur; VWR BDH 23826.464
Vanillin	ReagentPlus, 99%, Sigma-Aldrich, S/No: V1104
Sulphuric acid	ACS Reagent, 95.0-98.0 %, Sigma-Aldrich, S/No: 320501

6.5.3 UHPLC-Columns

Waters ACQUITY UPLC® BEH Phenyl 1.7 µm, 2,1 x 100mm Column, S/No: 01373502715781

Waters ACQUITY UPLC® BEH C18 1.7 µm, 2,1 x 50mm Column, S/No: 02533505015754

Waters ACQUITY UPLC® CSH™ C18 1.7 µm, 2,1 x 100mm Column, S/No: 01273504015754

Waters ACQUITY UPLC® CSH™ Fluoro-Phenyl 1.7 µm, 2,1 x 100mm Column, S/No: 01103504916012

Waters ACQUITY UPLC® HSS T3 1.8 µm, 2,1 x 100mm Column, S/No: 01643501416082

Waters ACQUITY UPLC® BEH C18 1.7 µm, 2,1 x 100mm Column, S/No: 02523502115739

6.5.4 SFC-Column

Waters Viridis® BEH 5 µm, 4.6 x 250mm Column, S/No: 01093504816102

6.5.5 HPLC-Column for HPLC-CAD

Agilent Zorbax SB-C18, 4.6 x 150 mm, 3.5 Micron

6.5.6 Spraying Reagents for TLC analysis

Vanillin/H_2SO_4 spraying reagent

Solution 1: 5 % methanolic H_2SO_4

15 ml concentrated H_2SO_4 are diluted with 285 ml MeOH

Solution 2: 1 % methanolic Vanillin solution

4 g Vanillin are dissolved in 400 ml MeOH

6.5.7 TLC-Plates

TLC silica gel 60 F_{254}, aluminum sheets 20 x 20 cm, 0.2 mm, Merck, 1.0554.0001

6.6 Parameters for Experimental Analysis

6.6.1 Optical Rotation

Optical rotations were measured at 20 °C in MeOH on a Perkin-Elmer 341 polarimeter (Perkin-Elmer Waltham, Massachusetts).

6.6.2 IR Measurements

IR spectra were acquired on a Bruker Tensor 27 spectrometer (Bruker, Billerica, Massachusetts).

6.6.3 NMR-Analysis for Structure Elucidation

1D- and 2D- NMR experiments were performed by using a Bruker spectrometer (Bruker, Billerica, Massachusetts) equipped with a Prodigy cryo probe, operating at 500 MHz. The samples (~1 mg) were measured in MeOD (calibrated to the residual nondeuterated solvent signals).

6.6.4 HRMS Measurements

High resolution mass spectroscopy (HR-MS) analyses were performed on a maXis HD ESI-Qq-TOF mass spectrometer (Bruker Daltonics, Bremen, Germany) equipped with electrospray ionization (ESI) in the positive and negative modes: capillary voltage, 2.0 to 4.5 kV (individually optimized); nebulizer, 0.4 bar (N_2); dry gas flow, 4 L/min (N_2); dry temperature, 200 °C. Samples were directly infused into the ESI source at a flow rate of 3 μL/min. Fragment ion spectra of the $[M+H]^+$, the $[M+Na]^+$ and either the $[M-H]^-$ or the $[M+HCOO]^-$ ion were recorded, whereby the collision energy was manually optimized. The sum formulas of the ions were determined using Bruker Compass DataAnalysis 4.2 based on the mass accuracy (Δ *m/z* ≤ 2 ppm for MS1 and ≤ 3 ppm for MS/MS) and isotopic pattern matching (SmartFormula algorithm).

7 REFERENCES

Websites:

Global Biodiversity Information Facility:
http://www.gbif.org/species/5249216/classification; Effective: July 2016

Mycoweb:
http://mycoweb-stv.ru/fungi/Submitted/ODG/ODG1_Gloeophyllum_odoratum_04_KVN_20091115.jpg; Effective: June 2016

Journal of Endocrinology:
http://joe.endocrinology-journals.org/content/212/2/99/F1.large.jpg; Effective: June 2016

Pilzforum:
http://www.pilzforum.eu/board/thema-gloeophyllum-odoratum-fenchelporling; Effective: August 2016

RCSB Protein Data Bank:
http://www.rcsb.org/pdb/images/1NN2_bio_r_500.jpg?bioNum=1; Effective: August 2016

Biology Tutorvista:
http://images.tutorvista.com/cms/images/38/influenza-virus.png; Effective: August 2016

Pharmacopeia Online:
http://www.uspbpep.com/bp2008/bp2008/bp_images/bp2008_v4_01_10_05_appendix_v/large/227opticalrotation_3_2008_56_eq.png; Effective: August 2016

Waters UPLC:
http://www.waters.com/waters/en_GB/UPLC---Ultra-Performance-Liquid-Chromatography-Beginner%27s-Guide/nav.htm?cid=134803622&locale=en_GB; Effective: August 2016

Waters SFC:
http://www.waters.com/waters/en_GB/Supercritical-Fluid-Chromatographx/nav.htm?locale=en_GB&cid=10145739; Effective: September 2016

Dionex:
http://www.dionex.com/en-us/webdocs/4035-BR-Dionex-ASE-150-350-BR70913_E.pdf; Effective: September 2016

Books:

Lindsay S. (1992) *High Performance Liquid Chromatography* – Analytical Chemistry by Open Learning (2nd edition). London: John Wiley & Sons, 264 pages.

Pharmacopoea Europaea, 8th edition, 2.2.7 "Optical Rotation"

Rösecke, J. (2000) Isolierung und Identifizierung von Inhaltsstoffen aus Holz zersetzenden Basidiomyceten, Dissertation, Univ. Hamburg.

Papers:

Anderson, C. G., Epstein, W. W. (1971). Metabolic intermediates in the biological oxidation of lanosterol to eburicoic acid. *Phytochemistry*, *10*(11), 2713–2717. https://doi.org/10.1016/S0031-9422(00)97269-8

Cateni, F., Lucchini, V., Zacchigna, M., Procida, G., Doljak, B., Anderluh, M. (2015). New Triterpenes from the Fungus *Gloeophyllum odoratum*. *Chem. Nat. Compd.*, *51*(1), 74–80. https://doi.org/10.1007/s10600-015-1207-x

Chang, S. T., Miles, P. G. (1992). Mushroom biology - a new discipline. *The Mycologist*, *6*(2), 64–65. https://doi.org/10.1016/S0269-915X(09)80449-7

Desfontaine, V., Guillarme, D., Francotte, E., Nováková, L. (2015). Supercritical fluid chromatography in pharmaceutical analysis. *J. Pharm. Biomed. Anal.*, *113*, 56–71. https://doi.org/10.1016/j.jpba.2015.03.007

Dresch, P., D´Aguanno, M. N., Rosam, K., Grienke, U., Rollinger, J. M., Peintner, U. (2015). Fungal strain matters: colony growth and bioactivity of the European medicinal polypores *Fomes fomentarius, Fomitopsis pinicola* and *Piptoporus betulinus*. *AMB Express*, *5*(1), 4. https://doi.org/10.1186/s13568-014-0093-0

Duru, M. E., Çayan, G. T. (2015). Biologically active terpenoids from mushroom origin: A review. *Rec. Nat. Prod.*, *9*(4), 456–483.

Grienke, U., Schmidtke, M., von Grafenstein, S., Kirchmair, J., Liedl, K. R., Rollinger, J. M. (2012). Influenza neuraminidase: A druggable target for natural products. *Nat. Prod. Rep.*, *29*(1), 11–36. https://doi.org/10.1039/C1NP00053E

Grienke, U., Zöll, M., Peintner, U., Rollinger, J. M. (2014). European medicinal polypores - A modern view on traditional uses. *J. of Ethnopharmacol.*, *154*(3), 564–583. https://doi.org/10.1016/j.jep.2014.04.030

Halsall, T. G., Hodges, R. (1954). The chemistry of the triterpenes and related compounds. Part XXIV. The conversion of polyporenic acid A into a lanosterol derivative. *J. Chem. Soc.(Resumed)*, (0), 2385. https://doi.org/10.1039/jr9540002385

Jagadesh, A., Salam, A. A. A., Mudgal, P. P., Arunkumar, G. (2016). Influenza virus neuraminidase (NA): a target for antivirals and vaccines. *Arch. Virol.*, *161*(8), 2087–2094. https://doi.org/10.1007/s00705-016-2907-7

Lindequist, U., Niedermeyer, T. H. J., Jülich, W.-D. (2005). The Pharmacological Potential of Mushrooms. *J. Evidence-Based Complementary Altern. Med.*, *2*(3), 285–299. https://doi.org/10.1093/ecam/neh107

Ma, L., Chen, H., Dong, P., Lu, X. (2013). Anti-inflammatory and anticancer activities of extracts and compounds from the mushroom Inonotus obliquus. *Food Chemistry*, *139*(1–4), 503–508. https://doi.org/10.1016/j.foodchem.2013.01.030

Money, N. P. (2016). Are mushrooms medicinal? *Fungal Biol.*, *120*(4), 449–453. https://doi.org/10.1016/j.funbio.2016.01.006

Moscona, A. (2005). Neuraminidase Inhibitors for Influenza. *N. Engl. J. Med.*, *353*(13), 1363–1373. https://doi.org/10.1056/NEJMra050740

Mueller, J. W., Gilligan, L. C., Idkowiak, J., Arlt, W., Foster, P. A. (2015). The Regulation of Steroid Action by Sulfation and Desulfation. *Endocr. Rev.*, *36*(5), 526–563. https://doi.org/10.1210/er.2015-1036

Nussbaumer, P., Billich, A. (2004). Steroid sulfatase inhibitors. *Med. Res. Rev.*, *24*(4), 529–576. https://doi.org/10.1002/med.20008

Purohit, A., Foster, P. A. (2012). Steroid sulfatase inhibitors for estrogen- and androgen-dependent cancers. *J. Endocrinol.*, *212*(2), 99–110. https://doi.org/10.1530/JOE-11-0266

Quin, M. B., Flynn, C. M., Schmidt-Dannert, C. (2014). Traversing the fungal terpenome. *Nat. Prod. Rep.*, *31*(10), 1449–73. https://doi.org/10.1039/c4np00075g

Rižner, T. L. (2016). The Important Roles of Steroid Sulfatase and Sulfotransferases in Gynecological Diseases. *Front. Pharmacol.*, *7*(February), 1–16. https://doi.org/10.3389/fphar.2016.00030

Rösecke, J., König, W. A. (2000). Constituents of various wood-rotting basidiomycetes. *Phytochemistry*, *54*(6), 603–610. https://doi.org/10.1016/S0031-9422(00)00165-5

Shah, R., Singh, J., Singh, D., Jaggi, A. S., Singh, N. (2016). Sulfatase inhibitors for recidivist breast cancer treatment: A chemical review. *Eur. J. Med. Chem.*, *114*, 170–190. https://doi.org/10.1016/j.ejmech.2016.02.054

Sliva, D. (2006). Ganoderma lucidum in cancer research. *Leuk. Res.*, *30*(7), 767–768. https://doi.org/10.1016/j.leukres.2005.12.015

Stamets, P., Zwickey, H. (2014). Medicinal Mushrooms: Ancient Remedies Meet Modern Science. *Integrative Medicine: A Clinician's Journal*, *13*(1), 46–47. Retrieved from http://www.ncbi.nlm.nih.gov/pubmed/26770081

Taji, S., Yamada, T., Wada, S., Tokuda, H., Sakuma, K., Tanaka, R. (2008). Lanostane-type triterpenoids from the sclerotia of Inonotus obliquus possessing anti-tumor promoting activity. *Eur. J. Med. Chem.*, *43*(11), 2373–2379. https://doi.org/10.1016/j.ejmech.2008.01.037

Wasser, S. P. (2011). Current findings, future trends, and unsolved problems in studies of medicinal mushrooms. *App. Microbiol. Biotechnol.*, *89*(5), 1323–1332. https://doi.org/10.1007/s00253-010-3067-4

I have endeavored to find all owners of the image rights and to obtain their consent to the use of the pictures in this work. If nevertheless a copyright infringement becomes known, I request for message with me.

8 APPENDIX

8.1 Generation of an Extraction Protocol with ASE for non-polar Triterpenes for Subsequent Separation with SFC

8.1.1 HPLC-CAD Chromatograms of *Ganoderma lucidum* for Preliminary Tests

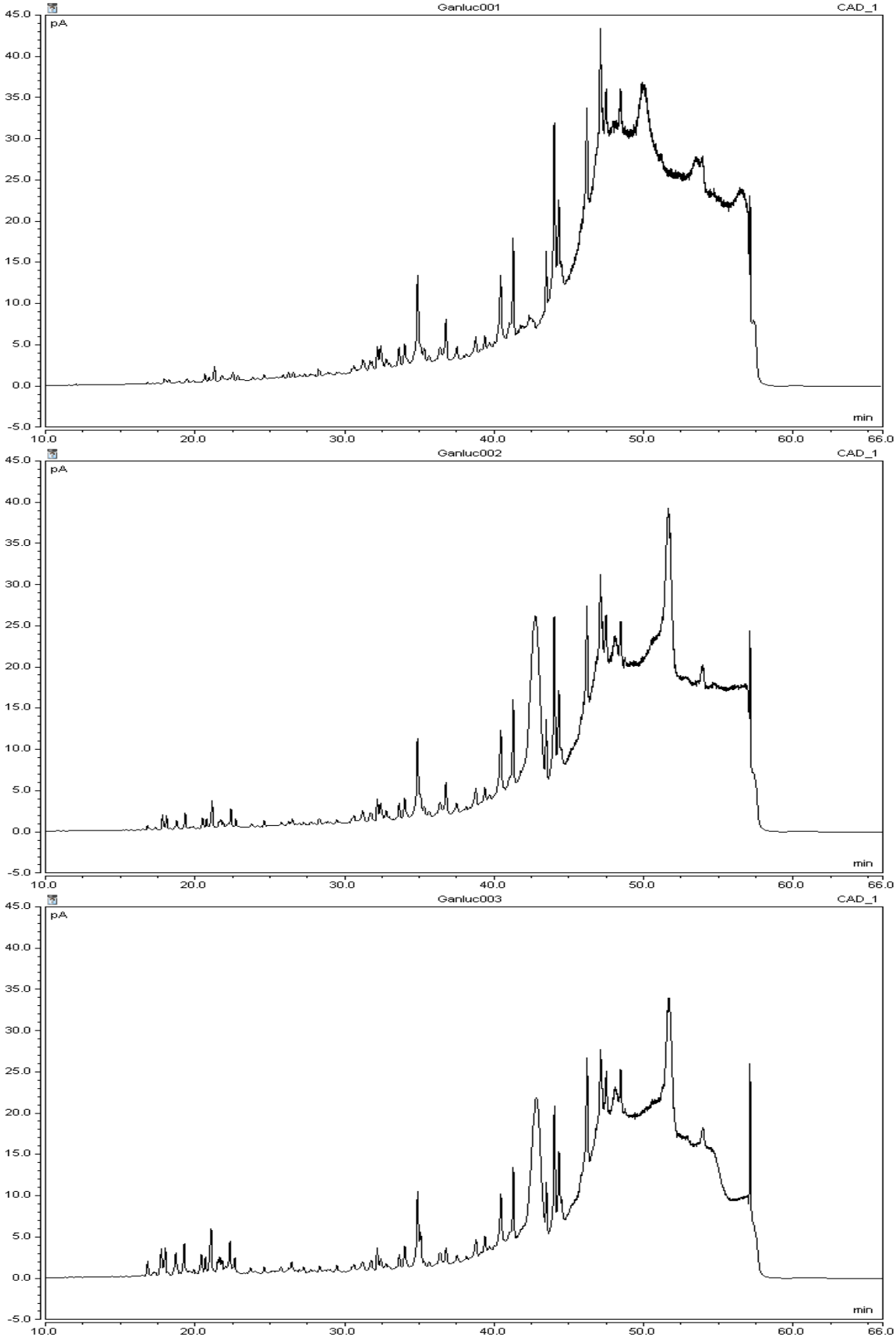

Figure 35 – Ganluc001-003

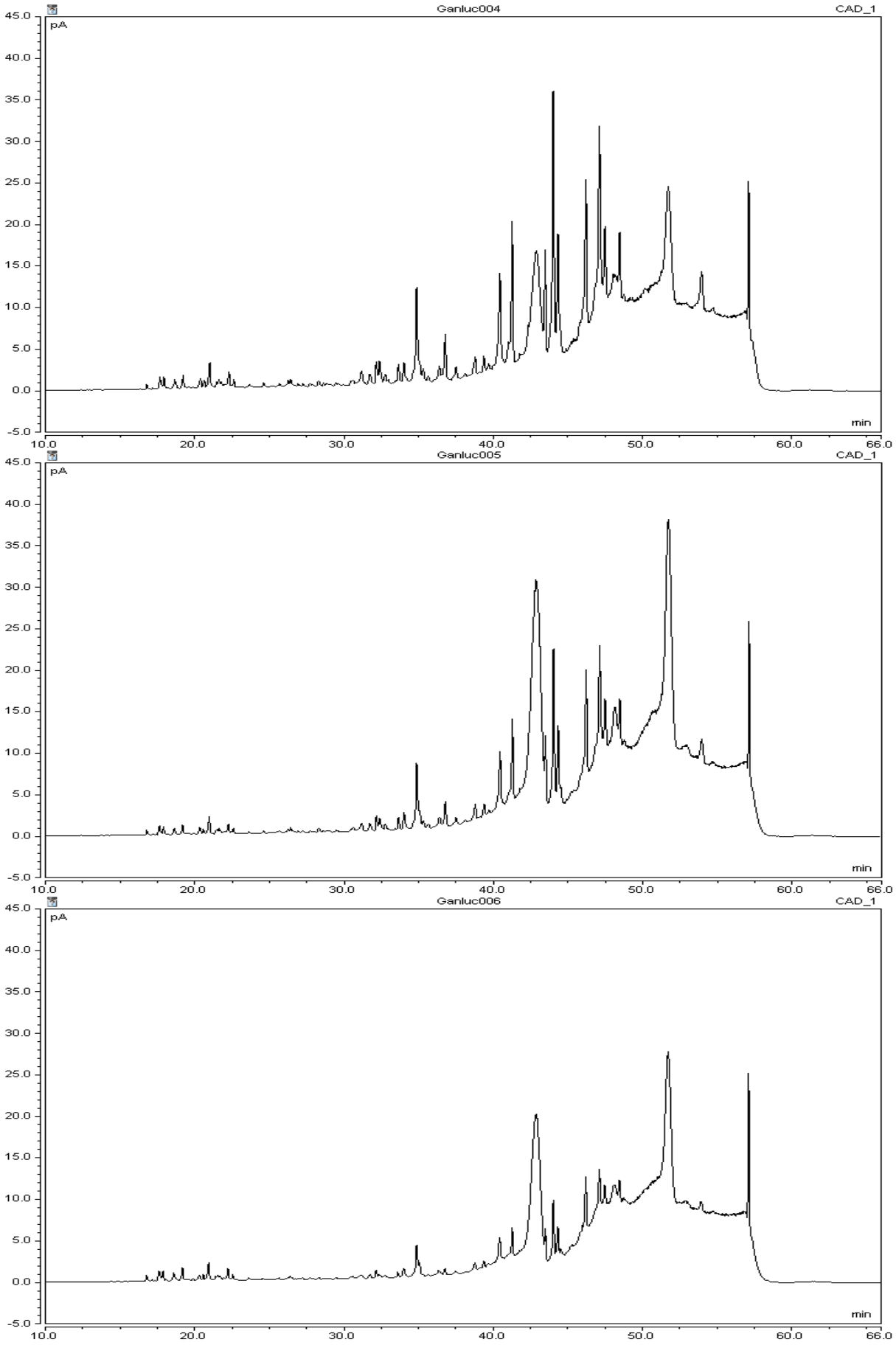

Figure 36 – Ganluc004-006

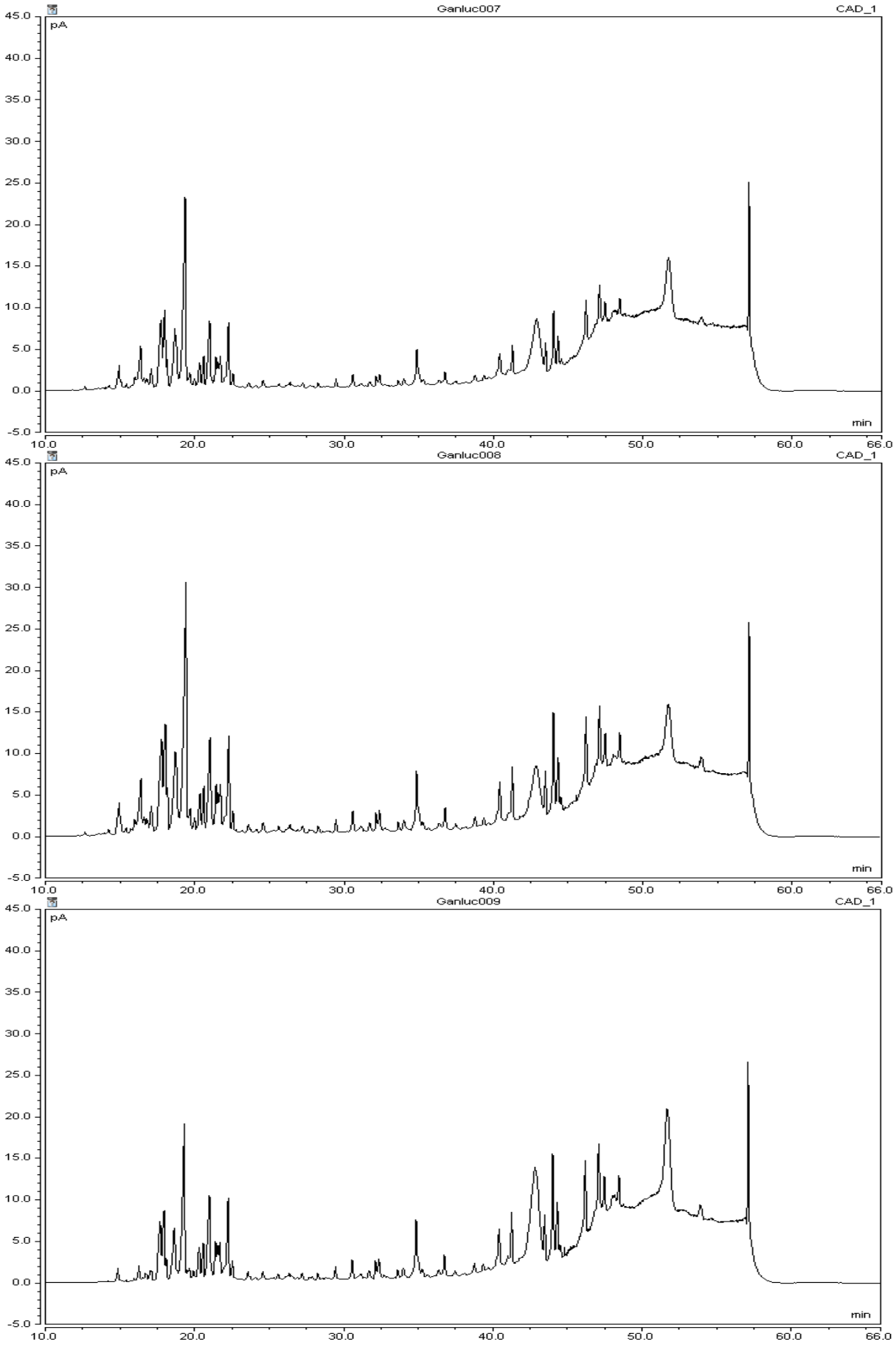

Figure 37 – Ganluc007-009

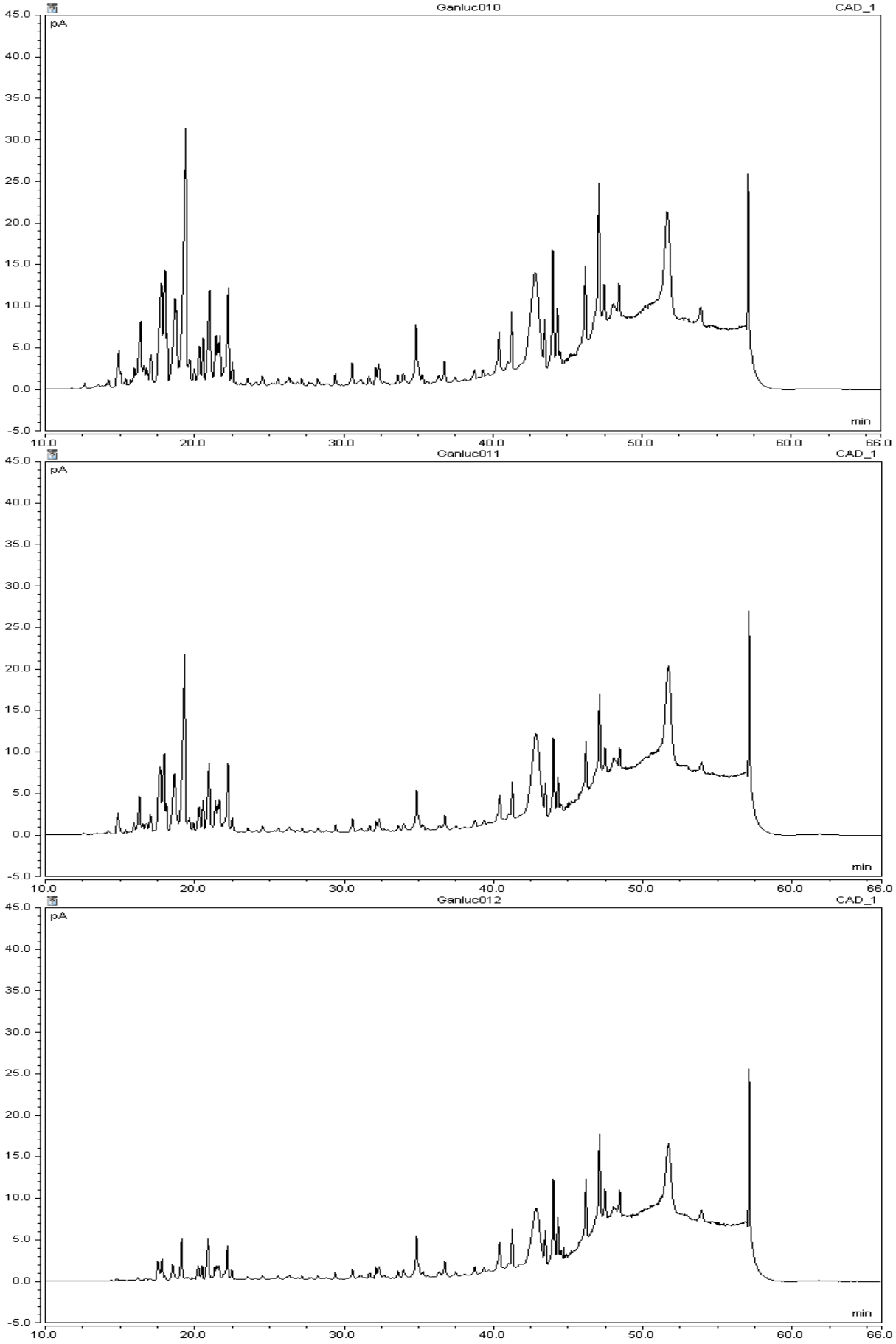

Figure 38 - Ganluc010-012

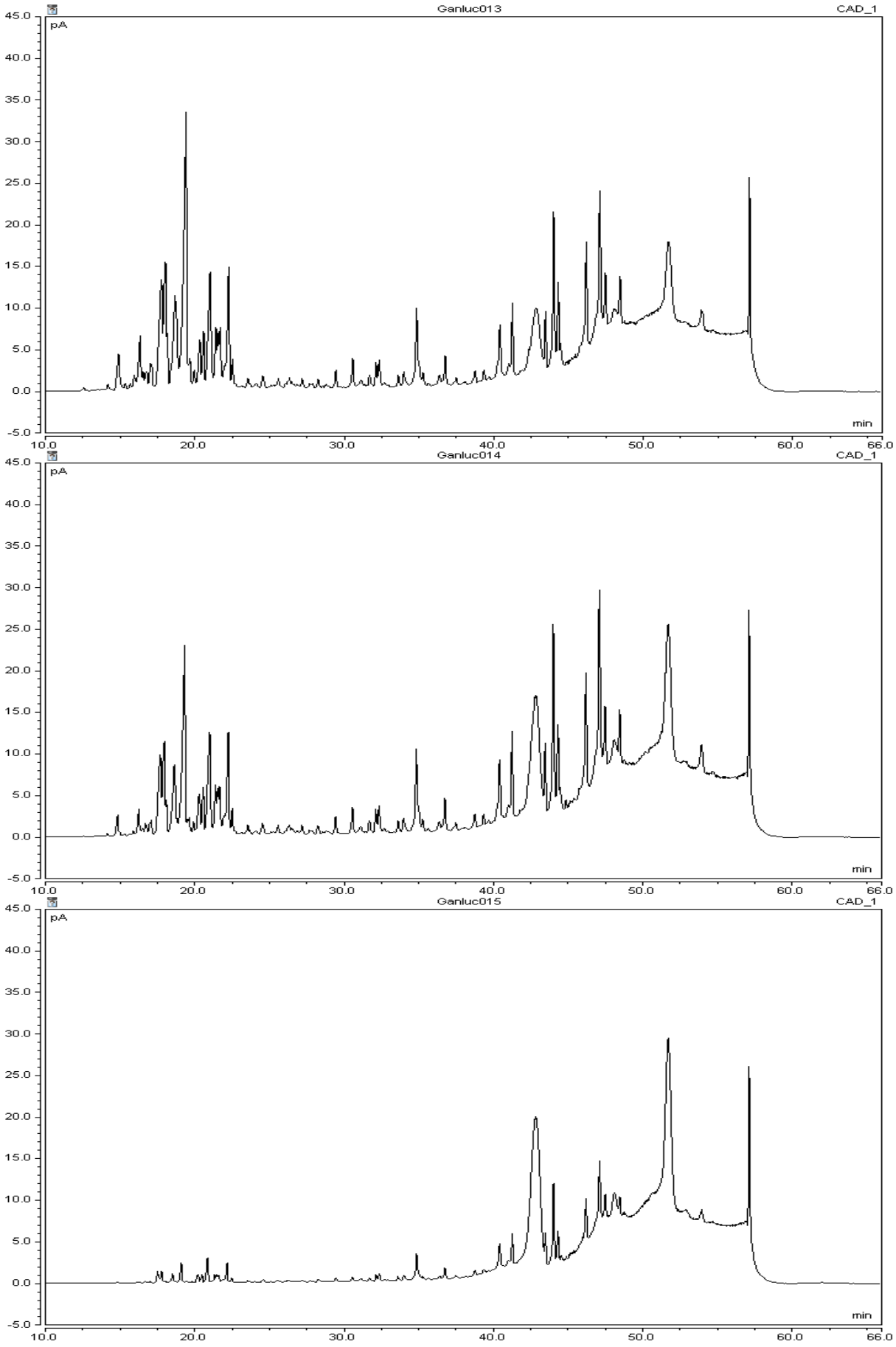

Figure 39 - Ganluc013-015

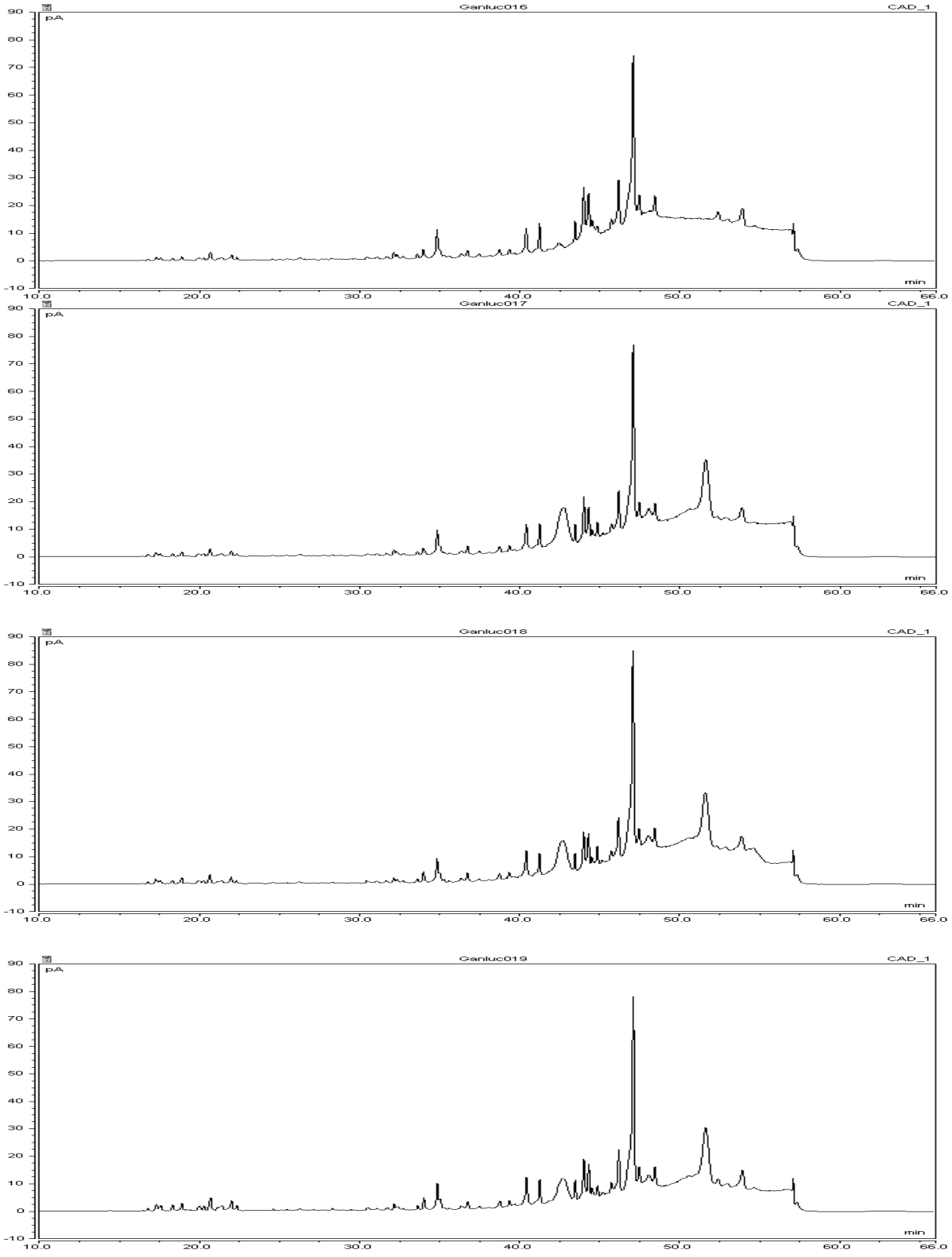

Figure 40 – Ganluc016-019

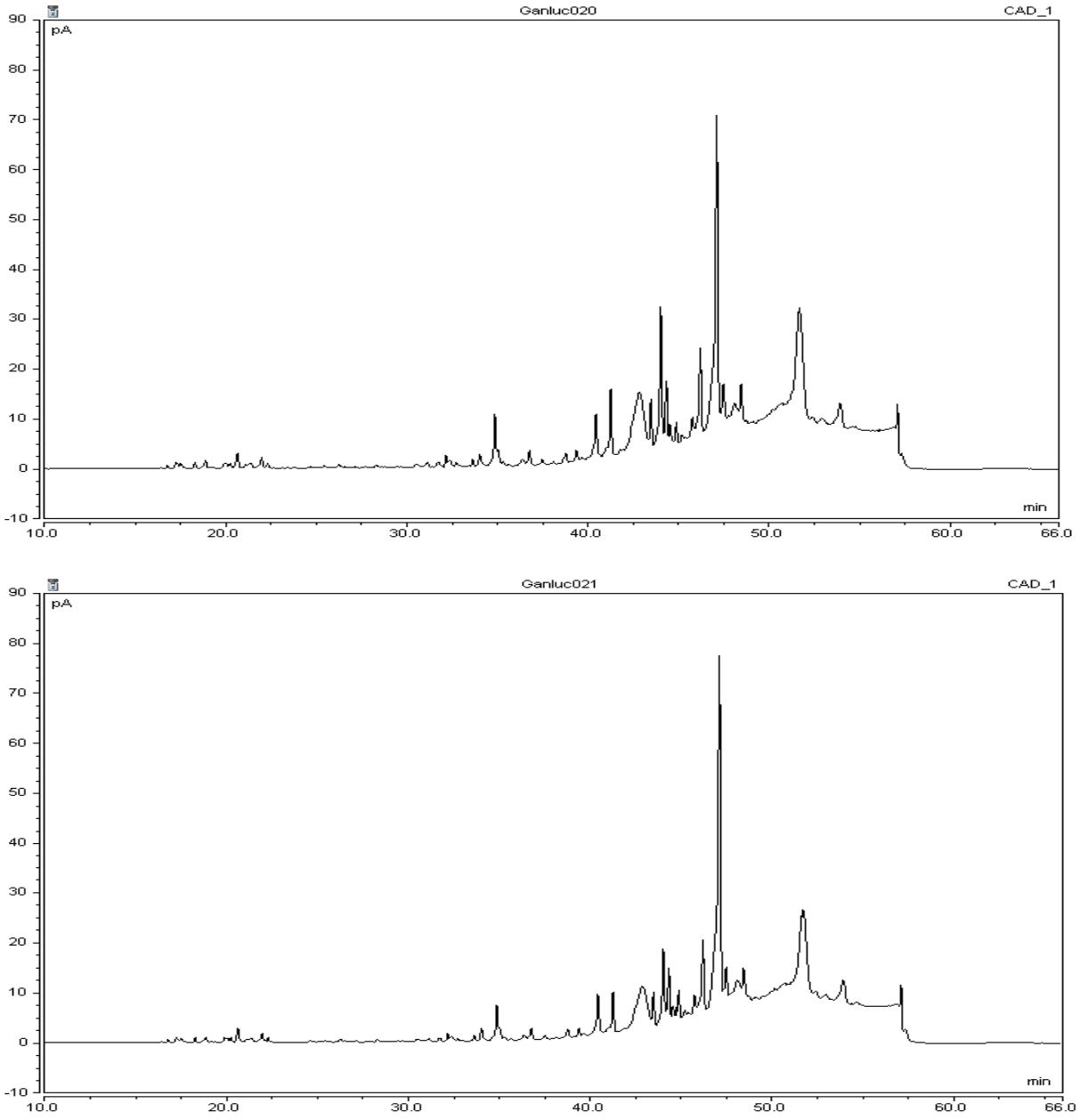

Figure 41 – Ganluc020-021

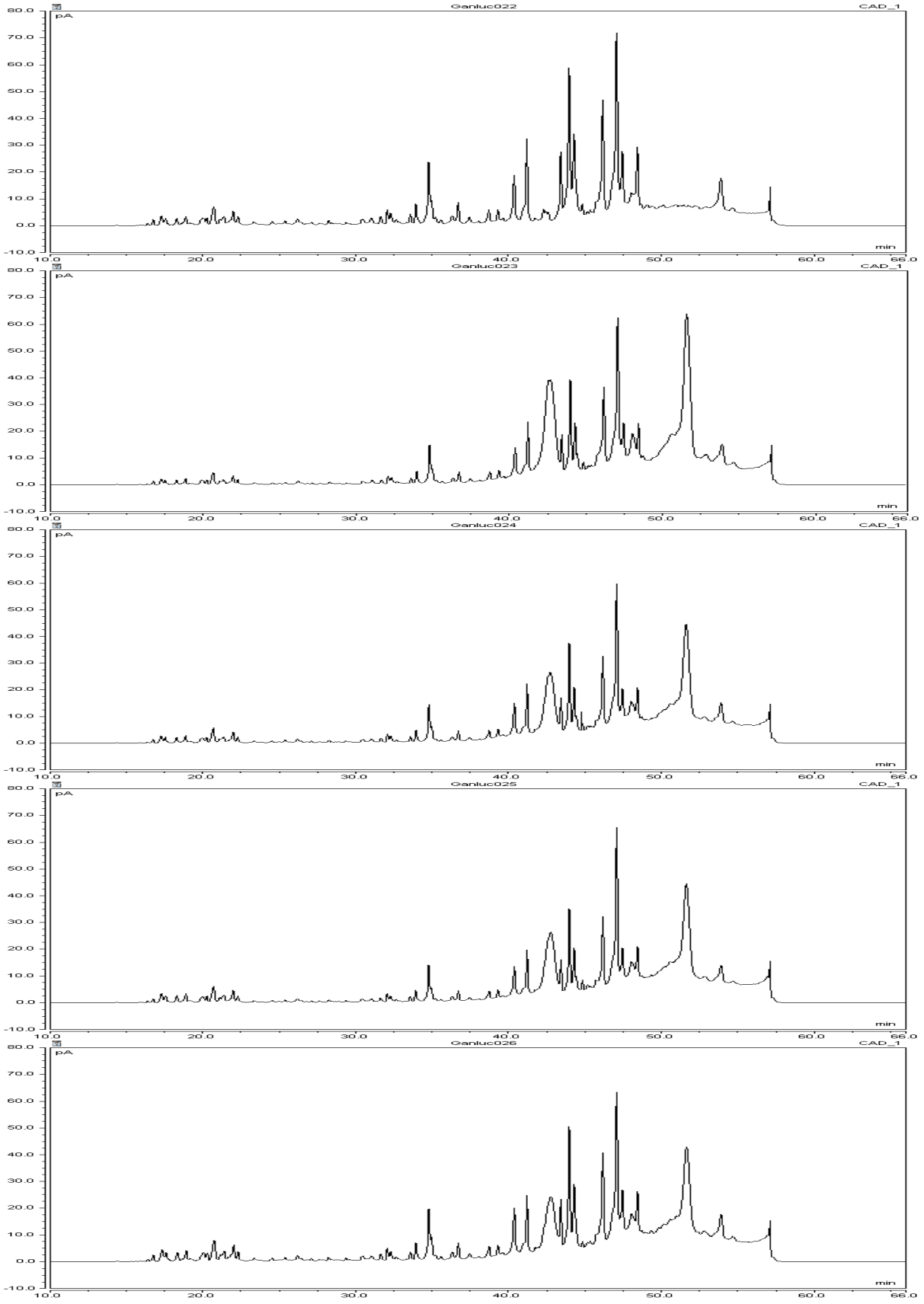

Figure 42 – Ganluc022-026

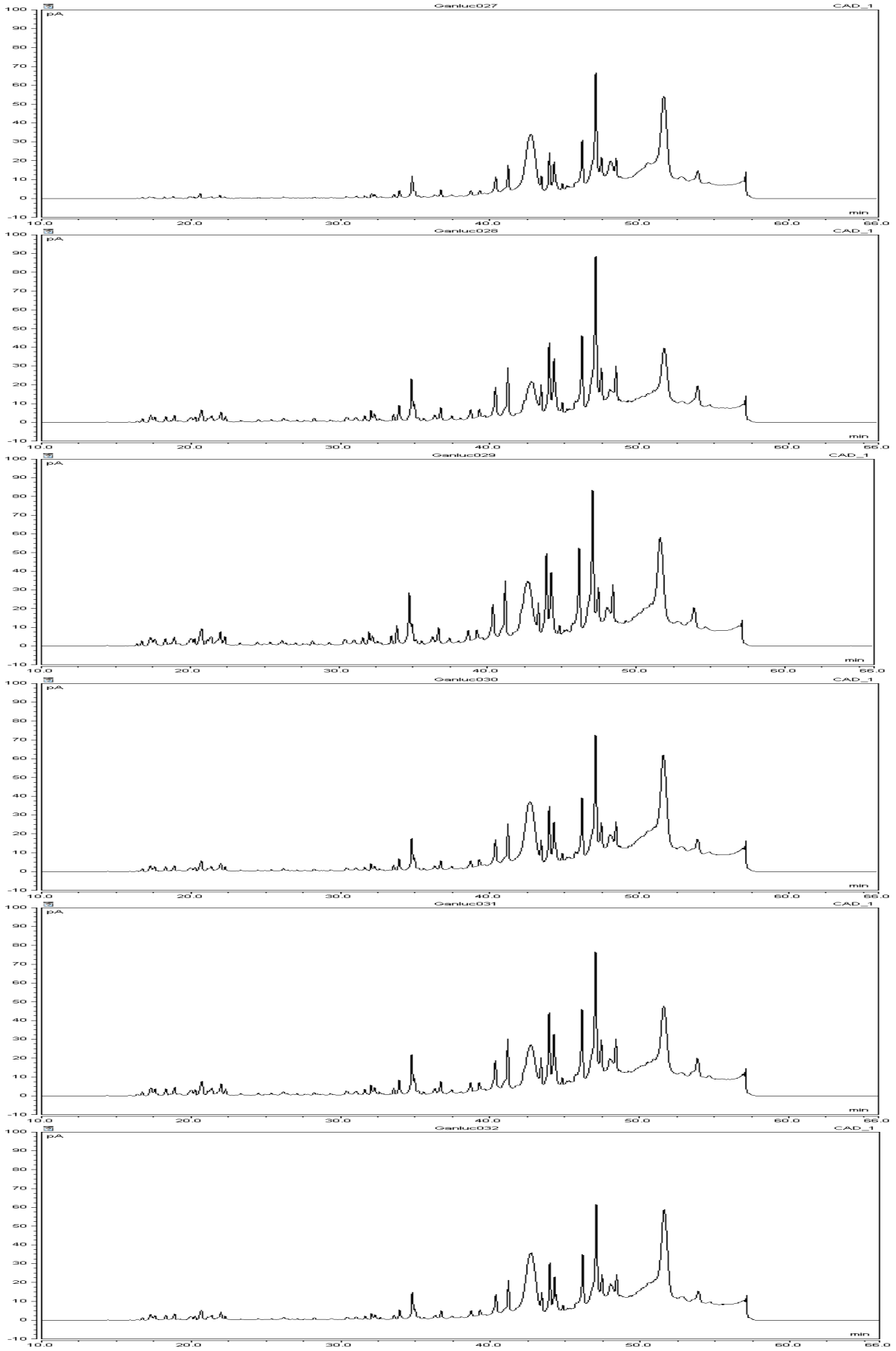

Figure 43 - Ganluc027-029

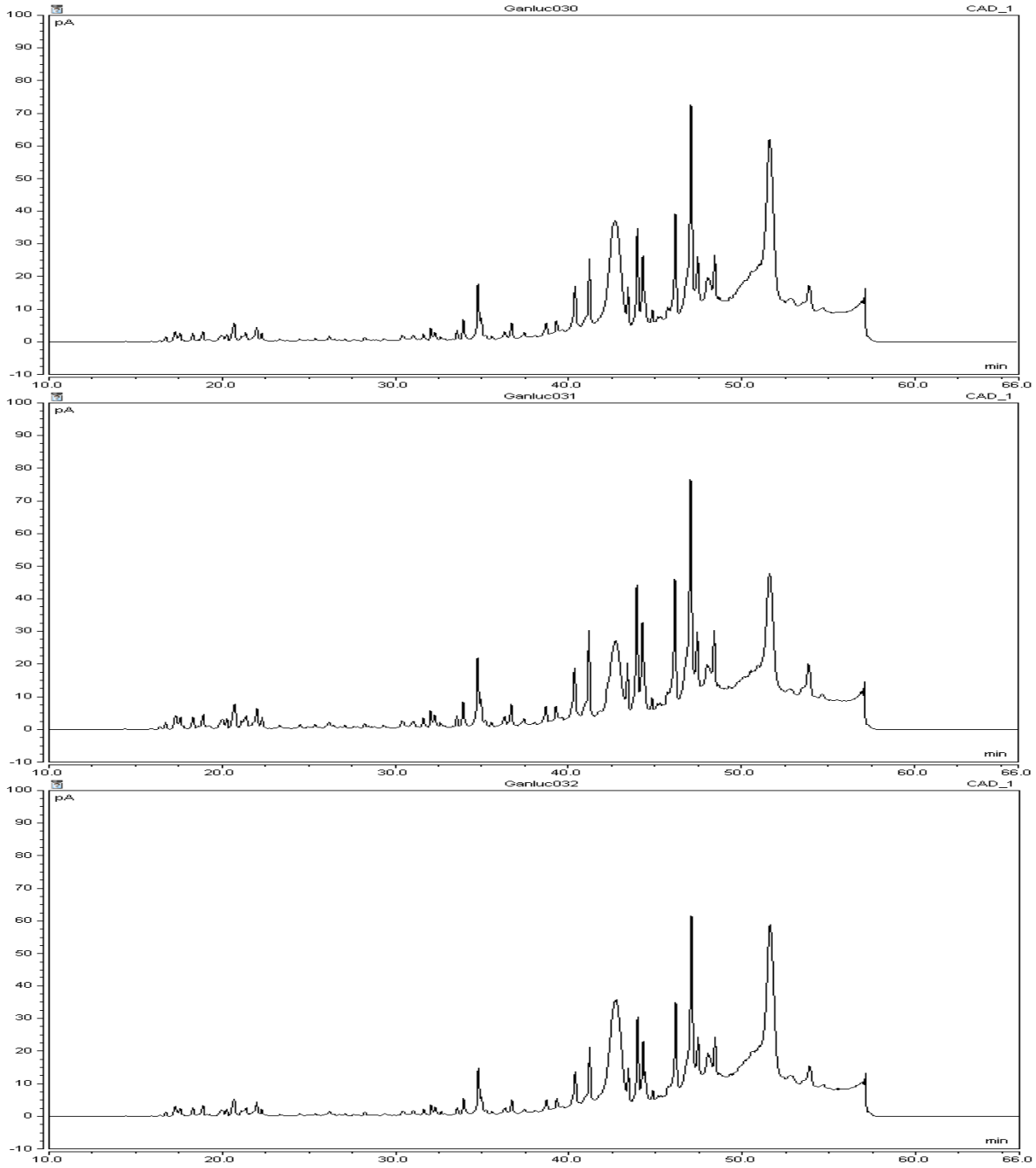

Figure 44 – Ganluc027-023

8.1.2 HPLC-CAD Chromatograms of Mushroom Extracts

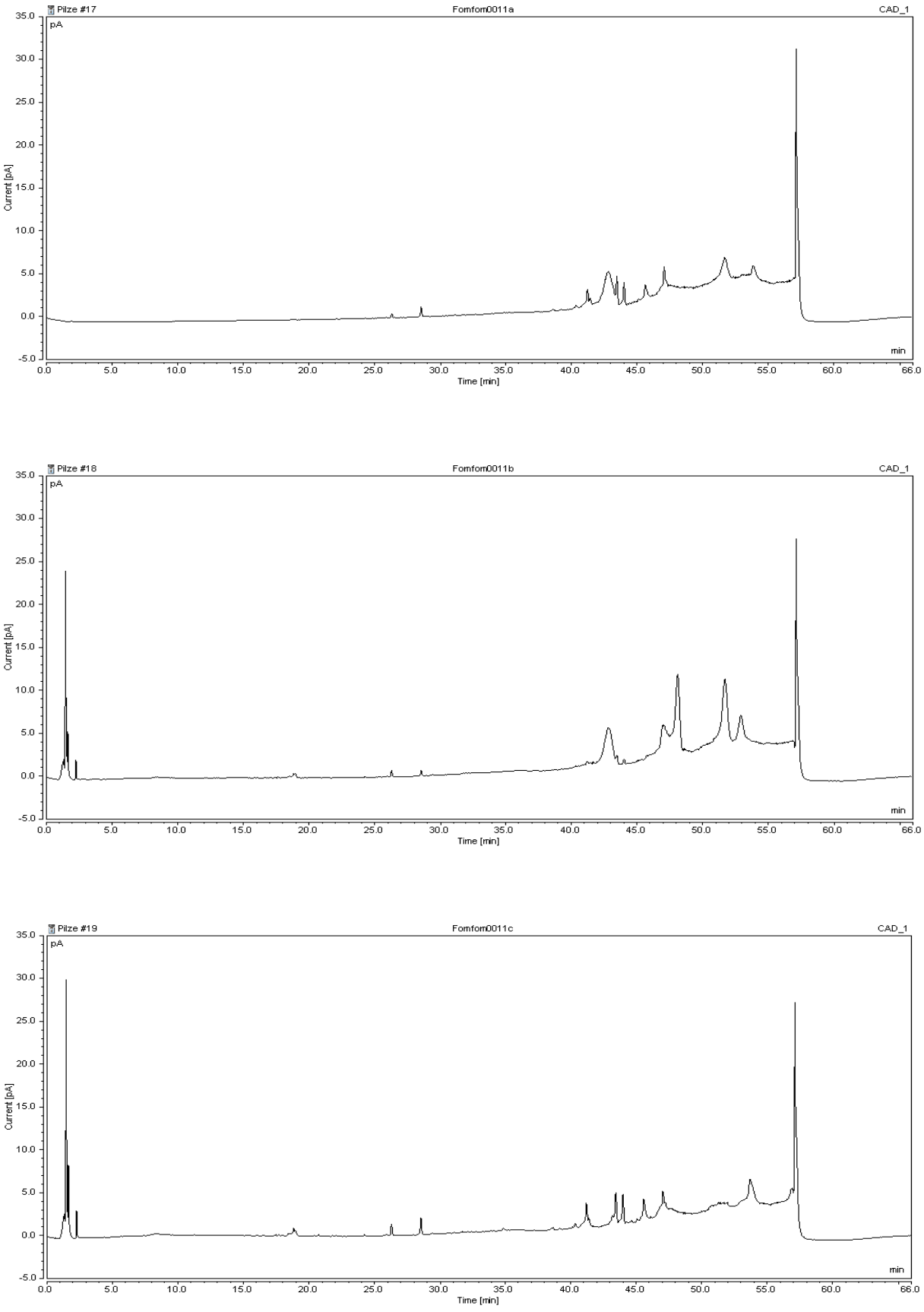

Figure 45 - Fomfom0011a-c

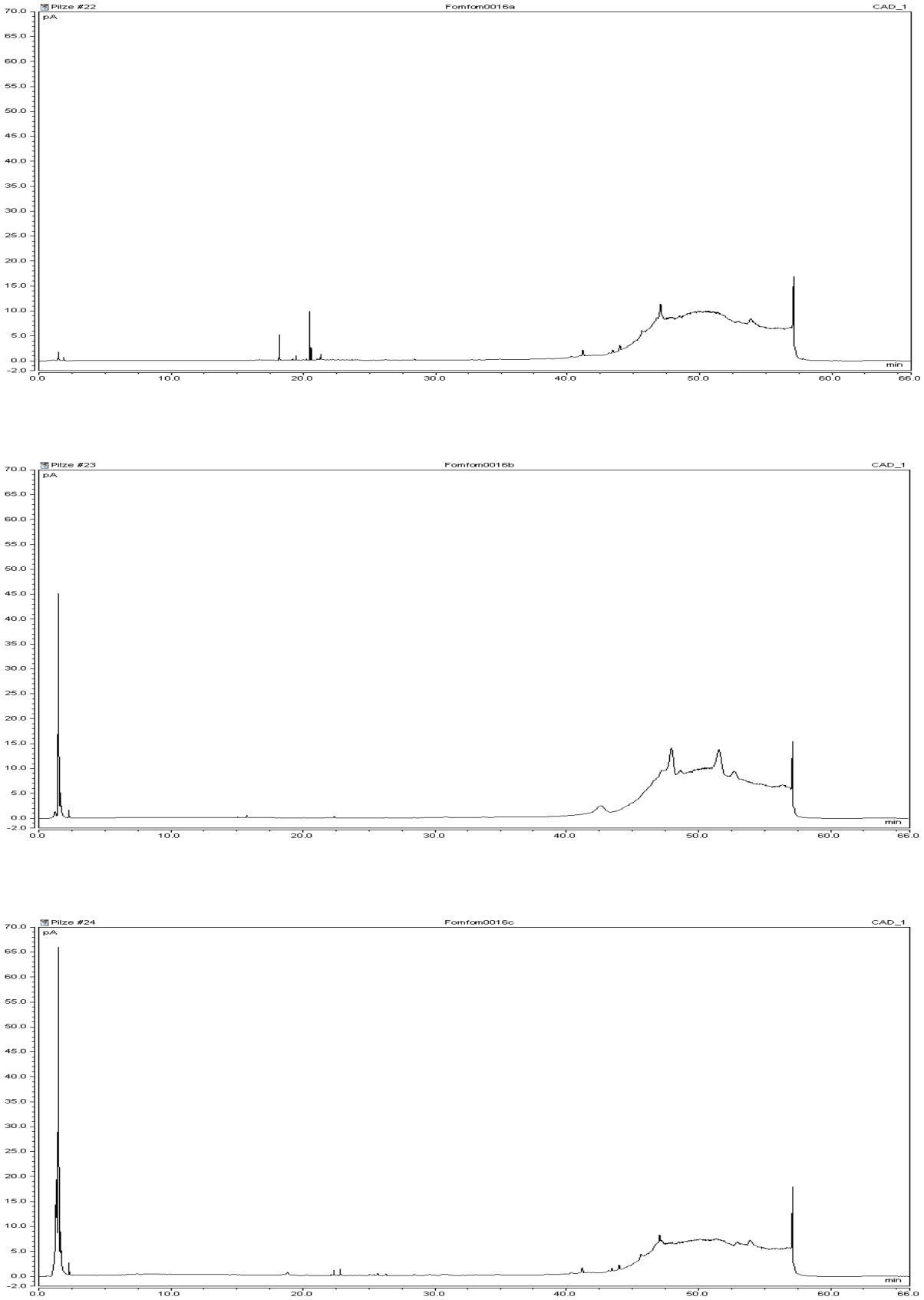

Figure 46 - Fomfom0016a-c

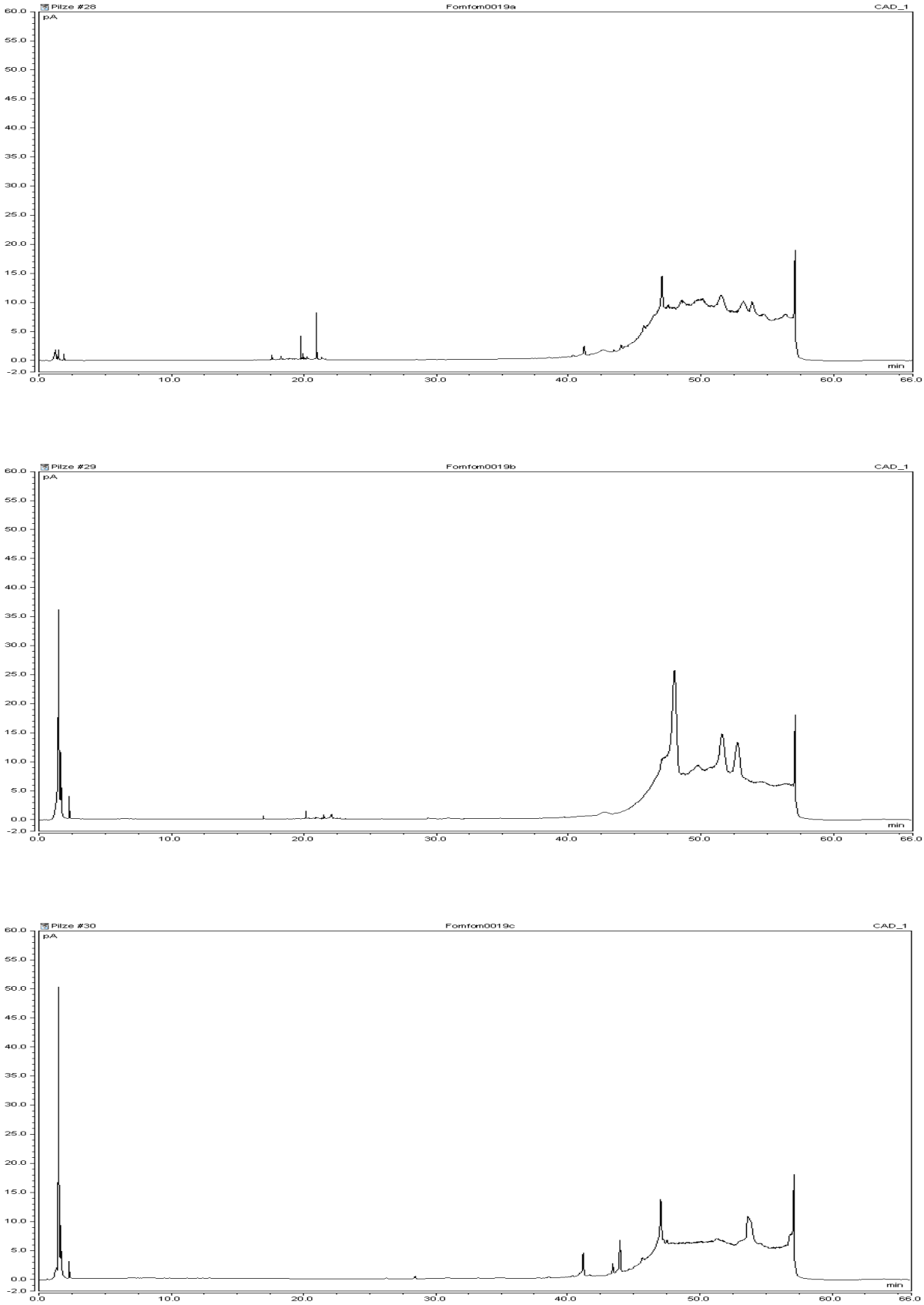

Figure 47 - Fomfom0019a-c

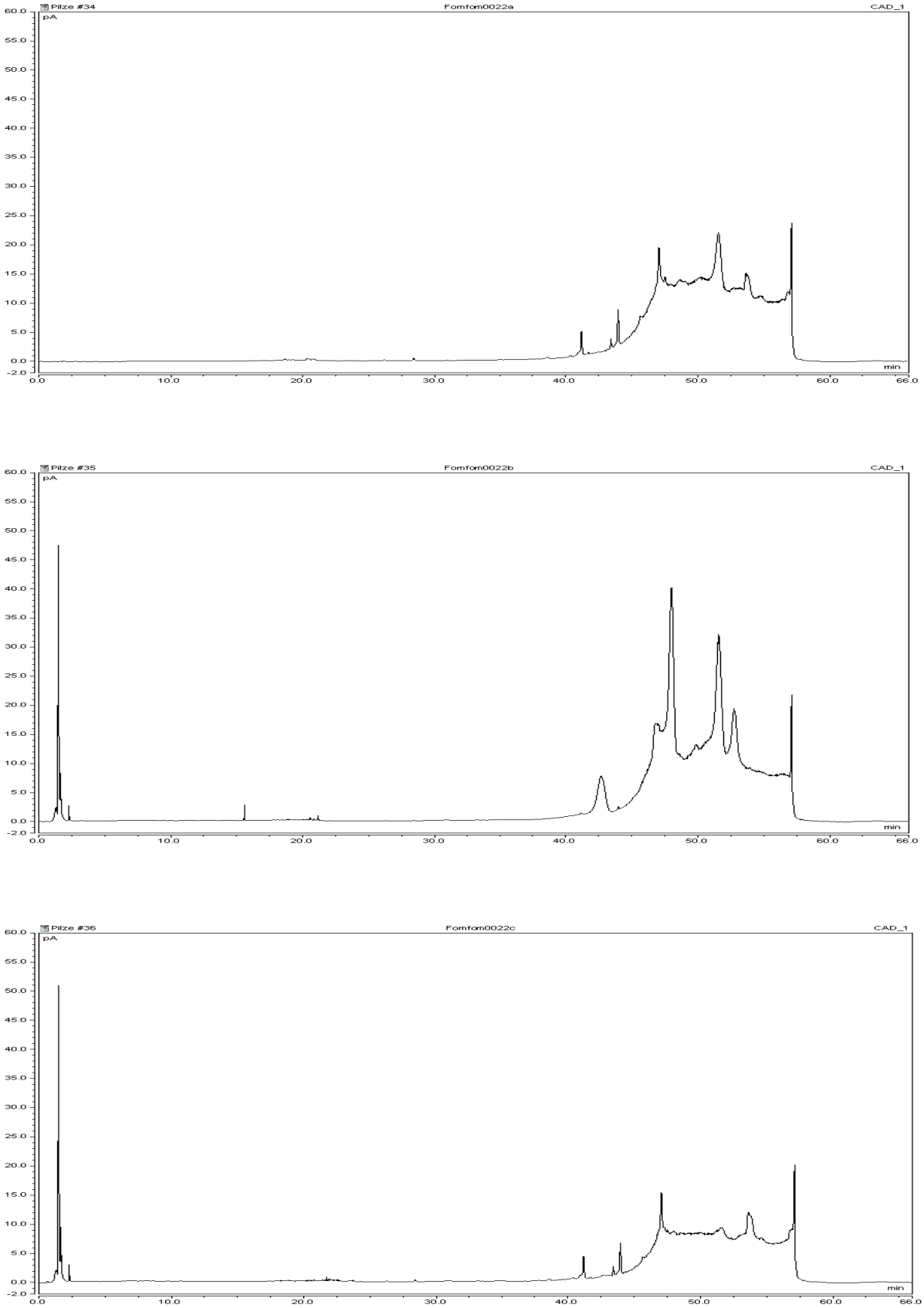

Figure 48 - Fomfom0022a-c

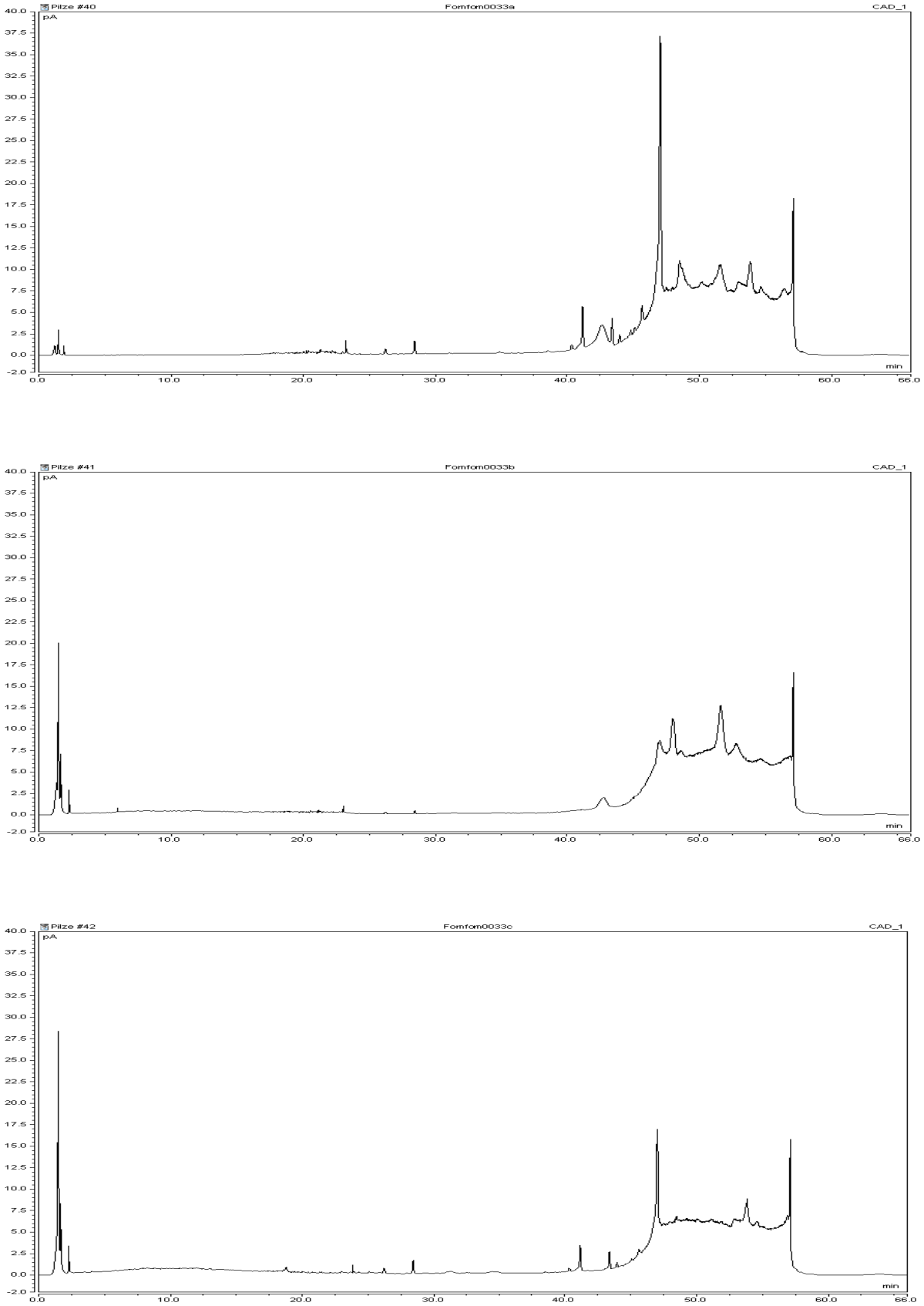

Figure 49 - Fomfom0033a-c

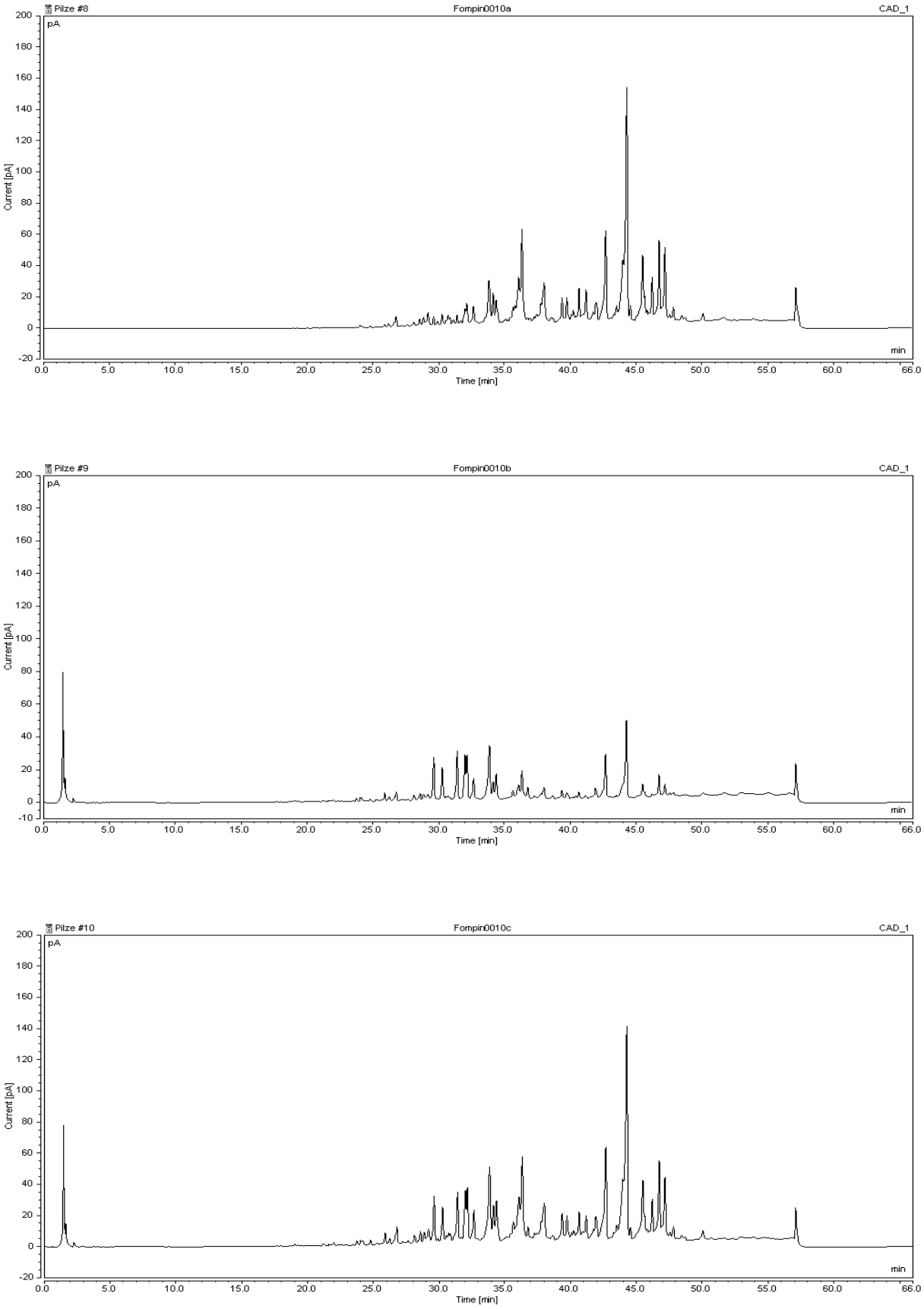

Figure 50 - Fompin0010a-c

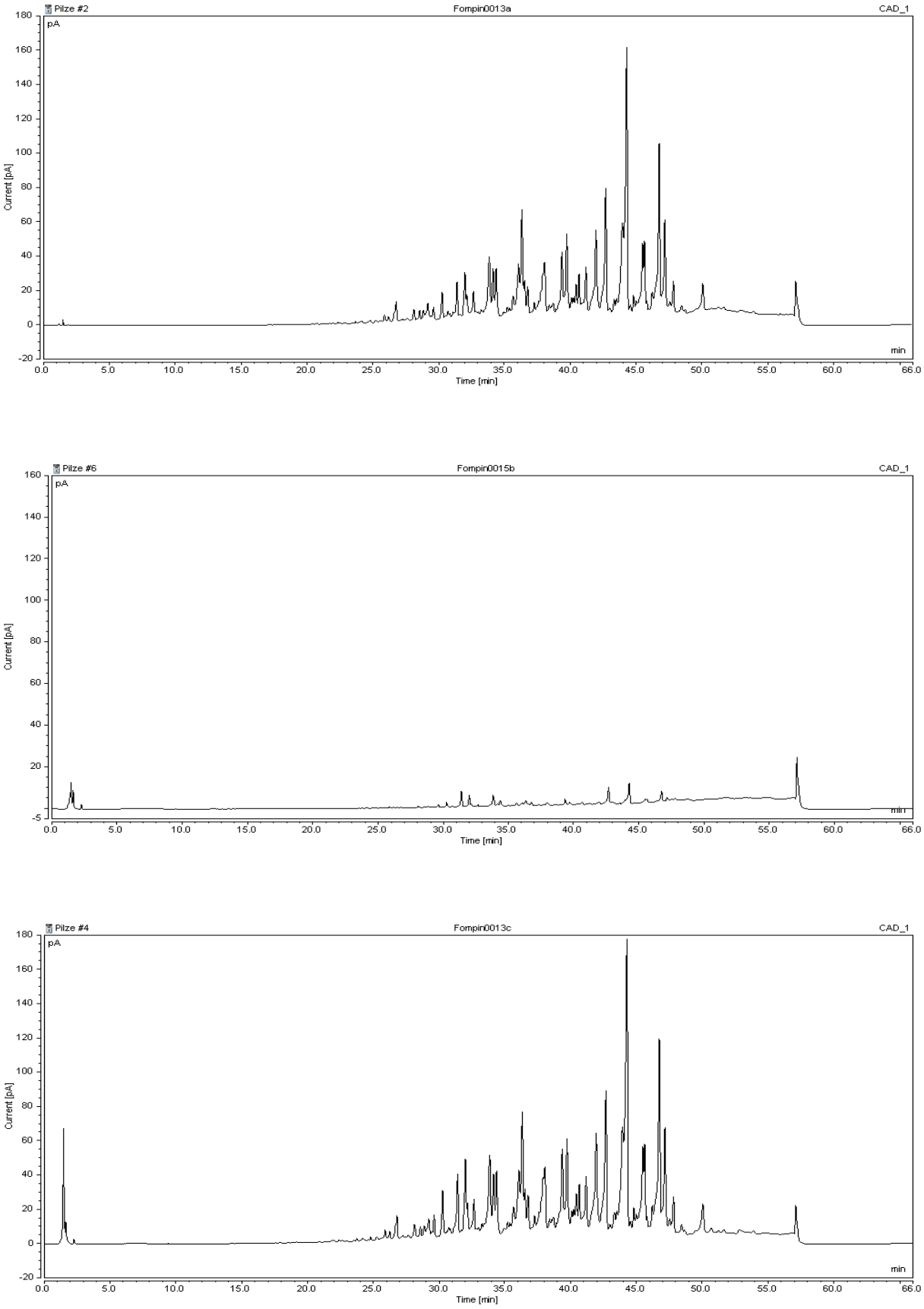

Figure 51 - Fompin0013a-c

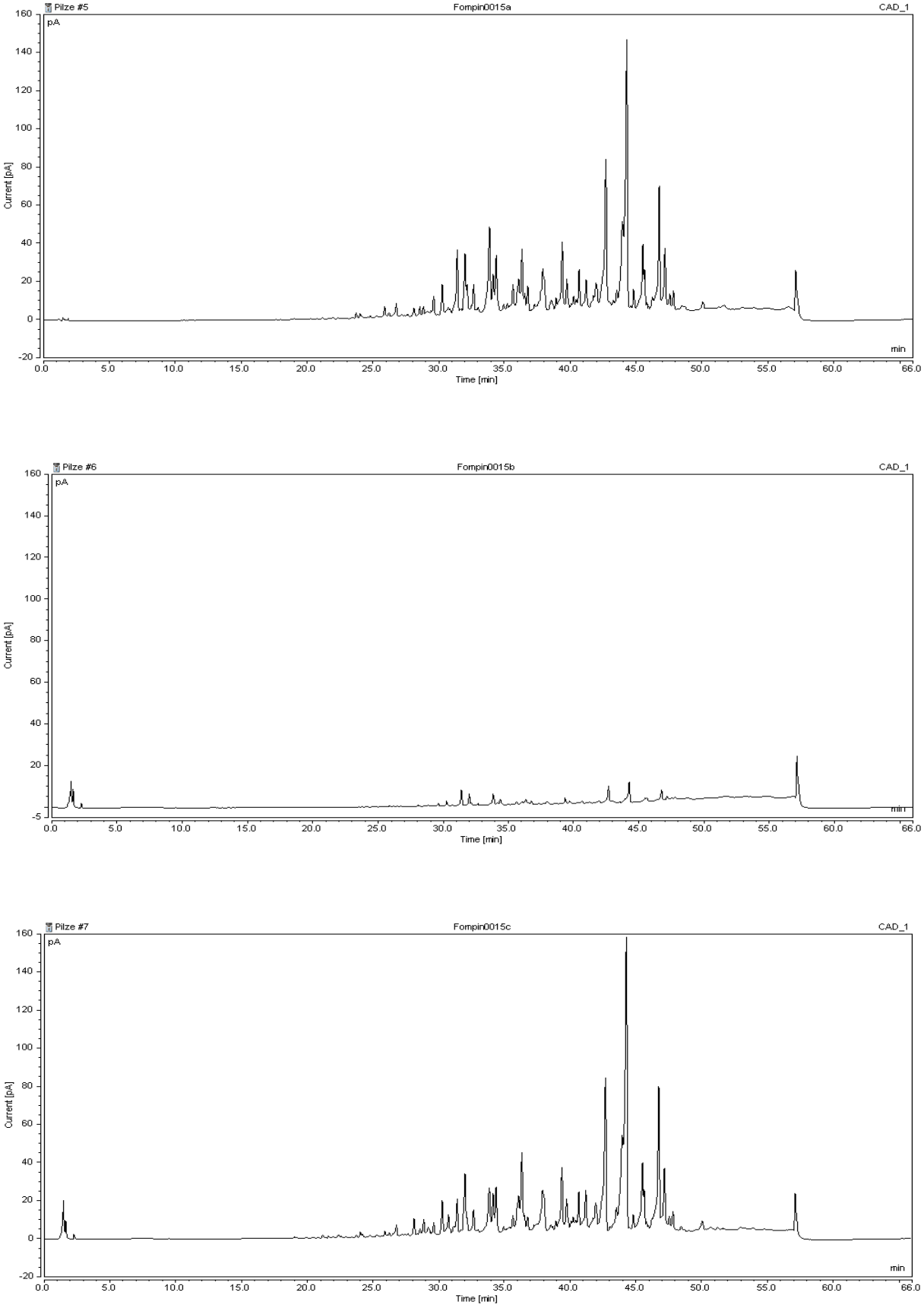

Figure 52 - Fompin0015a-c

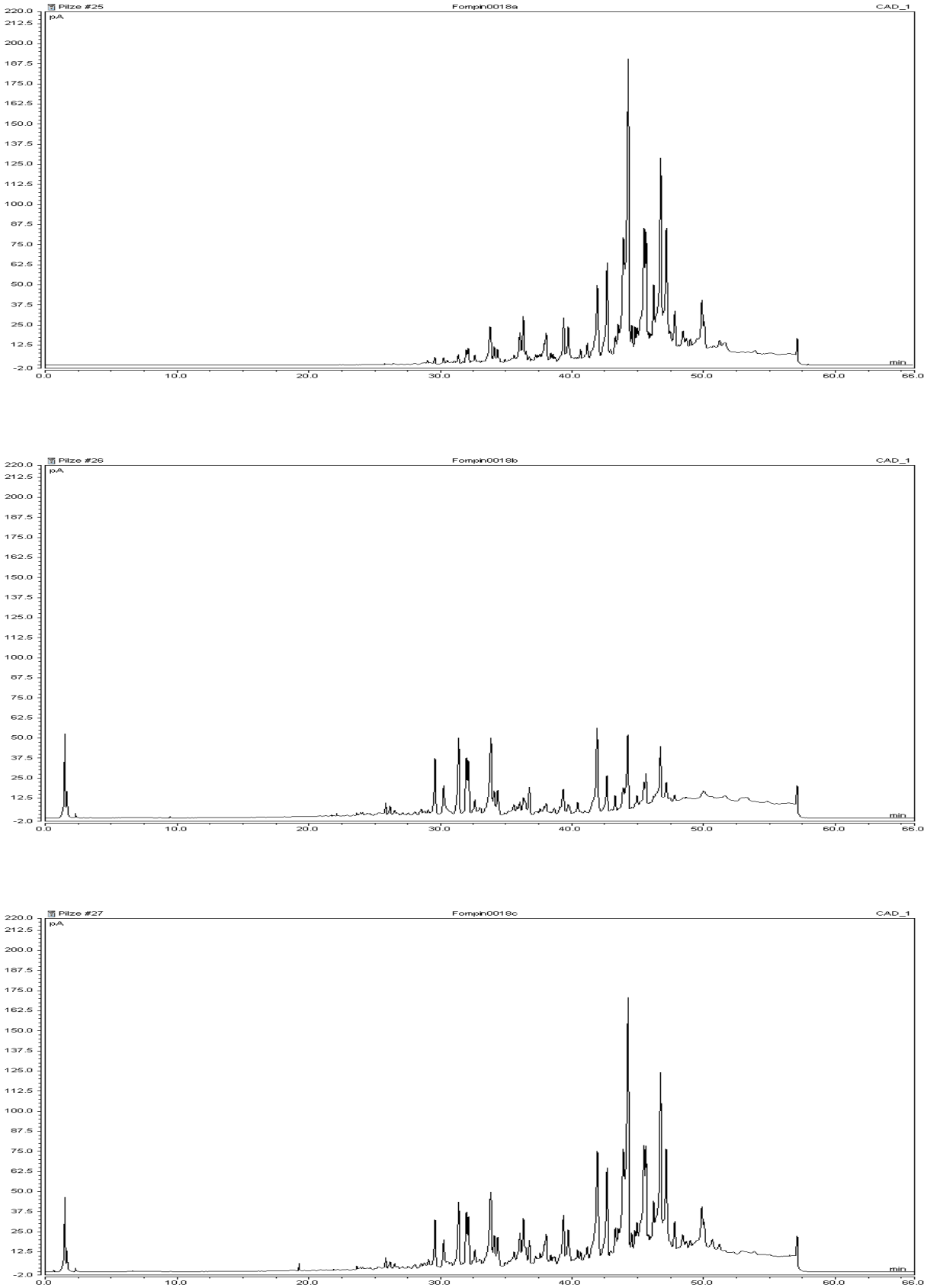

Figure 53 - Fompin0018a-c

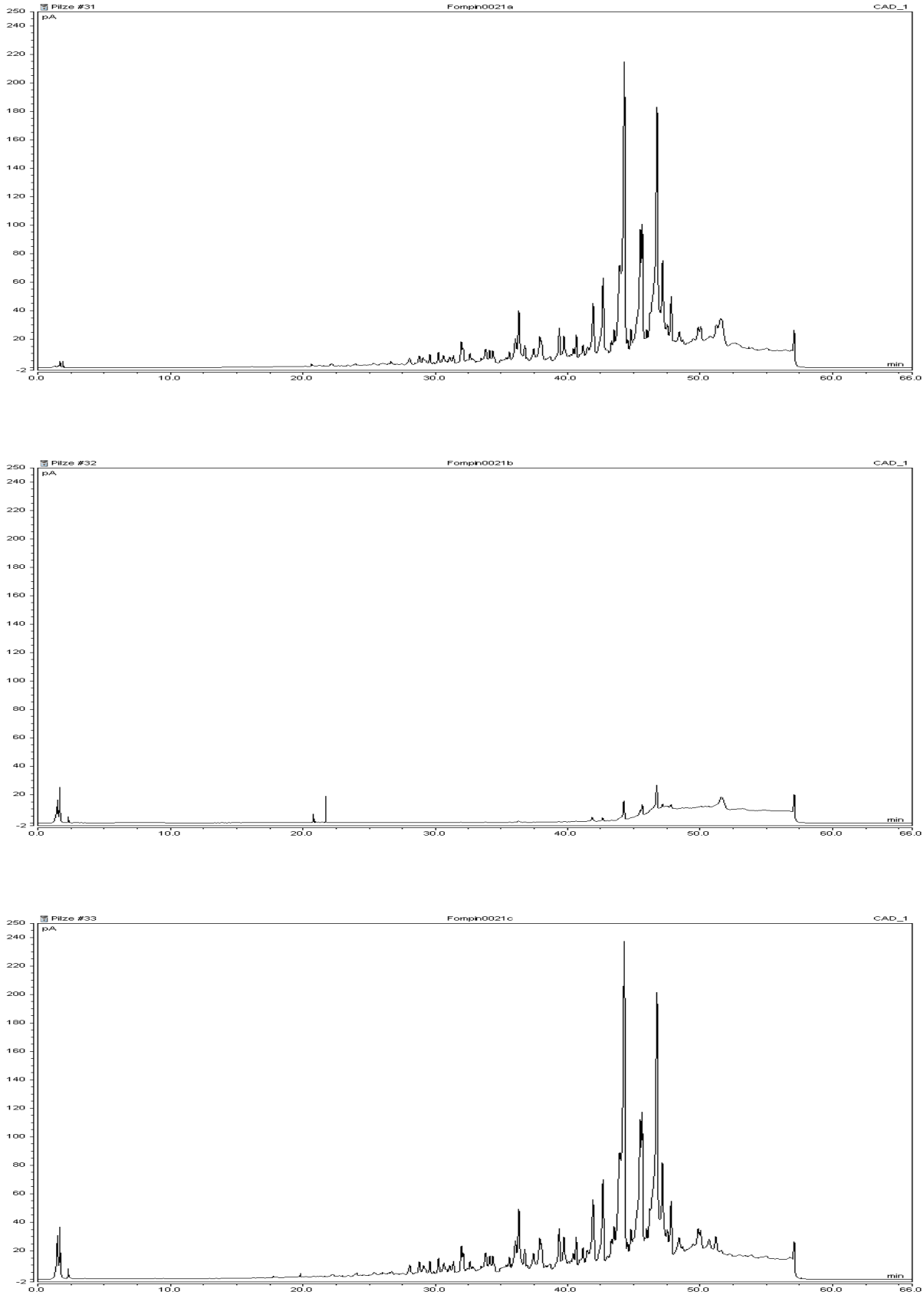

Figure 54 - Fompin0021a-c

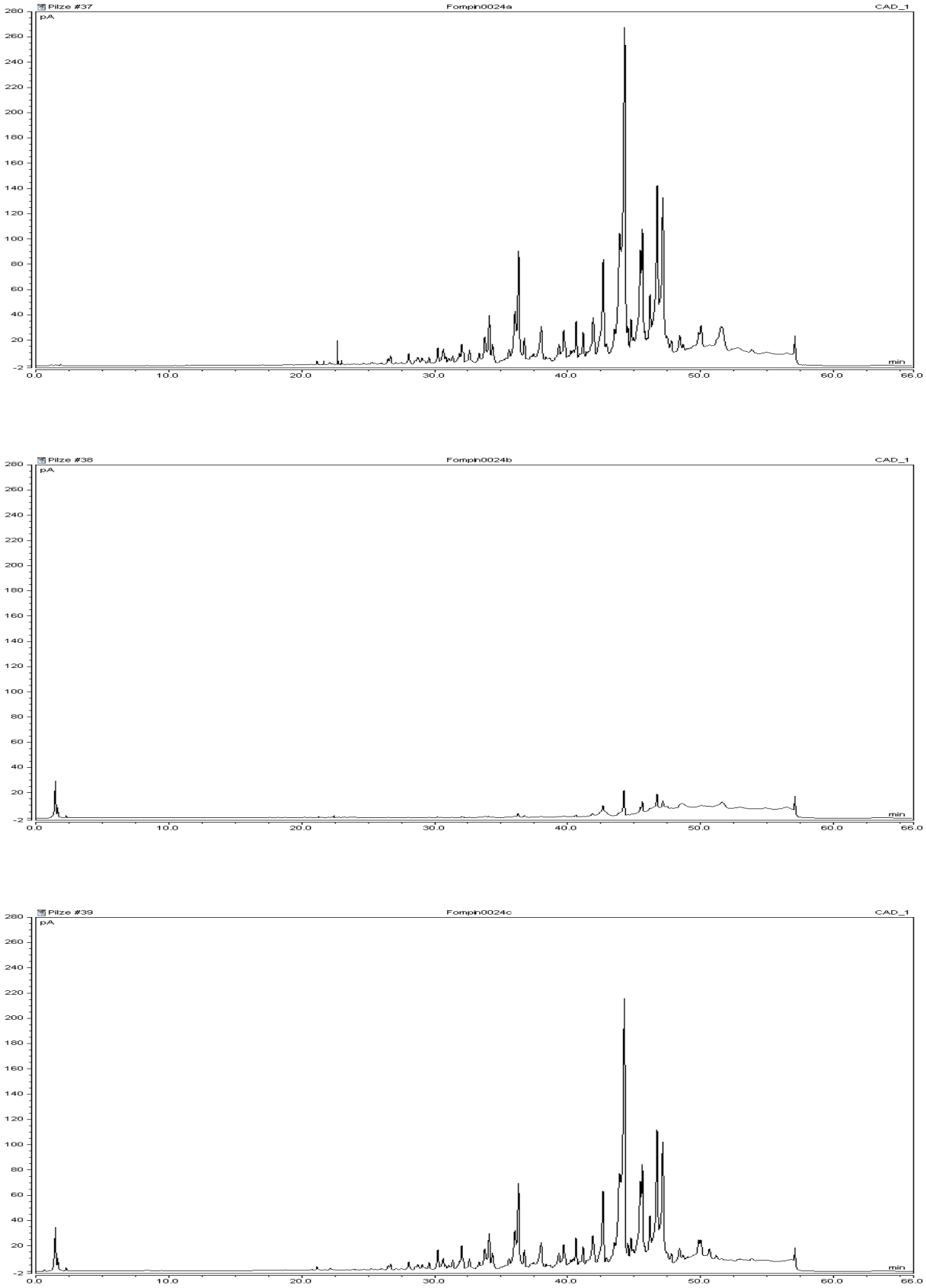

Figure 55 - Fompin0024a-c

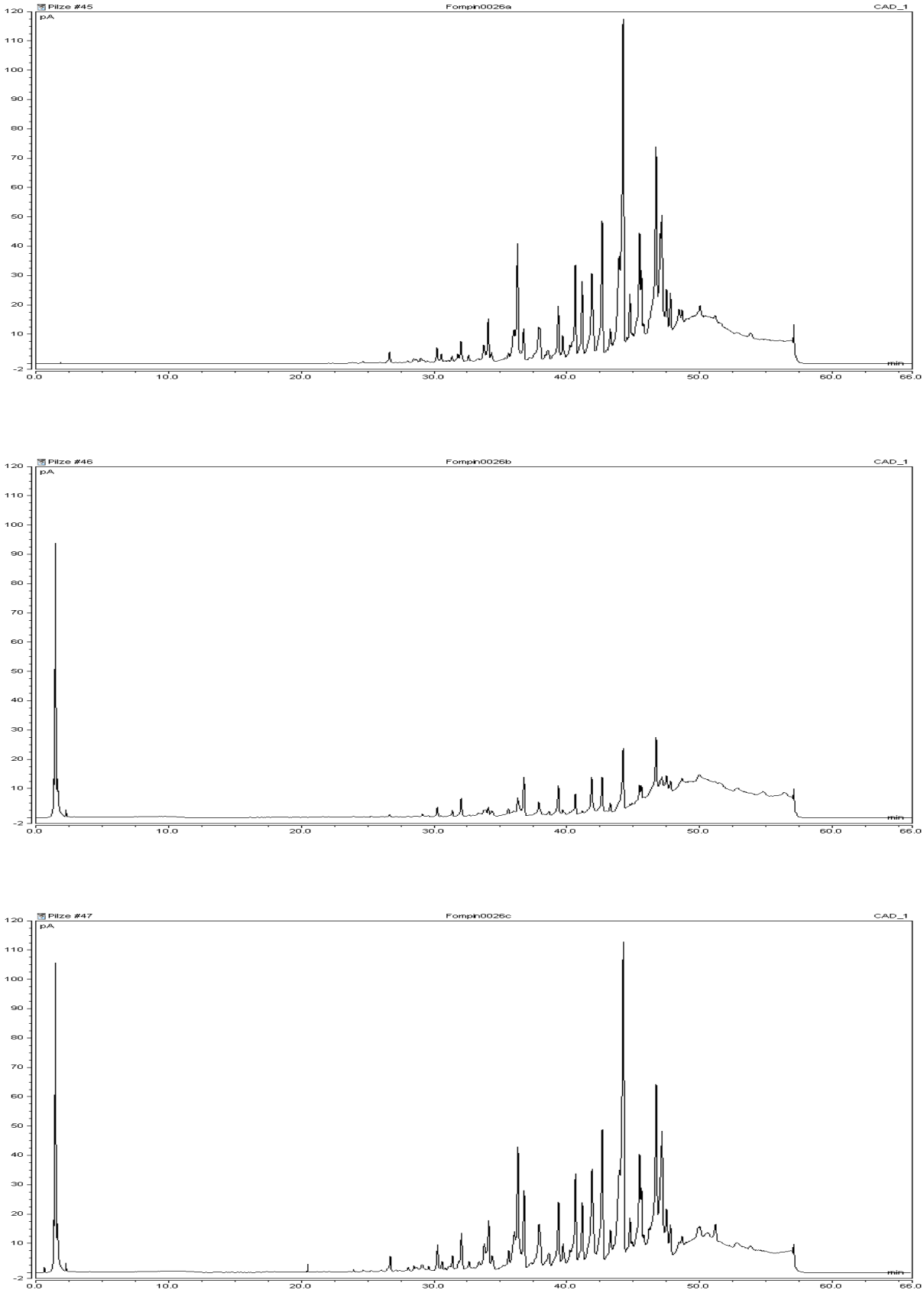

Figure 56 - Fompin0026a-c

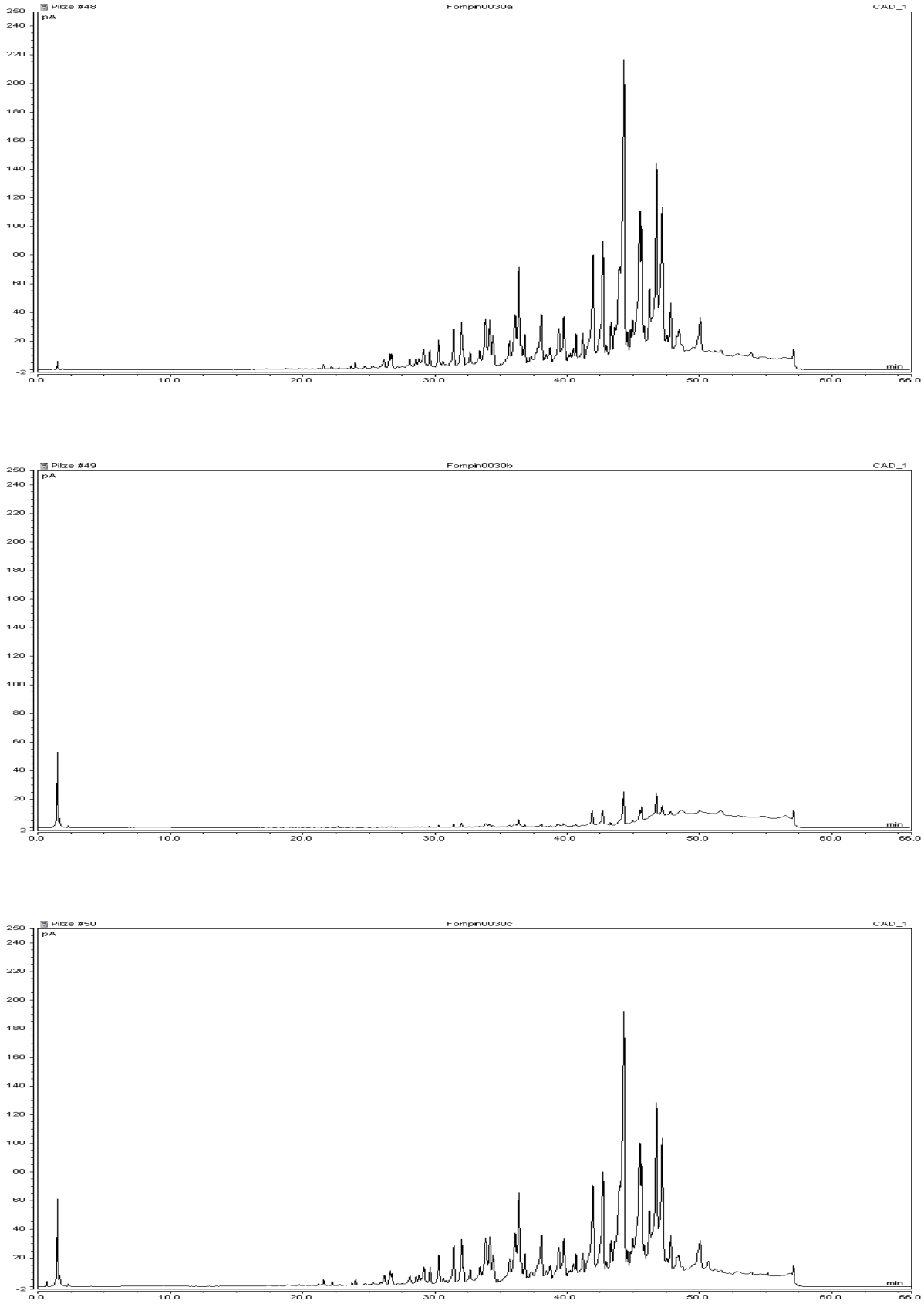

Figure 57 - Fompin0030a-c

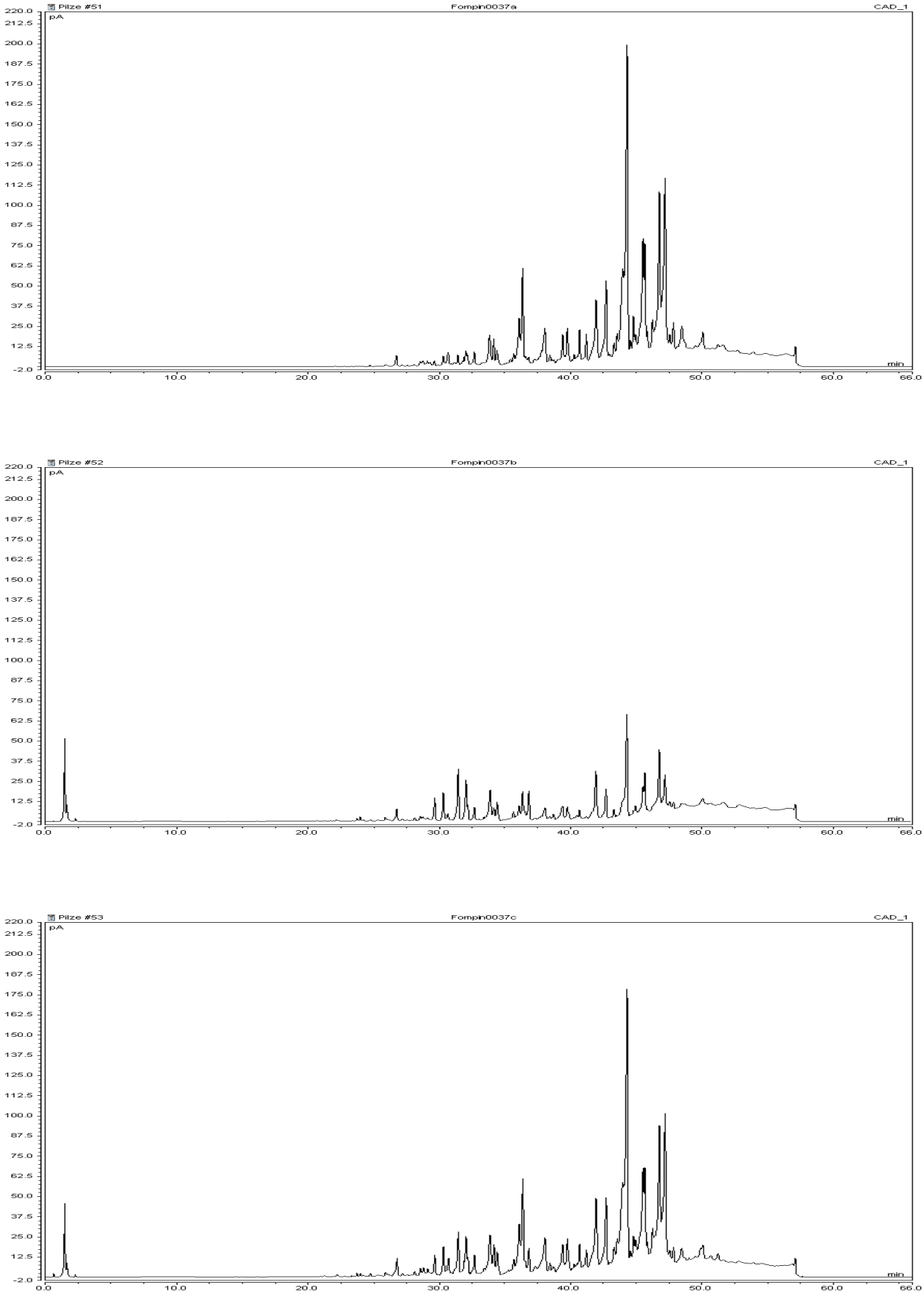

Figure 58 - Fompin0037a-c

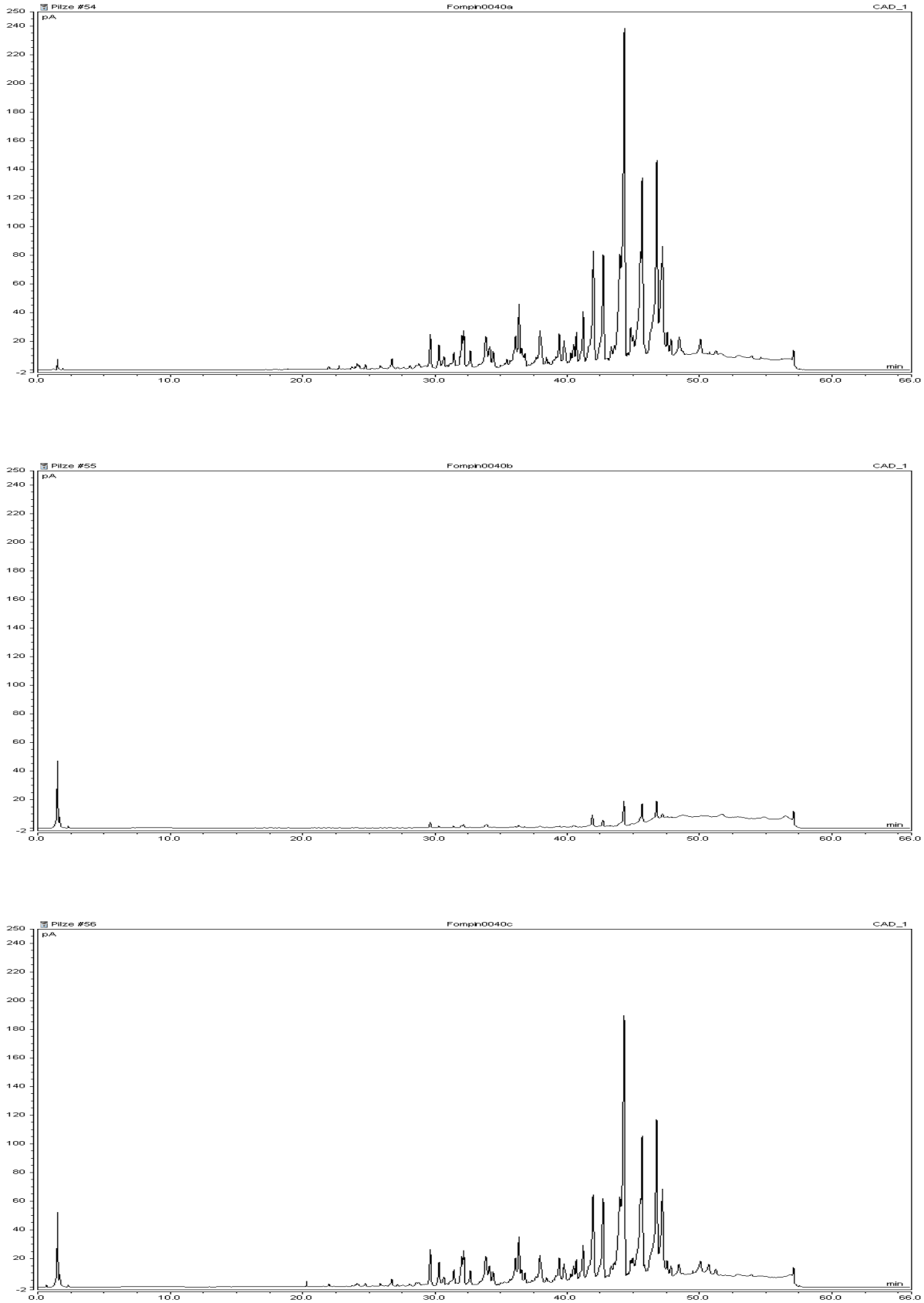

Figure 59 - Fompin0040a-c

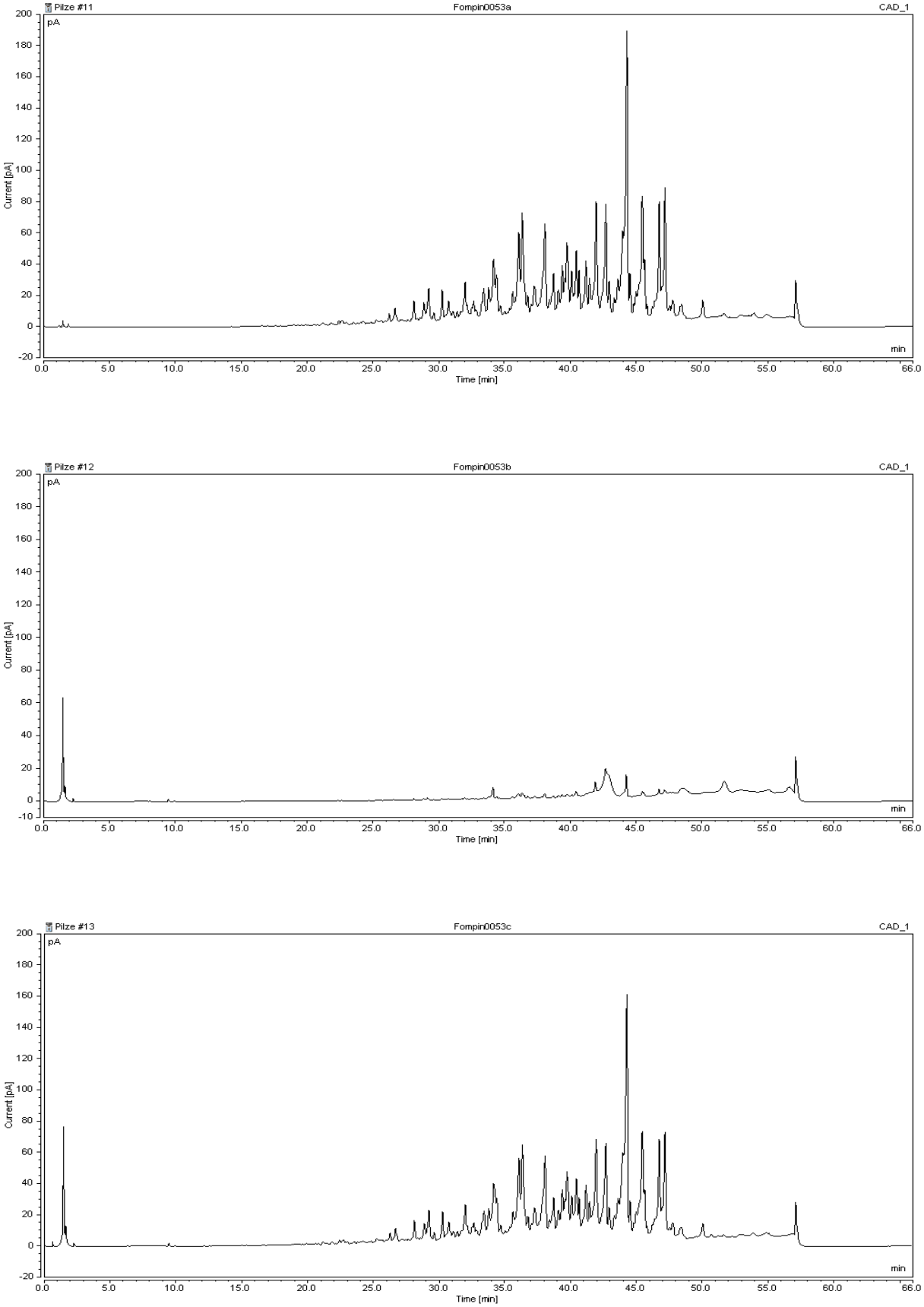

Figure 60 - Fompin0053a-c

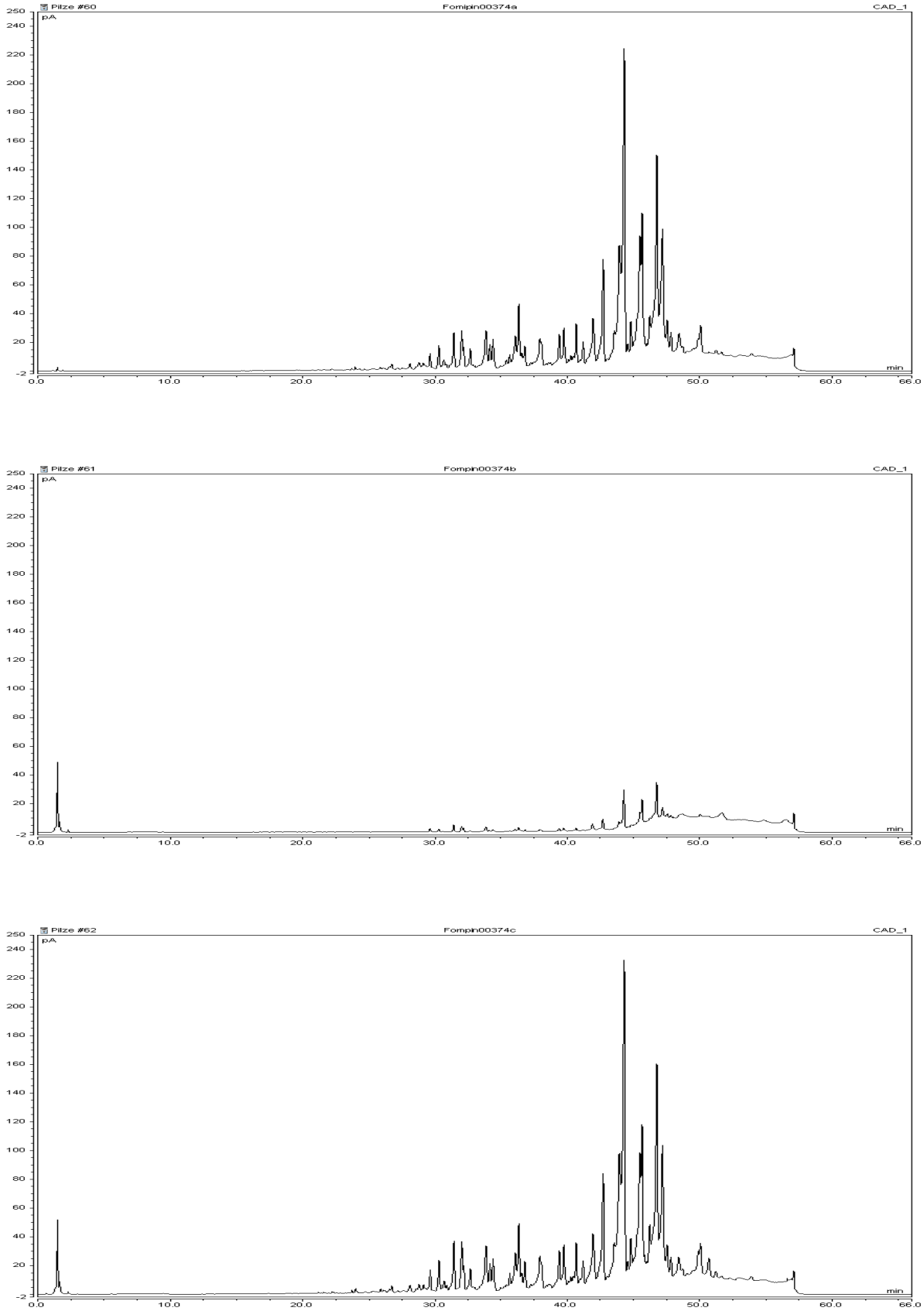

Figure 61 - Fompin00374a-c

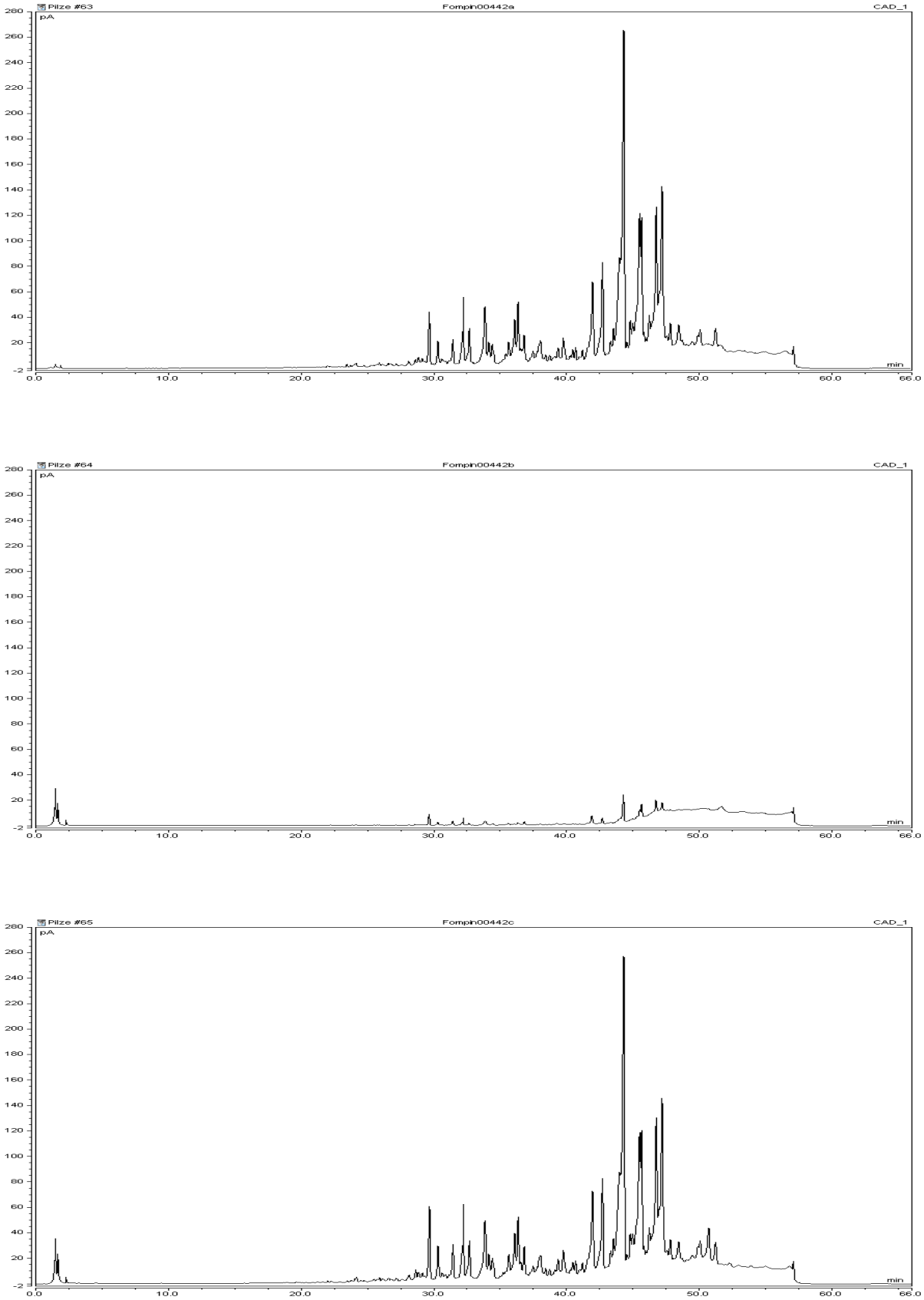

Figure 62 - Fompin00442a-c

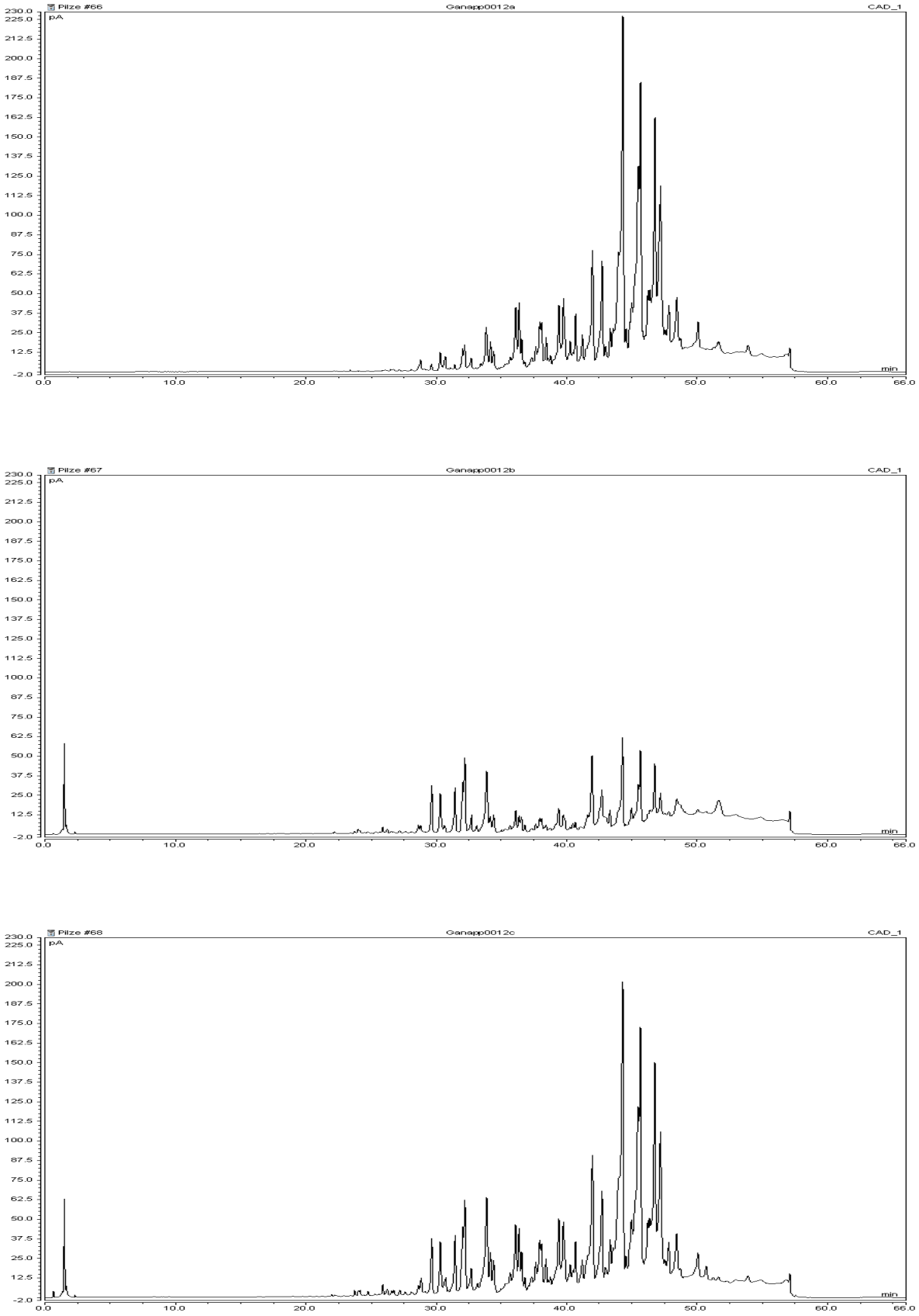

Figure 63 - Ganapp0012a-c

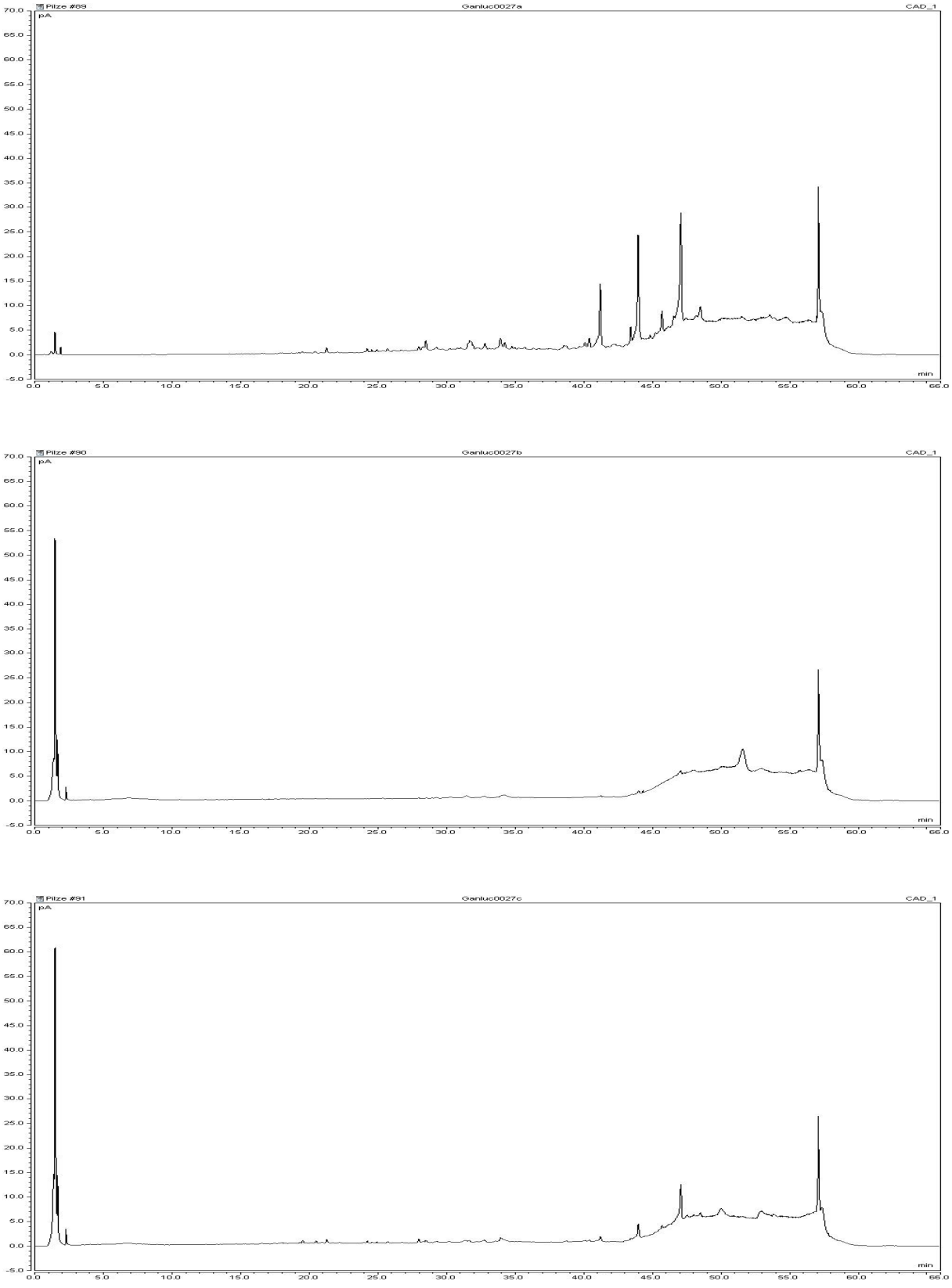

Figure 64 - Ganluc0027a-c

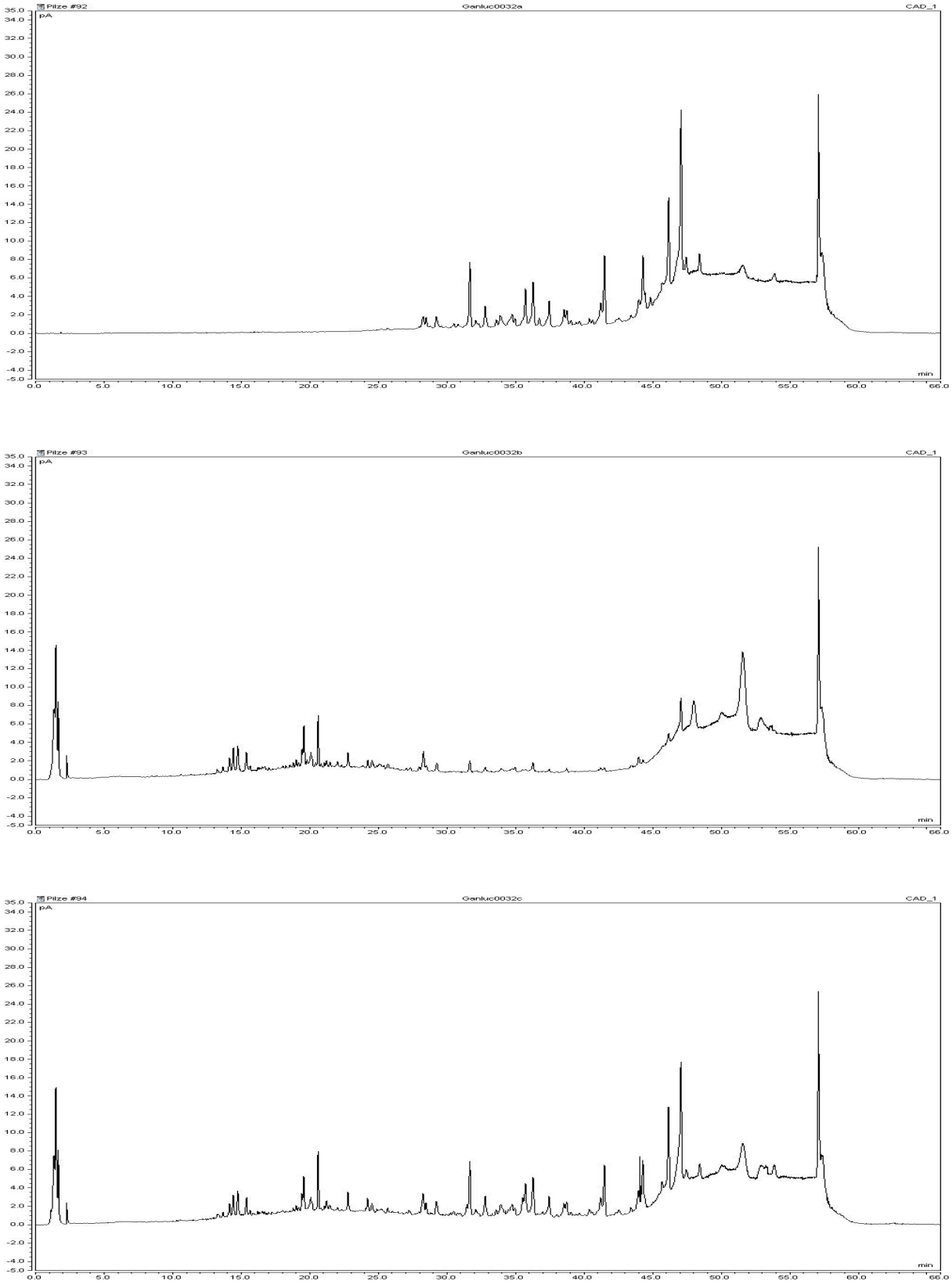

Figure 65 - Ganluc0032a-c

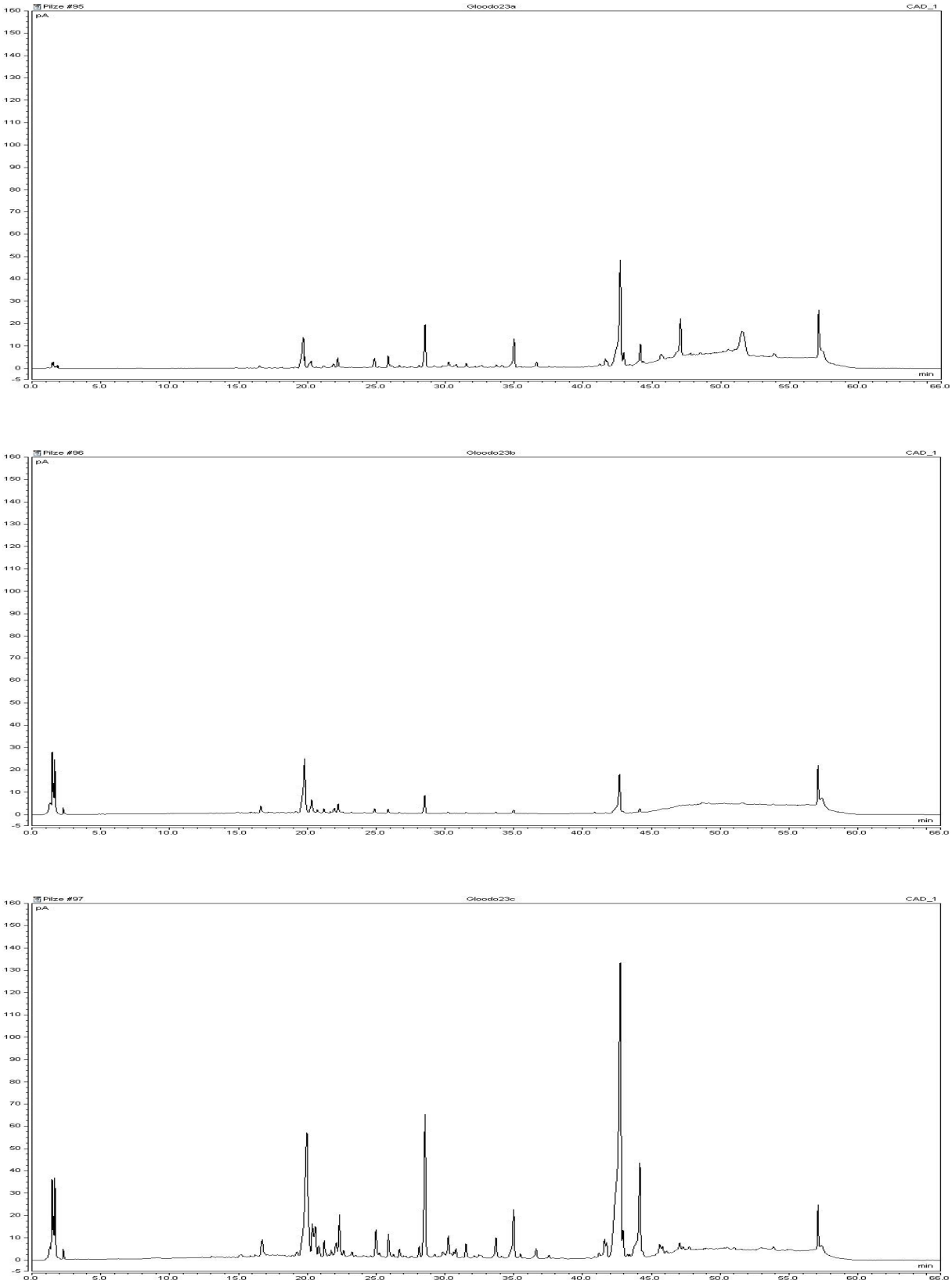

Figure 66 - Gloodo0023a-c

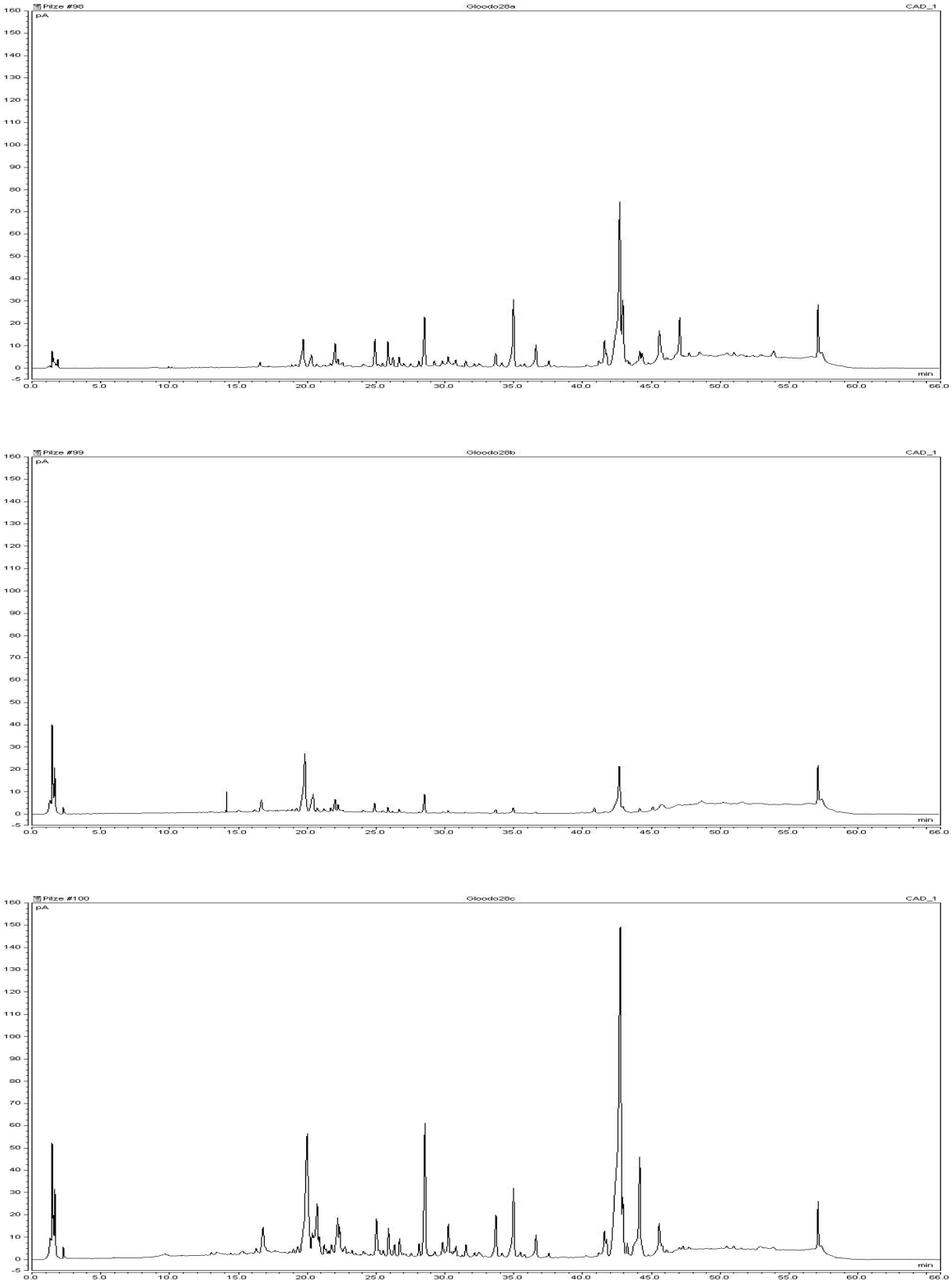

Figure 67 - Gloodo0028a-c

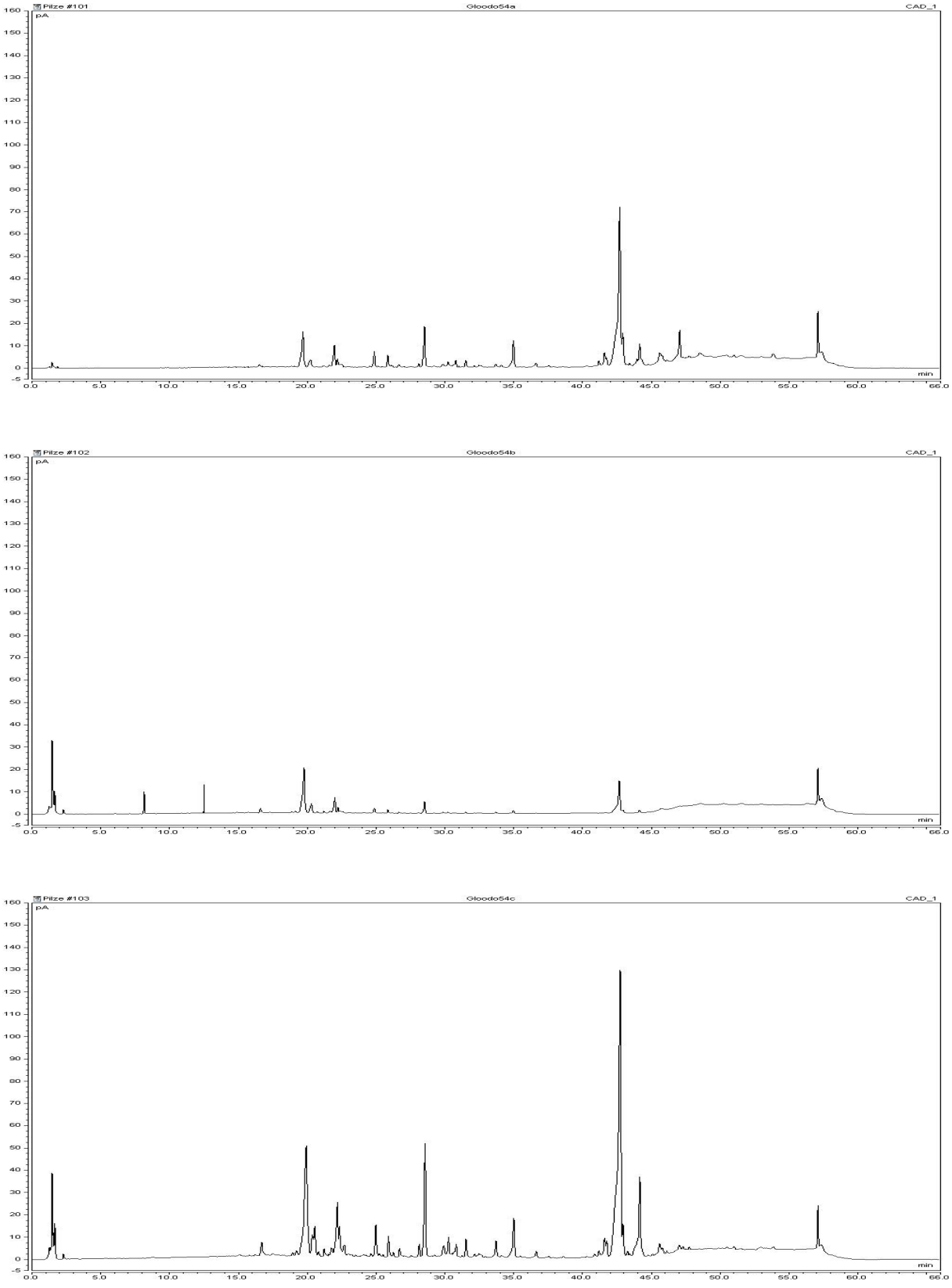

Figure 68 - Gloodo0054a-c

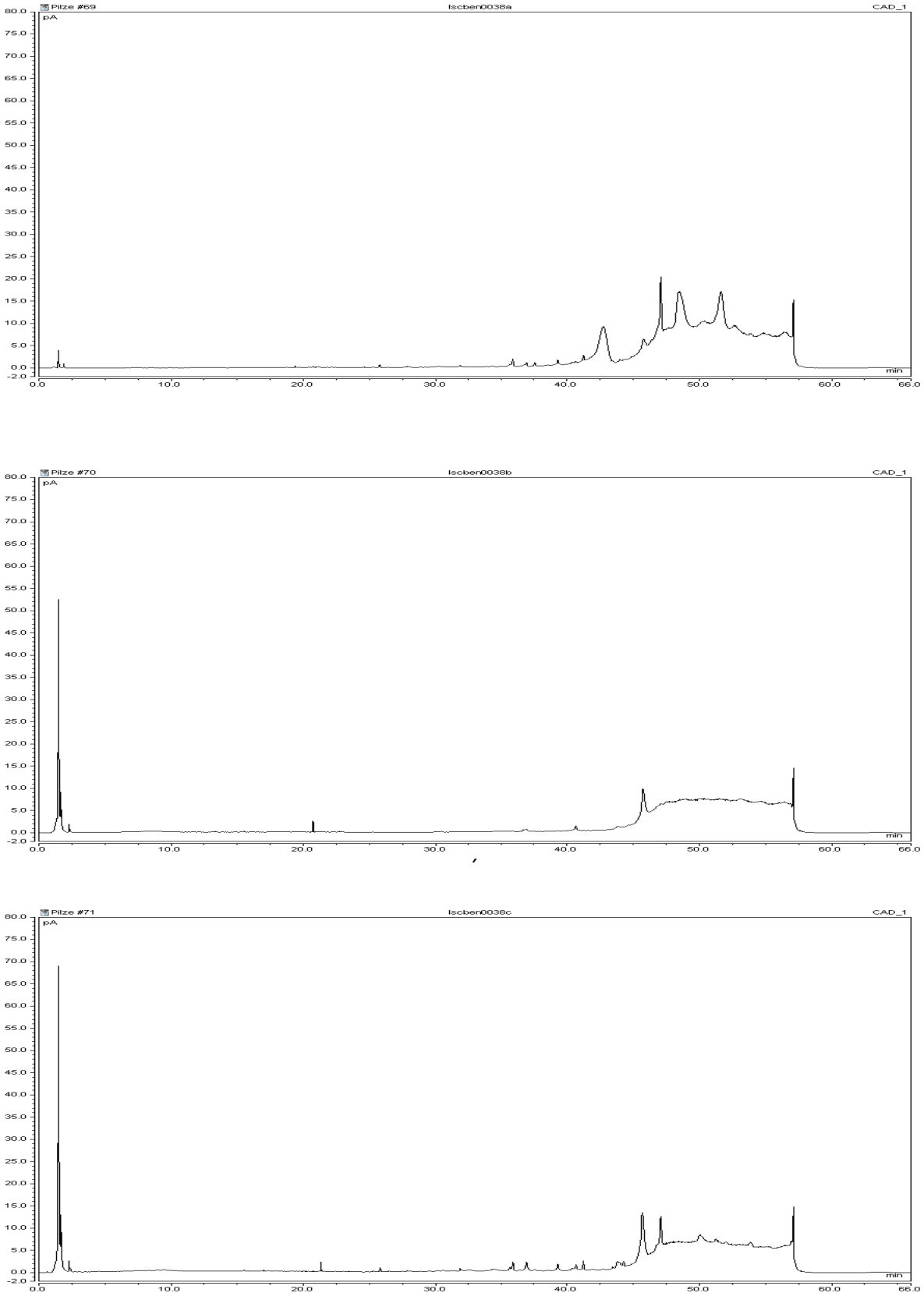

Figure 69 - Iscben0038a-c

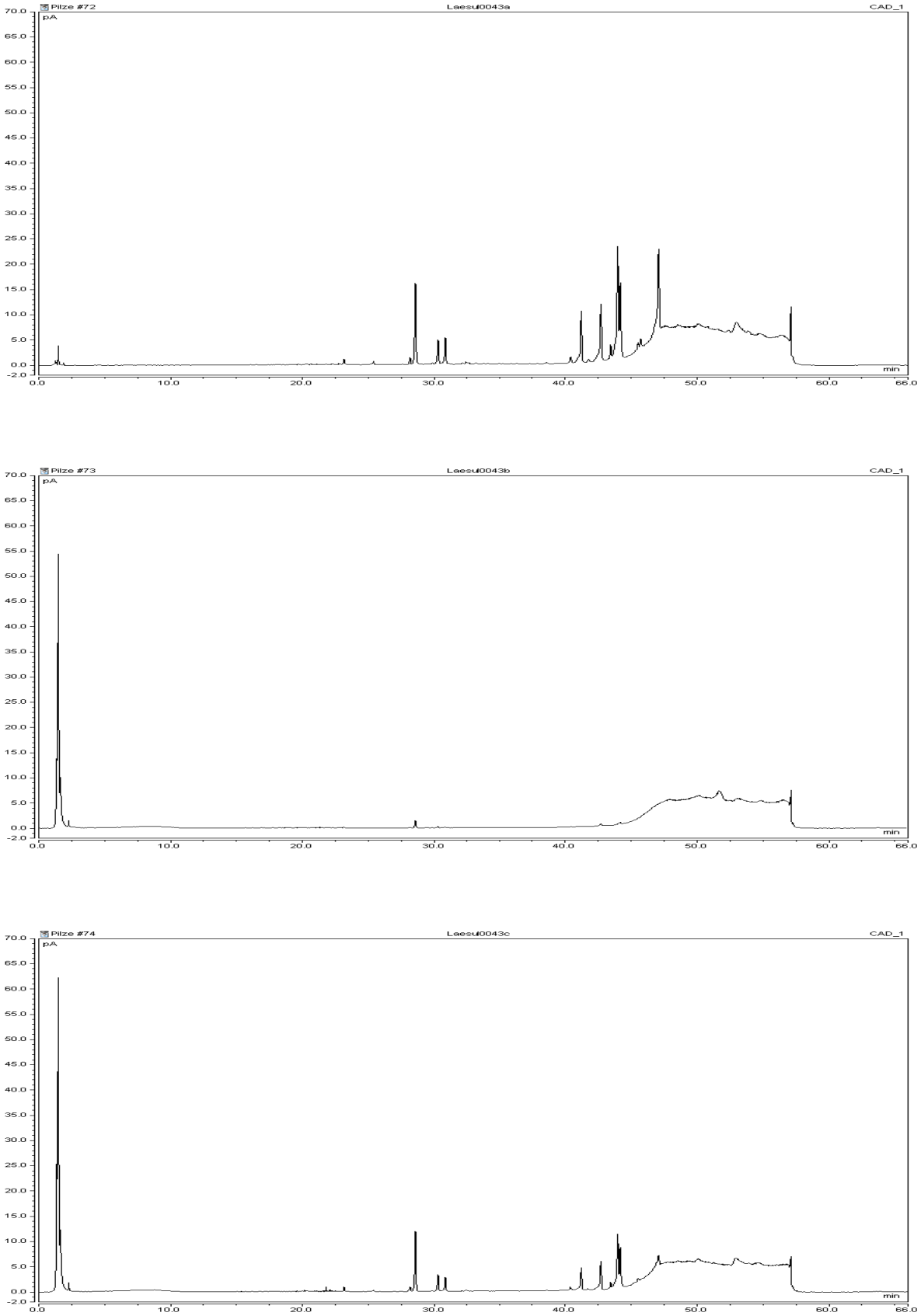

Figure 70 - Laesul0043a-c

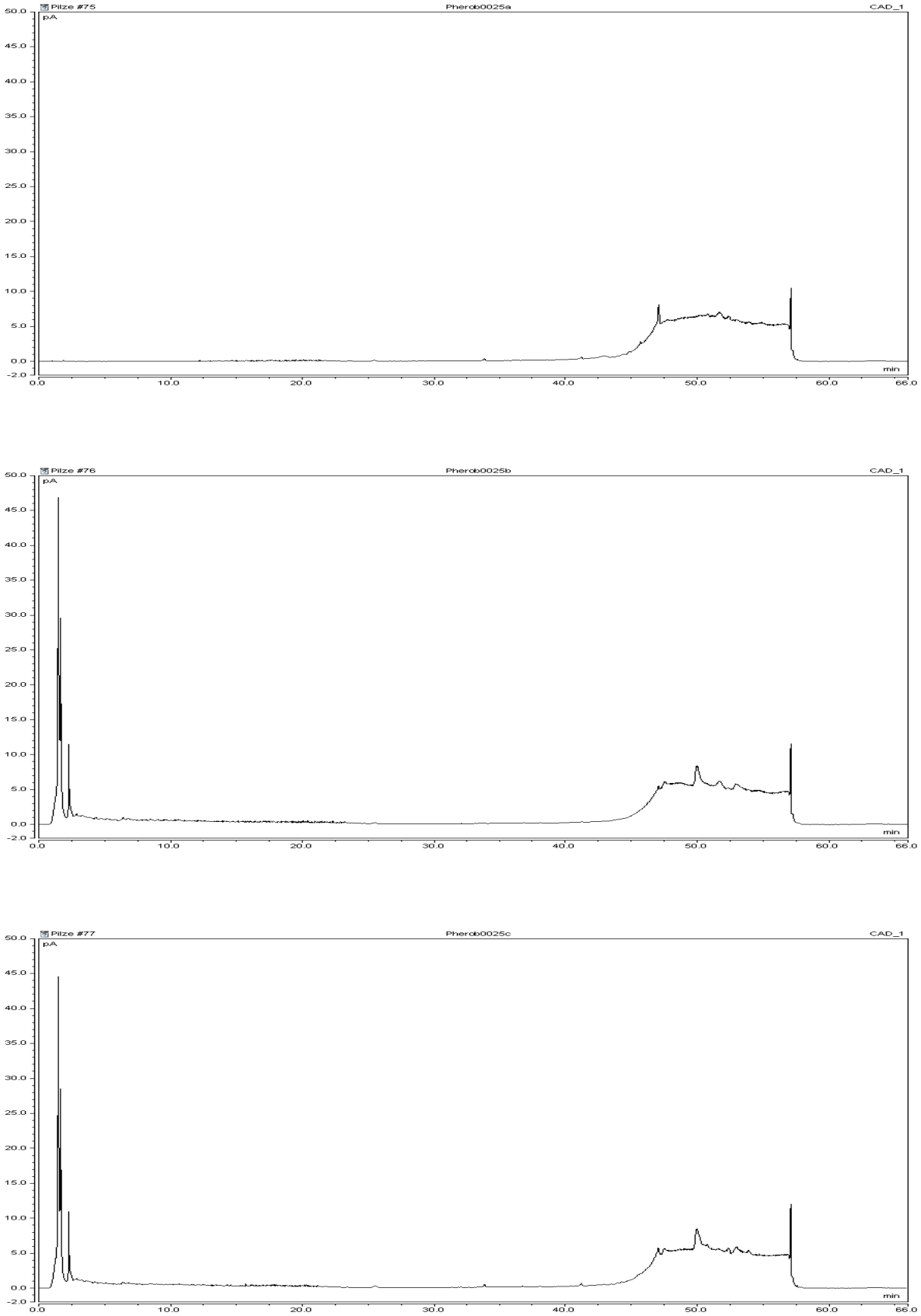

Figure 71 - Pherob0025a-c

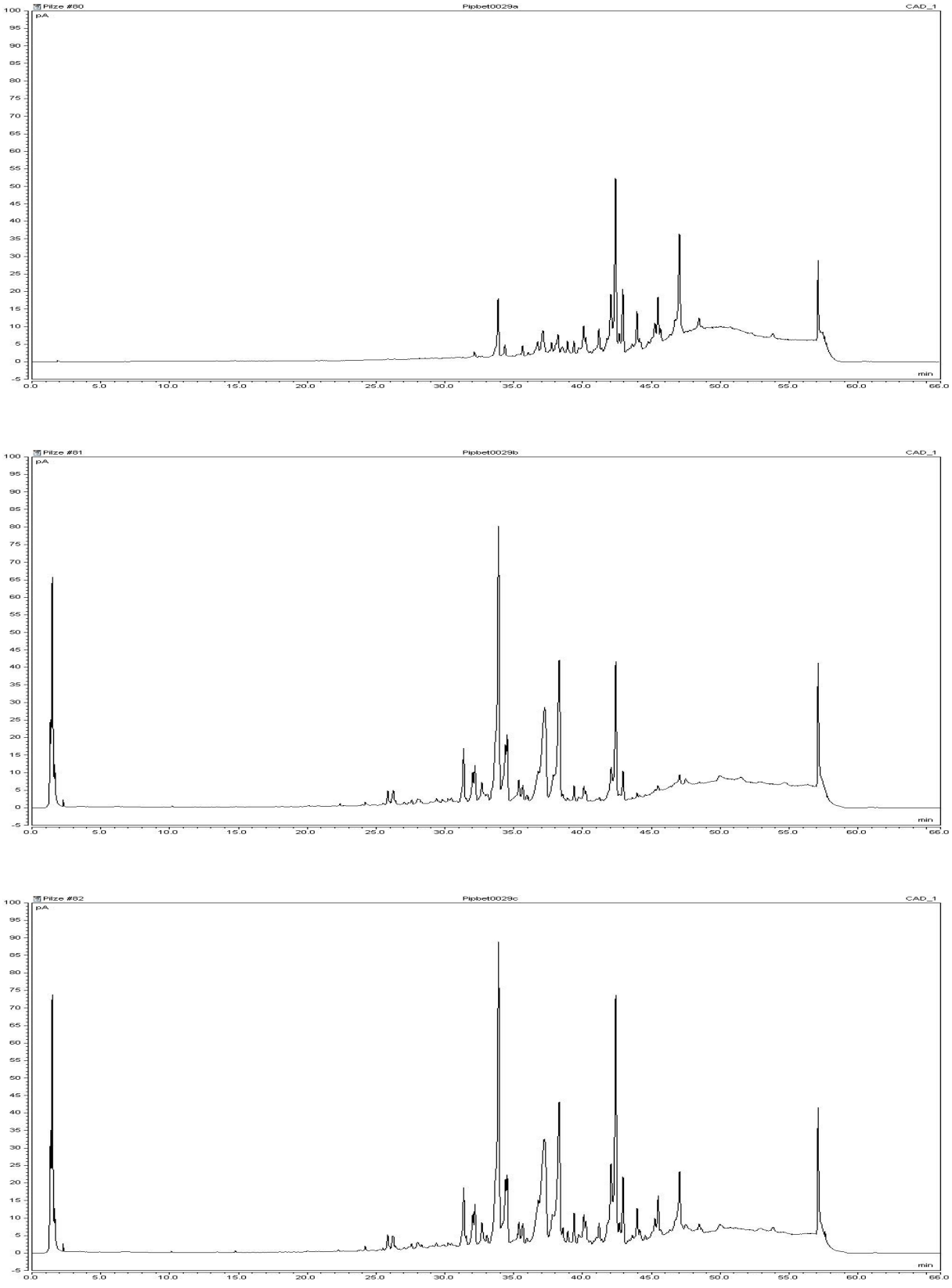

Figure 72 - Pipbet0029a-c

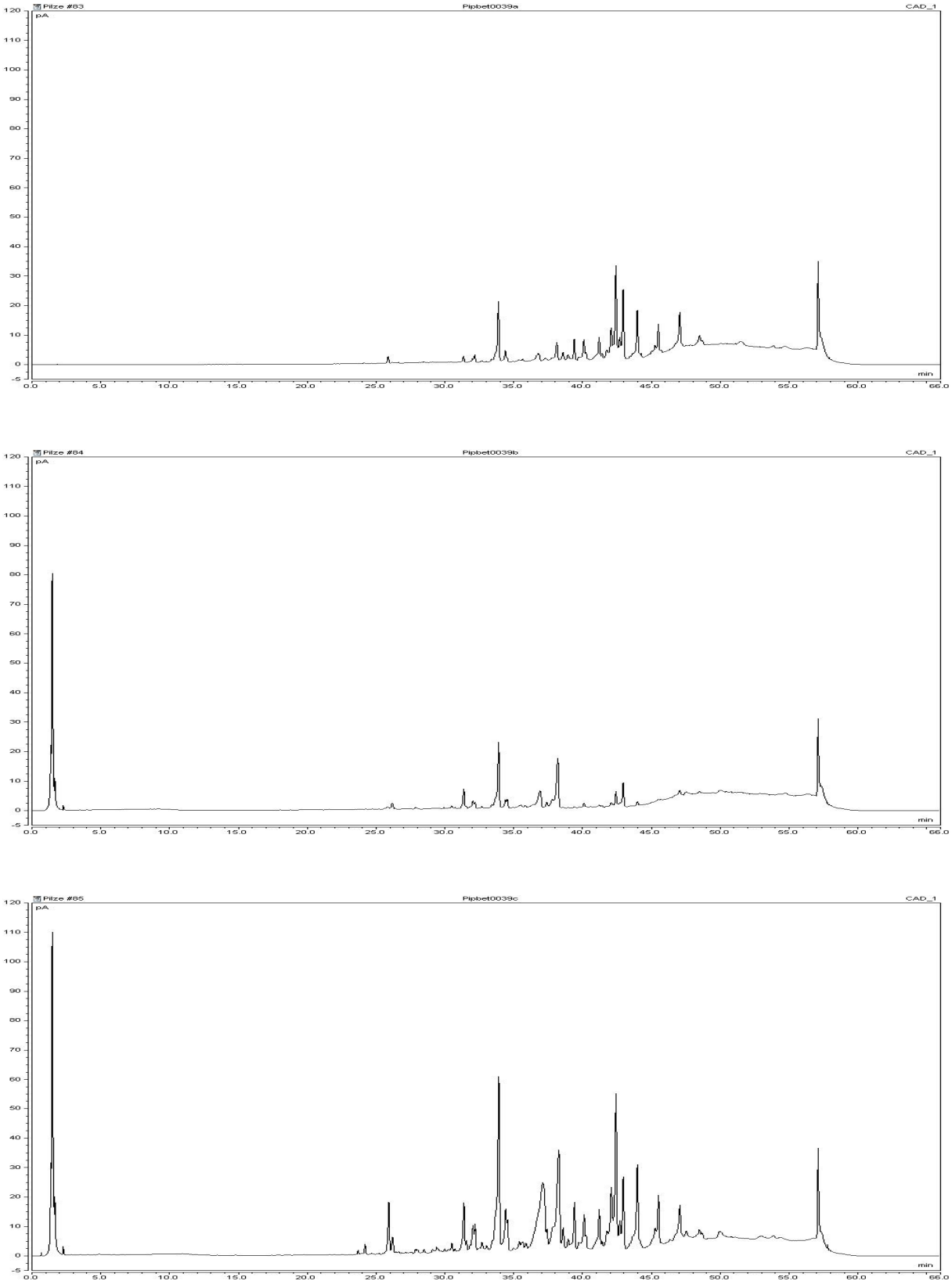

Figure 73 - Pipbet0039a-c

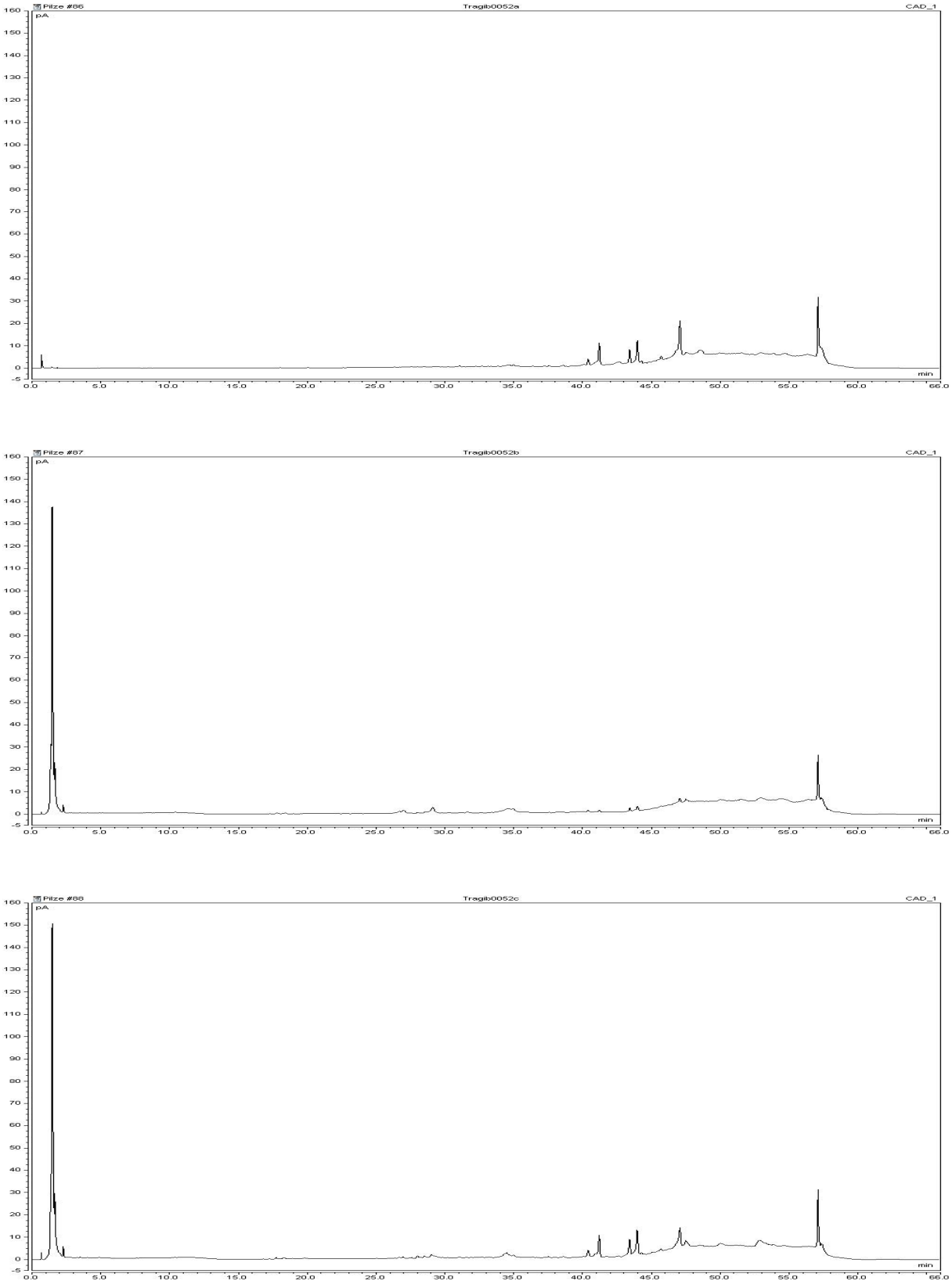

Figure 74 - Tragib0052a-c

8.1.3 SFC Chromatograms of PE Extracts

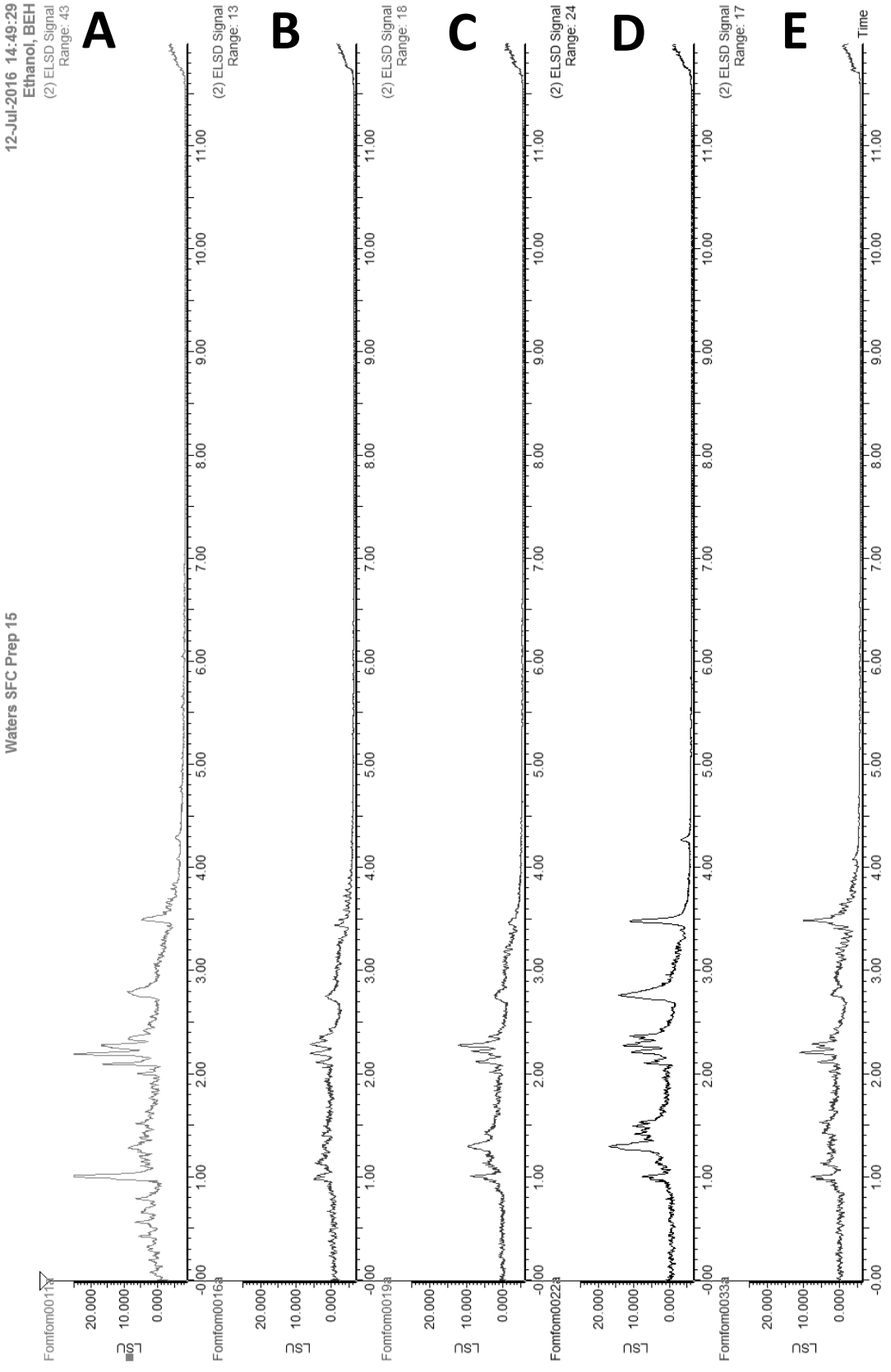

Figure 75- A: Fomfom0011a, B: Fomfom0016a, C: Fomfom0019a, D: Fomfom0022a, E: Fomfom0033a; ELSD Signals

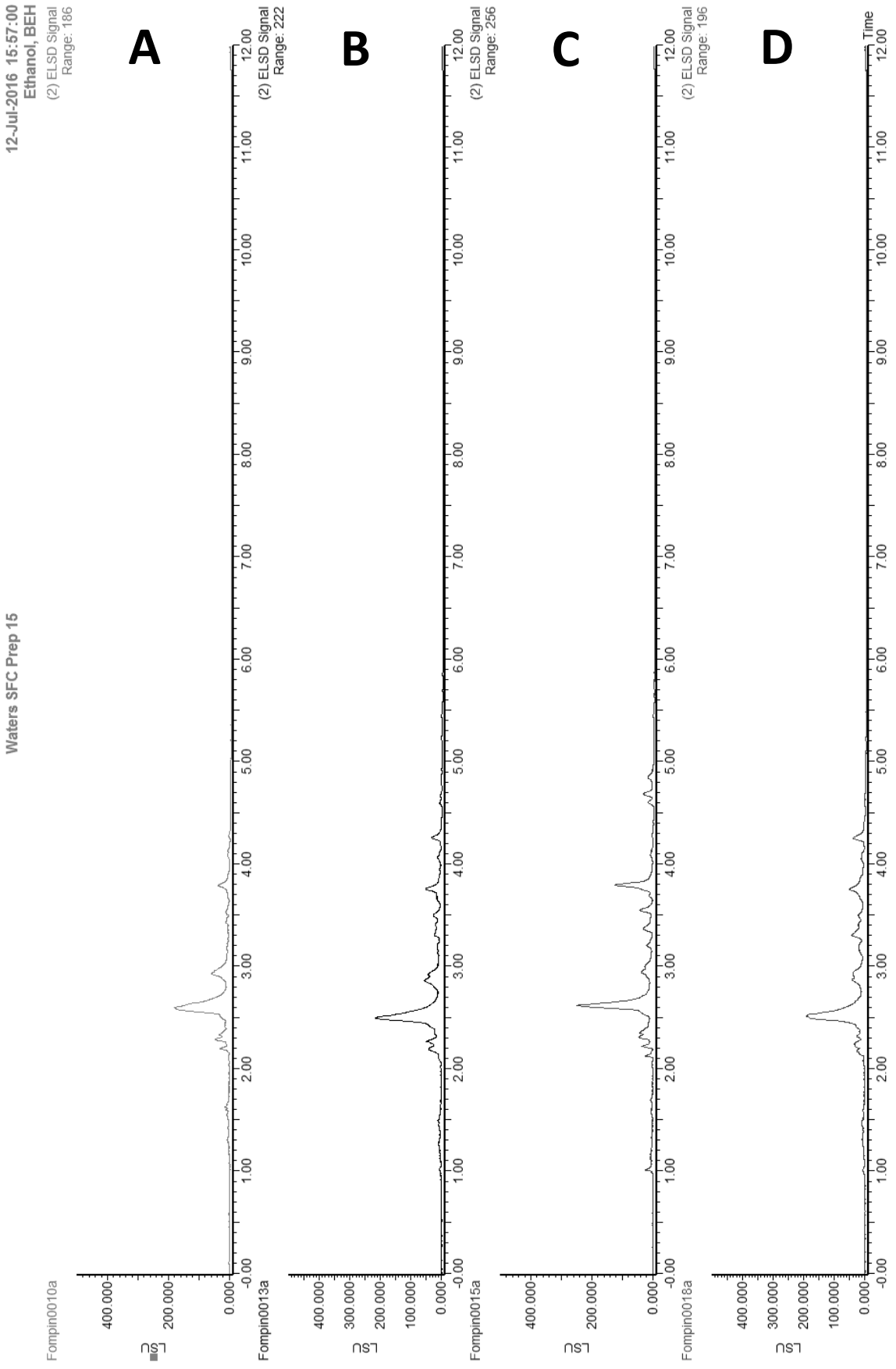

Figure 76 - A: Fompin0010a, B: Fompin0013a, C: Fompin0015a, Fompin0018a; ELSD Signals

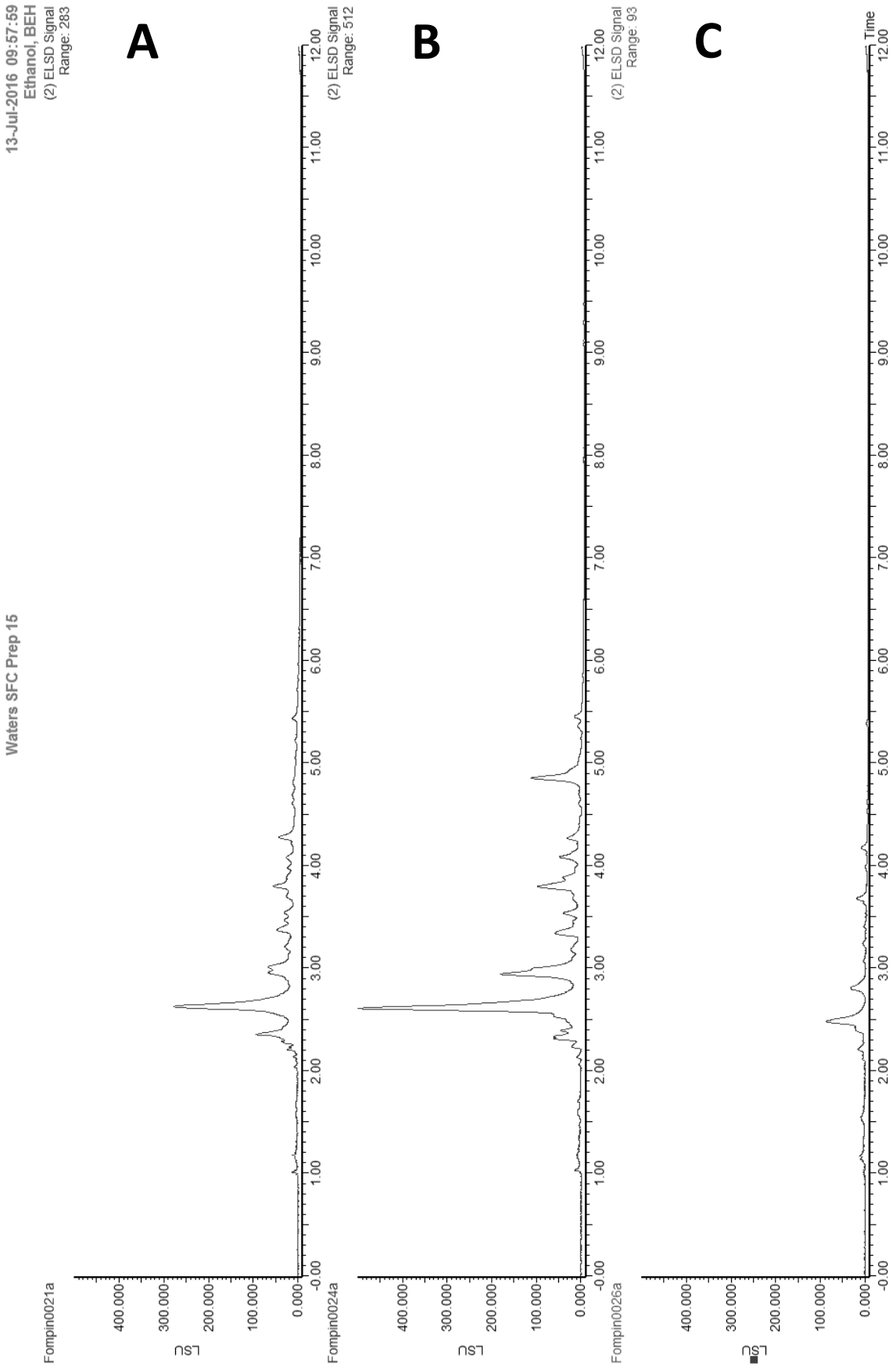

Figure 77 - A: Fompin0021a, B: Fompin0024a, C: Fompin0026a; ELSD Signals

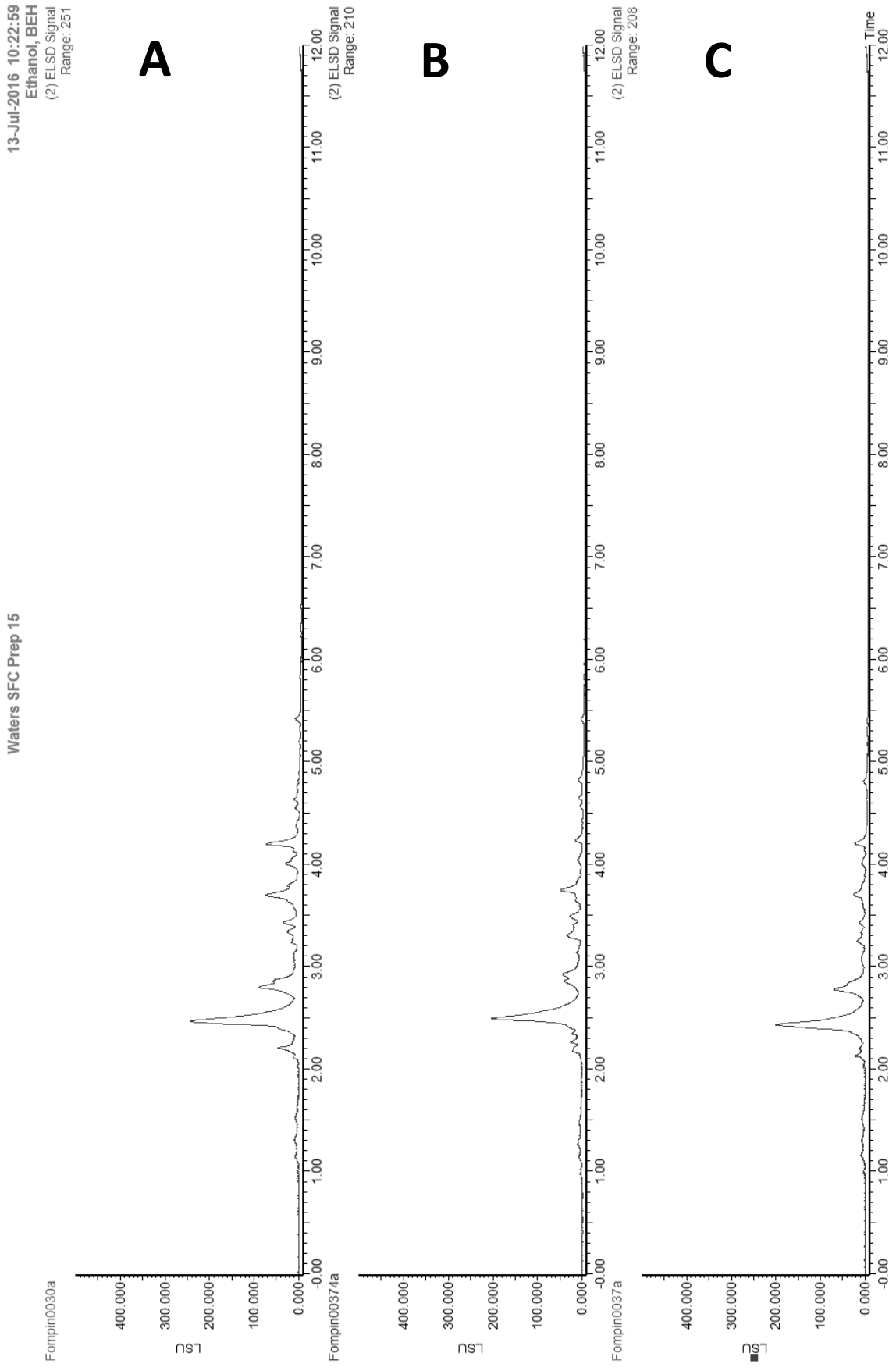

Figure 78 - A: Fompin0030a; B: Fompin00374a; C: Fompin0037a; ELSD Signals

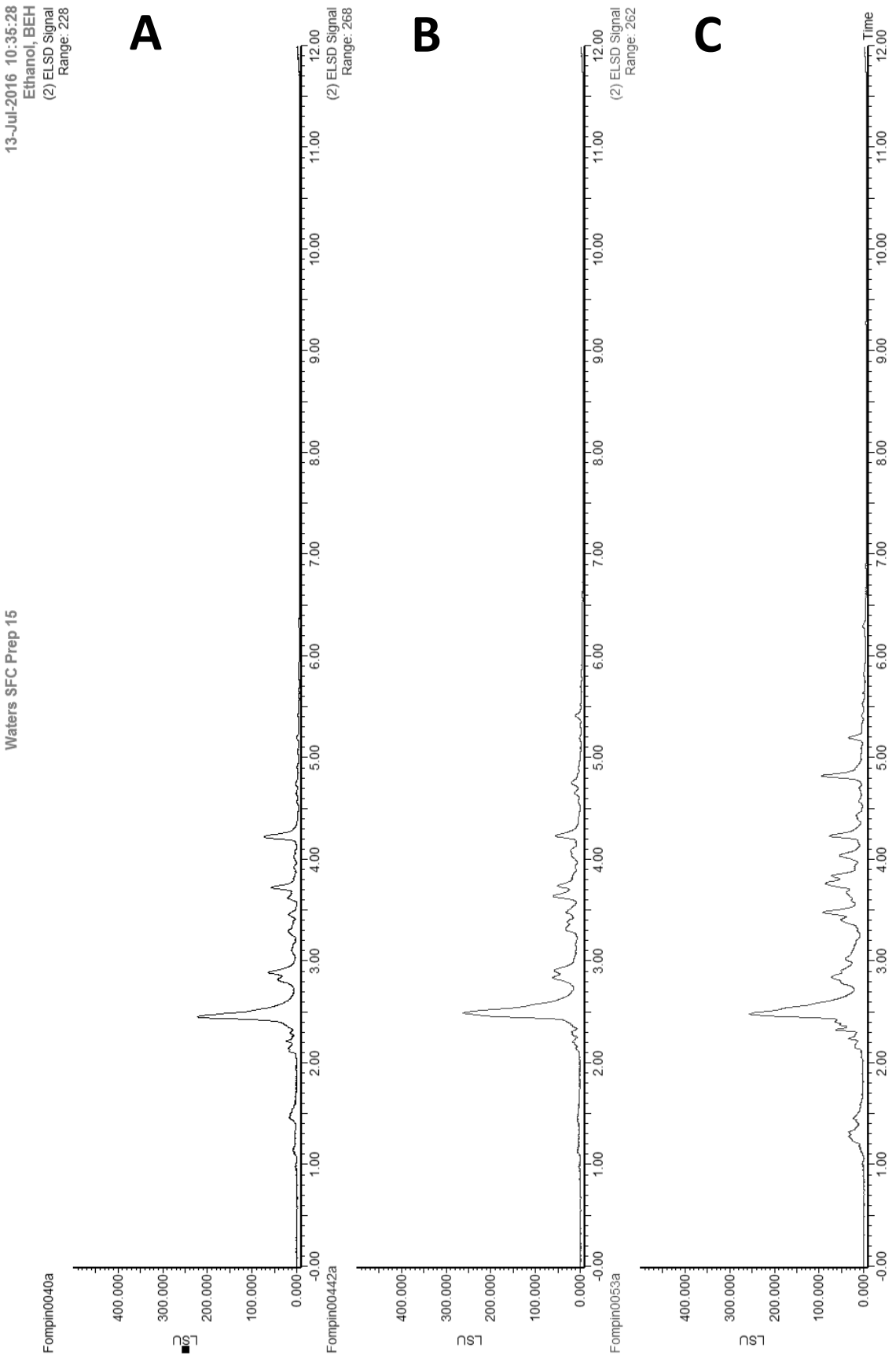

Figure 79 - A: Fompin0040a, B: Fompin00442a, C: Fompin0053a; ELSD Signals

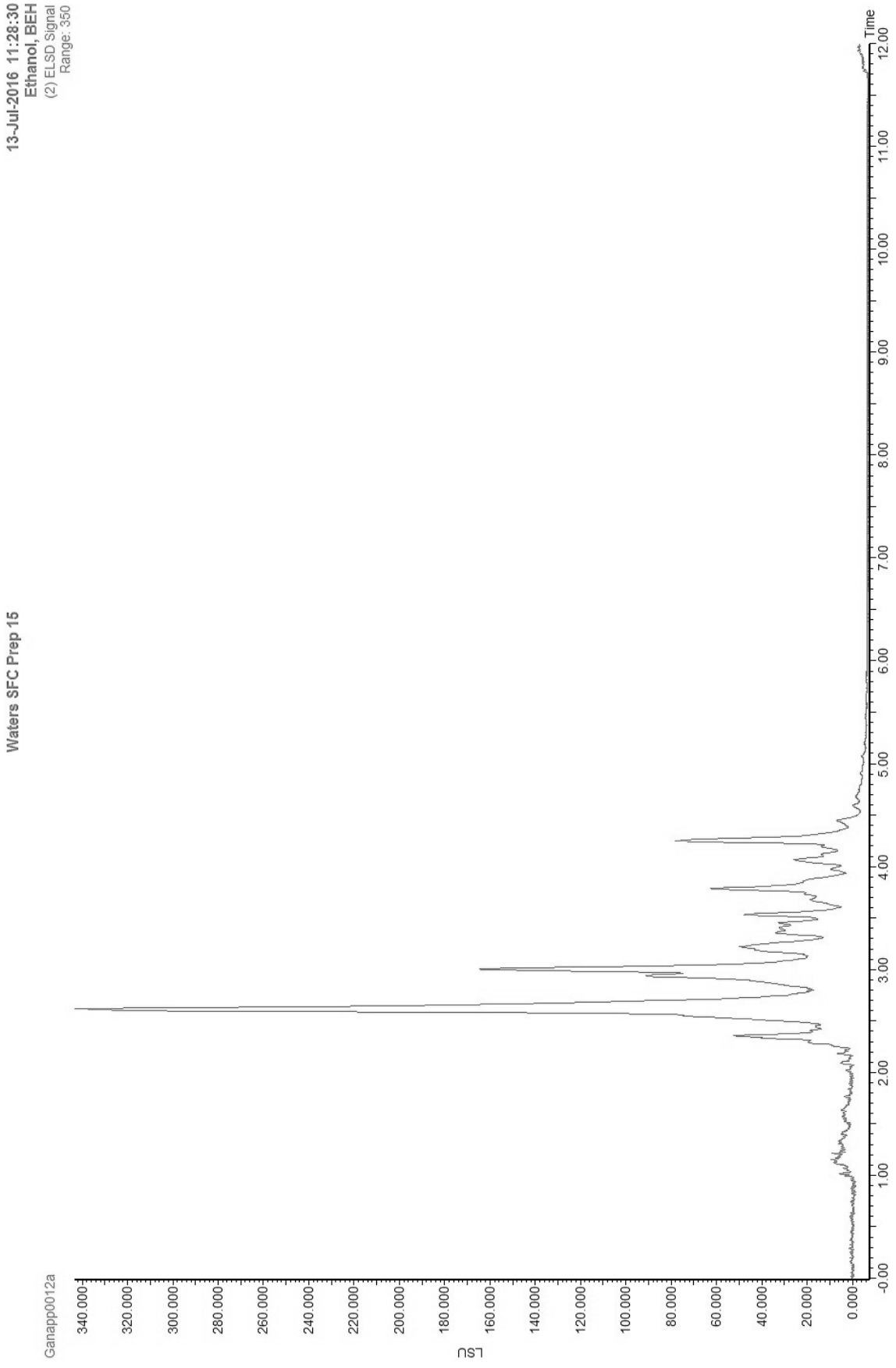

Figure 80 - Ganapp0012a; ELSD Signal

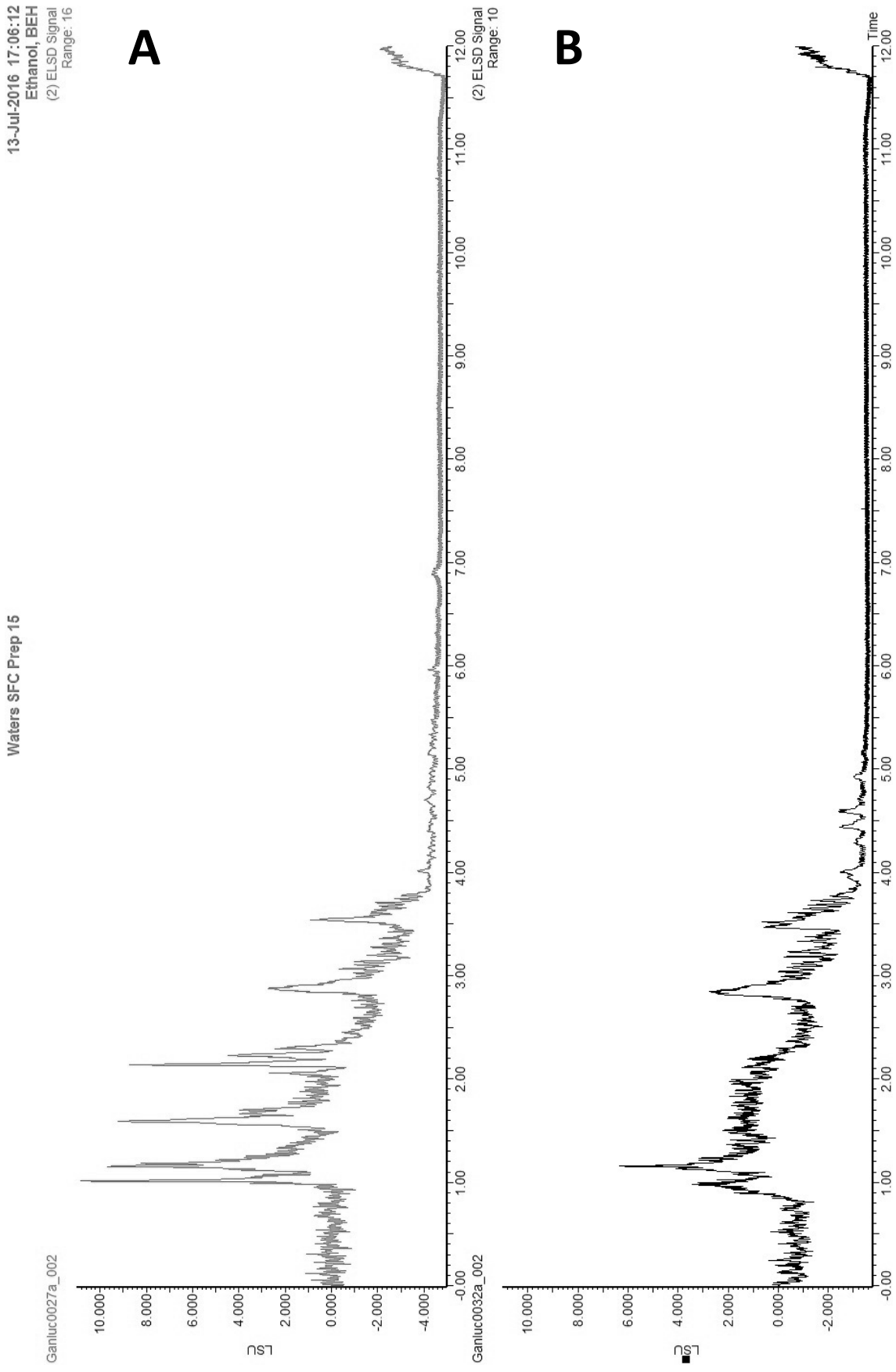

Figure 81 – A: Ganluc0027a; B: Ganluc0032a; ELSD Signals

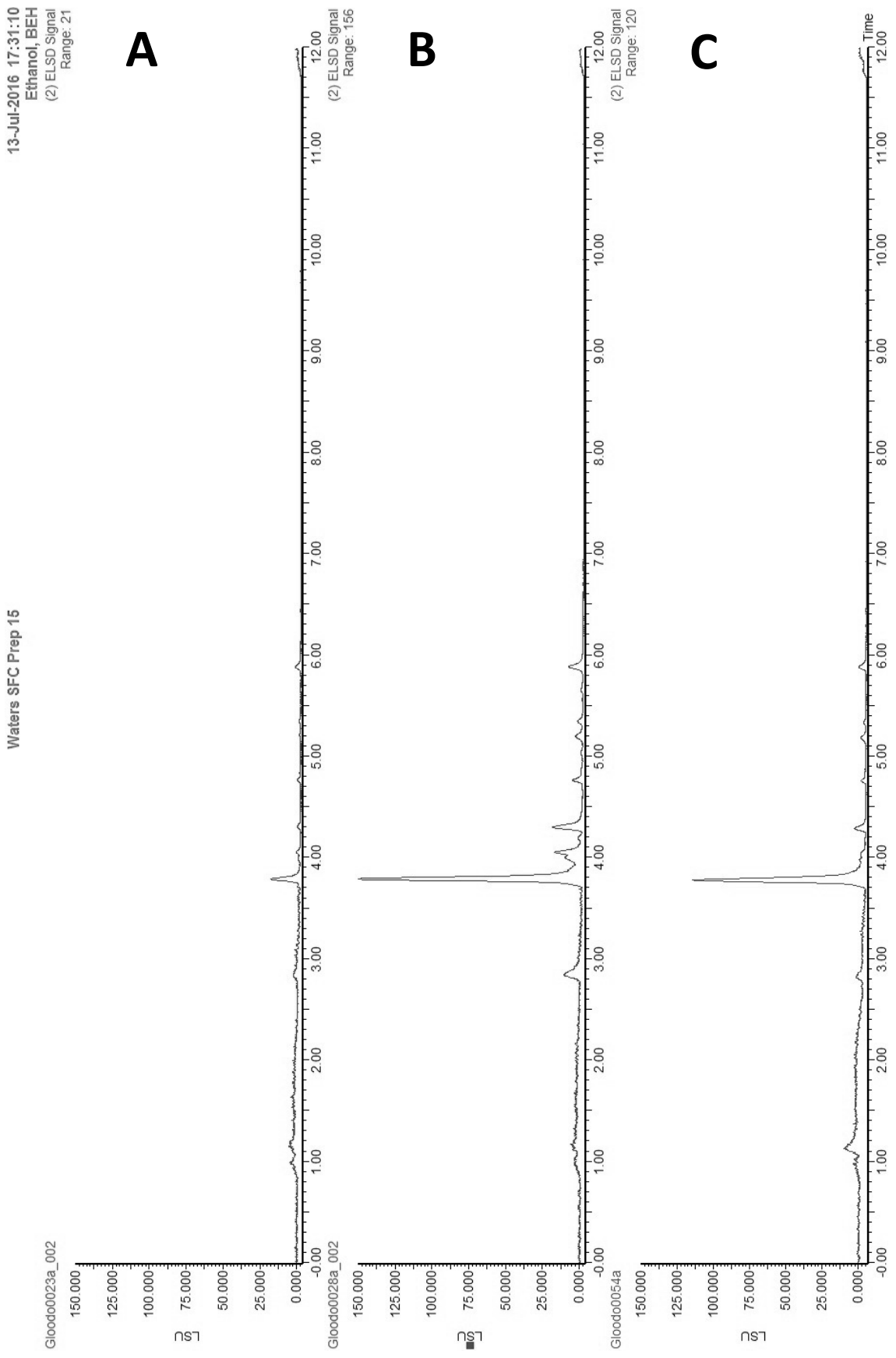

Figure 82 - A: Gloodo0023a; B: Gloodo0028a; C: Gloodo0054a; ELSD Signals

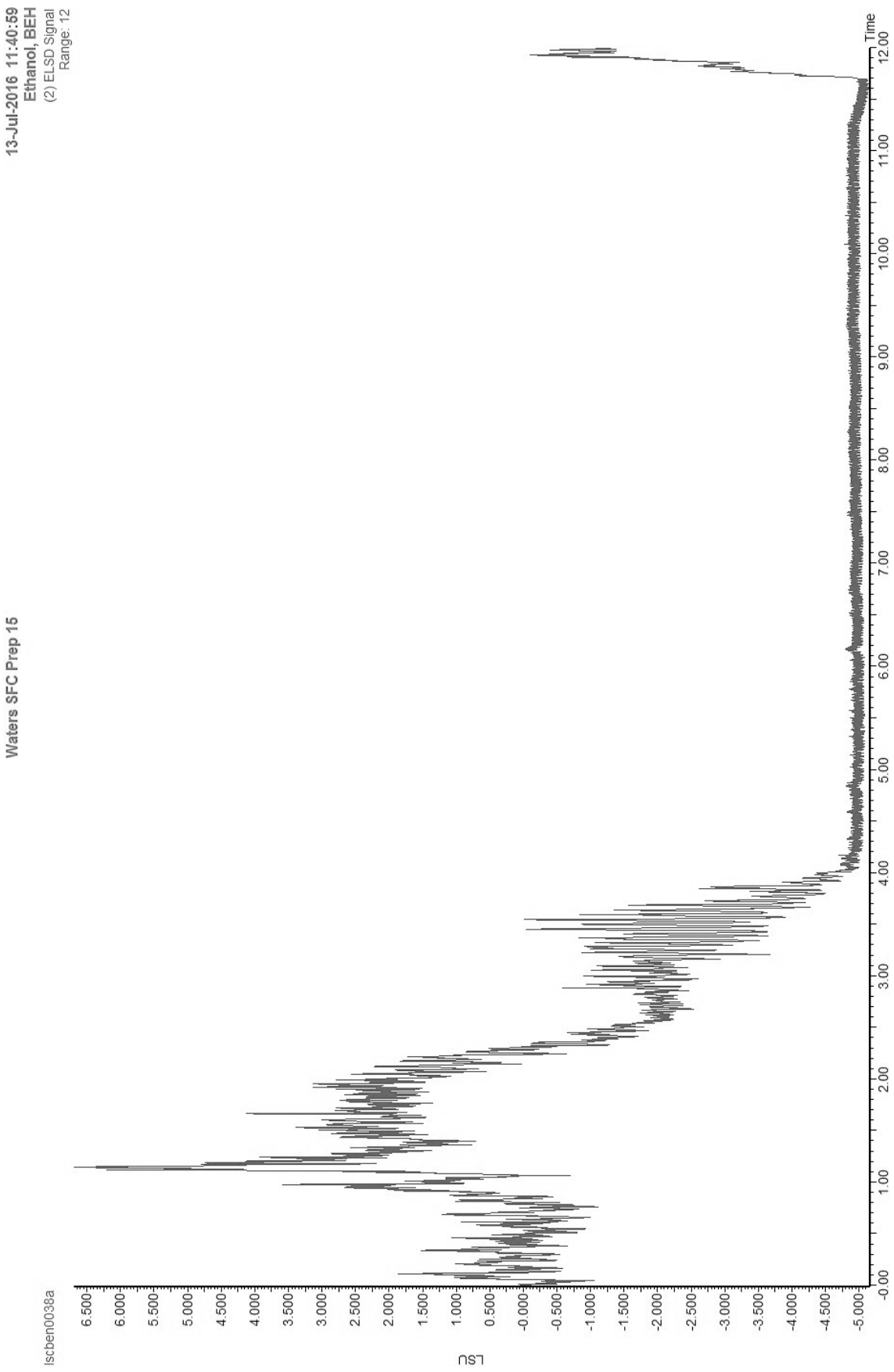

Figure 83 - Iscben0038a; ELSD Signal

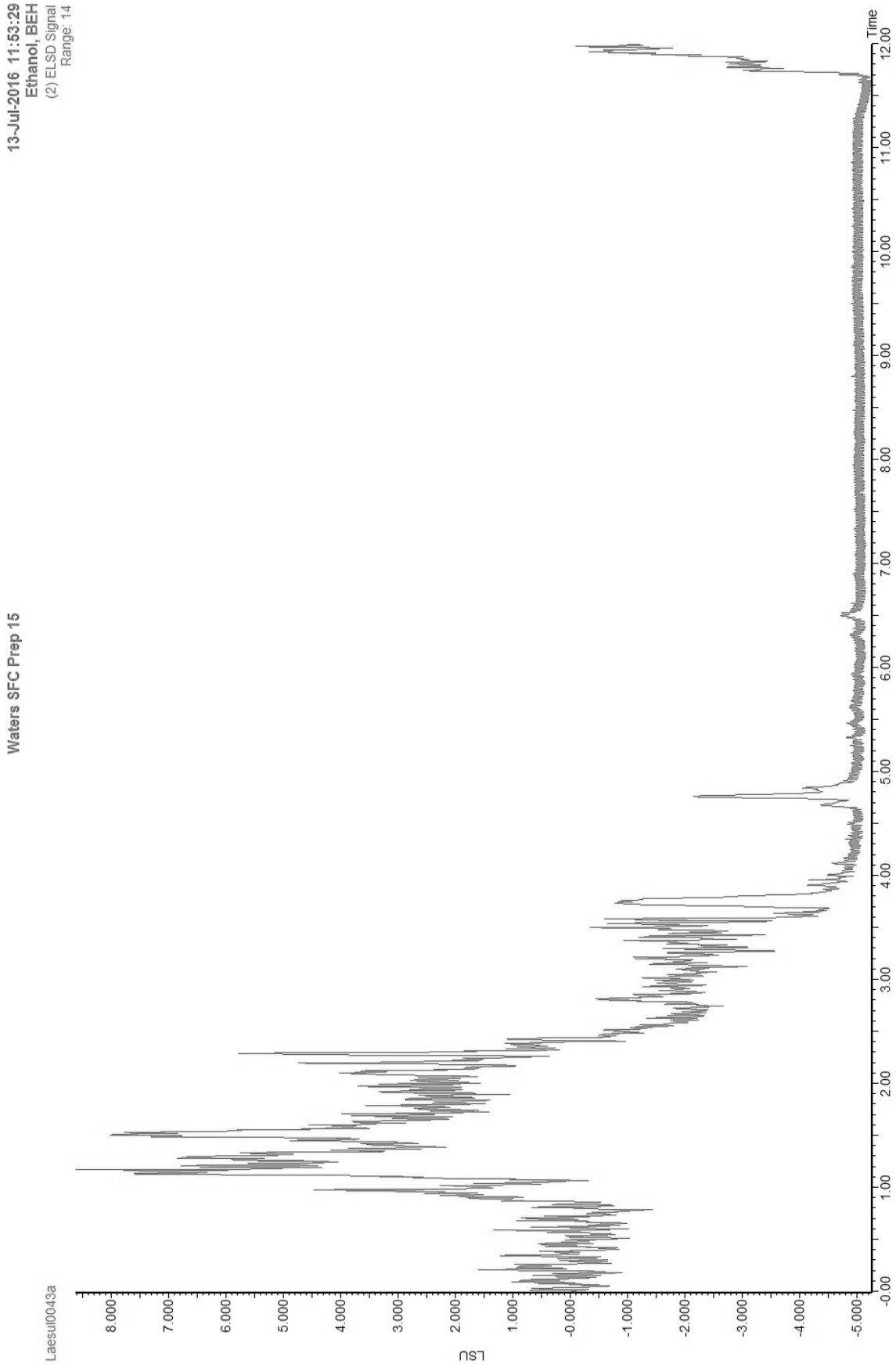

Figure 84 - Laesul0043a; ELSD Signal

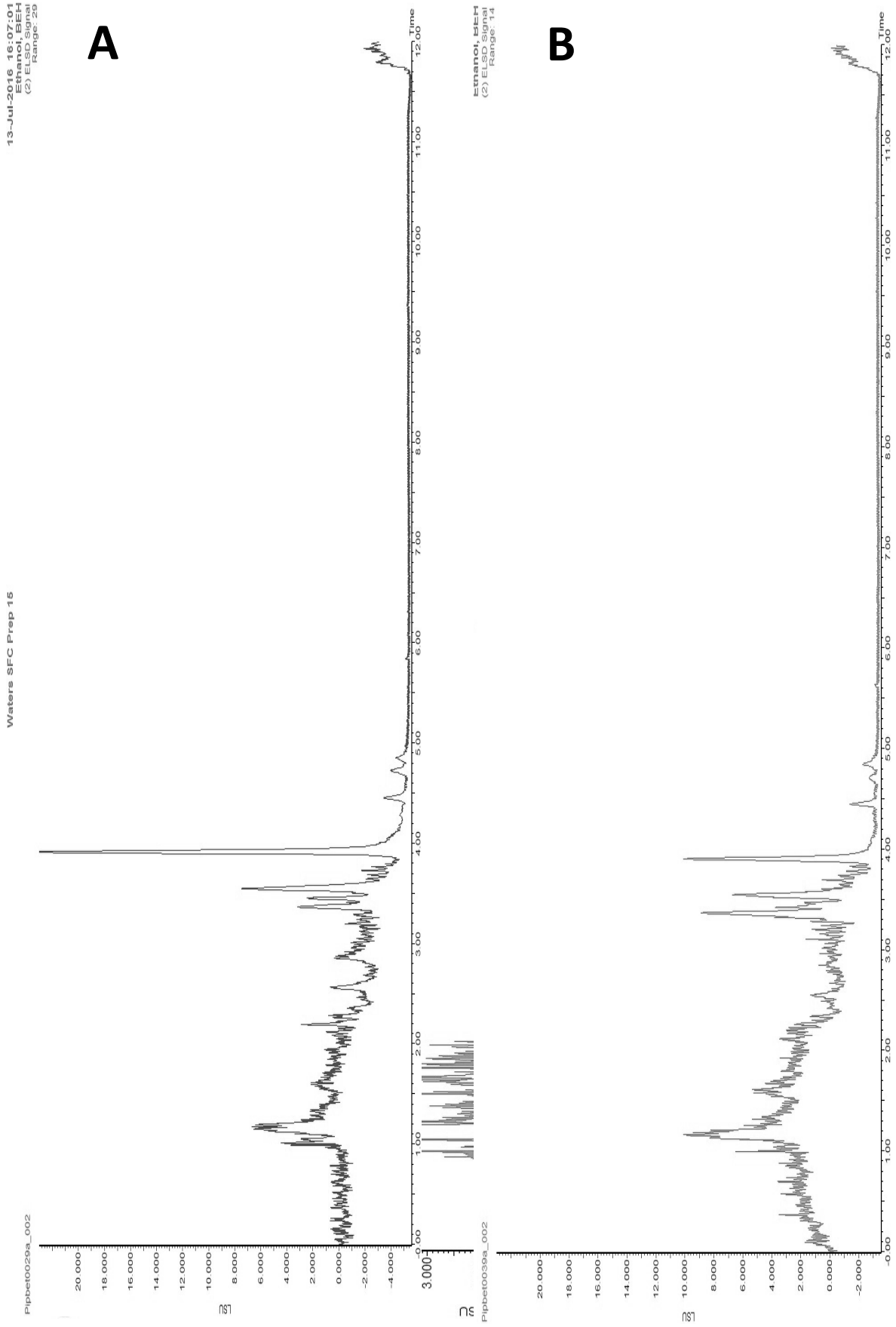

Figure 86 - A: Pipbet0029a ; B: Pipbet0039a; ELSD Signals

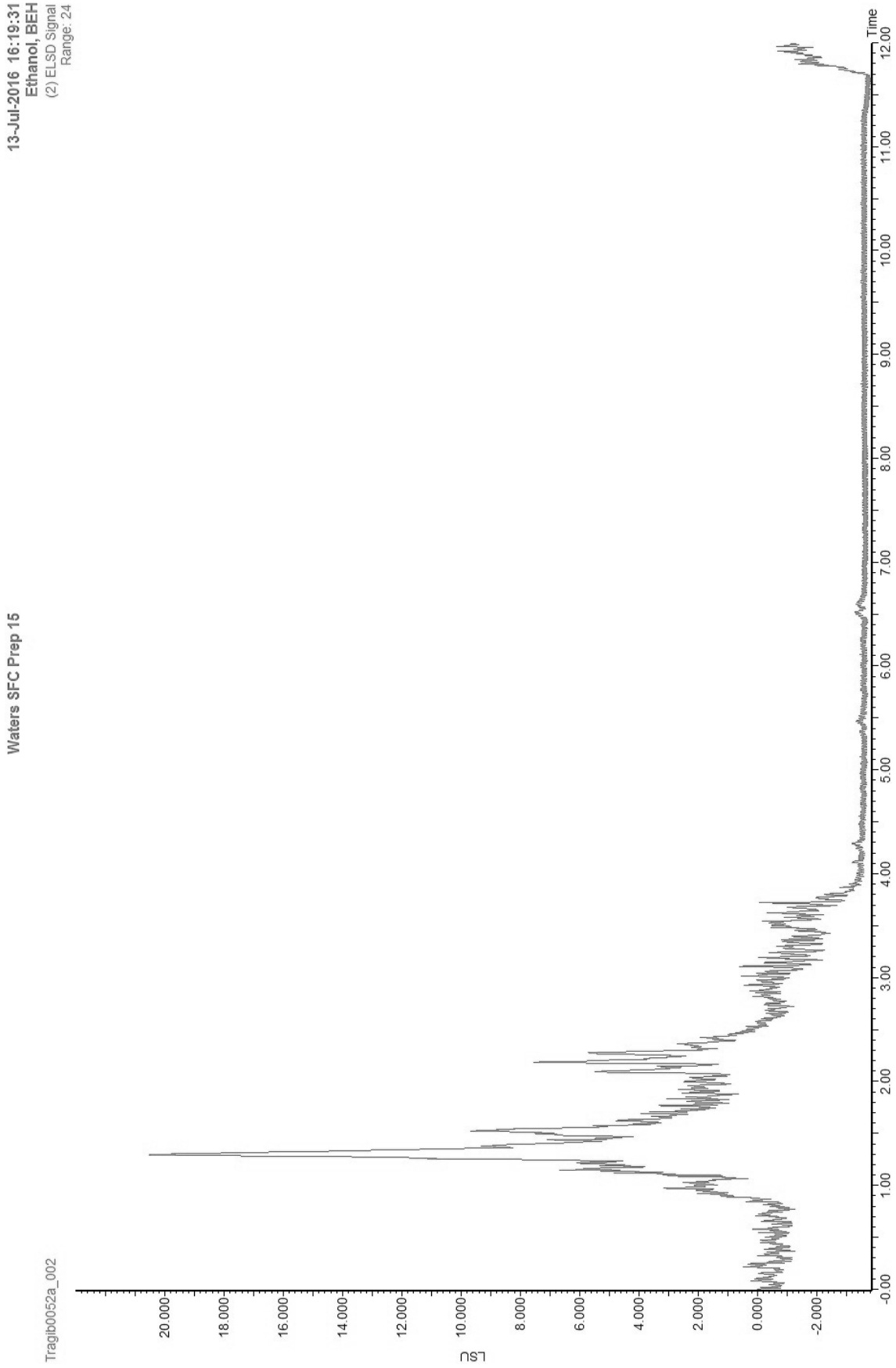

Figure 87 -Tragib0052a; ELSD Signal

8.2 Purification of Selected Fractions of *Gloeophyllum odoratum*

8.2.1 NMR-Spectra

8.2.1.1 GO36_01

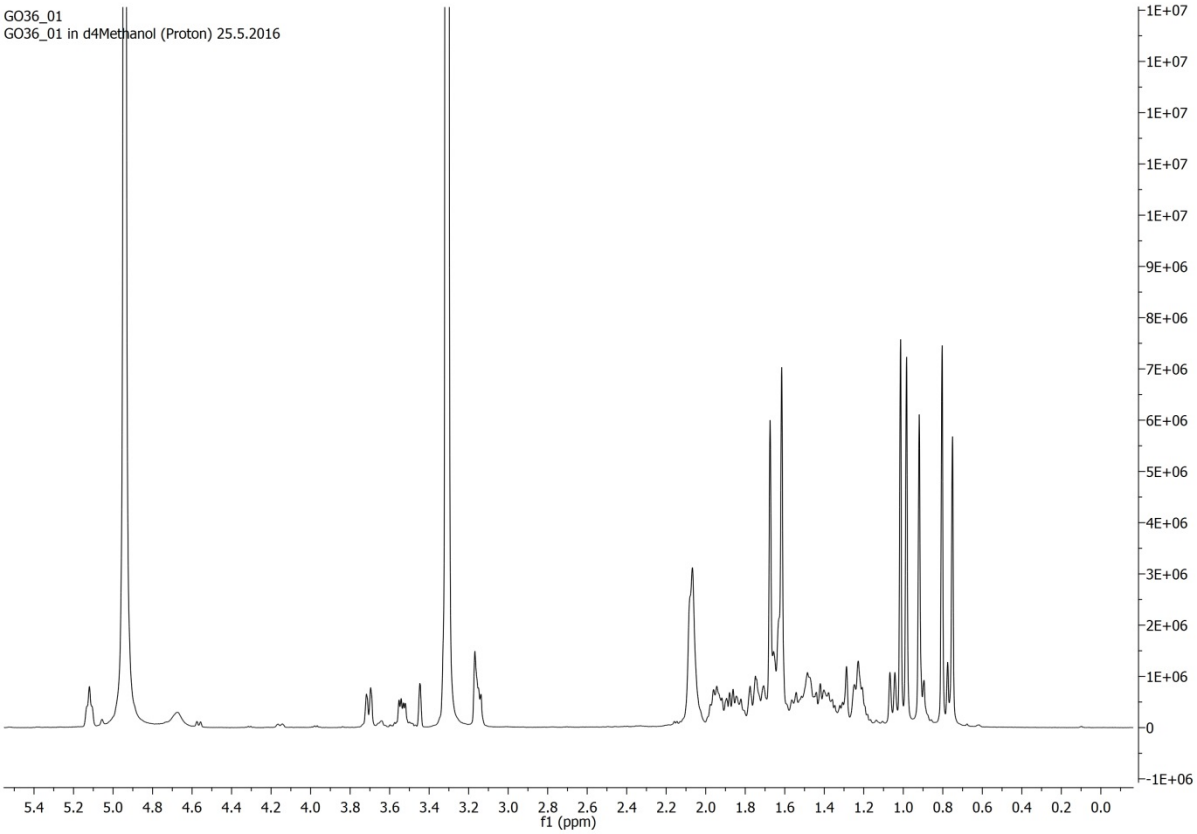

Figure 88 - 1H-NMR spectrum of GO54ED36_01; (CD3OD, ref.: δH 3.31 ppm, 500 MHz NMR, ~1 mg).

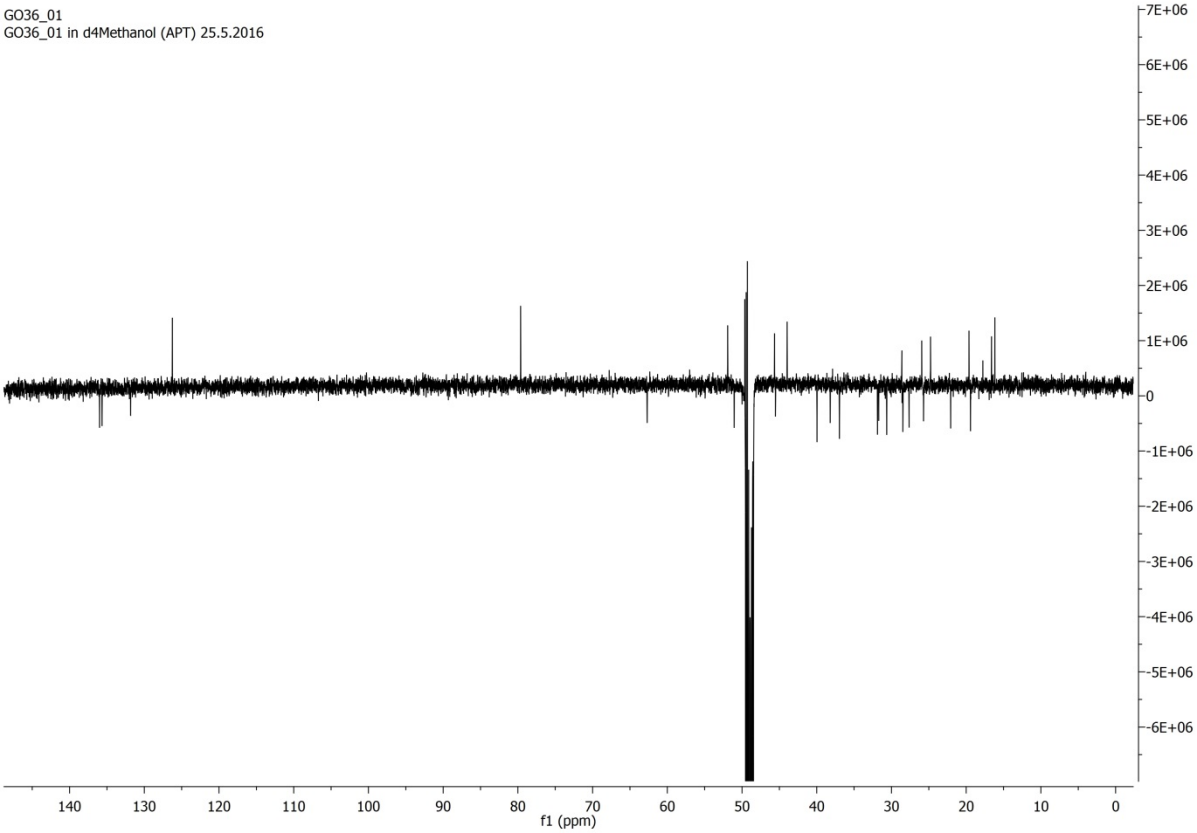

Figure 89 - 13C-APT spectrum of GO54ED36_01; (CD3OD, ref.: δC 49.00 ppm, 500 MHz NMR, ~1 mg).

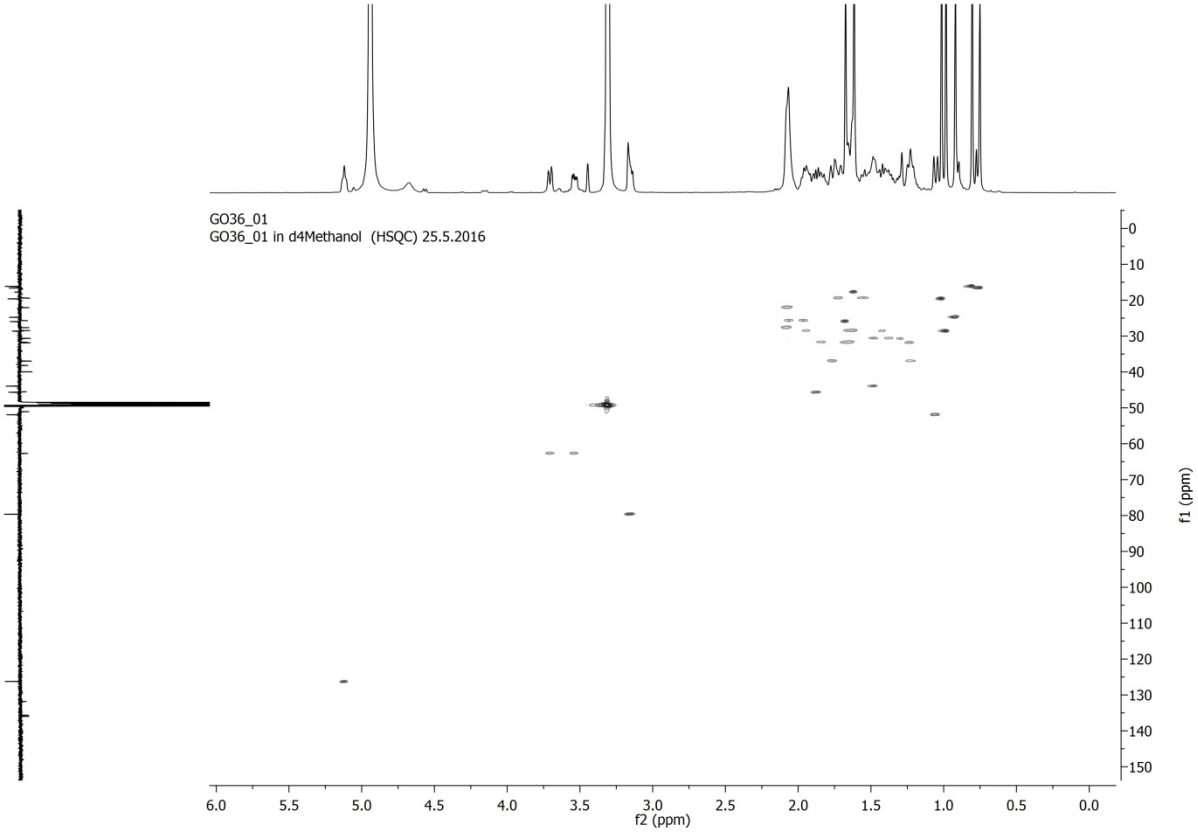

Figure 90 - HSQC spectrum (horizontal trace: 1H-NMR spectrum, vertical trace: 13C-APT) of GO54ED36_01; (CD3OD, ref.: δH 3.31 ppm, δC 49.00 ppm, 500 MHz NMR, ~1 mg).

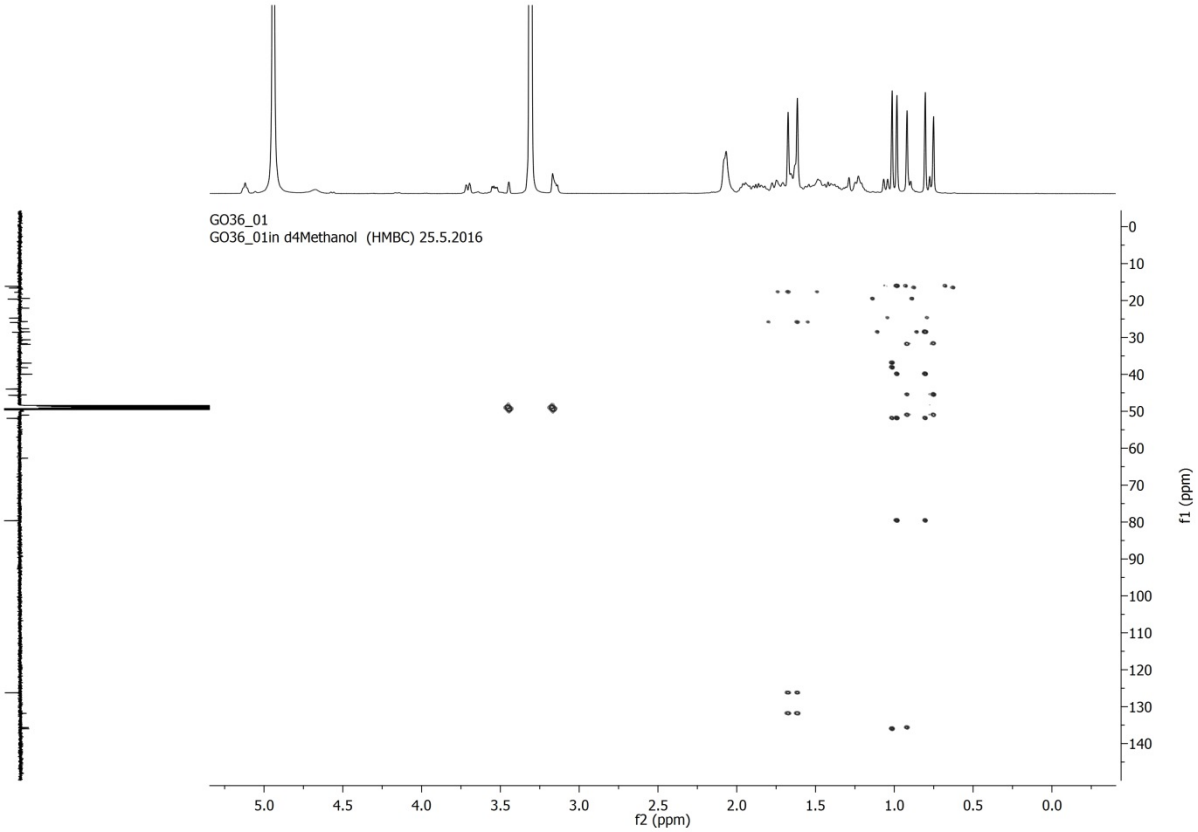

Figure 91 - HMBC spectrum (horizontal trace: 1H-NMR spectrum, vertical trace: 13C-APT) of GO54ED36_01; (CD3OD, ref.: δH 3.31 ppm, δC 49.00 ppm, 500 MHz NMR, ~1 mg).

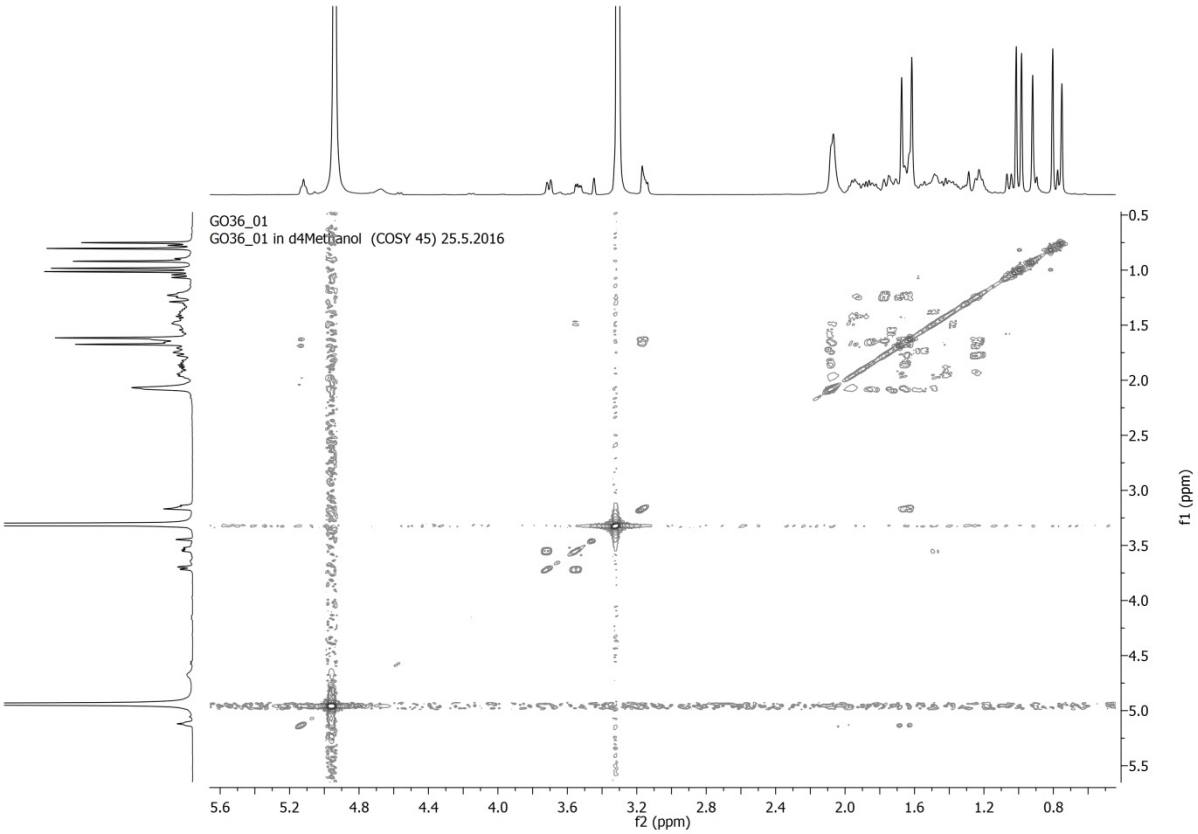

Figure 92 - HH-COSY spectrum (horizontal & vertical trace: 1H-NMR spectrum) of GO54ED36_01; (CD3OD, ref.: δH 3.31 ppm, 500 MHz NMR, ~1 mg).

8.2.1.2 GO36_02

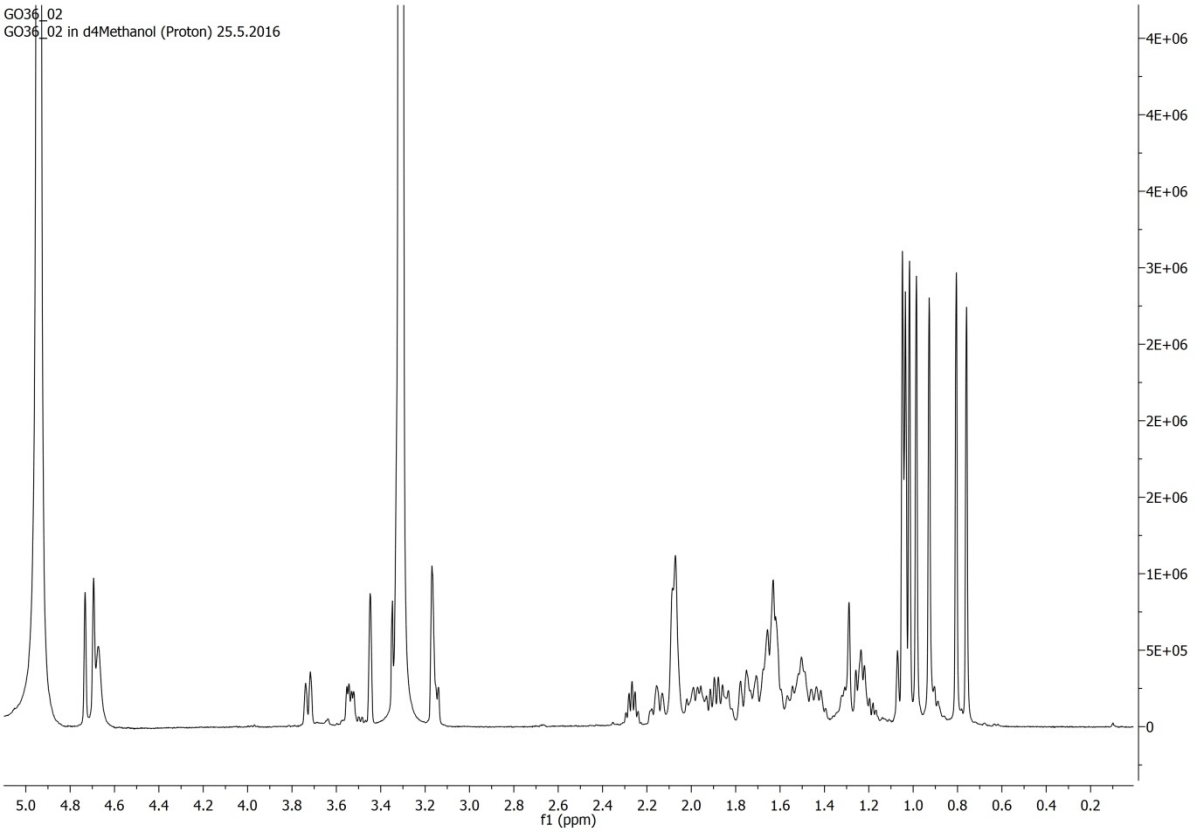

Figure 93 - 1H-NMR spectrum of GO54ED36_02; (CD3OD, ref.: δH 3.31 ppm, 500 MHz NMR, ~1 mg).

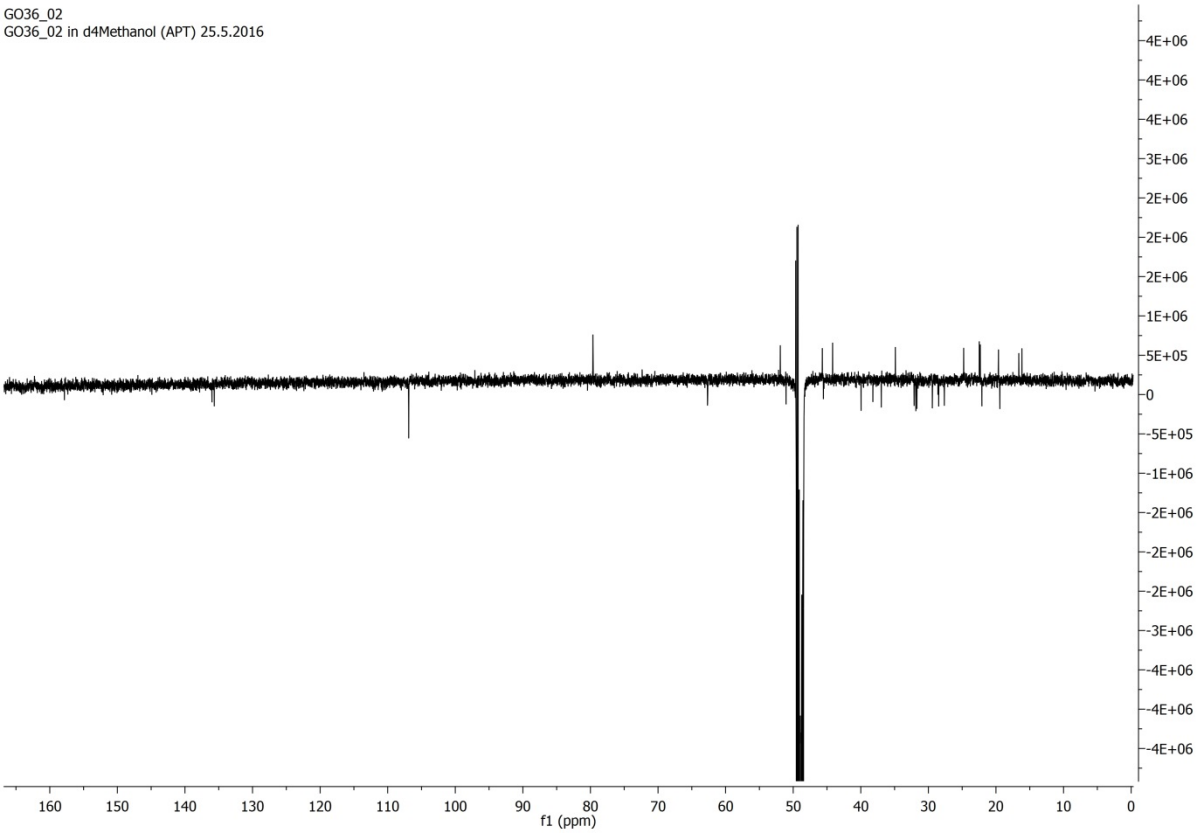

Figure 94 - 13C-APT spectrum of GO54ED36_02; (CD3OD, ref.: δC 49.00 ppm, 500 MHz NMR, ~1 mg).

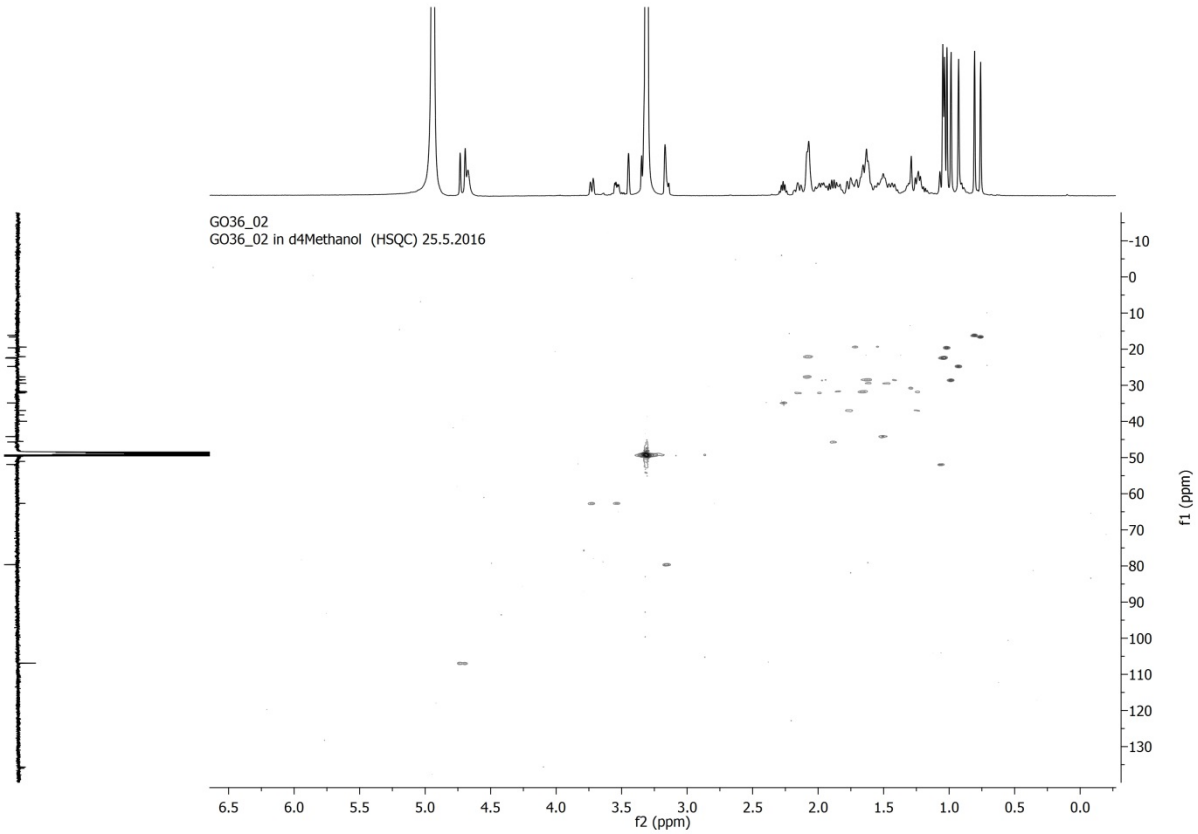

Figure 95 - HSQC spectrum (horizontal trace: 1H-NMR spectrum, vertical trace: 13C-APT) of GO54ED36_02; (CD3OD, ref.: δH 3.31 ppm, δC 49.00 ppm, 500 MHz NMR, ~1 mg).

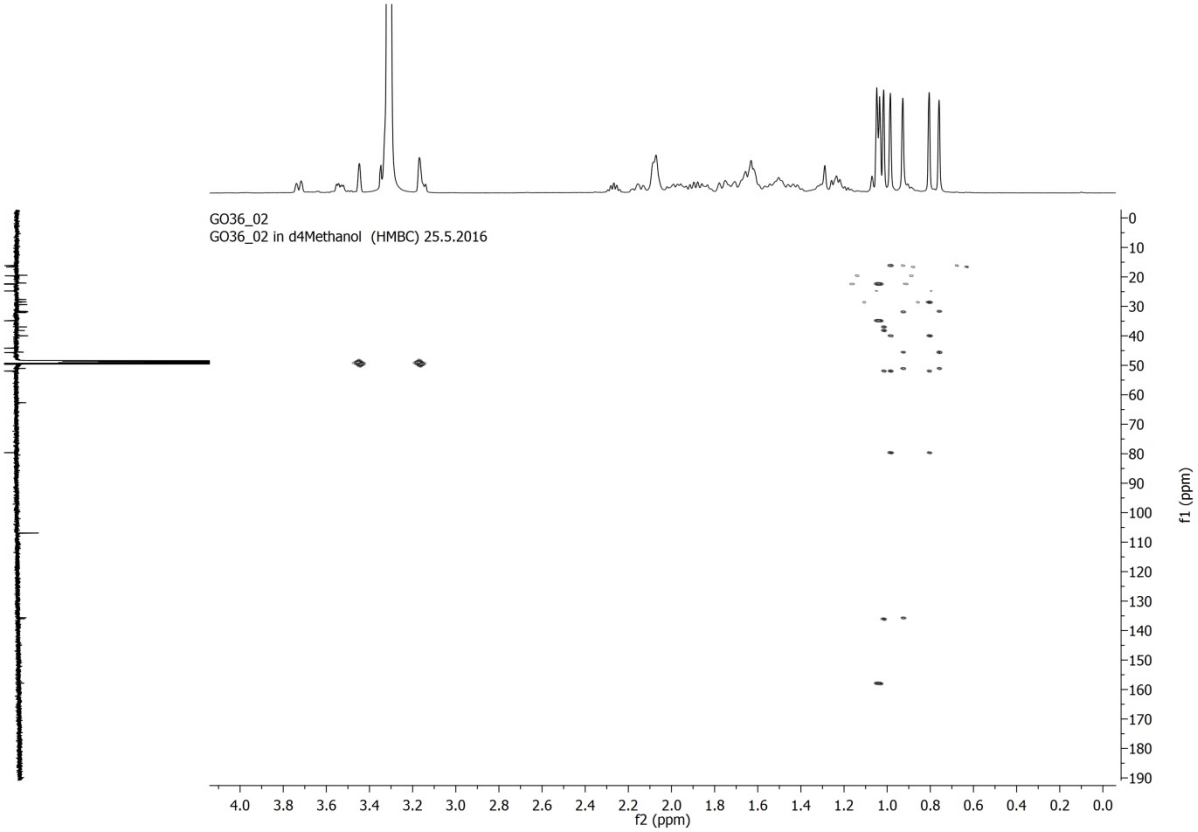

Figure 96 - HMBC spectrum (horizontal trace: 1H-NMR spectrum, vertical trace: 13C-APT) of GO54ED36_02; (CD3OD, ref.: δH 3.31 ppm, δC 49.00 ppm, 500 MHz NMR, ~1 mg).

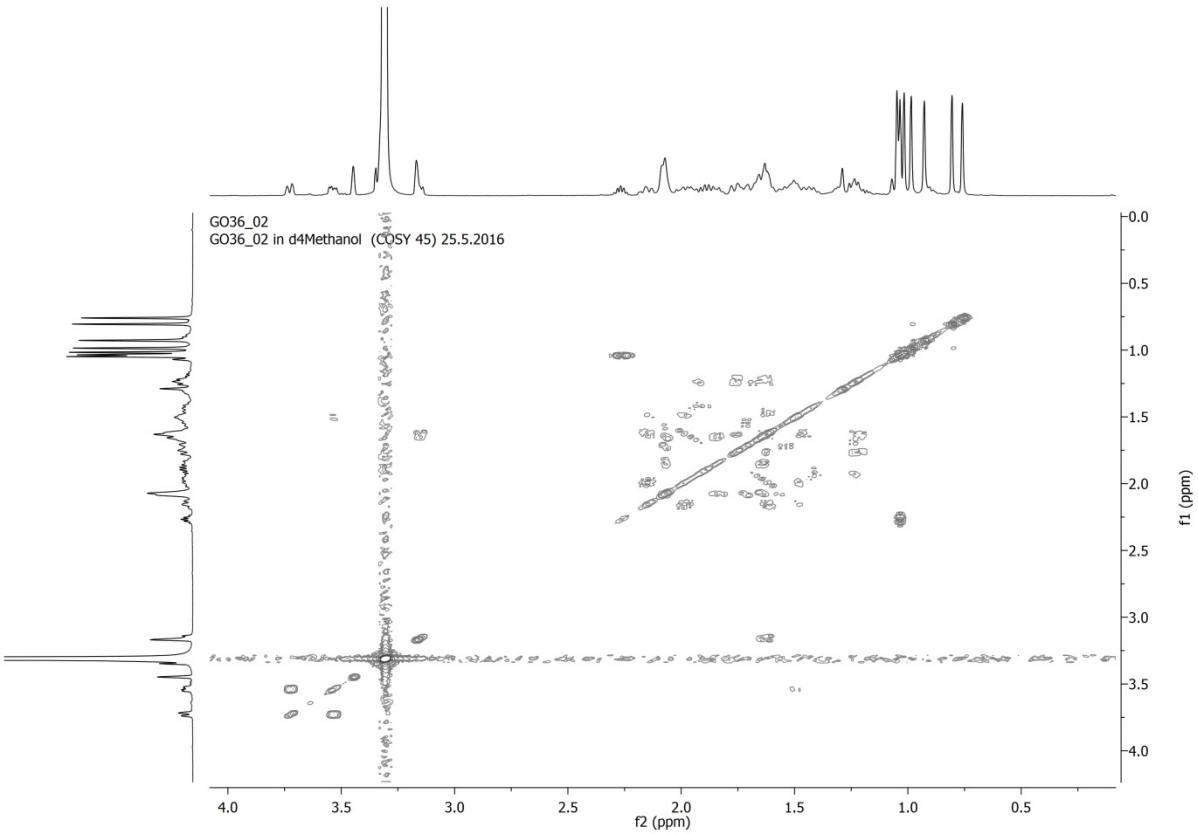

Figure 97 - HH-COSY spectrum (horizontal & vertical trace: 1H-NMR spectrum) of GO54ED36_02; (CD3OD, ref.: δH 3.31 ppm, 500 MHz NMR, ~1 mg).

8.2.2 HRMS Data

8.2.2.1 GO36_01

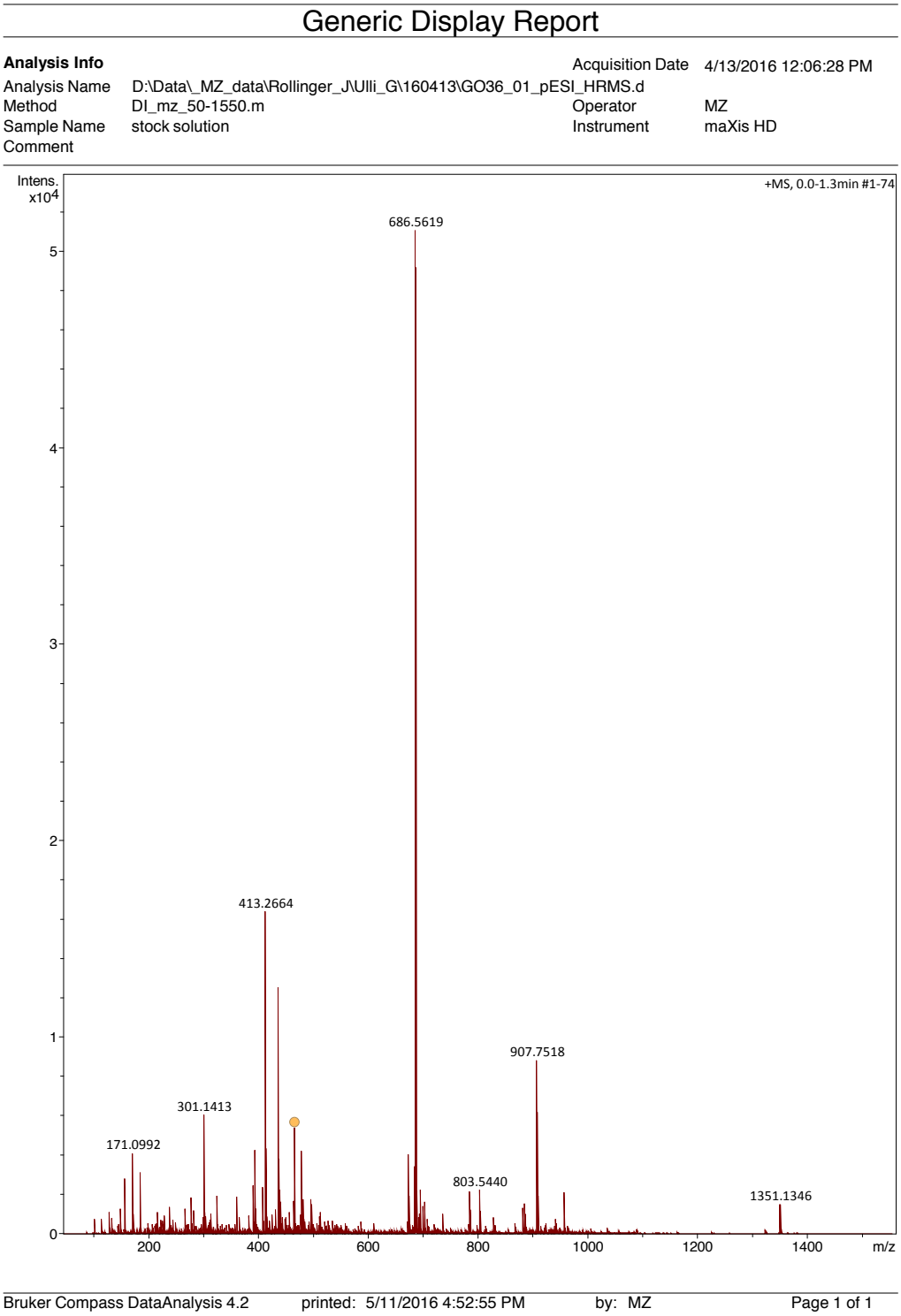

Figure 98 – pESI HRMS spectra of GO36_01

Generic Display Report

Analysis Info

Analysis Name	D:\Data_MZ_data\Rollinger_J\Ulli_G\160413\GO36_01_pESI_HRMS.d	Acquisition Date	4/13/2016 12:06:28 PM
Method	DI_mz_50-1550.m	Operator	MZ
Sample Name	stock solution	Instrument	maXis HD
Comment			

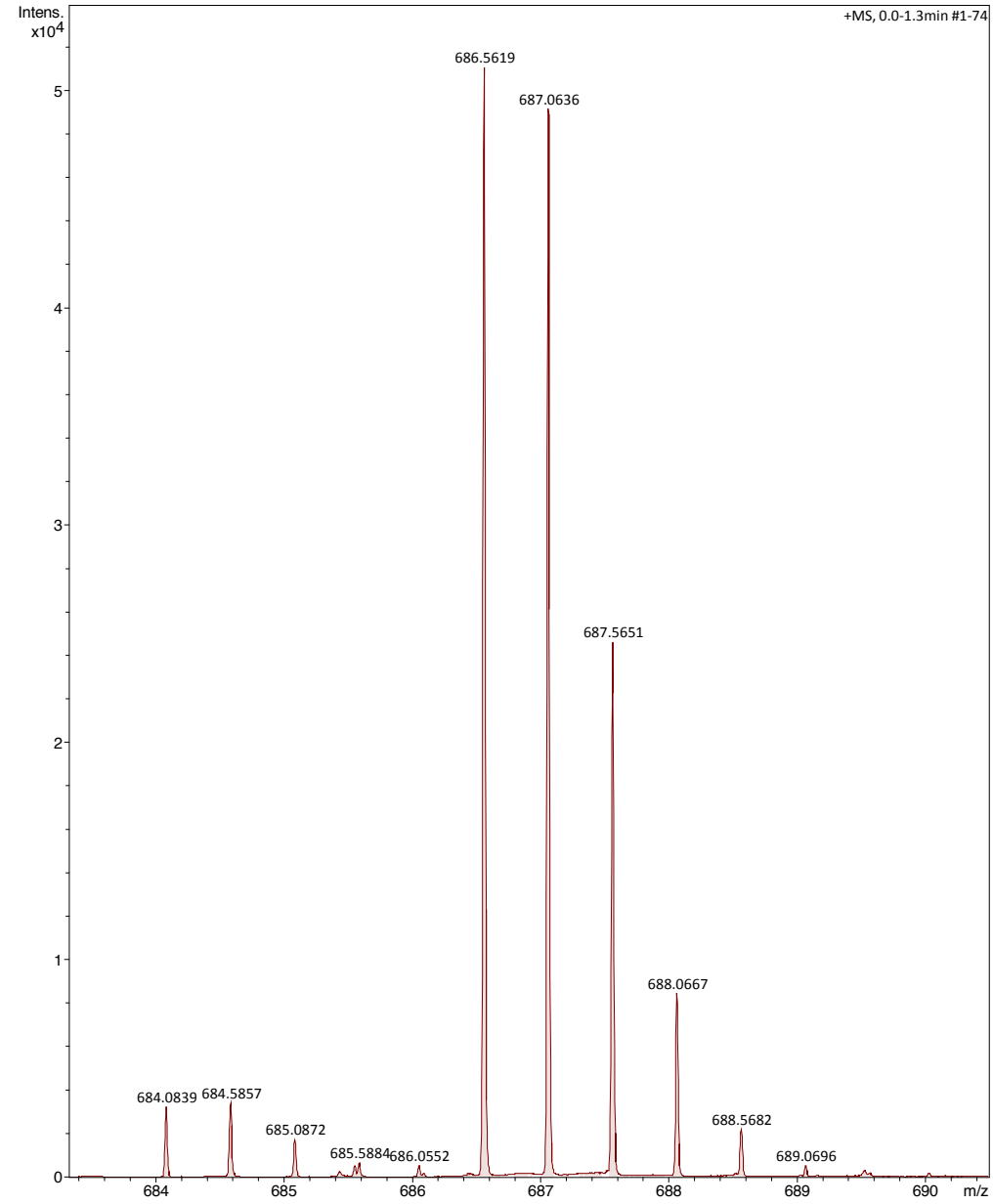

Bruker Compass DataAnalysis 4.2 printed: 5/11/2016 4:53:06 PM by: MZ Page 1 of 1

Figure 99 – pESI HRMS spectra of GO36_01

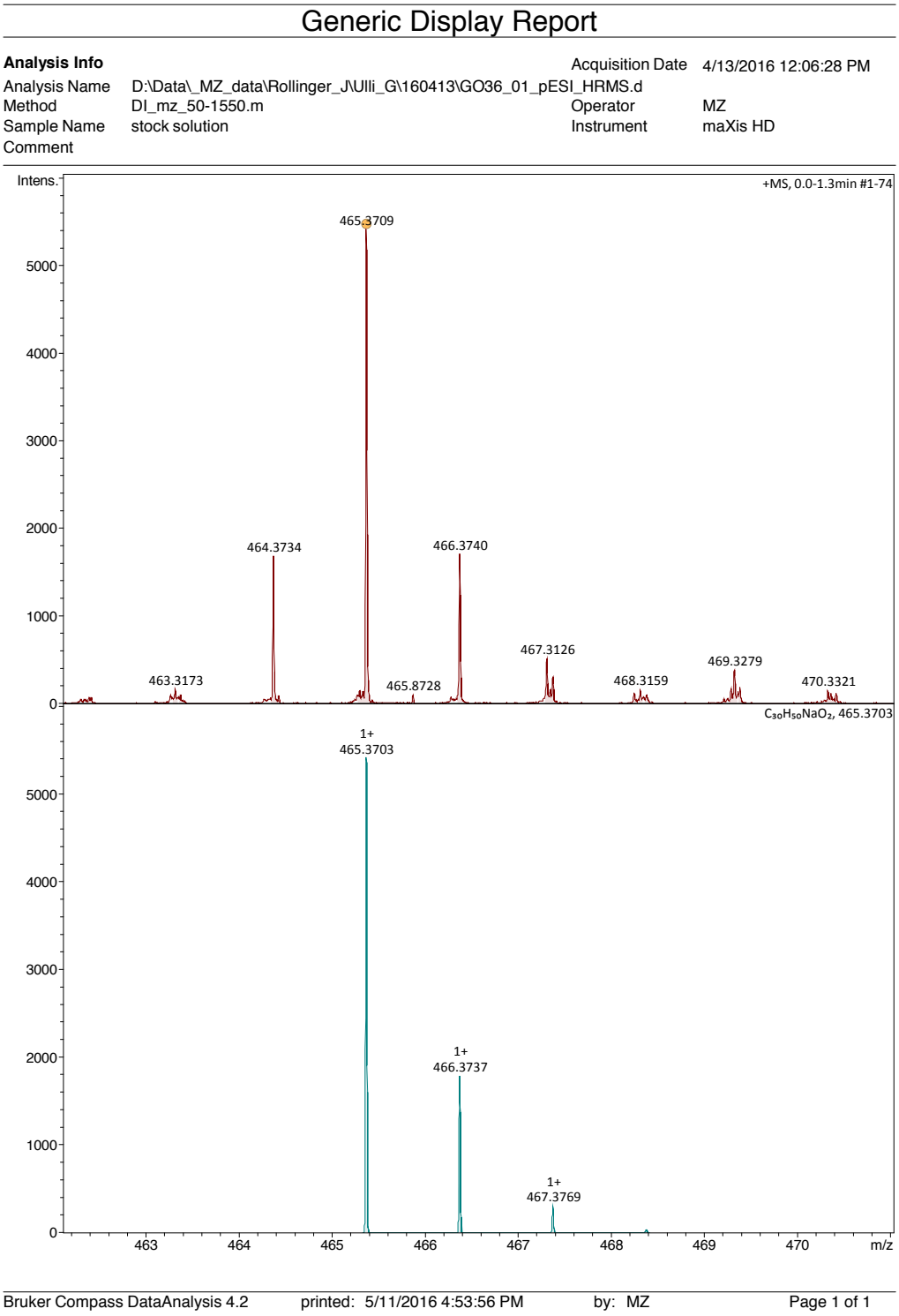

Figure 100 – pESI HRMS spectra of GO36_01

Mass Spectrum SmartFormula Report

Analysis Info

Analysis Name	D:\Data_MZ_data\Rollinger_J\Ulli_G\160413\GO36_01_pESI_HRMS.d	Acquisition Date	4/13/2016 12:06:28 PM
Method	DI_mz_50-1550.m	Operator	MZ
Sample Name	stock solution	Instrument	maXis HD 1820881.21300
Comment			

Acquisition Parameter

Source Type	ESI	Ion Polarity	Positive	Set Nebulizer	0.4 Bar
Focus	Active	Set Capillary	2100 V	Set Dry Heater	200 °C
Scan Begin	50 m/z	Set End Plate Offset	-500 V	Set Dry Gas	4.0 l/min
Scan End	1550 m/z	Set Charging Voltage	2000 V	Set Divert Valve	Waste
		Set Corona	0 nA	Set APCI Heater	0 °C

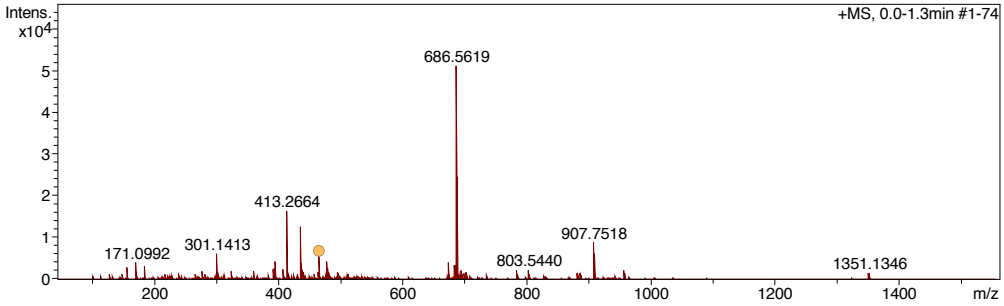

Meas. m/z	#	Ion Formula	m/z	err [ppm]	mSigma	# mSigma	Score	rdb	e⁻ Conf	N-Rule
465.3709	1	C30H50NaO2	465.3703	-1.3	8.7	1	100.00	5.5	even	ok

Figure 101 – pESI HRMS spectra of GO36_01

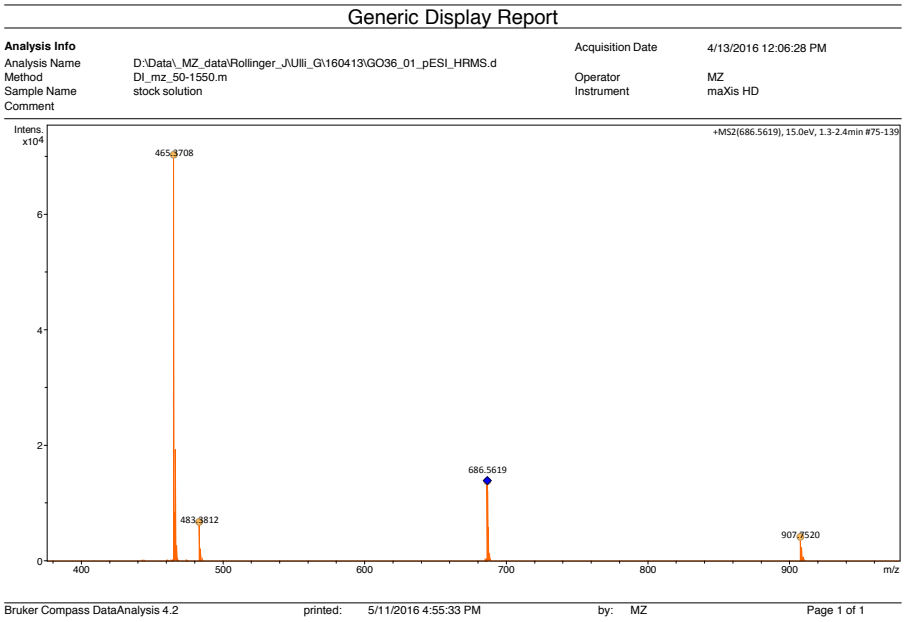

Figure 102 – pESI HRMS spectra of GO36_02

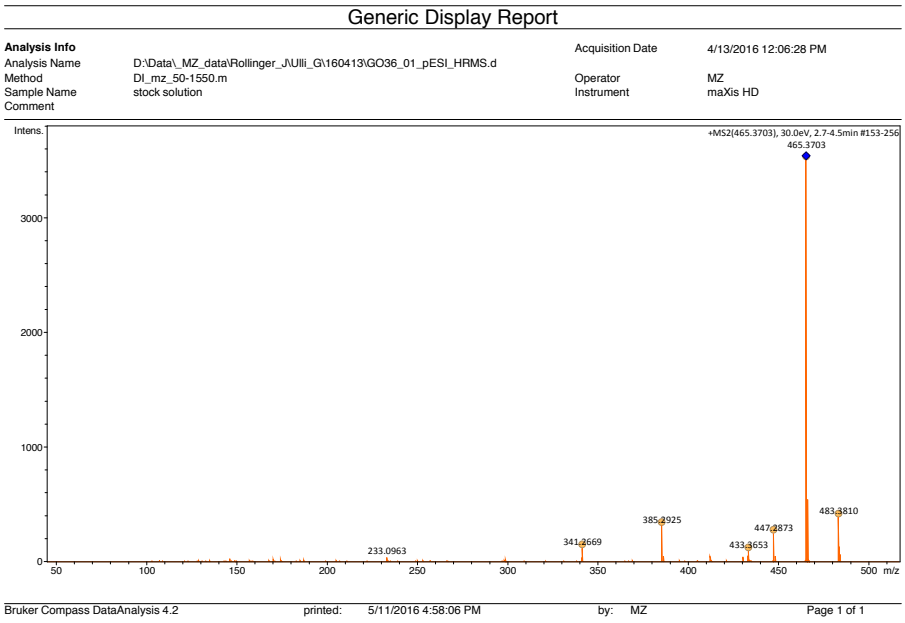

Figure 103 – pESI HRMS spectra of GO36_01

Mass Spectrum SmartFormula Report

Analysis Info

Analysis Name	D:\Data_MZ_data\Rollinger_J\Ulli_G\160413\GO36_01_pESI_HRMS.d	Acquisition Date	4/13/2016 12:06:28 PM
Method	DI_mz_50-1550.m	Operator	MZ
Sample Name	stock solution	Instrument	maXis HD 1820881.21300
Comment			

Acquisition Parameter

Source Type	ESI	Ion Polarity	Positive	Set Nebulizer	0.4 Bar
Focus	Active	Set Capillary	2100 V	Set Dry Heater	200 °C
Scan Begin	50 m/z	Set End Plate Offset	-500 V	Set Dry Gas	4.0 l/min
Scan End	1550 m/z	Set Charging Voltage	2000 V	Set Divert Valve	Waste
		Set Corona	0 nA	Set APCI Heater	0 °C

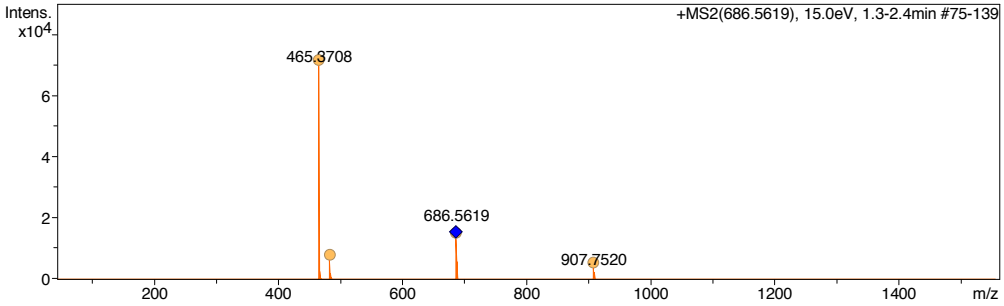

Meas. m/z	#	Ion Formula	m/z	err [ppm]	mSigma	# mSigma	Score	rdb	e⁻ Conf	N-Rule
465.3708	1	C30H50NaO2	465.3703	-1.2	32.4	1	100.00	5.5	even	ok
483.3812	1	C30H52NaO3	483.3809	-0.7	9.9	1	100.00	4.5	even	ok
686.5619	1	C32H73N9NaO5	686.5627	1.1	40.1	1	100.00	0.5	even	ok
907.7520	1	C60H100NaO4	907.7514	-0.7	13.5	1	100.00	10.5	even	ok
	2	C61H96N4Na	907.7527	0.8	22.6	2	62.37	15.5	even	ok

GO36_01_pESI_HRMS.d

Bruker Compass DataAnalysis 4.2 printed: 5/11/2016 4:58:22 PM by: MZ Page 1 of 1

Figure 104 – pESI HRMS spectra of GO36_01

Mass Spectrum SmartFormula Report

Analysis Info

Acquisition Date	4/13/2016 12:06:28 PM		
Analysis Name	D:\Data_MZ_data\Rollinger_J\Ulli_G\160413\GO36_01_pESI_HRMS.d		
Method	DI_mz_50-1550.m	Operator	MZ
Sample Name	stock solution	Instrument	maXis HD 1820881.21300
Comment			

Acquisition Parameter

Source Type	ESI	Ion Polarity	Positive	Set Nebulizer	0.4 Bar
Focus	Active	Set Capillary	2100 V	Set Dry Heater	200 °C
Scan Begin	50 m/z	Set End Plate Offset	-500 V	Set Dry Gas	4.0 l/min
Scan End	1550 m/z	Set Charging Voltage	2000 V	Set Divert Valve	Waste
		Set Corona	0 nA	Set APCI Heater	0 °C

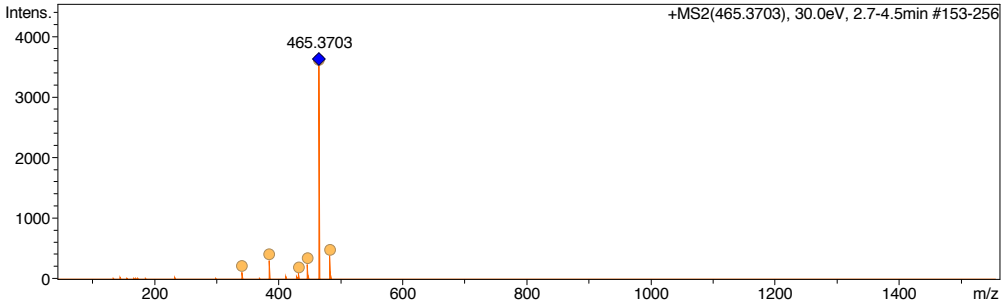

Meas. m/z	#	Ion Formula	m/z	err [ppm]	mSigma	# mSigma	Score	rdb	e⁻ Conf	N-Rule
341.2669	1	C19H34N4Na	341.2676	1.9	n.a.	1	100.00	4.5	even	ok
	2	C18H38NaO4	341.2662	-2.0	n.a.	2	99.21	-0.5	even	ok
385.2925	1	C20H42NaO5	385.2924	-0.1	45.0	1	100.00	-0.5	even	ok
433.3653	1	C26H50NaO3	433.3652	-0.3	n.a.	1	100.00	1.5	even	ok
447.2873	1	C13H36N12NaO4	447.2875	0.4	15.3	1	100.00	1.5	even	ok
	2	C28H40NaO3	447.2870	-0.8	78.6	2	14.14	8.5	even	ok
465.3703	1	C30H50NaO2	465.3703	-0.0	106.7	1	100.00	5.5	even	ok
483.3810	1	C30H52NaO3	483.3809	-0.3	85.4	1	100.00	4.5	even	ok

Figure 105 – pESI HRMS spectra of GO36_01

8.2.2.2 GO36_02

Generic Display Report

Analysis Info

Acquisition Date	4/13/2016 2:49:22 PM		
Analysis Name	D:\Data_MZ_data\Rollinger_J\Ulli_G\160413\GO36_02_recal_pESI_HRMS.d		
Method	DI_mz_50-1550.m	Operator	MZ
Sample Name	stock solution	Instrument	maXis HD
Comment			

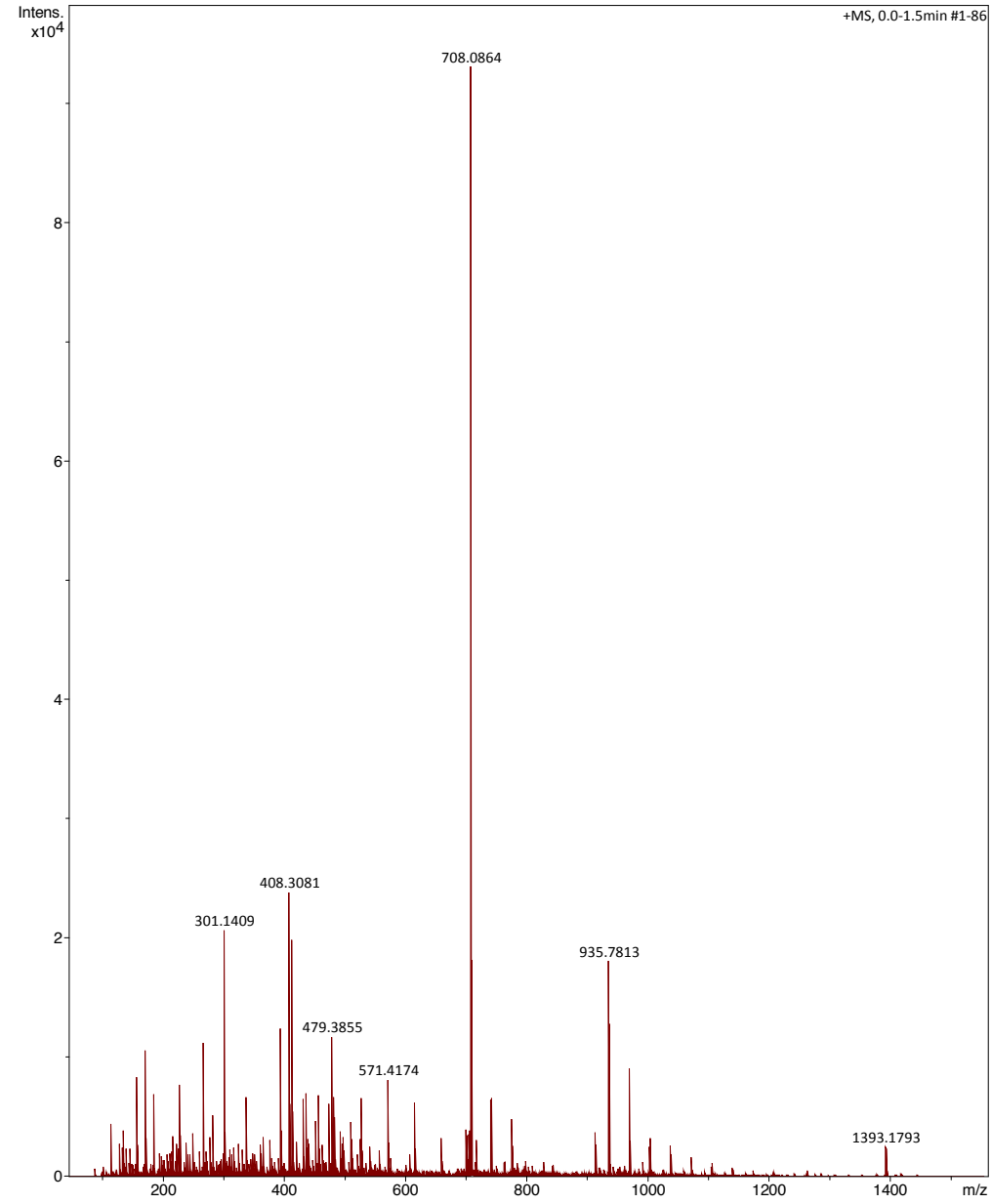

Bruker Compass DataAnalysis 4.2 printed: 5/11/2016 5:00:00 PM by: MZ Page 1 of 1

Figure 106 – pESI HRMS spectra of GO36_02

Generic Display Report

Analysis Info		Acquisition Date	4/13/2016 2:49:22 PM
Analysis Name	D:\Data_MZ_data\Rollinger_J\Ulli_G\160413\GO36_02_recal_pESI_HRMS.d		
Method	DI_mz_50-1550.m	Operator	MZ
Sample Name	stock solution	Instrument	maXis HD
Comment			

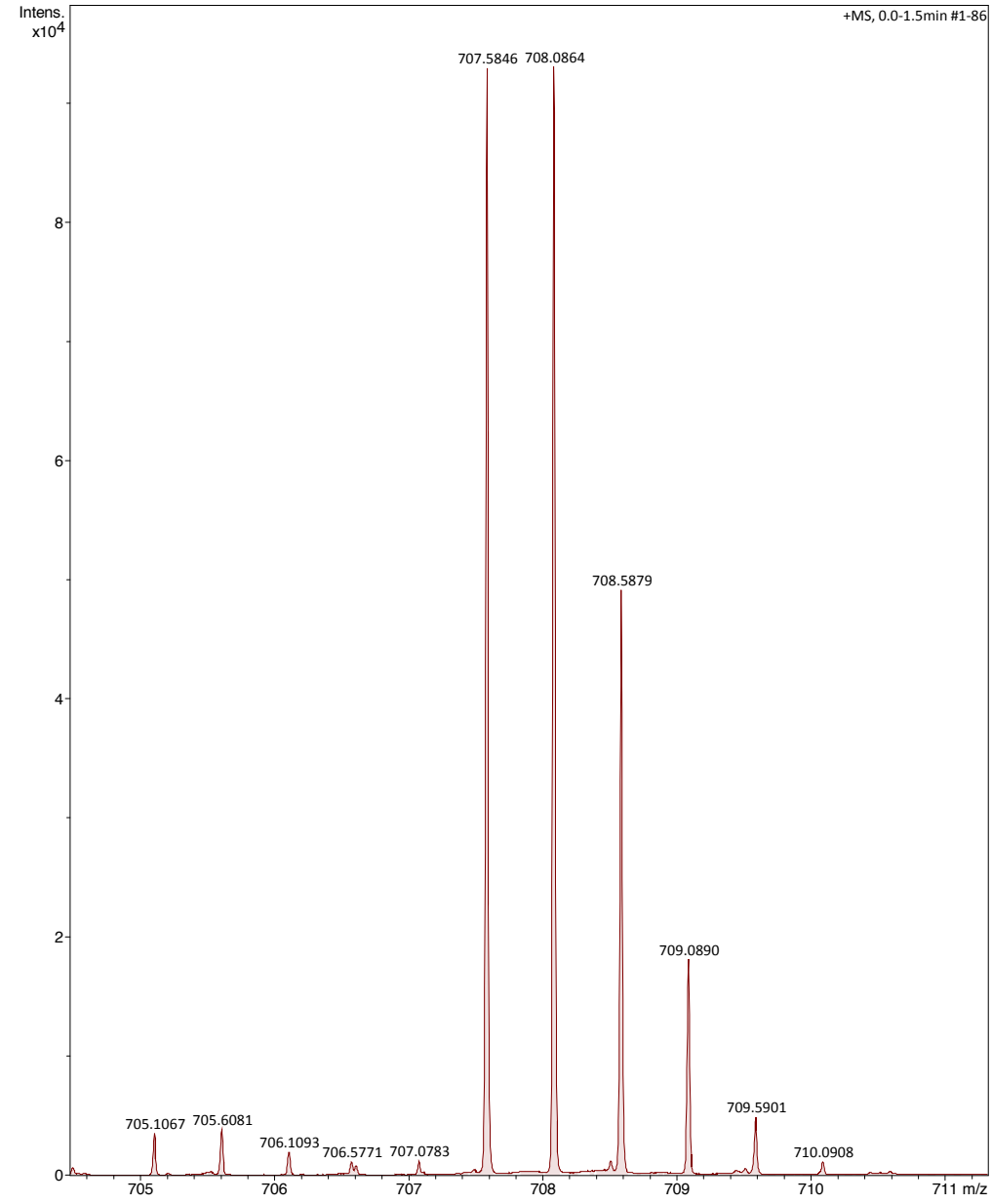

Bruker Compass DataAnalysis 4.2 printed: 5/11/2016 5:00:16 PM by: MZ Page 1 of 1

Figure 107 – pESI HRMS spectra of GO36_02

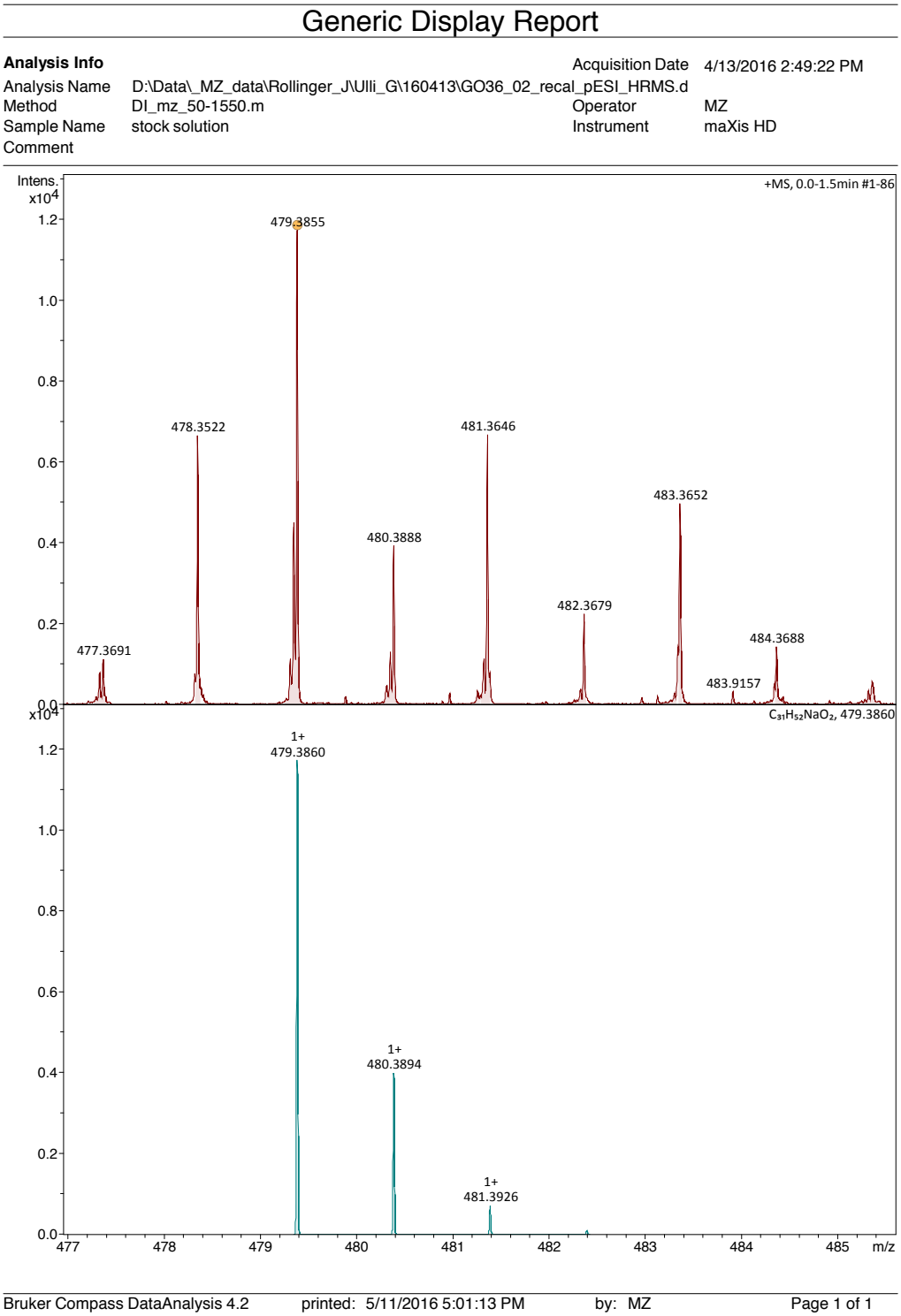

Figure 108 – pESI HRMS spectra of GO36_02

Mass Spectrum SmartFormula Report

Analysis Info

Acquisition Date	4/13/2016 2:49:22 PM		
Analysis Name	D:\Data_MZ_data\Rollinger_J\Ulli_G\160413\GO36_02_recal_pESI_HRMS.d		
Method	DI_mz_50-1550.m	Operator	MZ
Sample Name	stock solution	Instrument	maXis HD 1820881.21300
Comment			

Acquisition Parameter

Source Type	ESI	Ion Polarity	Positive	Set Nebulizer	0.4 Bar
Focus	Active	Set Capillary	2300 V	Set Dry Heater	200 °C
Scan Begin	50 m/z	Set End Plate Offset	-500 V	Set Dry Gas	4.0 l/min
Scan End	1550 m/z	Set Charging Voltage	2000 V	Set Divert Valve	Waste
		Set Corona	0 nA	Set APCI Heater	0 °C

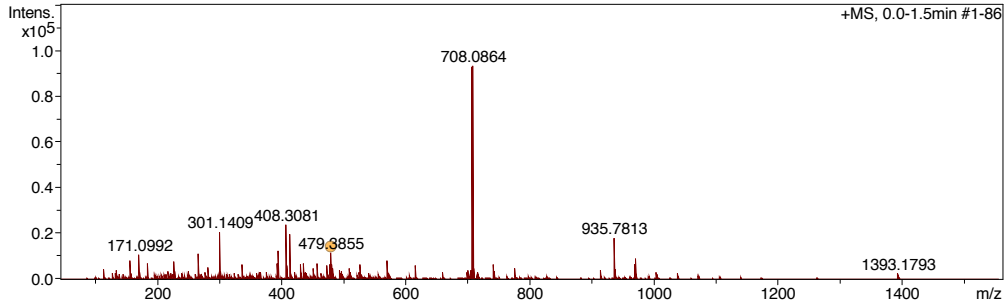

Meas. m/z	#	Ion Formula	m/z	err [ppm]	mSigma	# mSigma	Score	rdb	e⁻ Conf	N-Rule
479.3855	1	C31H52NaO2	479.3860	0.9	30.8	1	100.00	5.5	even	ok

Figure 109 – pESI HRMS spectra of GO36_02

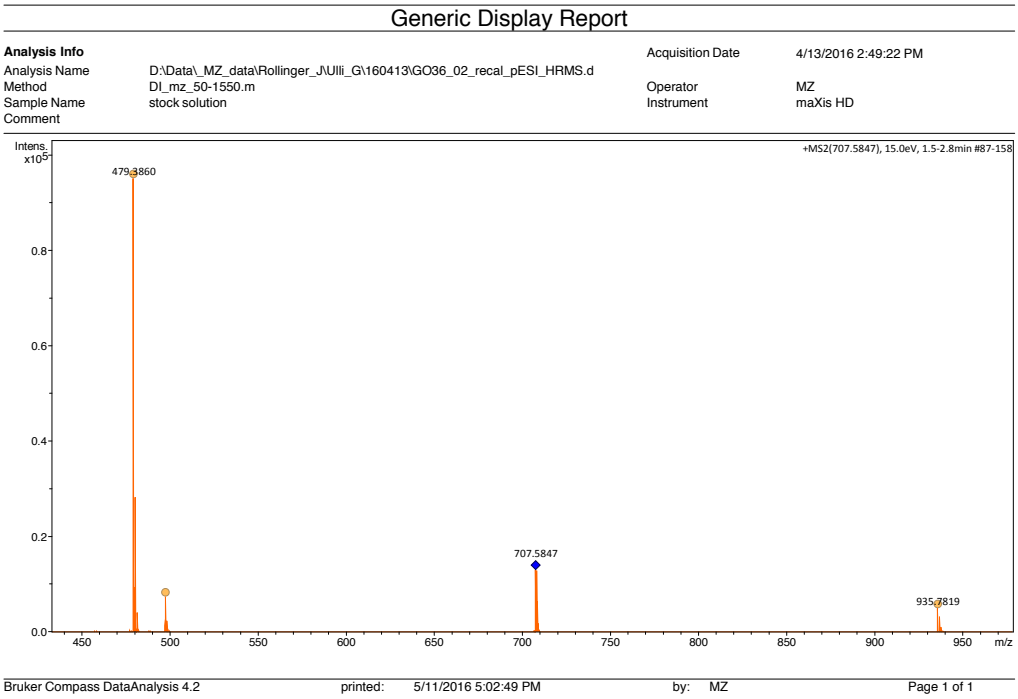

Figure 110 – pESI HRMS spectra of GO36_02

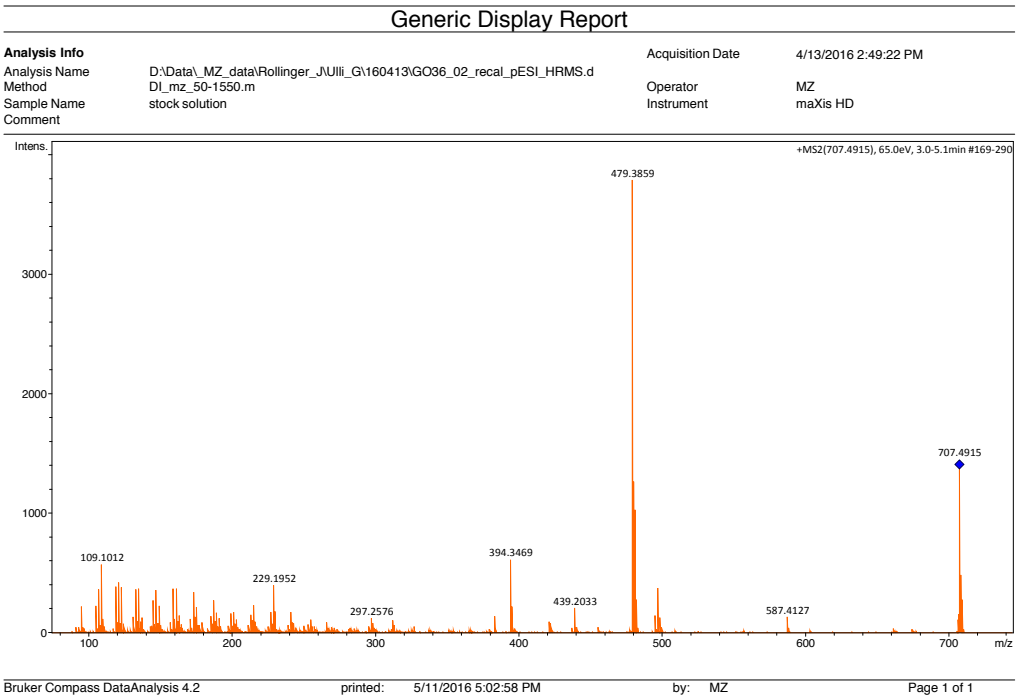

Figure 111 – pESI HRMS spectra of GO36_02

Mass Spectrum SmartFormula Report

Analysis Info

Acquisition Date	4/13/2016 2:49:22 PM		
Analysis Name	D:\Data_MZ_data\Rollinger_J\Ulli_G\160413\GO36_02_recal_pESI_HRMS.d		
Method	DI_mz_50-1550.m	Operator	MZ
Sample Name	stock solution	Instrument	maXis HD 1820881.21300
Comment			

Acquisition Parameter

Source Type	ESI	Ion Polarity	Positive	Set Nebulizer	0.4 Bar
Focus	Active	Set Capillary	2300 V	Set Dry Heater	200 °C
Scan Begin	50 m/z	Set End Plate Offset	-500 V	Set Dry Gas	4.0 l/min
Scan End	1550 m/z	Set Charging Voltage	2000 V	Set Divert Valve	Waste
		Set Corona	0 nA	Set APCI Heater	0 °C

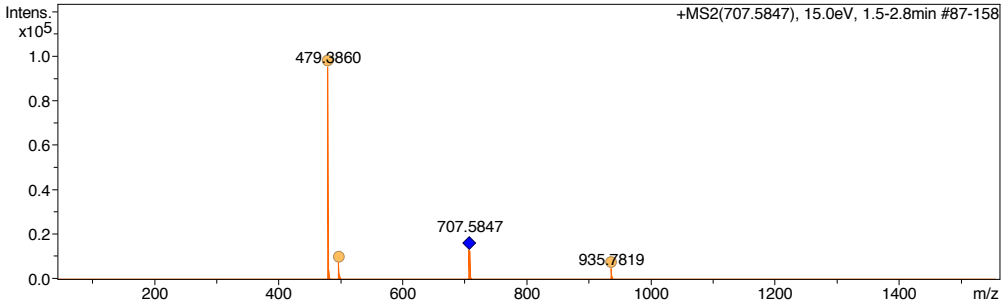

Meas. m/z	#	Ion Formula	m/z	err [ppm]	mSigma	# mSigma	Score	rdb	e⁻ Conf	N-Rule
479.3860	1	C31H52NaO2	479.3860	-0.1	24.0	1	100.00	5.5	even	ok
497.3963	1	C31H54NaO3	497.3965	0.5	13.6	1	100.00	4.5	even	ok
935.7819	1	C58H100N6NaO2	935.7800	-2.0	6.8	1	53.61	11.5	even	ok
	2	C62H104NaO4	935.7827	0.9	20.1	2	100.00	10.5	even	ok

Figure 112 – pESI HRMS spectra of GO36_02

Mass Spectrum SmartFormula Report

Analysis Info

Analysis Name	D:\Data_MZ_data\Rollinger_J\Ulli_G\160413\GO36_02_recal_pESI_HRMS.d	Acquisition Date	4/13/2016 2:49:22 PM
Method	DI_mz_50-1550.m	Operator	MZ
Sample Name	stock solution	Instrument	maXis HD 1820881.21300
Comment			

Acquisition Parameter

Source Type	ESI	Ion Polarity	Positive	Set Nebulizer	0.4 Bar
Focus	Active	Set Capillary	2300 V	Set Dry Heater	200 °C
Scan Begin	50 m/z	Set End Plate Offset	-500 V	Set Dry Gas	4.0 l/min
Scan End	1550 m/z	Set Charging Voltage	2000 V	Set Divert Valve	Waste
		Set Corona	0 nA	Set APCI Heater	0 °C

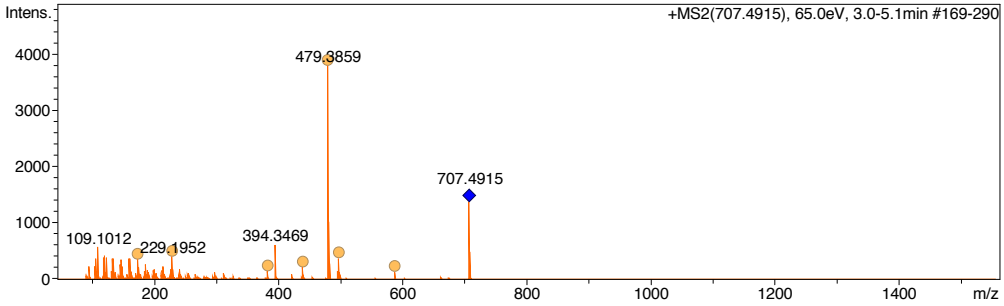

Meas. m/z	#	Ion Formula	m/z	err [ppm]	mSigma	# mSigma	Score	rdb	e⁻ Conf	N-Rule
109.1012	1	C8H13	109.1012	-0.5	66.8	1	100.00	2.5	even	ok
173.1326	1	C13H17	173.1325	-0.8	378.8	1	100.00	5.5	even	ok
229.1952	1	C17H25	229.1951	-0.6	157.9	1	100.00	5.5	even	ok
383.1406	1	C27H20NaO	383.1406	0.0	n.a.	1	100.00	17.5	even	ok
	2	C12H16N12NaO2	383.1411	1.4	n.a.	2	80.06	10.5	even	ok
439.2033	1	C31H28NaO	439.2032	-0.2	n.a.	1	100.00	17.5	even	ok
	2	C16H24N12NaO2	439.2037	0.9	n.a.	2	86.61	10.5	even	ok
479.3859	1	C31H52NaO2	479.3860	0.1	30.9	1	100.00	5.5	even	ok
497.3967	1	C31H54NaO3	497.3965	-0.4	31.8	1	100.00	4.5	even	ok
587.4127	1	C30H60NaO9	587.4130	0.5	n.a.	1	100.00	0.5	even	ok
	2	C27H52N10NaO3	587.4116	-1.8	n.a.	2	66.87	6.5	even	ok

Figure 113 – pESI HRMS spectra of GO36_02

Generic Display Report

Analysis Info

Acquisition Date	4/13/2016 2:57:44 PM		
Analysis Name	D:\Data_MZ_data\Rollinger_J\Ulli_G\160413\GO36_02_ISD50_pESI_HRMS.d		
Method	DI_mz_50-1550.m	Operator	MZ
Sample Name	stock solution	Instrument	maXis HD
Comment			

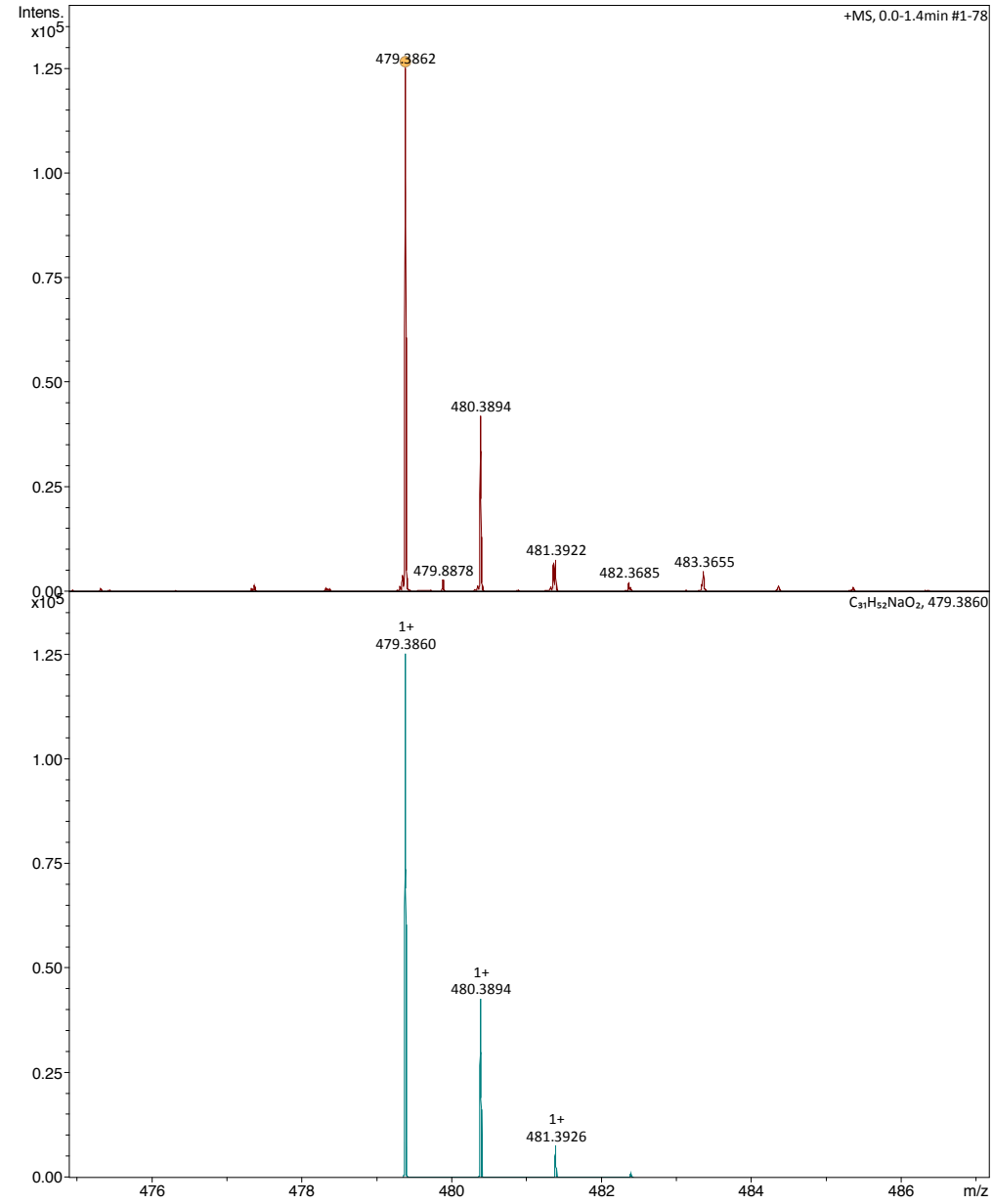

Bruker Compass DataAnalysis 4.2 printed: 5/11/2016 5:07:53 PM by: MZ Page 1 of 1

Figure 114 - ISD50 pESI HRMS spectra of GO36_02

Mass Spectrum SmartFormula Report

Analysis Info

Acquisition Date	4/13/2016 2:57:44 PM		
Analysis Name	D:\Data_MZ_data\Rollinger_J\Ulli_G\160413\GO36_02_ISD50_pESI_HRMS.d		
Method	DI_mz_50-1550.m	Operator	MZ
Sample Name	stock solution	Instrument	maXis HD 1820881.21300
Comment			

Acquisition Parameter

Source Type	ESI	Ion Polarity	Positive	Set Nebulizer	0.4 Bar
Focus	Active	Set Capillary	2200 V	Set Dry Heater	200 °C
Scan Begin	50 m/z	Set End Plate Offset	-500 V	Set Dry Gas	4.0 l/min
Scan End	1550 m/z	Set Charging Voltage	2000 V	Set Divert Valve	Waste
		Set Corona	0 nA	Set APCI Heater	0 °C

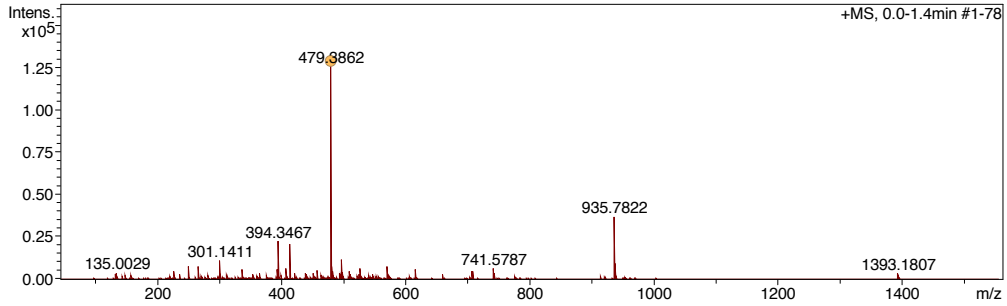

Meas. m/z	#	Ion Formula	m/z	err [ppm]	mSigma	# mSigma	Score	rdb	e⁻ Conf	N-Rule
479.3862	1	C31H52NaO2	479.3860	-0.5	3.0	1	100.00	5.5	even	ok

Figure 115 - ISD50 pESI HRMS spectra of GO36_02